

**C-type lectin receptors in
cell-specific targeting and malaria infection**

Inaugural-Dissertation

to obtain the academic degree

Doctor rerum naturalium (Dr. rer. nat.)

submitted to the Department of Biology, Chemistry, and Pharmacy
of Freie Universität Berlin

by

Maha Fay Binudin Maglinao

2013

Reviewers: **Prof. Dr. Markus Wahl**
Prof. Dr. Peter H. Seeberger

Date of defense: **17 June 2013**

Acknowledgement

I am very grateful to Prof. Dr. Peter H. Seeberger for giving me the opportunity and support for my thesis. I would like to express my deepest gratitude to Dr. Bernd Lepenies for being a wonderful Group Leader. His patience, understanding, excellent guidance, and unwavering support helped me overcome challenges and finish this dissertation. I am especially grateful to Prof. Dr. Markus Wahl who was willing to become my examiner even at a late notice.

I would like to thank Prof. Dr. Robert Klopffleisch for a fruitful collaboration and for the instrumental contributions he provided for the malaria research. I would also like to thank Dr. Mark Schlegel who, aside from being a supportive friend, has been an excellent collaborator.

I am thankful to Dr. Dan Gruenstein, Dr. Raghavendra Kikkeri, Dr. Mayeul Collot, Dr. Gonçalo Bernardes, and Prof. Dr. Hans Börner for the productive collaborations.

I would like to thank Dr. Daniel Kolarich and Kathirvel Alagesan for sequencing of the fusion proteins, to Dr. Anish Chakkumkal and Felix Broecker for the assistance with the protein conjugation, to Sebastian Götze for the help with the microarray, and to Kathrin Stavenhagen and Uwe Möglinger for the support with the MALDI analysis.

I would like to thank the members of the Glycoimmunology Group---past and present---Magdalena, Susanne, Uwe, Markus, Julia, Timo, Sandra, and Stephanie for the pleasant and enjoyable working environment. In particular, I would like to thank Magdalena for being a great colleague cum partner through all the bumps, big and small.

I would also like to thank Nahid, Bopanna, Daniel, and the rest of the Department of Biomolecular Systems for the constructive feedback and overall collegial atmosphere.

I would like to thank Ivan, Alex, Carl, Cullen, François, Bopanna, Rajan, and Cheng-chung who were not just colleagues but more importantly, dear friends. Their friendship, support, and encouragement have helped push me through my research.

I would like to thank my family for the steadfast faith and support which are indispensable throughout my studies.

Lastly, I would like to thank Daniele for his quiet patience and tolerance to my moods, and for never ceasing to be my source of strength and everything wonderful.

Amino acid code

Alanine	A
Arginine	R
Asparagine	N
Aspartic acid	D
Cysteine	C
Glutamine	Q
Glutamic acid	E
Glycine	G
Histidine	H
Isoleucine	I
Leucine	L
Lysine	K
Methionine	M
Phenylalanine	F
Proline	P
Serine	S
Threonine	T
Tryptophan	W
Tyrosine	Y
Valine	V

Abbreviations

ABTS	2,2'-azino-bis(3-ethylbenzothiazoline-6-sulphonic acid)
Amp	Ampicillin
APC	Allophycocyanin
APC	Antigen-presenting cell
ASGPR	Asialoglycoprotein
RBC	Red blood cell
bp	Base pair
BSA	Bovine serum albumin
CARD9	Caspase recruitment domain-containing protein 9
CD	Cluster of differentiation
Cd	Cyclodextrin
cDNA	Complementary DNA
CLR	C-type lectin receptor
CM	Cerebral malaria
ConA	Concanavalin A
CRD	Carbohydrate-recognition domain
DAMP	Danger-associated molecular pattern
DC	Dendritic cell
DC-SIGN	DC-specific ICAM3-grabbing nonintegrin
DCIR	Dendritic cell immunoreceptor
DNA	Deoxyribonucleic acid
dNTP	Deoxyribonucleotide triphosphate
DSAP	Disuccinimido adipate
DTT	Dithiothreitol
ECL	Enhanced chemiluminescence
ECM	Experimental cerebral malaria
EDC	<i>N</i> -ethyl- <i>N'</i> -(diethylaminopropyl)-carbodiimide
EDTA	Ethylenediaminetetraacetic acid
ELISA	Enzyme-linked immunosorbent assay
FACS	Fluorescent-activated cell sorting
FCS	Fetal calf serum
FITC	Fluorescein isothiocyanate

Foxp3	Forkhead/winged helix transcription factor 3
GPI	Glycosylphosphatidylinositol
HE	Hematoxylin and eosin stain
HRP	Horseradish peroxidase
ICAM-1	Intercellular adhesion molecule – 1
IFN	Interferon
Ig	Immunoglobulin
IL	Interleukin
i.p.	Intraperitoneal
IRF	Interferon regulatory factor
ITAM	Immunoreceptor tyrosine-based activation motif
ITIM	Immunoreceptor tyrosine-based inhibition motif
kDa	KiloDalton
KO	Knockout
LPS	Lipopolysaccharide
MCL	Macrophage-restricted C-type lectin
MGL	Macrophage galactose-type C-type lectin
MICL	Myeloid inhibitory C-type lectin
MHC-I/II	Major histocompatibility complex class I/II
MR	Mannose receptor
mRNA	Messenger RNA
NHS	<i>N</i> -hydroxysuccinimide
NK	Natural killer cell
NLR	NOD-like receptor
NOD	Nucleotide-binding oligomerization domain
OD _x	Optical density (x = wavelength in nm)
OT	Ovalbumin transgene
OVA	Ovalbumin
PAMP	Pathogen-associated molecular pattern
PbA	<i>Plasmodium berghei</i> ANKA
PBA	Phosphate buffered saline
PCR	Polymerase chain reaction
PerCP	Peridinin chlorophyll protein
PE	Phycoerythrin

pRBC	Parasitized red blood cells
PRR	Pattern-recognition receptor
RBC	Red blood cell
RLR	Rig-1-like receptor
RNA	Ribonucleic acid
ROS	Reactive oxygen species
rpm	Revolutions per minute
RT	Room temperature
SDS	Sodium dodecyl sulfate
SDS-PAGE	SDS polyacrylamide gel electrophoresis
SEM	Standard error of the mean
SHP	<i>Src</i> homology domain-containing phosphatase
Syk	Spleen tyrosine kinase
TAE	Tris-acetate-EDTA
TBE	Tris-borate-EDTA
TCR	T cell receptor
T _H	T helper cell
TLR	Toll-like receptor
TNF	Tumor necrosis factor
TNFR	TNF receptor
T _{reg}	Regulatory T cell

Table of Contents

1. Introduction

1.1 Immunity	1
1.1.1 Innate immunity	1
1.1.2 Dendritic cells	3
1.1.3 CLRs	4
1.1.3.1 Dectin 1	6
1.1.3.2 SIGNR3	7
1.1.3.3 DCIR	8
1.1.3.4 MICL	8
1.1.3.5 Clec12b	9
1.1.3.6 MGL	9
1.1.3.7 MCL	9
1.2 Lectin targeting	10
1.2.1 Multivalency in carbohydrate ligand presentation	10
1.2.2 Targeting lectins for induction of immune response	11
1.2.3 Targeting CLRs on DCs	12
1.3 CLRs in infection	14
1.4 Malaria	15
1.4.1 Severe malaria	17
1.4.2 Murine models of malaria	17
1.4.3 PRRs in cerebral malaria	19
1.5 Scope and limitation of the study	20

2. Materials and Methods

2.1 Materials	22
2.1.1 Instruments and special implements	22
2.1.2 Consumables	23
2.1.3 Chemicals	23
2.1.4 Bacterial strain, cell lines, mouse strains, and parasite strain	23
2.1.5 Materials for molecular biology and biochemistry methods	24
2.1.5.1 Antibodies, enzymes, reagents, kits, and supplements	24
2.1.5.2 Buffers and supplements	26
2.1.5.3 Vectors and primers	28
2.1.6 Materials for cell biology methods	28
2.1.6.1 Media and buffers	28
2.2 Methods	30
2.2.1 Molecular biology and biochemistry methods	30
2.2.1.1 mRNA extraction from murine splenic cells	30
2.2.1.2 cDNA synthesis	30
2.2.1.3 Polymerase Chain Reaction (PCR)	30
2.2.1.4 Cloning into pDrive vector	31
2.2.1.5 DNA gel electrophoresis	31
2.2.1.6 DNA concentration determination	32
2.2.1.7 Transformation into <i>E. coli</i> DH5- α competent cells	32
2.2.1.8 Plasmid purification	32
2.2.1.9 Analytical digestion	32

2.2.1.10 Ligation with pFuse	32
2.2.1.11 Protein purification	33
2.2.1.12 Protein concentration determination	33
2.2.1.13 SDS-PAGE, Western Blot	33
2.2.1.14 OVA-carbohydrate conjugation	34
2.2.2 Biophysical methods	35
2.2.2.1 Carbohydrate microarray printing	35
2.2.2.2 Detection of lectin-carbohydrate interactions	35
2.2.2.3 Determination of lectin-carbohydrate kinetics (SPR)	35
2.2.2.4 Quantification of carbohydrates conjugated on OVA	37
2.2.3 Cell biology methods	38
2.2.3.1 ELISA	38
2.2.3.2 ELISpot	38
2.2.3.3 Flow cytometry	39
2.2.3.4 CBA	39
2.2.3.5 Uptake studies in HepG2 cells	39
2.2.3.6 Apoptosis studies in HepG2 cells	40
2.2.3.7 Stimulation studies of PECs	41
2.2.3.8 Stable transfection into CHO cells	42
2.2.3.9 Fusion protein production in bioreactors	43
2.2.3.10 Isolation of spleen cell subsets	43
2.2.3.11 <i>In vitro</i> stimulation by OVA-carbohydrate conjugates	44
2.2.4 <i>In vivo</i> methods	44
2.2.4.1 Ethics statement	44
2.2.4.2 Adoptive transfer	44
2.2.4.3 Immunization	45
2.2.4.4 Stabilate preparation	45
2.2.4.5 PbA infection of mice	45
2.2.4.6 Brain histology	45
2.2.4.7 Determination of spleen and brain cell population	46
2.2.4.8 Binding studies with pRBCs	46
2.2.5 Statistical analysis	47
3. Results	
3.1 Lectin targeting	48
3.1.1 Affinity and kinetics of lectin-multivalent carbohydrate system interaction	48
3.1.2 Carbohydrate-functionalized dendrimers and liposomes in <i>in vitro</i> cellular uptake and drug delivery	50
3.1.3 Cell stimulation by carbohydrate-functionalized fiber meshes	53
3.1.4 Platform for CLR targeting for immune modulation	54
3.1.4.1 Production of CLR fusion proteins	54
3.1.4.2 Glycan microarray reveals novel ligands of CLRs	56
3.1.4.3 Carbohydrate modification of OVA leads to increased T _H 1 cytokine production <i>in vitro</i>	60
3.1.4.4 CLR targeting <i>in vivo</i> using OVA conjugates dampens humoral response	62
3.2 Role of CLRs in malaria	64
3.2.1 Role of DCIR in cerebral malaria	64

3.2.1.1 Genotyping of DCIR ^{-/-} mice	64
3.2.1.2 Reduced CM incidence in DCIR ^{-/-} mice	64
3.2.1.3 Reduced T cell sequestration in brain of DCIR ^{-/-} mice	65
3.2.1.4 Reduced TNF- α levels in serum of DCIR ^{-/-} mice	69
3.2.1.5 Modulated T cell activation in spleen of DCIR ^{-/-} mice	69
3.2.2 Role of SIGNR3 ^{-/-} in cerebral malaria	71
3.2.2.1 Genotyping of SIGNR3 ^{-/-} mice	71
3.2.2.2 Reduced CM incidence in SIGNR3 ^{-/-} mice	71
3.2.2.3 Similar T cell sequestration in brain of SIGNR3 ^{-/-} and wild-type mice	72
3.2.2.4 Decreased TNF- α but increased IFN- γ expression	72
3.2.2.5 Modulated spleen cell activation in SIGNR3 ^{-/-} mice	73
4. Discussion	
4.1 Lectin targeting	76
4.1.1 Multivalency enhances carbohydrate-lectin interaction	76
4.1.2 Multivalent carbohydrate presentation affords cell-specific targeting	77
4.1.3 CLR targeting modulates immune response	78
4.1.4 Platform for surveying CLR adjuvanticity	79
4.2 CLRs in cerebral malaria	82
4.3 Conclusion	86
Supplemental Information	
SI.1 Fusion protein sequences	89
SI.2 Genotyping protocols from the Consortium for Functional Glycomics	104
SI.3 List of microarray carbohydrates	106
Summary	108
Summary in German	109
List of publications	110
References	111

1. Introduction

1.1 The immune system

Immunity is a complex system of defense reactions of the body. The reactions are targeted against foreign substances, termed non-self antigens, and in certain instances, against self antigens of the host. The reaction itself may or may not be protective, but it is aimed essentially at maintaining the physiological integrity of the individual host. It is classified as either innate or adaptive immunity. Innate immunity encompasses many rapid defense mechanisms to infections and other challenges. The reaction features the rapid recognition of pathogen or tissue and the signaling to the cells of the adaptive immune system of the presence of danger. It consists of phagocytic cells, natural killer (NK) cells, complement, and cytokines such as interferons (IFNs) (1, 2). The adaptive immune response, on the other hand, is initiated more slowly, in days, and has two key features: specificity for antigens and a durable memory to elicit a protective immune response upon re-exposure to antigen. The response changes its quality and magnitude with each successive encounter with the antigen. Adaptive responses are either immunogenic, providing resistance to infection and cancer, or tolerogenic (3), leading to down-modulation of immune responses which is desirable in transplantation, autoimmunity, and allergy (4).

1.1.1 Innate immunity

Cells of the innate immune system use a variety of pattern recognition receptors (PRRs) to recognize molecular patterns shared between pathogens, for instance bacterial lipopolysaccharide (LPS) and other capsular polysaccharides, flagellin, or CpG motifs of bacterial DNA (1). PRRs are germline-encoded receptors recognizing pathogen-associated molecular patterns (PAMPs). Additionally, PRRs are involved in sensing endogenous 'danger' signals by recognizing danger-associated molecular patterns (DAMPs). They are predominantly expressed by cells of the innate immune system and have critical roles in host protection from invading pathogens. Upon recognition of PAMPs or DAMPs by the PRRs, an inflammatory response is triggered which is characterized by the secretion of cytokines, stimulation of antimicrobial peptides, recruitment of phagocytes, and/or pyroptotic cell death (5). The innate immune system constitutes multiple signaling pathways and exacting coordination among these pathways is critical to the efficient clearance of pathogens and other molecular threats. The main families of PRRs are the Toll-like receptors (TLRs), the NOD-

like receptors (NLRs), the RIG-1-like receptors (RLRs), and the the C-type lectin receptors (CLRs).

TLRs are the best characterized among the PRRs to date. TLRs recognize PAMPs from bacteria, fungi, parasites, and viruses such as the lipid-based bacterial cell wall component LPS, microbial protein component flagellin, and double-stranded nucleic acid CpG DNA (6). They also recognize DAMPs for instance heat shock proteins and extracellular protein fragments. Interaction of TLRs with the respective PAMPs or DAMPs initiates signaling cascades which activates transcription factors such as AP-1, NF- κ B and interferon regulatory factors (IRFs). This then results in crucial inflammatory responses, production of interferons, pro-inflammatory and effector cytokines, which help direct the adaptive immune response (7). NLRs are described as containing a tripartite domain organization with a conserved nucleotide-binding oligomerization domain (NACHT/NOD), leucine-rich repeats implicated in microbial sensing and an *N*-terminal effector region consisting of a protein-protein interaction domain such as the CARD, pyrin or BIR domain. The primary role of NLRs is to recognize cytoplasmic PAMPs and endogenous ‘danger’ signals, and consequently, induce immune responses. However, most of their ligands are not identified and only the function of few out of the 20 NLRs in mammals is known (8). RLRs are cytoplasmic RNA helicases crucial for antiviral responses of the host. Activation of RLRs such as RNA sensors RIG-1, MDA-5, and LGP2 lead to the stimulation of transcription factors which control the gene expression encoding of interferons and other cytokines (9). CLRs encompass a large family of proteins that bind to carbohydrate moieties of various pathogens. Their role in innate immunity will be further discussed below.

The host’s defense relies on a concerted action of both innate immunity and adaptive immunity. The innate immune system plays a crucial role in prompting the adaptive immunity to develop an effective and enduring immunological memory as it not only precedes but also enhances the adaptive immune system. This sophisticated and potent interplay between the innate and adaptive immunity needs to be instructed and regulated by antigen-presenting cells (APCs) (10). The effector cells of the immune system, mostly T and B lymphocytes, are tasked to eliminate infected cells and remove toxic substances. APCs are honed to initiate the development of lymphocyte activation. Dendritic cells (DCs), macrophages, and B lymphocytes are classified as professional APCs. They express major histocompatibility complex (MHC) molecules and exhibit mechanisms for effective antigen uptake and expression of costimulatory molecules that induce T cell activation (11, 12).

1.1.2 Dendritic cells

DCs are unique APCs because they are the strongest inducers of primary immune responses, thus permitting establishment of immunological memory. DCs are crucial for both recognition of a variety of antigens and presentation of antigen fragments to T cells thus inducing effector functions such as proliferation or cytokine secretion (13). Upon stimulation, DCs migrate to T cell areas of the draining lymph nodes, where they interact with T cells recognizing the MHC-presented peptides and induce them to proliferate. The antigens are broken down in the cytosol by the proteasome and enter the endoplasmic reticulum wherein peptides bind to newly formed MHC-I molecules for presentation on the cell surface. DCs are specialized to capture and process antigens *in vivo*, converting proteins to peptides that are presented on MHC class I and class II molecules and recognized by CD8⁺ and CD4⁺ T cells, respectively (1). For MHC-I presentation, short, intracellularly derived peptides are presented on the cell surface for recognition by CD8⁺ T cells. These peptides may stem from self proteins, tumor proteins, or from microbial pathogens which, in most cases, are viruses. DCs are capable of cross-presentation in which extracellular antigens are presented on MHC-I molecules enabling the initiation of CD8⁺ T cell responses (14). In this process, antigens are taken up by phagocytosis or receptor-mediated endocytosis into the cytosol which finally stimulates CD8⁺ cytotoxic T cells.

For MHC-II presentation to stimulate CD4⁺ T helper cells, the antigens are taken up also by phagocytosis or receptor-mediated endocytosis, but in this case, to endosomes wherein proteolysis follows. The peptides enter a vesicular compartment containing MHC-II molecules where they bind and are subsequently transported to the cell surface. Presentation of antigens by DCs alone does not suffice to induce effective T cell responses against pathogens.

In addition to antigen recognition, processing, and presentation, the expression of costimulatory molecules is a key function of DCs. These costimulatory molecules on the surface of DCs consist of members from the B7 family, TNF family, and intracellular adhesion molecules and they play key roles in activating T cells as well as the accurate homing of DCs before and after antigen recognition (15). CD4⁺ T cells play a prominent regulatory role among the cellular players of the immune system (13). They differentiate into different T cell lineages depending on the cytokine composition of the microenvironment. These lineages are highly specialized for each different pathogen. Initial recognition of these pathogens is mediated by the signaling of PRRs, which upon activation, trigger the expression of genes that provide the information necessary for priming of CD4⁺ T cells. The subsequent

expression of costimulatory molecules enhances T cell responses and production of cytokines that trigger the transcription of master transcription factors in CD4⁺ T cells and guide them into the T_H1, T_H2, T_H17 or regulatory T cell lineage (13).

1.1.3 C-type lectin receptors (CLRs)

DCs express many kinds of CLRs on their surface which contribute to antigen capture. CLRs are defined by their ability to bind carbohydrates usually in a Ca²⁺-dependent manner and the carbohydrate-binding activity is mediated by a conserved carbohydrate recognition domain (CRD) (16). CLRs recognize specific carbohydrate structures on the surface of pathogens, and also autoantigens (5). Based on their molecular structures, CLRs are divided into two families of transmembrane receptors, type I or type II, which have their *N* termini

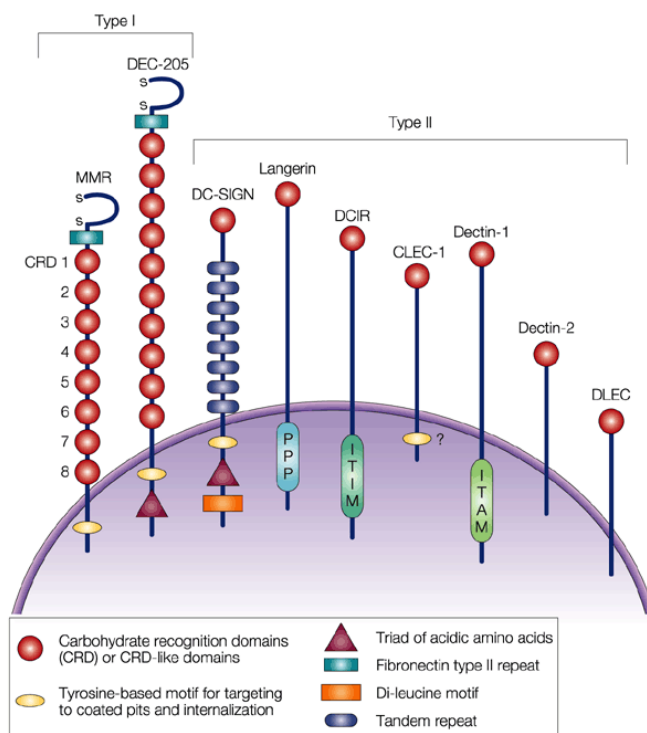


Figure 1. CLRs are divided into Type I or Type II family of transmembrane receptors. MR and DEC-205 are Type I CLRs, which have their *N* termini pointing outward from the cytoplasm and have multiple CRDs. Type II CLRs such as Dectin 1 and DCIR have their *N* termini pointing into the cytoplasm and have only one CRD at their carboxy-terminal extracellular domain. Figure taken from (5).

However, CLRs are not only involved in the recognition of glycostructures on pathogens, but also interact with glycans expressed on host cells, thus contributing to homeostatic regulation of the immune system. This is particularly important since the glycosylation pattern on the cell surface changes extensively during inflammatory processes

pointing outward or into the cytoplasm, respectively (Figure 1). One group is a type I transmembrane protein family with multiple CRDs, which includes the mannose receptor (MR, CD206), DEC-205 (CD205), and Endo 180 (CD280). The other group comprises type II transmembrane proteins with a single CRD, such as the macrophage galactose-type C-type lectin (MGL, CD301), DC-specific ICAM3-grabbing nonintegrin (DC-SIGN, CD209), langerin (CD207) and the members of the DCIR and the Dectin 1 family of lectins. Both groups of CLRs are capable of recognizing a variety of antigens, ranging from self-molecules to pathogens. Furthermore, CLRs have been reported to be exploited for targeted drug delivery.

and these alterations play a direct role in stimulation and/or modulation of T cell responses, i.e. modifying the inflammatory phenotype of the DC into an anti-inflammatory phenotype or shifting the T_{H1}/T_{H2} balance (13, 14). The two classes of glycans include the *N*-linked glycans (attached to asparagine residues of proteins) and the *O*-linked glycans (attached to serine or threonine residues). Changes in glycosyltransferase levels can lead to modifications in the core structure of *N*- or *O*-linked glycans (15). Activation of $CD4^+$ and $CD8^+$ T cells leads to changes in terminal *N*-glycan structures corresponding to an altered expression of sialyltransferases and galactosyltransferases responsible for the synthesis of these structures (16, 17).

CLR-triggered responses are shaped by an exquisitely controlled process integrating signals from the activating or inhibitory function of each receptor. These complex interactions, which regulate the quality as well as the magnitude of the ultimate response, are critically dependent on two short, loosely conserved motifs found in the intracellular domain of various signaling proteins. These motifs, termed immunoreceptor tyrosine-based activation motif (ITAM) or immunoreceptor tyrosine-based inhibitory motif (ITIM), provide the basis for two contrasting signaling elements that dictate the control of cellular activation within the immune system. The most crucial intracellular signaling molecule in CLR signaling belongs to the spleen tyrosine kinase (Syk)-family which operate in the proximal intracellular signaling pathways of cells of the innate immune system. SYK is a non-receptor protein tyrosine kinase that is widely expressed in hematopoietic cells (18, 19). CLR coupling to SYK can be indirect through one or more copies of the ITAM, whose sequence is defined as $Y_{xx}L/I_{(x_6-8)}Y_{xx}L/I$ (where x denotes any amino acid), or direct via a single tyrosine-based motif, termed hemITAM, in the cytoplasmic domains of the CLRs. It couples the activated immunoreceptors to downstream signaling events that mediate diverse cellular responses, including proliferation, differentiation, and phagocytosis. ITAM-containing CLRs include Dectin 2, hBDCA2, mDCAR, mDCAR1, Mincle, and MDL1, while those bearing the hemITAM domain are Dectin 1, CLEC2, DNGR1, and SIGNR3. The inhibitory pathway is initiated through phosphorylation of the ITIMs, defined by the sequence of amino acids $I/V/L/SxY_{xx}L/V$ (where x denotes any amino acid), and as a consequence, negatively regulating signaling through the recruitment of phosphatases Src homology 2-containing protein tyrosine phosphatase 1 and 2 (SHP-1 and SHP-2, respectively) (19). CLRs classified in this group are DCIR, MICL, and Clec12b. On the other hand, there are CLRs which do not have either ITIM or ITAM. They are generally involved in the endocytic process and facilitate antigen presentation to T cells. CLRs which do not have ITIMs/ITAMs are MR, DEC-205,

DC-SIGN, SIGNR1, Langerin, hMGL, mMGL1, mMGL2, CLEC-1, DCAL-1, MCL, LOX-1, and LSECTin (20-22).

The primary focus of this thesis is on CLRs expressed by myeloid cells (Figure 2), which also represent CLRs with different signaling motifs: hemITAM (Dectin 1 and SIGNR3), ITIM (DCIR, MICL, and Clec12b), and ITIM/ITAM-independent (MGL1 and MCL).

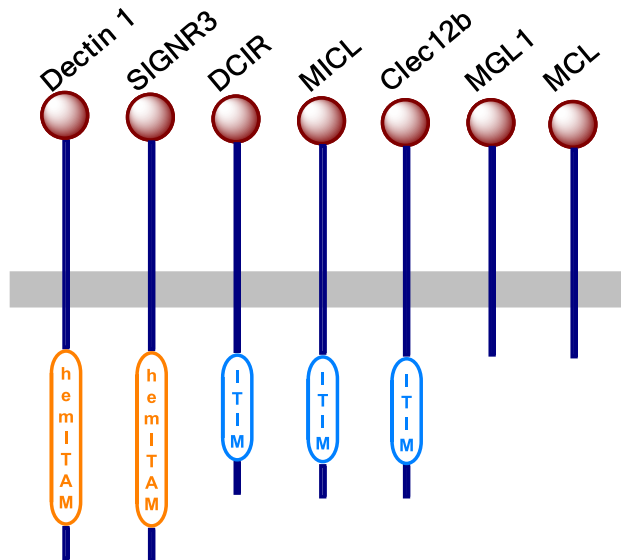


Figure 2. Myeloid CLRs investigated in this thesis. Dectin 1 and SIGNR3 contain hemITAM, whereas DCIR, MICL, and Clec12b have ITIM. MGL1 and MCL neither have ITAM nor ITIM.

1.1.3.1 Dectin 1

Among the CLRs investigated in this study, the best characterized is Dectin 1 (Clec7a). Mouse Dectin 1 is expressed by DCs, monocytes, macrophages, neutrophils and a subset of $\gamma\delta$ T cells (23, 24). In humans, Dectin 1 is also expressed by the same cell subsets and, additionally, by B cells, eosinophils, and mast cells (25-27). Dectin 1 is the archetype of hemITAM-bearing CLRs (Figure 3) (28).

Dectin 1 has an atypical CRD and binding to its ligand, β -1,3-linked glucans in the cell wall of fungi, some bacteria, and

plants, is Ca^{2+} -independent (29, 30). Additionally, Dectin 1 can recognize unidentified endogenous T cell and mycobacterial ligands (31). Upon binding to its ligands, Dectin 1 activates a range of cellular responses including phagocytosis, reactive oxygen species (ROS) production and cytokine secretion via multiple signaling pathways. The most prominent Dectin 1 signaling pathway is the Syk-Caspase recruitment domain-containing protein 9 (CARD9) pathway, which leads to the activation of the canonical NF κ B subunits, c-Rel and p65, and, subsequently, the production of pro-IL-1 β , IL-6, IL-10, IL-23 and TNF- α (32). Dectin 1 can also activate the non-canonical NF κ B subunit RelB in a NIK-dependent pathway, a feature unique to itself (33). This pathway directs the modulation of cytokine production via the development of inactive RelB-p65 dimers, which are important for inducing T_H1/T_H17 cytokine profiles through increased expression of cytokines IL-1 β and IL-12p40, and the modulation of NF- κ B gene transcription, thereby reducing IL-1 β and IL-12p40, while increasing the expression of CCL17 and CCL22 (17). Dectin 1 also activates the

kinase Raf-1, independent of Syk signaling, which regulates NF κ B gene expression. The activation of Raf-1 results in an increase in p65 transcriptional activity and reduction of RelB activity through the formation of inactive RelB-p65 dimers. Syk-dependent Dectin 1 signaling activates the NLRP3 inflammasome by ROS mediation which leads to the production of bioactive IL-1 β (34, 35). Inflammasome activation by Dectin 1 might play a role in the balance between tolerance to commensal flora and inflammation at mucosal surfaces as demonstrated by investigating the invasion of *Candida albicans* (36). Additionally, through the Ca²⁺-mediated NFAT pathway, Dectin 1 can induce the production of IL-2 and IL-10 by macrophages and DCs stimulated with *C. albicans* or zymosan, a fungal particle found in *Saccharomyces cerevisiae* (37).

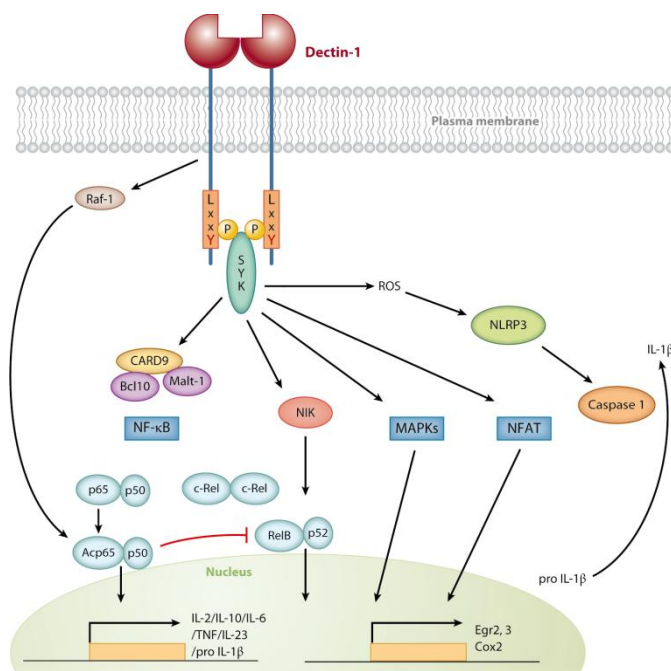


Figure 3. Dectin 1 as a model hemITAM-coupled receptor. Upon activation of Dectin 1 by ligand recognition, Syk is recruited through a phosphotyrosine residue in the hemITAM motif. Syk stimulates ROS production and leads to the activation of the NALP3 inflammasome, and consequently, to the processing of pro-IL-1 β . Syk is also involved in the activation of NF- κ B at different levels. Dectin 1 activation also precedes Syk-independent activation of Raf-1, resulting in acetylation of p65/p50 and modulation of NF- κ B. Figure taken from (43).

As in the case with Dectin 1, SIGNR3 signaling is dependent on Syk and on the tyrosine residue in the YxxL motif, that it is proposed that SIGNR3 possesses hemITAM (42). Additionally, it can mediate endocytosis and degradation of glycoprotein ligands (38).

1.1.3.2 SIGNR3

DC-specific ICAM3-grabbing nonintegrin (DC-SIGN) is an adhesion molecule that facilitates attachment of T cells to DCs and was identified as a pathogen-binding receptor (38). DC-SIGN mediates adhesion with T cells by acting to stabilize the contact region between DCs and T cells (39). It captures HIV-1 by binding to the HIV-1 envelope glycoprotein gp120 and facilitates its transport to T cells (40).

SIGNR3 is one mouse homologue that closely resembles the human DC-SIGN. Both SIGNR3 and DC-SIGN are expressed by monocytes, DCs, and macrophages (41). Similar to DC-SIGN, SIGNR3 binds to high mannose and fucose-terminated glycans.

1.1.3.3 Dendritic cell immunoreceptor (DCIR)

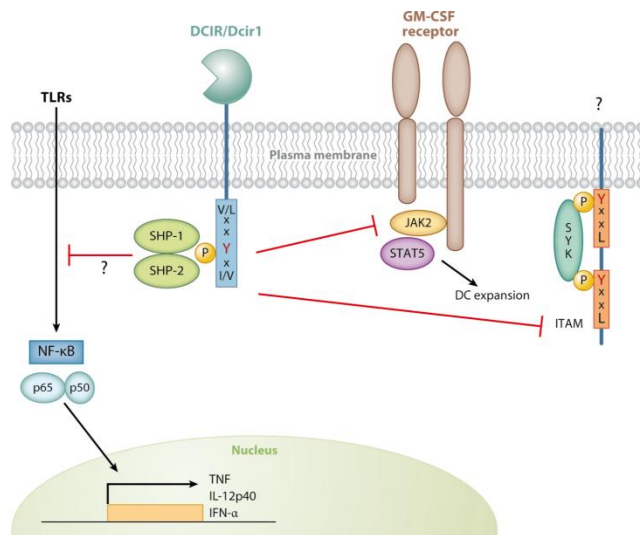


Figure 4. DCIR/DCIR1 as model ITIM-bearing CLR. Phosphorylation of the tyrosine in the ITIM allows for binding of SHP-1 and SHP-2 phosphatases. ITIM signaling inhibits signals that are activated by ITAM. Figure taken from (43).

Dendritic cell immunoreceptor (DCIR, Clec4a) signaling is mediated through ITIM (Figure 4) and it is mainly expressed by DCs, but also by macrophages, monocytes, and B cells (43, 44). Human DCIR has four homologs in mouse which are also expressed by the same cell types and, additionally, by neutrophils (43, 45). In murine rheumatoid models, DCIR-deficient mice exhibited increased numbers of DCs and developed autoimmunity (46). Human DCIR was found to be involved in CD8⁺

T cell cross-priming in the spleen (47) and was exploited for DC targeting using DCIR-specific antibodies (48). Ligands for DCIR have not yet been identified. One of the possible roles of mouse DCIR is to regulate DC expansion, and hence, maintaining homeostasis, as demonstrated by the high degree of STAT5 phosphorylation as a result of cultivation in GM-CSF among bone marrow-derived DCs from DCIR1^{-/-} mice (46). ITIM signaling essentially inhibits signaling induced by ITAM. The phosphotyrosine residue present in the human DCIR ITIM associates with phosphorylated SHP-1 and nonphosphorylated SHP-2 (49). In addition, DCIR inhibits B cell receptor (BCR) signaling after coligation of BCR and a chimeric Fcγ receptor IIB containing the cytoplasmic portion of DCIR (44).

1.1.3.4 Myeloid inhibitory C-type lectin (MICAL)

Human myeloid inhibitory C-type lectin receptor (MICAL, Clec12a, DCAL-2, KLRL-1, CLL-1) is predominantly expressed by granulocytes, monocytes, macrophages and DCs (50-52). Mouse MICAL is expressed by the same cell subsets and also by B cells, T cells in peripheral blood, and NK cells in the bone marrow (53, 54). It recognizes an endogenous ligand present in the bone marrow, thymus, heart, spleen, and kidney which suggests that it plays a role in homeostasis (54). It contains an ITIM which can inhibit cell activation and is capable of recruiting SHP-1 and SHP-2, but not SHIP-1 (50, 51).

1.1.3.5 Clec12b

Clec12b, which belongs to the Dectin 1 cluster, is a poorly characterized CLR. It is broadly expressed by cells of myeloid and lymphocyte lineage (55). It contains an ITIM and its inhibiting capacity is demonstrated via recruitment of the phosphatases SHP-1 and SHP-2 (56). This characteristic suggests that it might be capable of suppressing the activity of monocyte-derived cells in inflammation and the identity of its ligand would elucidate its biological role. However, no ligand has yet been identified.

1.1.3.6 Macrophage galactose-like lectin (MGL)

The human macrophage galactose-like lectin (MGL) is expressed by DCs and macrophages (57, 58) and it has neither ITAM nor ITIM (42). Its CRD recognizes *N*-acetylgalactosamine (GalNAc, Tn) residues on glycoproteins and glycolipids (59). MGL recognizes antigens from different pathogens (60-63) and is involved in the maintenance of homeostasis (64). In cancer, MGL has been shown to play a role in enabling DCs to sense glycosylation (65) and in recognizing tumor-associated glycoproteins (66). There are two murine homologues of MGL, MGL1 and MGL2 (67, 68) which are also expressed by the same cell types as the human MGL (69). MGL1 is highly specific for Lewis X and Lewis A structures, while MGL2, similar to human MGL, binds to GalNAc and additionally to galactose (70). MGL1 was demonstrated to be engaged in immune regulation (71), tumor recognition (72, 73), and apoptotic cell removal during embryogenesis (74, 75). Nevertheless, the mechanism and signaling pathways underlying MGL1 involvement are still to be elucidated. On the other hand, MGL2 promotes both MHC-I and MHC-II antigen presentation in DCs (76).

1.1.3.7 Macrophage-restricted C-type lectin (MCL)

Macrophage-restricted C-type lectin (MCL, Clec4d, Clecsf8), a member of the Dectin 2 CLR cluster, is primarily expressed by neutrophils and monocytes in both human and mouse. Similar to MGL, MCL does not contain ITIM or ITAM. Unlike the other CLRs which contain the conserved residues necessary for carbohydrate interactions, MCL only possesses the residues required for Ca²⁺ coordination but not the amino acid triplet motif, EPN, that is generally associated with carbohydrate recognition and binding (20). Nonetheless, no carbohydrate ligand has yet been identified to bind to MCL. It is also not known whether MCL is associated with any adaptor molecule. However, it was reported to play a role in

stimulating cellular activation through its capability to induce phagocytosis, cytokine production, and respiratory burst (77).

1.2 Lectin targeting

Carbohydrates play an important role in many biological systems by virtue of the lectins which recognize them. Carbohydrate-lectin interactions are involved in expansively diverse biological processes which include embryonic development, intracellular trafficking, cell-cell recognition, cell activation, cell adhesion, cell homing, endocytosis, phagocytosis, inflammation, tumor cell metastasis, and apoptosis (78). Targeting of lectins through the use of their ligands can be employed to induce an immune response. This strategy has been found to be lucrative in understanding the role of carbohydrate-lectin interactions. It sheds light into the influence of such interactions in mediating signaling and antigen delivery, in understanding the role of lectins, and more interestingly, in surveying the potential of lectins in immunotherapy.

1.2.1 Multivalency in carbohydrate ligand presentation

One main drawback for investigating carbohydrate-lectin interactions is the weak affinity of the binding which will require enhanced tools to analyze carbohydrate-lectin interplay. Carbohydrate-lectin interactions are relatively weak with dissociation constants often in the micromolar to millimolar range. While affinity pertains to the apparent binding of the ligand to its lectin, avidity is used to take into account multivalent interactions. Detection and read-out of binding can be improved by multivalent probes since they amplify the weak interactions and reinforce the potency of carbohydrate ligands.

Detailed investigation of multivalent carbohydrate-protein interactions has gained increasing interest in glycosciences and thus a great deal of research has been devoted to the design and synthesis of chemical tools, such as multivalent glycan presentation of various architectures (Figure 5). These multivalent carbohydrate-based tools come in different architectures such as quantum dots, dendrimers, polymers, liposomes, and other types of nanoparticles as well as carbohydrates built on templates of cyclodextrin (Cd) and calixarene (79-82), and possess unique properties, e.g. autofluorescence or self-assembly capabilities. These multivalent probes can be functionalized with carbohydrates with principal consideration on valency, the spatial arrangement of the target lectin's multiple binding sites, and the response to external stimuli. With these devices in hand, a number of assays and biophysical methods including, but not limited to, surface plasmon resonance (SPR) (83),

enzyme-linked lectin assays (ELLA) (84), hemagglutination inhibition assay (HIA) (85) and isothermal titration calorimetry (ITC) (86) can be utilized to probe carbohydrate–lectin interactions. It is known that the binding affinity of a ligand to the lectin is influenced by factors such as size, spatial assembly and/or valency of the ligands. Additionally, it is important to optimize the presentation of the sugar ligand(s) to further understand the mechanistic details of a specific binding event and to enhance the affinity of binding.

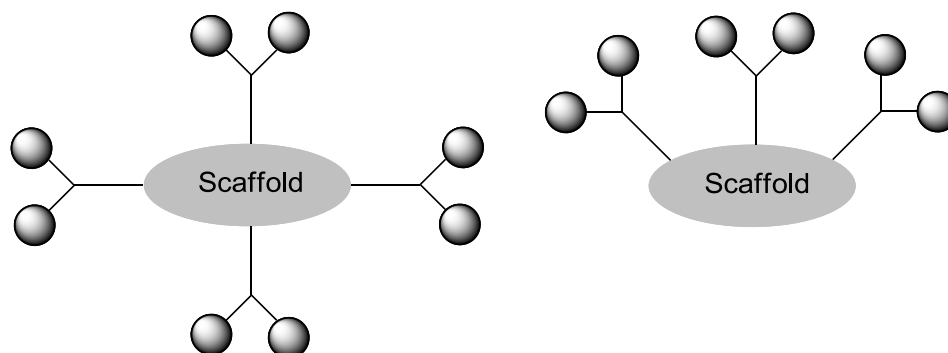


Figure 5. Representative architectural templates of multivalent carbohydrate structures. The scaffold represents the carrier system (e.g. liposomes, quantum dots). It can also bear dyes or tags which are used to enable tracking of the whole structure or for immobilization, depending on the method used to examine the interaction. Grey balls represent carbohydrates.

1.2.2 Targeting lectins for induction of immune response

Carbohydrate-based therapies hold great promise and glycan binding receptors have been targeted for cell-specific drug and gene delivery (79, 87, 88). Most carbohydrate-based targeting strategies have exploited the lectin-mediated endocytotic uptake of carbohydrate-containing drug delivery systems. Specific binding of isolated and synthetic carbohydrates to endogenous lectins on cell surfaces resulted in cell-specific binding and uptake (89). Upon internalization, the drug is then released from the carrier to target a specific subcellular organelle and foster a biological activity (90). Several endogenous ligands have been employed to study the design and development of carbohydrate-based delivery systems, namely the asialoglycoprotein receptor (ASGPR) (90-92), galectins (galectin 1, galectin 3) (93, 94), selectins (E-selectin, L-selectin) (95, 96), mannose receptor (MR, mannose-binding protein (MBP)) (97), and hyaluronic acid receptors (CD44, receptor for hyaluronan-mediated motility (RHAMM)) (98).

ASGPR is a CLR that is a particularly attractive target for liver-specific drug delivery since it is expressed exclusively on parenchymal hepatocytes (91). It is the most widely used in targeting studies as it serves as the prototype of CLRs. The main function of ASGPR is to maintain homeostasis of serum glycoprotein levels by binding and uptake of desialylated

(galactosyl-terminated) glycoproteins (99). Human ASGPR consists of two subunits, H1 and H2. The H1 subunit mediates Ca^{2+} -dependent galactose/GalNAc recognition whereas the H2 subunit is responsible for functional configuration (100). Recent studies describe the use of natural ASGPR ligands or synthetic ligands with galactosylated cholesterol, glycolipids, or polymers (101-103). Specific targeting of hepatocytes has enabled gene delivery (104), for example using galactosylated DNA lipid nanocapsules as the vector (105). Binding of galactose and GalNAc to ASGPR strongly depends on the valency of the ligands with a binding hierarchy increasing from monoantennary to tetraantennary ligands (106). It is also known that ASGPR exhibits a 10–50 fold higher affinity to GalNAc compared to galactose residues (107). Furthermore, the distance between the terminal galactose/GalNAc residues is important for optimal spatial orientation resulting in maximal binding to the heterooligomeric ASGPR (81). The other CLR which is also exploited for targeting is MR. MR is a transmembrane CLR which contains eight CRDs. Surface-bound MR is highly expressed by DCs as well as macrophages and hepatic endothelial cells. It is involved in mediating endocytosis and processing of glycoprotein antigens that expose mannose and fucose residues, for presentation of antigen-derived peptides by MHC-II molecules. Drug delivery systems targeting MR may have therapeutic application in macrophage-mediated diseases. MR-mediated interactions have been extensively studied using different mannose-functionalized delivery systems such as liposomes and nanoparticles to deliver drugs, immunomodulators, or oligonucleotides to macrophages via MR-mediated interactions (97, 108).

1.2.3 Targeting CLRs on DCs

The intrinsic facility of DCs to recognize and take up antigens confers a valuable tool for targeted delivery of antigens. Additionally, the strategy can be carefully designed as to enable a restricted MHC-I or MHC-II presentation. For MHC-I presentation, antigens or DNA constructs encoding antigens are directly delivered into the cytosol. On the other hand, targeting of antigens to DC via its surface receptors will result in MHC-II presentation (109). Still, it is feasible to deliver these antigens to the MHC-I pathway via cross-presentation (109, 110).

Targeting CLRs on DCs has also been studied to exploit the potential influence CLRs have on the induction of immunity or tolerance (111). The most widely used strategy is the use of antibodies to target CLRs. Antigens attached to antibodies are used as a tool with the advantage that the antibodies are very specific towards their respective CLR. DEC-205 has been the most probed CLR and numerous studies have outlined its use in targeting of antigens

to human DCs (111-113). Targeting of antigens to the DEC-205 receptor increased the efficiency of T cell activation upon vaccination (114). Ligands highly specific for MR elicited an enhanced humoral response and T cell immunity both *in vitro* and *in vivo* when administered in combination with endotoxins (115). Targeting MICL on DCs to deliver an antigen was found to be an effective strategy to foster humoral responses (53). Specific delivery of antigens to Clec9a using ovalbumin (OVA) antibody conjugates developed potent humoral immunity, CD4⁺ T cell proliferation, and cross-presentation to T cells (116-118). Targeting DCIR using anti-DCIR2 antibody on human plasmacytoid DCs resulted in more efficient antigen presentation and impeded with IFN- γ production (119). Nevertheless, the use of antibodies to target CLR has posed issues in terms of tissue penetration, which is hindered because of the antibody's bulkiness, as well as Fc receptor binding, which can be induced by the Fc part (111). In order to circumvent the problems posed by the size of antibodies, the smaller single chain Fv antibody (scFv) has been used as an alternative. Targeting DEC-205 using scFv was found to enhance antigen presentation as well as T cell responses (113, 120). Additionally, murine antibodies also incur the disadvantages of having a short half-life in serum and the ability to trigger unwanted anti-antibody immune responses (121). Humanized antibodies were developed to address these shortcomings. Humanized antibodies consist of the variable domains of a rodent antibody attached to the constant fragments of human antibodies or in a more sophisticated design, the antigen-binding loops of the rodent antibody are incorporated into a human antibody (122). The latter strategy was applied to generate humanized anti-DC-SIGN to target DCs and naïve and recall T cell responses were effectively induced (123). Targeting of CLR has also been shown to induce tolerance. Delivery of type 1 diabetes antigen to DEC-205 has resulted in tolerance of reactive CD8⁺ T cells in diabetic NOD mice (124). In another study, T_{reg} proliferation was boosted upon targeting CD8 α ⁻ cells by anti-DCIR antibodies (125).

Targeting CLR using their carbohydrate ligands has also been surveyed since this approach affords the means to overcome the problems prompted by the use of antibodies (111). Antigens can be modified with carbohydrate ligands instead of antibodies to target CLR. This provides insight into the role of CLR in mediating signaling upon encountering antigens in physiological conditions. Moreover, some CLR bind to the same carbohydrate which can enable targeting of multiple CLR at the same time. Nanoparticles have also been used as targeting carriers systems. One notable advantage that nanoparticles have is the versatility in their sizes which can take advantage of the mechanisms of endocytosis that direct their entry into DCs. Protein antigen functionalized on particles of 1–5 μm is cross-

presented at significantly higher levels compared with soluble protein (126). Macropinocytosis is employed to internalize smaller solutes such as macromolecules and particularly small nanoparticles (<50 nm) (127); whereas phagocytosis takes place to allow entry for larger nanoparticles (>500 nm) (128). These carriers can deliver antigens to DCs by the natural propensity for DCs to take up matter or by directly targeting CLR ligands (129). Thus, CLRs are promising targets for multivalent presentations of carbohydrate ligand for immune modulation.

1.3 CLRs in infection

CLRs have been found to interact with microbial pathogens and although some of these interactions do not influence the immune response directed towards the pathogen, still a considerable number have been implicated to orchestrate innate responses to microbial pathogens. The CLRs DCIR, Dectin 1, Dectin 2, MR, DC-SIGN, the mouse homologs of DC-SIGN (SIGNR1 and SIGNR3), and Mincle are not only involved in serum glycoprotein homeostasis, cellular trafficking and DC-T cell interaction, but also recognize a number of microorganisms that exploit these interactions to generate immune induction, suppression, or deviation in the infected host (42, 130).

DCIR plays a protective role by reducing the inflammatory response induced by the mosquito-born Chikungunya virus (131). It also binds to the human immunodeficiency virus 1 (HIV-1) resulting in viral proliferation thereby promoting infection (132). SIGNR3 has been identified to bind to the virus HIV-1 envelope glycoprotein gp120 (40). DC-SIGN is utilized by HIV-1 to escape immunosurveillance and to promote its survival by hiding within DCs and by reducing their antigen-presenting capacities (40, 133), which is also the case for the bacterium *Mycobacterium tuberculosis* upon targeting DC-SIGN and MR (134-136). Additionally, DC-SIGN interacts with *M. tuberculosis* bacilli and its mycobacterial surface glycan, mannosylated lipoarabinomannan (ManLam), to induce the production of pro-inflammatory cytokine TNF- α (137). *M. tuberculosis* is also recognized by Dectin 1 and Mincle, but unlike the interaction between the bacteria and DC-SIGN or MR, the host is not exploited by the pathogen. Dectin 1 is not required for host defense against *M. tuberculosis* (138), and it is mainly Mincle which induces a CARD9-dependent protection against *M. tuberculosis* (139, 140). Binding of *Helicobacter pylori* to DC-SIGN blocks skewing of the naïve T cells towards T_H1 cells, preventing *H. pylori* from being eliminated by the host immune response (141). Fungal pathogens such as *C. albicans* are recognized by CLRs Dectin 1, Dectin 2, MR, DC-SIGN, SIGNR1, and Mincle. More importantly, the initiation of the

innate response to *Candida* infection is regulated by CARD9 by controlling the signaling of Dectin 1, the receptor for recognizing β -1,3-glucans in cell walls in nearly all fungi, a process which is independent of TLR signaling pathways (142). Furthermore, mice deficient in Dectin 1 were shown to be more susceptible to chemically induced colitis as a result of altered immunity to commensal fungi in the gut (143). These studies demonstrate the key role that CLRs play to employ a versatile system in order to initiate varied outcomes during infections.

Such a role is not only evident in viral, bacterial, and fungal interactions, but in parasitic recognition as well (144). MR participates in the recognition of different *Leishmania* species (*donovani* and *amazonensis*) and its expression is up-regulated during the initial stages of infection (145, 146). MGL1 and MGL2 were found to be novel markers for type II cytokine dependent alternatively activated macrophages in the chronic stage of infection with *Trypanosoma brucei* (147). On the other hand, the interaction of MR with *T. cruzi* is a mechanism exploited by the parasite to evade the immune response (148). In murine malaria infection, Clec9a⁺DCs were demonstrated to mediate the development of cerebral malaria. Ablation of Clec9a⁺DCs resulted in complete resistance to the symptom and reduction of CD8⁺ T cell sequestration, and its activated phenotype, in the brain (149). The helminth *Schistosoma mansoni* interacts with DC-SIGN and thereby causes a shift towards a T_H2 response, which is crucial for the persistence of this pathogen (60). Binding of MR to the glycosylated excretory/secretory materials released by the schistosome larvae, a process crucial for the infection of the host, modulates the production of IFN- γ by CD4⁺ T cells (150). Hence, these studies indicate the importance of CLRs in innate immunity during microbial infections.

1.4 Malaria

Malaria is one of the main global causes of death from infectious diseases, resulting in more than 200 million clinical cases and 655,000 deaths per year with 86% of those infected are children below three years of age (151). It is caused by parasites classified under the protozoan genus *Plasmodium*. Humans can be infected with any of the following species: *P. falciparum*, *P. vivax*, *P. ovale*, *P. knowlsei*, and *P. malariae*. The parasite is primarily transmitted through the bite of an infected female *Anopheles* mosquito injecting sporozoites which then migrate into the liver. Infection can also occur through blood transfusion and congenital transmission. During the asymptomatic pre-blood phase inside the parenchymal hepatocytes, the sporozoites undergo a transformation which gives rise to thousands of merozoites. Budding of merozoite-filled vesicles with cell membranes derived from

hepatocytes, termed merozoites, allow for the migration of parasites into the bloodstream (152). Mature merozoites are released into the bloodstream wherein they infect red blood cells (RBCs) and initiate the blood stage. The infecting merozoite forms a vacuole and changes into a uninucleated ring form whereupon maturation, divides into a multinucleated schizont. Upon schizont rupture, merozoites are yet again released into the bloodstream and infect naïve RBCs. Additionally in *P. falciparum* infection, parasitized RBCs (pRBCs) adhere to the endothelium and the placenta to evade clearance of pRBCs by the spleen (153). During the blood stage, a fraction of merozoites will develop into gametocytes which will be taken up by the *Anopheles* mosquitoes, clinching the sexual stage of the *Plasmodium* life cycle (Figure 6) (154). The pathology of malaria is exclusively due to the blood stage. Symptoms usually occur within 10–15 days after infection. The majority of patients experience fever, chills, headaches, and diaphoresis. Other symptoms include dizziness, nausea, abdominal pain, vomiting, mild diarrhea, and dry cough (155).

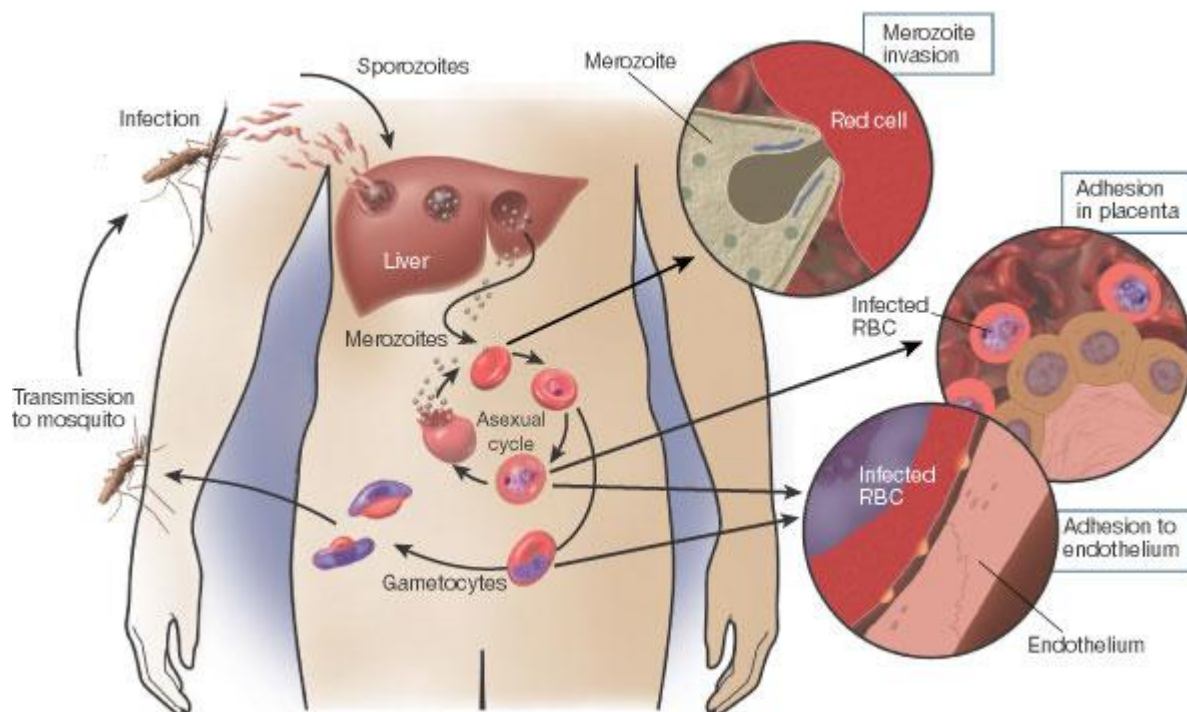


Figure 6. The *Plasmodium* life cycle. The events leading up to the formation of gametocytes shape the severity of malaria. The *Anopheles* mosquito injects sporozoites into the host transmitted through the blood to the liver where they invade hepatocytes. The sporozoites are transformed into merozoites which then mature into schizonts. Merozoites facilitate passage of merozoites into the bloodstream. Thus far, the infection is non-pathogenic and clinically silent. The schizonts rupture releasing merozoites which infect naïve RBCs. The pathology of the disease occurs during the blood stage. In *P. falciparum* infection, parasitized RBCs infected with *P. falciparum* binds to the endothelium or placenta to escape spleen-dependent clearance. Figure taken from (153).

1.4.1 Severe malaria

The vast majority of severe malaria cases and deaths are caused by *P. falciparum*, which is endemic mainly in sub-Saharan Africa and in tropical regions of the world. *P. vivax* and *P. ovale* also induce severe symptoms, but the cases are rare. Severe pathology results in grave complications, debilitating relapses, and even death (156, 157). The World Health Organization (WHO) laid out the criteria for severe malaria based on clinical and epidemiological studies. The major symptoms of severe malaria include cerebral malaria (CM), severe anemia, pulmonary edema, metabolic acidosis, hypoglycemia, acute renal failure, and impaired circulation (153). Patients can exhibit one or more of these symptoms, which can develop rapidly and can lead to death within mere hours or days.

CM is the most acute manifestation of severe malaria which occurs from infection with *P. falciparum*. The fatality rate ranges from 9% among children in Africa to 15% in adults in Southeast Asia (158, 159). Metabolic acidosis conveys a higher risk of death, nonetheless, CM accounts for a significant proportion of mortality, and even for those who survive, there is still a high likelihood that they suffer from neurological defects. CM involves heightened encephalopathy characterized by impaired consciousness with fever, convulsions with neurological consequences, and eventually an unrousable coma. The common feature is vascular sequestration of infected erythrocytes into the brain, though perivascular hemorrhages and immune cell infiltration within brain micro-vessels are also fairly observed (160, 161). If left untreated, CM is fatal within 24-74 hours upon the onset of the symptoms (162).

1.4.2 Murine models of malaria

Information on the pathogenesis of severe malaria cannot be solely discerned from clinical studies. An investigation that is limited to pre-mortem studies in patients cannot meet the challenges that abound as *Plasmodium* species have developed sophisticated strategies to avert the immune response of the host. A detailed investigation into the pathogenesis using human subjects is to a large extent not ethically, financially, and practically possible (163). Furthermore, *in vitro* studies also have limitations particularly in interpreting the characteristics of the host immune cells. Animal models for investigating the pathogenesis caused by malaria infection are useful because these allow for a careful scrutiny of specific processes through the range and degree of methodical findings provided by the use of animals. In so doing, it is important to choose the particular experimental animal with the appropriate *Plasmodium* species which mimics the specific human disease pattern (164). The significant

advantage of using murine models is that there are four *Plasmodium* species which can be used namely *P. yoelii*, *P. chabaudi*, *P. vinckei*, and *P. berghei* with different strains each of which demonstrates varying pathogenicity. Moreover, inbred and congenic mouse strains are available with well-defined MHC haplotypes as well as an immune system bearing well-defined defective components. The nonlethal strain *P. yoelii* 17XNL is used to survey the immune mechanisms of protection while the lethal *P. yoelii* YM strain is used to test vaccine candidates. *P. chabaudi* and *P. vinckei* strains are used to investigate immunity and susceptibility to drugs (165).

The *P. berghei* ANKA (PbA) infection of mice is an established model of experimental cerebral malaria (ECM) (165, 166). PbA infects reticulocytes and mature red blood cells (RBCs) in C57BL/6 and CBA mice which results in the manifestation of ECM exhibiting fatal cerebral pathology with clinical signs such as ataxia, respiratory distress, and coma (167). Symptoms shared with its human counterpart include neurological complications (convulsions, paralysis, and coma), loss of vascular cell integrity, congestion of microvessels with infected erythrocytes, hemorrhages, mononuclear cell adherence to the vascular endothelium, and pro-inflammatory cytokine expression (168). The period between infection and onset of clinical signs occur between 5-10 days post-infection, the range of which is attributable to the infection dose, the genetic background of the host, and the specific clone of the parasite (167). Once the clinical signs become evident, the condition of the infected mice deteriorates rapidly with death ensuing within 4-5 hours after the onset of the neurological symptoms. Blood brain barrier disruption, characterized by vascular leakage involving the cortex, cerebellum, and olfactory bulb, is observed in PbA-infected mice (169, 170) with accumulation of pRBCs within blood vessels (171). Cognitive dysfunction, as an effect of PbA infection, is characterized by impaired visual memory, which is directly correlated with haemorrhage and inflammation as well as microglial activation (172). Essentially, the accumulation of monocytes and macrophages and the activation of brain mononuclear cells, including astrocytes and microglial cells, are considered key features of ECM (173-175).

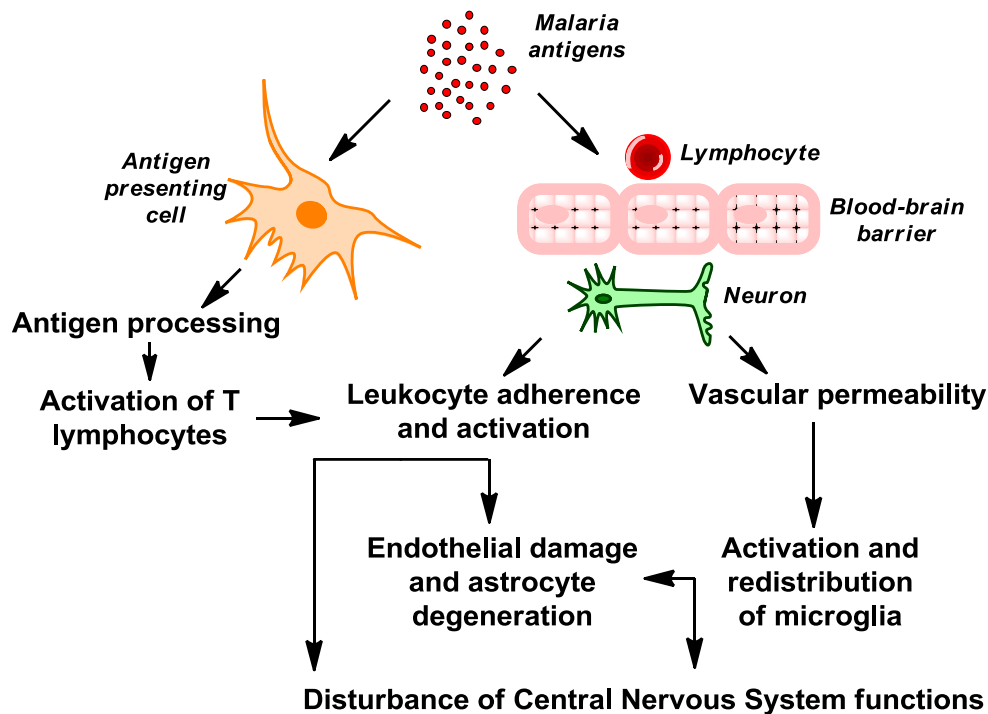


Figure 7. Course of events leading to the development of cerebral malaria. Malaria antigens are processed and presented to T cells by APCs. Activated T cells produce cytokines which may enhance the events occurring at the vasculature, increasing the permeability of the blood brain barrier and stimulate the endothelium to up-regulate the expression of adhesion molecules such as ICAM-1. This disturbance enables the malfunctioning of astrocytes and microglia. Astrocytes degrade due to loss of support functions. Microglia also demonstrates changes as a result of stimulation by malarial exoantigens which enter through the compromised blood brain barrier. The increased permeability of the blood brain barrier, loss of integrity of astrocytes and microglia, and the secretion of damaging factors to sequestered leukocytes all contribute to the disturbance of the central nervous system (CNS) manifested by cerebral symptoms, coma, and eventual death.

1.4.3 PRRs in cerebral malaria

Host defense to malaria infection involves multiple strategies. The role of T cells and cytokines in the course of ECM has been intensively studied. In PbA infection of mice, sequestration of CD8⁺ T cells into the brain (176), accompanied by the release of the cytolytic molecules granzyme B and perforin (177), promotes CM development. CD8⁺ T cells also mediate the accumulation of PbA-infected red blood cells, pRBCs, in the brain (178). ECM is associated with high levels of pro-inflammatory cytokines (179, 180) with TNF- α and IFN- γ playing a crucial role in CM induction (181, 182). Consistently, IFN- γ -producing CD4⁺ T cells were shown to trigger the enhanced CD8⁺ T cell accumulation in the brain thus inducing ECM (183). In contrast, the immune modulatory cytokine IL-10 plays a key role in protection against severe malaria (184).

While adaptive immunity during the course of malaria has been investigated intensively, little is known about the role of innate immunity in CM induction. Innate immunity is of crucial importance as a first line of defense against infections (185) with

dendritic cells (DCs) playing a pivotal role in antigen presentation and initiation of a protective immune response (1). A number of studies indicated that DC functions such as maturation and the ability to cross-present malaria antigens are compromised by the interaction with pRBCs (163, 186, 187), while other studies indicated that DCs from malaria-infected mice were still efficient in presenting pRBC-derived antigens to CD4⁺ T cells (188, 189). In recent years, the contribution of DC subsets to immunity but also malaria-associated pathology has started to be unraveled (190-192). Still little is known about which PRRs expressed by DCs are involved in host defense to malaria on the one hand and how they might contribute to CM development on the other hand.

TLRs have been implicated to play a role in innate immunity to malaria as well as CM development (193, 194). However, the role of TLRs in malaria is still under debate (195-197). Besides TLRs, members of the TNF and TNF receptor superfamily were also shown to affect the outcome of malaria infection such as the interaction of LIGHT (TNFSF14) with the lymphotoxin β receptor that is involved in CM induction (198, 199). CLRs recognize specific carbohydrate structures on the surface of pathogens and self-antigens (5, 42) and orchestrate innate responses to a number of pathogens including bacteria, viruses, fungi, and helminths (42). In the case of malaria, DCs expressing the CLR Clec9a are critically involved in CM development. Ablation of Clec9a⁺ DCs resulted in complete resistance to ECM and reduction of CD8⁺ T cell sequestration in the brain (149). In another study, the role of CARD9, adaptor protein involved in signaling of CLRs such as Dectin 1 or Dectin 2, was investigated. CARD9 deficiency did not affect CM induction indicating that CLR signaling through CARD9 plays a limited role in CM development (200).

1.5 Scope and limitation of the study

This thesis is aimed at using carbohydrate ligands to elucidate the role of CLRs in immune modulation and employing animal models to study their role in infection. Known lectin-carbohydrate interactions were initially explored as proof-of-principle investigations to explore the effect of multivalent presentation of ligands in lectin-ligand binding as well as to test biological assays which might become relevant to understanding the function of CLRs. Novel ligands of some of the CLRs pertinent to this study, namely Dectin 1, DCIR, MCL, MICL, Clec12b, and MGL1 were identified and used in targeting CLRs on DCs *in vitro* and *in vivo* to investigate their roles in immune modulation. This approach is directed towards a rational strategy that will integrate tools that will bring about a comprehensive platform for studying the potential of CLR ligands as adjuvants.

Furthermore, the role of CLR_s in murine CM was investigated and the role of one specific CLR, the ITIM-bearing DCIR, in this process is described in detail in this thesis. To shed light into the different effects involved by virtue of the distinct signaling motifs of CLR_s, the role of SIGNR3, a hemITAM-containing CLR, in CM is succinctly presented.

2. Materials and Methods

2.1 Materials

2.1.1 Instruments and special implements

Analytical balance	
Agarose gel system	Biozym, Hamburg, Germany
Autoclave	Laboclav, steriltechnik AG, Detzel Schloss, Germany
Cell counter	Mettler Toledo, Columbus, OH, USA
Centrifuges	5810R & 5417R, Eppendorf, Wesseling-Berzdorf, Germany
Electrophoresis system	Biorad, Munich, Germany
ELISA plate reader	Infinite M200, Tecan, Crailsheim, Germany
Elispot reader	Bioreader 5000, BioSys, Karben, Germany
Flow cytometer	FACS Canto II, BD Pharmingen, Heidelberg, Germany
Freezer	Liebherr, Ahrensfelde, Germany
Gel imager (agarose gel)	Intas GDS, Goettingen, Germany
Heating Block	Thermomixer Comfort, Eppendorf, Wesseling-Berzdorf, Germany
Incubator for bacteria	Memmert, Schwabach, Germany
Incubator for cell culture	C150, Binder, Tuttlingen, Germany
Magnetic stirrer	MR Hei-Tec, Heidolph, Schwabach, Germany
Microarray printer	SciFlexarrayer, Scienion, Berlin, Germany
Fluorescent scanner	Genepix 4300A, Molecular Devices, Sunnyvale, CA, USA
Microscopes	Hund, Wilovert, Buckinghamshire, UK
Microwave	Panasonic, Hamburg, Germany
Multi-pipette	Eppendorf, Wesseling-Berzdorf, Germany
Multichannel pipette	Eppendorf, Wesseling-Berzdorf, Germany
NanoQuant plate	NanoQuant, Maennedorf. Switzerland
Oven	Binder, Tuttlingen, Germany
PCR thermocycler	C1000 Thermal Cycler, Biorad, Munich, Germany
pH meter	Mettler Toledo, Columbus, OH, USA
Pipettes	Eppendorf, Wesseling-Berzdorf, Germany
Refrigerator	Liebherr, Ahrensfelde, Germany
Shaker	Neolab, Heidelberg, Germany
Shaker for bacteria	Infors HT Multitron, Basel, Switzerland
Spectrophotometer	Spectrometer Ultraspec63, GE Healthcare, Uppsala, Sweden
Sterile bench	Herasafe KS, Thermo Scientific, Bonn, Germany
Surface plasmon resonance	Biacore T100, GE Healthcare, Uppsala, Sweden
UV table	Intas UV System, Goettingen, Germany
Vortexer	Vortex Gene, Scientific Industries, Bohemia, NY, USA
Water bath	Memmert, Schwabach, Germany
Water deionizer	Integra UV Plus, Neolab, Heidelberg, Germany

2.1.2 Consumables

Amicon [®] Ultra-4 Centrifugal Filters	Millipore, Bedford, MA, USA
Bioreactors	CELLine 350, Integra Biosciences, Zizers, Switzerland
Cell culture flasks	Corning, Corning, NY, USA
Cell culture plates	Corning, Corning, NY, USA
Cell strainer (40 µm)	Thermo Scientific, Waltham, MA, USA
Centricon [®] Centrifugal Filters	Millipore, Bedford, MA, USA
CM5 chip	GE Healthcare, Uppsala, Sweden
Combitips	Eppendorf, Wesseling-Berzdorf, Germany
Cryotubes	Corning, Corning, NY, USA
ELISA plates	Greiner, Frickenhausen, Germany
Elispot plates	Millipore, Bedford, MA, USA
FACS tubes	Sarstedt, Nuremberg, Germany
Falcon tubes	Corning, Corning, NY, USA
Epoxy-derivatized glass slides	Scienion, Berlin, Germany
HiTrap Protein G column	GE Healthcare, Uppsala, Sweden
Microscope slide	Sarstedt, Nuremberg, Germany
Needles	B. Braun, Melsungen, Germany
Nitrocellulose membrane	Biorad, Munich, Germany
Pasteur pipettes	Roth, Karlsruhe, Germany
Petri dishes	Corning, Corning, NY, USA
Pipettes	Corning, Corning, NY, USA
Sterile flasks	Corning, Corning, NY, USA
Sterile filters	Roth, Karlsruhe, Germany
Sterile pipettes	Corning, Corning, NY, USA
Syringes	B. Braun, Melsungen, Germany
Eppendorf tubes	Eppendorf, Wesseling-Berzdorf, Germany

2.1.3 Chemicals

All chemicals used in this study were acquired from the following companies: Sigma-Aldrich (Munich, Germany) and Roth (Karlsruhe, Germany). Chemicals used for SPR studies were purchased from GE Healthcare (Uppsala, Sweden).

2.1.4 Bacterial strain, cell lines, mouse strains, and parasite strain

Bacterial strain

E. coli DH5- α

Cell lines

CHO (CCL-61)

HepG2

Mice strains

Balb/c	Charles River, Sulzfeld, Germany; Max Planck Institute for Infection Biology, Berlin, Germany
C57BL/6	Charles River, Sulzfeld, Germany; Max Planck Institute for Infection Biology, Berlin, Germany
DCIR ^{-/-}	Consortium for Functional Glycomics
SIGNR3 ^{-/-}	Consortium for Functional Glycomics
OT-II transgenic	Max Planck Institute for Infection Biology, Berlin, Germany

Parasite strain

Plasmodium berghei ANKA (MRA-311) MR4/ATCC. Manassas, VA, USA

2.1.5 Materials for molecular biology and biochemistry methods**2.1.5.1 Antibodies, enzymes, reagents, kits and supplements**Antibodies

Annexin V-FITC	eBioscience, Frankfurt, Germany
Goat anti-human IgG-HRP	Dianova, Hamburg, Germany
Goat anti-human IgG-PE	BD Pharmingen, Heidelberg, Germany
Goat anti-mouse IgG (H+L)	DAKO, Hamburg, Germany
Mouse anti-human IgG1-AF488	Invitrogen, Carlsbad, CA, USA
Rabbit polyclonal anti-human CD3	DAKO, Hamburg, Germany
Rabbit polyclonal anti-granzyme B	Abcam, Cambridge, MA, USA
Rat anti-mouse CD4-FITC	eBioscience, Frankfurt, Germany
Rat anti-mouse CD8-APC-H7	BD Pharmingen, Heidelberg, Germany
Rat anti-mouse CD16/32	BD Pharmingen, Heidelberg, Germany
Rat anti-mouse CD19-FITC	BD Pharmingen, Heidelberg, Germany
Rat anti-mouse CD31	Dianova, Hamburg, Germany
Rat anti-mouse CD62L-PE	BD Pharmingen, Heidelberg, Germany
Rat anti-mouse CD69-PerCP-Cy5.5	eBioscience, Frankfurt, Germany
Rat anti-mouse IFN- γ -APC	BD Pharmingen, Heidelberg, Germany
Rat anti-mouse IFN- γ (capture)	BD Pharmingen, Heidelberg, Germany
Rat anti-mouse IFN- γ (detection)	BD Pharmingen, Heidelberg, Germany
Rat anti-mouse IL-2 (capture)	BD Pharmingen, Heidelberg, Germany
Rat anti-mouse IL-2 (detection)	BD Pharmingen, Heidelberg, Germany
Rat anti-mouse IL-4 (capture)	BD Pharmingen, Heidelberg, Germany
Rat anti-mouse IL-4 (detection)	BD Pharmingen, Heidelberg, Germany
Rat anti-mouse TNF- α -AF488	BD Pharmingen, Heidelberg, Germany

Enzymes

AMV Reverse Transcriptase	NEB, Ipswich, MA, USA
<i>Bgl</i> II	NEB, Ipswich, MA, USA
<i>Eco</i> R1-HF	NEB, Ipswich, MA, USA
<i>Nco</i> I	NEB, Ipswich, MA, USA
T4 DNA Ligase	Promega, Madison, WI, USA
<i>Taq</i> DNA Polymerase	Promega, Madison, WI, USA

Reagents, kits and supplements

ABTS	AppliChem, Darmstadt
Acrylamide/bis-acrylamide (29:1)	Sigma-Aldrich, St. Louis, MO, USA
Agar	Sigma-Aldrich, St. Louis, MO, USA
Agarose	Biomol, Hamburg, Germany
Amicon centrifugal filters	Millipore, Bedford, MA, USA
Ammonium persulfate (APS)	Sigma-Aldrich, St. Louis, MO, USA
Annexin V Apoptosis Detection Kit	BD Pharmingen, Heidelberg, Germany
Avidin-HRP	PeptoTech, Rocky Hill, NJ, USA
BSA	Biomol, Hamburg, Germany
Coomassie Protein Assay	Biorad, Munich, Germany
Cytometric Bead Assay (CBA; murine IFN- γ , TNF- α , IL-10, IL-6, IL-12p70, IL-4)	BD Bioscience, San Jose, CA, USA
DNA molecular weight ladder (100 bp)	Fermentas, St. Leon-Rot, Germany
dNTPs	Promega, Madison, WI, USA
DTT	Promega, Madison, WI, USA
ECL Western Blot Detection Reagent	Biorad, Munich, Germany
Ethidium bromide	Sigma-Aldrich, St. Louis, MO, USA
OligoDT primer	Biorad, Munich, Germany
OVA	Innovagen, Lund, Sweden
OVA ³²³⁻³³⁹ peptide	Innovagen, Lund, Sweden
LPS	Sigma-Aldrich, St. Louis, MO, USA
Milk powder	Sigma-Aldrich, St. Louis, MO, USA
Murine IL-12p40 and IL-2 ELISA Kit	PeptoTech, Rocky Hill, NJ, USA
PCR cloning kit	Qiagen, Hilden, Germany
Plasmid miniprep kit	Qiagen, Hilden, Germany
Protein G columns	GE Healthcare, Uppsala, Sweden
Protein molecular weight ladder	NEB, Ipswich, MA, USA
Reverse Transcriptase 10x buffer	Promega, Madison, WI, USA
RNasin	Promega, Madison, WI, USA
QIAEX gel extraction kit	Qiagen, Hilden, Germany
Streptavidin-HRP	PeptoTech, Rocky Hill, NJ, USA
Sulfo-NHS-LC-biotin reagent	Thermo Scientific, Waltham, MA, USA
<i>Taq</i> DNA Polymerase 10 buffer	Promega, Madison, WI, USA
TEMED	Sigma-Aldrich, St. Louis, MO, USA
Tissue freezing medium	Leica Biosystems, Wetzlar, Germany
TRI Reagent [®]	Sigma-Aldrich, St. Louis, MO, USA
Tween-20	Sigma-Aldrich, St. Louis, MO, USA
X-gal	Promega, Madison, WI, USA
Yeast extract	Sigma-Aldrich, St. Louis, MO, USA
Zeocin	Invitrogen, Carlsbad, CA, USA

2.1.5.2 Buffers and supplements

Stock solutions

Ampicillin in water	100 mg/ml
Kanamycin in water	30 mg/ml
X-gal stock solution in dimethylformamide (toxic)	40 mg/ml

Ammonium persulfate (APS)

10% in H₂O

Binding buffer (Protein G column)

20 mM sodium phosphate, pH 7.0

Blocking buffer (Western Blot)

5% milk powder in PBS

Blocking buffer (Glycan Array)

10mM HEPES (11.9 g)
1mM MgCl₂ (5 mL from 1M MgCl₂)
1mM CaCl₂ (5 mL from 1M CaCl₂)
2% BSA (IgG free)
In 500 ml water

Elution buffer (Protein G column)

0.1 M Glycine-HCl, pH 2.7

LB (Luria Bertani)

10 g Tryptone
5 g Yeast extract
10 NaCl
in 1 L water, pH 7.0

LB low salt

10 g Tryptone
5 g Yeast extract
5 g NaCl
in 1 L water, pH 7.5

Lectin buffer (Glycan array)

10mM HEPES (11.9 g)
1mM MgCl₂ (5 mL from 1M MgCl₂)
1mM CaCl₂ (5 mL from 1M CaCl₂)
In 500 ml water

SOB (- glucose)

0.5 % Yeast extract
2% Tryptone
10 mM NaCl
10 mM MgCl₂
2.5 mM KCl
10 mM MgSO₄
in 1 L water

SOC (+ glucose)

SOB
20 mM Glucose

10x TBE

0.89 M Tris base
0.89 M boric acid
20 mM Na₂EDTA·2H₂O

10x TBS

24 g Tris-HCl
5.6 g Tris base
88 g NaCl
in 1L water, pH 7.6

10x Transferring/Blotting buffer (Western Blot)

144 g glycine
30.3 g Tris base
In H₂O up to 1 L water

TBST

25 ml 10X TBST
500 µl Tween 20
in 250 ml water

TBST with milk

7.5 g milk
 12 ml 10X TBST
 300 µl Tween 20
 in 250 ml water

2.1.5.3 Vectors and primersVectors

pDrive cloning vector	Invivogen, Toulouse, France
pFuse-hIgG1-Fc2 vector	Invivogen, Toulouse, France

Primers

All primers were obtained from MWG (Ebersberg, Germany).

CLR primers:

DCIR:	Forward 5'-GAATTCGCTACTTCTCCTGCTGCTGG-3'
	Reverse 5'-AGATCTTCCAGTCTTCCAACGGTAAA-3'
Clec12b:	Forward 5'-ACTTTCTCCTAGGATGTCTG-3'
	Reverse 5'-GCATGGGTTTGCAATAGGTC-3'
Dectin 1:	Forward 5'-GAATTCTTCAGGGAGAAATCCAGAGG-3'
	Reverse 5'-AGATCTTGAAGAAGTATTGCAGATTTGGTT-3'
MICL:	Forward 5'-GAATTCTTTGGCAACAGAAATGATAA-3'
	Reverse 5'-AGATCTGCCATTCAACACACTTTCCA -3'
MCL:	Forward 5'-GAATTCTCATTACTTTTTACGCTGGA-3'
	Reverse 5'-AGATCTACAAATCCTTCTCACCTCAAAG-3'

2.1.6 Materials for cell biology methods**2.1.6.1 Media and buffers**Solutions

DMEM (without L-glutamine and sodium pyruvate)	PAN Biotech, Aidenbach, Germany
IMDM (without L-glutamine and sodium pyruvate)	PAN Biotech, Aidenbach, Germany
RPMI 1640 (without L-glutamine and sodium pyruvate)	PAN Biotech, Aidenbach, Germany
10000 U/ml penicillin, 10 mg/ml streptomycin	PAN Biotech, Aidenbach, Germany
200 mM stable glutamine	PAN Biotech, Aidenbach, Germany
Fetal calf serum (FCS)	PAN Biotech, Aidenbach, Germany

ABTS solution

0.4 mg/ml ABTS
 0.03% H₂O₂
 In 0.1 M citrate buffer, pH 4.0

Complete DMEM

500 ml DMEM
10% FCS
1% glutamine
1% penicillin/streptomycin

Complete RPMI

500 ml RPMI 1640
10% FCS
1% glutamine
1% penicillin/streptomycin

ELISA coating buffer

NaCO₃/NA₂HCO₃, pH 9.4

ELISA blocking buffer

1% BSA in PBS

ELISA reagent diluent

1% BSA
0.05% Tween 20
in PBS

ELISA washing buffer

0.05% Tween 20 in PBS

Erythrocyte lysis buffer

10% 0.1 M Tris-HCl (pH 7.5)
90% 0.16 M NH₄Cl

FACS staining buffer

0.5% BSA
2 mM EDTA
in PBS

2.2 Methods

2.2.1 Molecular biology and biochemistry methods

2.2.1.1 mRNA extraction from eukaryotic cells

Total RNA was isolated from eukaryotic cells by a single extraction using the acid guanidinium thiocyanate-phenol-chloroform (AGPC) mixture as described by Chomczynski and Sacchi (201). The isolation was done, under RNase-free conditions, using the TRI Reagent[®] solution following manufacturer's instructions.

2.2.1.2 cDNA synthesis

First-strand complementary DNA was synthesized by reverse transcription in 20- μ l reaction mixtures prepared as follows:

MgCl ₂ (25 mM)	4 μ l
Reverse Transcriptase 10x buffer	2 μ l
dNTP mixture (10 mM)	2 μ l
RNasin	0.5 μ l
AMV Reverse Transcriptase	0.6 μ l
Oligo DT primers	1 μ l
RNA	5 μ l
Nuclease-free H ₂ O	4.9 μ l

2.2.1.3 Polymerase Chain Reaction (PCR)

Polymerase Chain Reaction (PCR) is a technique which uses thermal cycling to amplify a specific DNA sequence. This is done by separating the two strands of DNA, marking the location of the specific sequence with primers, and incubating with DNA polymerase to assemble a copy alongside each segment and continuously copy the copies until the DNA sequence is exponentially amplified (202).

PCR was used to amplify desired DNA fragments. Thereof, a PCR reaction mix was prepared as follows:

10x <i>Taq</i> DNA polymerase buffer	2.5 μ l
dNTPs (10 mM)	0.5 μ l
Forward primer (10 μ M)	2.5 μ l
Reverse primer (10 μ M)	2.5 μ l
cDNA template	2.0 μ l
<i>Taq</i> DNA polymerase	0.2 μ l
dH ₂ O up to	25 μ l

The amplification was performed on a ThermoCycler using the following PCR program:

Initial denaturation	95°C	3 min	(× 35 cycles)
Denaturation	95°C	30 sec	
Annealing	(varies)		
Elongation	72°C	1 min	
Final elongation	72°C	5 min	

Annealing temperatures for amplification of DCIR, Clec12b, Dectin 1, MICL, and MCL DNA sequences were 64.3°C, 61.6°C, 65.3°C, 58.7°C, and 60.5°C, respectively.

For genotyping DCIR^{-/-} and SIGNR3^{-/-} mice, genomic DNA was obtained from the tail biopsies of knockout, heterozygous, and wild-type mice. PCR was performed according to the protocol as outlined in Consortium for Functional Glycomics.

2.2.1.4 Cloning into pDrive vector

The pDrive cloning vector allows for the insertion and removal of DNA and which altogether can be stably maintained in bacterial cells for cloning. pDrive contains the enzyme restriction sites which are compatible with the restriction enzymes used in designing the primers encoding the extracellular regions of the CLRs. Additionally, the vector allows for ampicillin selection and blue/white screening of inserted DNA, both of which were utilized in this thesis. PCR products were cloned into the pDrive cloning vector according to the manufacturer's instructions.

2.2.1.5 DNA gel electrophoresis

Each DNA sample was mixed with loading buffer and the mixture was loaded onto 0.7% agarose gel. The electrophoresis ran for 30 minutes at 100 V using TBE as running

buffer. Staining was done using 1 µg/ml ethidium bromide in TBE buffer for 10 minutes followed by destaining in water for 30 minutes. The gel was imaged using the Gel imager.

2.2.1.6 DNA concentration determination

DNA concentration was measured using Nanoquant plate and subsequent measurement was done at 260 nm with A_{260}/A_{280} using the Tecan Microplate Reader.

2.2.1.7 Transformation into DH5- α competent cells

50 ng of the plasmid was added into 100 µl of thawed DH5- α competent cells. The mixture was incubated in ice for 30 minutes. The cells were heat shocked at 42°C for 2 minutes and then rescued at 37°C for 1 hour with minimal shaking on a thermomixer. 40 µl of X-Gal stem solution was spread on LB (50 µg/ml Amp) plates. The cells were spread on the plates and inoculated at 37°C for 18 hours. White colonies were picked out and inoculated in SOC media (50 µg/ml Amp) at 37°C for 16 hours with shaking.

2.2.1.8 Plasmid purification

Plasmid DNA was isolated based on the alkaline lysis method to precipitate the DNA (203). Plasmid DNA was purified using Miniprep kit following the manufacturer's instructions.

2.2.1.9 Analytical digestion

Double digestion was performed using the restriction enzymes *EcoRI*-HF and *Bgl*III for DCIR, Dectin 1, MICL, MCL cloning and the vector pFuse, and *NcoI* and *Bgl*III for Clec12b cloning. The reaction was allowed to proceed at 37°C for 2 hours while shaking.

2.2.1.10 Ligation with pFuse

The CRD-containing extracellular regions of the CLRs Dectin 1, MICL, DCIR, MCL, and Clec12b were fused with the human IgG₁-Fc2 using the expression vector pFuse. The vector has several features; the most important are the hIgG₁-Fc2, hEF1-HTLV promoter, IL2 signal sequence, and the zeocin resistance gene. The hIgG₁-Fc2 contains the CH2 and CH3 domains of the hIgG₁ heavy chain and the hinge region. The latter works as a flexible spacer between the two parts of the Fc fusion protein. hEF1-HTLV is a dual promoter: the Elongation Factor-1 α (EF-1 α) (204) as the core promoter and the R segment and a fragment of the U5 sequence (R-U5') of the Human T cell Leukemia Virus (HTLV) Type 1 Long (205).

The EF-1 α promoter generates long lasting *in vivo* expression of a transgene, while the coupling of R-U5' to EF-1 α boosts RNA stability. The IL2 signal peptide undergoes intracellular cleavage which promotes the secretion of the fusion protein. The *Sh ble* gene from *Streptoalloteichus hindustanus* affords the resistance to the antibiotic zeocin which serves as a selection marker in CHO cells after transfection.

pFuse ligation was done using T4 DNA ligase according to the manufacturer's instructions. The mixture was prepared as follows:

pFuse vector DNA	1 μ l
CLR DNA	9 μ l
10x T4 DNA Ligase Buffer	2 μ l
Nuclease-free water	7 μ l
Ligase	1 μ l

The mixture was allowed to incubate at RT for 10 minutes.

2.2.1.11 Protein purification

Fusion proteins were purified by running cell supernatants through HiTrap Protein G columns according to the manufacturer's instructions. Thereafter, the elution buffer was exchanged with PBS. Using Amicon[®] Ultra-4 centrifugal filters with a membrane cutoff of 30 kDa, the eluted sample was placed on the reservoir and the tube was centrifuged at 4000 \times g for 10 minutes. The filtrate was then discarded. PBS was added to the reservoir up to the maximum volume and the whole process was repeated twice.

2.2.1.12 Protein concentration determination

To quantify the purified proteins, the copper-based method, BCA Protein Assay as described by Smith (206), was performed following the manufacturer's instructions using BSA as the standard protein.

2.2.1.13 SDS-PAGE and Western Blot

Protein samples were mixed with loading buffer, heated at 95°C for 5 minutes, and loaded onto a 12% SDS-PAGE gel. Separated proteins in the gels were electrophoretically transferred onto a nitrocellulose membrane at 250 mA for 1 hour. The blotted membrane was washed twice with PBS and blocked with 5% skim milk in TBS-T for 1 hour. After washing the membrane three times with TBST, goat anti-human IgG-HRP, diluted 1:1000 in TBST

was added and incubated for 1 hour. The membrane was then washed three times with TBST followed by detection using the ECL detection system as outlined by the manufacturer.

2.2.1.14 OVA-carbohydrate conjugation

Amino-linked 1,3-lactosamine and Gb5 (synthesized by Dr. Mark Schlegel) were conjugated to ovalbumin (OVA) using a disuccinimido adipate (DSAP) linker (Figure 8). The DSAP linker contains an amine-reactive *N*-hydroxysuccinimide (NHS) ester located on both ends of the 6-carbon spacer arm. These NHS esters can react with primary amines at pH 7-9 to form stable amide bonds (207). DSAP can be used to conjugate amino-linked synthetic carbohydrates to primary amines in the side chain of lysine residues on the surface of the protein. The linker was dissolved in DMSO and activated by 10 μ l triethylamine. Carbohydrates dissolved in DMSO were added dropwise and allowed to react for 1.5 hours. 250-500 μ l phosphate buffer was added and the unreacted linker was removed by adding 10 ml of chloroform followed by centrifugation at $3000 \times g$ for 3 minutes. Bound carbohydrate-linker was pipetted from the aqueous phase and this chloroform extraction was repeated twice. Carbohydrate-linker was incubated overnight with OVA in 250-500 μ l sodium phosphate buffer (pH 7.4). Samples were concentrated using a 10 kDa Centricon[®] centrifuge unit and dissolved in either water for MALDI-TOF-MS analysis or in sterile PBS.

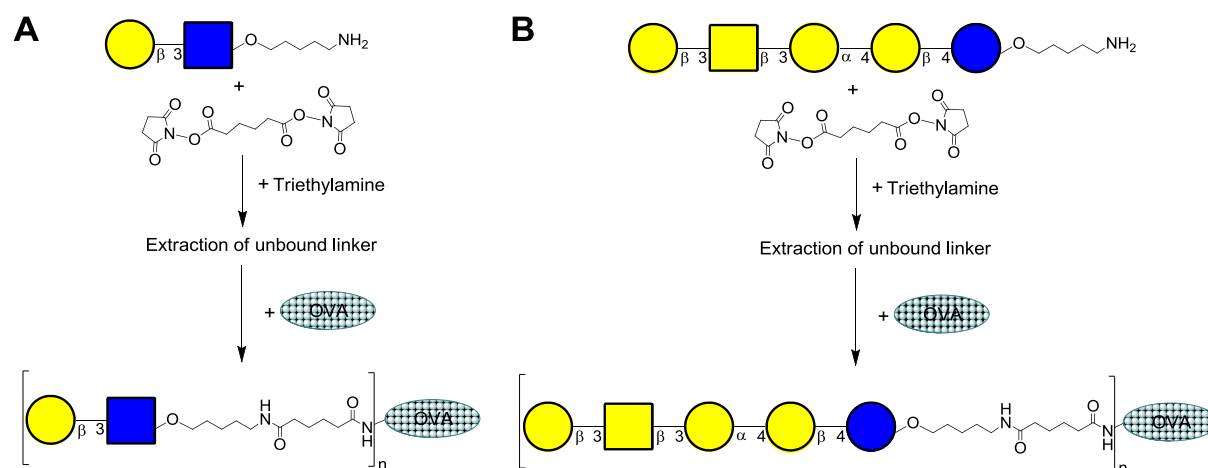


Figure 8. Schematic representation of OVA-carbohydrate conjugation. Amino-linked (A) 1,3-lactosamine and (B) Gb5 were conjugated to OVA using a DSAP linker.

2.2.2 Biophysical methods

2.2.2.1 Carbohydrate microarray printing

Amino- and thiol-functionalized carbohydrates synthesized by former and current members of the department (208-218), diluted in varying concentrations in 50 mM sodium phosphate, were printed at approximately 1.2 nL per feature/spot on epoxy-derivatized glass slide at 30% humidity using a piezoelectric microarray with an uncoated glass nozzle. 16 replicate subarrays were printed per slide, with each carbohydrate probe spotted in triplicates per subarray. Thereafter, the slides were stored in a dark moisture chamber at RT for 24 hours, washed twice with distilled water, and centrifuged at 2000 rpm for 5 minutes.

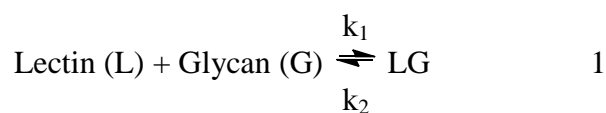
2.2.2.2 Detection of lectin-carbohydrate interactions

The carbohydrate microarray slide was quenched just before use by washing three times with distilled water and incubating in quenching solution at 50°C in the dark for 1 hour. The slides were washed three times with distilled water and centrifuged at 2000 rpm for 5 minutes. The slide was then placed on 16-well gasket slide and incubation cassette system, mildly shaken, and protected from light for the subsequent steps. Each subarray was blocked with blocking buffer at RT for 1 hour and washed three times with lectin buffer for 5 minutes. 1 µg of protein sample, diluted in lectin buffer supplemented with 2% Tween 20, was applied to a subarray and incubated at RT for 1 hour. The subarrays were washed three times with lectin buffer for 5 minutes. Monoclonal goat anti-human IgG-PE was incubated at a 1:100 dilution in lectin buffer with 5% BSA on the subarrays at RT for 1 hour and washed once with lectin buffer. The slide was then removed from the gasket slide, placed in a petri dish, washed twice with lectin buffer, and washed once with distilled water. The slide was centrifuged at 1000 rpm for 5 minutes and scanned with a Genepix scanner. Binding affinities were determined by measuring the Mean Fluorescent Intensities (MFI) using Genepix Pro 7 (Molecular Devices, Sunnyvale, CA, USA).

2.2.2.3 Determination of protein-carbohydrate kinetics (SPR)

Surface plasmon resonance (SPR) is a valuable tool for analyzing lectin-carbohydrate interaction in real time and for providing insights into the affinity and kinetics of binding (219). SPR is a technique for measuring the association and dissociation kinetics of ligand, termed analyte, with a receptor. The analyte or the receptor can be immobilized on a sensor chip which bears a gold film. The association of the analyte and receptor with one or the

other, depending which one is immobilized, induces a change in the refractive index of the layer in contact with the gold film. This is measured as a change in the refractive index at the surface layer and is recorded as the SPR signal in resonance units (RU). Binding is measured in real time and information about the association and dissociation kinetics can thus be obtained, which in turn can be used to obtain K_a and K_d from Equations 2 and 3.



$$K_A = [\text{LG}]/[\text{L}][\text{G}] = k_1/k_2 \quad 2$$

$$K_D = [\text{L}][\text{G}]/[\text{LG}] = 1/K_a = k_2/k_1 \quad 3$$

For the preparation of Concanavalin A (Con A)-coated surfaces, Con A was immobilized at high (Con A-HD) and low (Con A-LD) densities at a flow rate of 10 $\mu\text{L}/\text{min}$. The CM5 chip was activated by injection of a mixture of *N*-ethyl-*N'*-(diethylaminopropyl)-carbodiimide (EDC) and *N*-hydroxysuccinimide (NHS) for 10 minutes and functionalized by injecting 100 $\mu\text{g}/\text{mL}$ and 10 $\mu\text{g}/\text{mL}$ Con A in acetate buffer pH 5.5 for Con A-HD and Con A-LD, respectively, for 7 minutes. The remaining activated carboxyl groups were then capped by injection of 1 M ethanolamine for 10 minutes. Control flow cells were treated with EDC/NHS followed by ethanolamine as described. Concentration gradients of the different ruthenium complexes (5 μM , 10 μM , 20 μM , 30 μM , 40 μM , and 50 μM) (Figure 9) were injected over the Con A-functionalized surfaces at 10 $\mu\text{L}/\text{min}$, allowing 60 seconds for contact and 300 seconds for dissociation times, followed by regeneration using 100 mM methyl- α -D-mannopyranoside at 30 $\mu\text{L}/\text{min}$ for 30 seconds. Experimental data were analyzed using Biacore S20 T100 Evaluation Software. Kinetic analyses based on a 1:1 interaction model for the Con A-Ru complexes interaction were performed using Scrubber2 (BioLogic Software, Campbell, Australia).

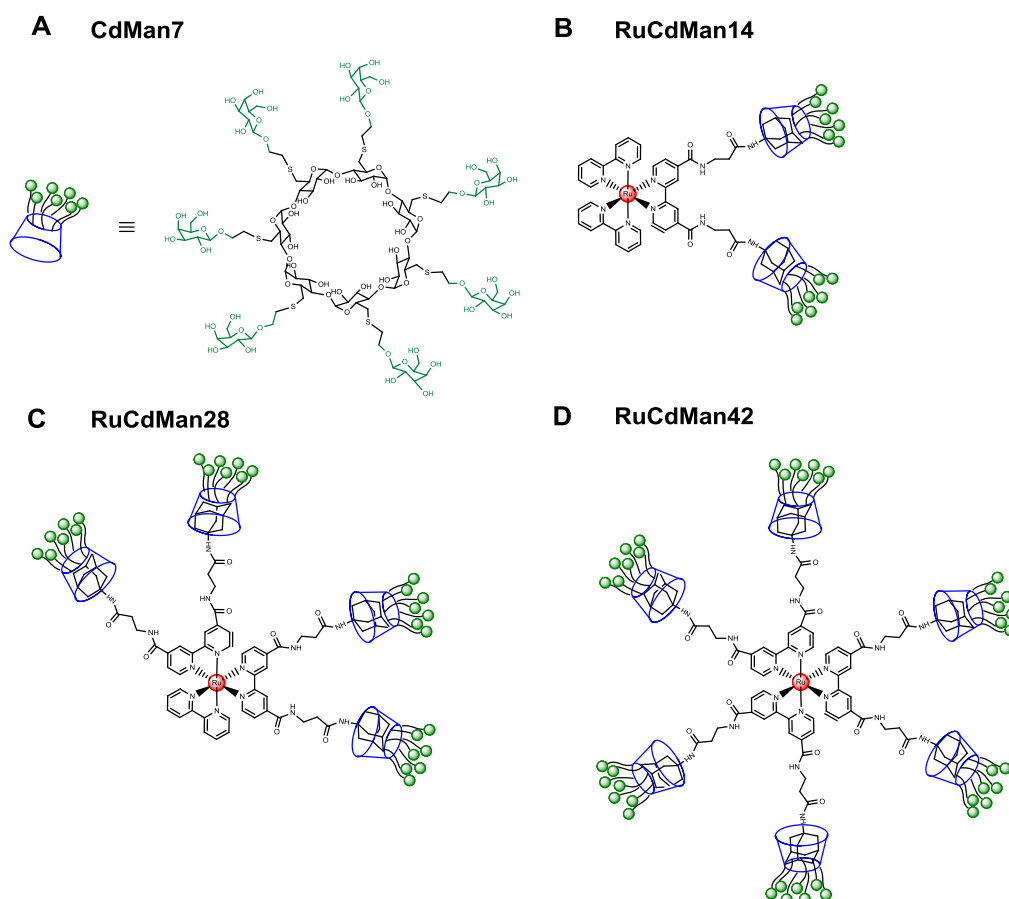


Figure 9. Schematic representation of the different carbohydrate-functionalized Ru(II) complexes. (A) Scheme of heptamannosylated cyclodextrin (CDMan). **(B-D)** Different Ru(II) complex structures functionalized with 2 (RuCdMan14), 4 (RuCdMan28), or 6 (RuCdMan42) heptamannosylated cyclodextrins (B, C, and D, respectively). Figure modified from (220).

2.2.2.4 Quantification of carbohydrates conjugated on OVA

In order to determine the average number of carbohydrates conjugated on each OVA molecule, matrix-assisted laser desorption/ionization time-of-flight mass spectrometry (MALDI-TOF-MS) analysis was performed using autoflex™ speed mass spectrometer. The instrument ran with smartbeam™ II laser optics running at 1000 Hz and was operated using FlexControl 3.3 software (Bruker Daltonics, Bremen, Germany). Equal amounts of 1 mg/ml of sample in water and 50 nmol/μl of the matrix, 2',4',6'-trihydroxyacetophenone monohydrate (THAP), in 50 % acetonitrile were mixed. 1 μL of the mixture was spotted onto a 384-spot, 600-μm polished steel MALDI target and allowed to dry at room temperature. Internal calibration was done using a standard calibration mix. MS spectra were acquired in linear-positive ion mode within the mass range of m/z 25000-65000. The spectra acquired were then adjusted for baseline correction and smoothed using Gaussian algorithm with m/z of 0.2 width and 1 cycle with the FlexAnalysis software (Bruker Daltonics, Bremen, Germany).

2.2.3 Cell biology methods

2.2.3.1 Enzyme-linked immunosorbent assay (ELISA)

For cytokine quantification, an indirect sandwich ELISA was performed according to the manufacturer's instructions (PeproTech). 1 µg/ml of capture antibody in PBS was added on ELISA plate wells and incubated at RT overnight. The wells were washed four times using the washing buffer. 300 µl of blocking buffer was then added and incubated at RT for 1 hour, afterwards, the wells were washed four times with washing buffer. 100 µl of standards (2 ng/ml to zero) and samples in diluent were added to each well in triplicates and incubated at RT for 2 hours. The wells were washed four times in washing buffer and 100 µl of IL-12p40 detection antibody was added and incubated at RT for 30 minutes. The wells were washed four times and 100 µl of avidin-HRP conjugate, diluted 1:2000 in diluent, was added and incubated at RT for 2 hours. The wells were washed four times and 100 µl of 0.25 µg/ml ABTS substrate solution was added and incubated at RT until color development ensued. OD was monitored using an ELISA plate reader at 405 nm with wavelength correction at 650 nm.

For determining antibody titers, 0.5 µg of capture molecule was prepared in 100 µl of coating buffer and incubated on ELISA plate wells at 4°C overnight or at RT for 2 hours. The wells were washed three times with washing buffer and 300 µl of blocking buffer was added and incubated at 4°C overnight or at RT for 2 hours. The wells were washed three times with washing buffer and 100 µl of each sample, in different dilutions, was added in triplicates and incubated at RT for 2 hours. The wells were washed three times with washing buffer and 100 µl of AP-conjugated detection antibody, diluted 1:1000, was added and incubated at RT for 1 hour. The wells were washed three times with washing buffer and 50 µl of 10 mg/ml pNPP substrate was added. The substrate was incubated until the color developed and the OD was determined using an ELISA plate reader at 405 nm.

2.2.3.2 ELISpot

ELISpot analyses were done for IFN-γ, IL-2, and IL-4. ELISpot plates were wetted with 20 µl of 35% ethanol for 1 minute, followed by washing three times with PBS. The wells were coated with 50 µl of 5 µg/ml anti-mouse capture antibody in PBS and incubated at 4°C overnight. The plates were rinsed twice with 100 µl complete RPMI medium and blocked with 200 µl RPMI medium at RT for 2 hours. The medium was decanted and 100 µl of medium alone (negative control), 50 µg/ml OVA₃₂₃₋₃₃₉ peptide, or 10 µg/ml anti-mouse CD3 and anti-mouse CD28 (positive control) were added to specified wells. 100 µl of splenic cells

containing 4×10^5 cells were added to the wells. The cells were incubated at 37°C with 5% CO_2 for 18 hours. The wells were washed 2 times with 100 μl water and allowed to soak for 3-5 minutes in each washing step. These were then washed three times with 200 μl washing buffer. 50 μl dilution buffer (PBS with 10% FCS) containing 2 $\mu\text{g/ml}$ detection antibody was added to each well and incubated at RT for 2 hours. The wells were then washed three times with washing buffer. 50 μl of streptavidin-HRP, diluted 1:200, in dilution buffer was added and incubated at RT for 1 hour. AEC stock solution containing 100 mg AEC in 10 ml DMF was prepared. The AEC substrate solution was made which consisted of 333.3 μl of AEC stock solution, 10 ml 0.1 M acetate solution, and 5 μl H_2O_2 . The wells were washed twice with 200 μl PBS and 100 μl of freshly prepared AEC substrate solution was added. The wells were allowed to develop until pink spots were visible. The development was stopped by adding water and the plates were then allowed to air dry. Once dried, the spots were enumerated using the Elispot analyzer BIOREADER 5000.

2.3.3.3 Flow cytometry

Cells were stained with respective fluorescently-labeled antibodies according to the respective method. After staining, the cells were washed twice with FACS buffer and resuspended in 200 μl FACS buffer. Cells were analyzed using FACS CantoTM II. Flow cytometry results were analyzed using FlowJo (Treestar Inc., Ashland, OR, USA).

2.3.3.4 Cytometric Bead Array (CBA)

For cytokine quantification, blood was taken from the tails of uninfected and PbA-infected mice. The cytokines $\text{TNF-}\alpha$, $\text{IFN-}\gamma$, IL-10, IL-12p70, IL-1 β , IL-4, and IL-6, were measured by cytometric bead array (CBA) according to the manufacturer's instructions (BD Pharmingen).

2.2.3.5 Uptake studies in HepG2 cells

Human hepatocellular carcinoma cell line, HepG2, was plated in 6-well plates and cultivated in complete DMEM medium. When cells were 70% confluent, different concentrations (10 μmol , 50 μmol , and 250 μmol) of rhodamine B-containing cyclodextrin (Cd) glycodendrimers (Figure 10A) were added to the cells. After incubation times between one and six hours, cells were washed with PBS. The cells were then collected with PBS containing 1% FCS by shearing force. Uptake of glycodendrimers was measured by flow

cytometry using a FACSCanto™ II flow cytometer. Excitation wavelength in the FACS experiments was 540 nm, which is the excitation wavelength of rhodamine B.

For analysis of glycoliposome uptake by the HepG2 cell line, cells were incubated with liposomes consisting of L- α -phosphatidylcholine and rhodamine-DHPE (negative control) or liposomes displaying additionally glycolipid *N*-Acetylglucosamine (GlcNAc; specificity control) or GalNAc on their surface (Figure 10B). After incubation times between one to six hours, cells were washed with PBS and collected from the plate. Detection of liposome uptake was performed as described above.

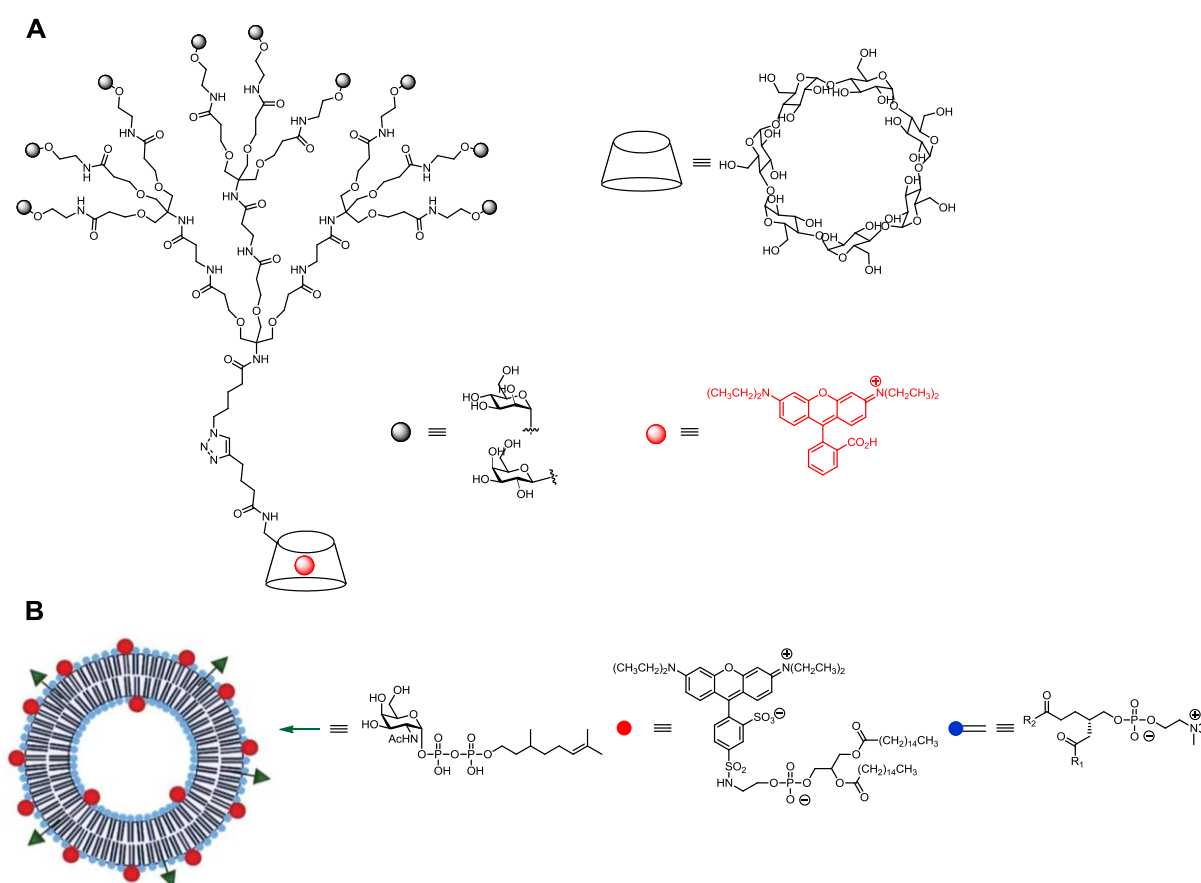


Figure 10. Schematic representation of the glycodendrimers and glycoliposome. (A) CD glycodendrimer consisting of CD (cylinder), the encaged fluorescent dye rhodamine B (red ball), and terminal D-Mannose or D-Gal residues (grey ball). (B) Glycoliposomes consisting of L- α -phosphatidylcholine (blue ball), the fluorescent lipid rhodamine-DHPE (red ball), and synthetic glycolipids containing either a terminal GalNAc or GlcNAc residue (green arrow). Figure modified from (221).

2.2.3.6 Apoptosis studies in HepG2 cells

For analysis of apoptosis, HepG2 cells were incubated with doxorubicin-loaded galactose-functionalized cyclodextrin (Figure 11) for 24 hours at concentrations of 1 μ g/ml, 5 μ g/ml, and 10 μ g/ml of the incorporated drug. The following controls were used: untreated cells (negative control), cells incubated with doxorubicin alone (positive control),

and cells treated with cyclodextrin-Gal only. The concentrations for doxorubicin and empty cyclodextrin-Gal were the same as those of doxorubicin-loaded cyclodextrin-Gal. After incubation, the adherent cells were detached from the growth surface using Trypsin/EDTA. The staining procedure was performed according to the protocol in the Annexin V-APC Apoptosis Detection Kit. Detection of apoptotic cells was done by flow cytometry as described above.

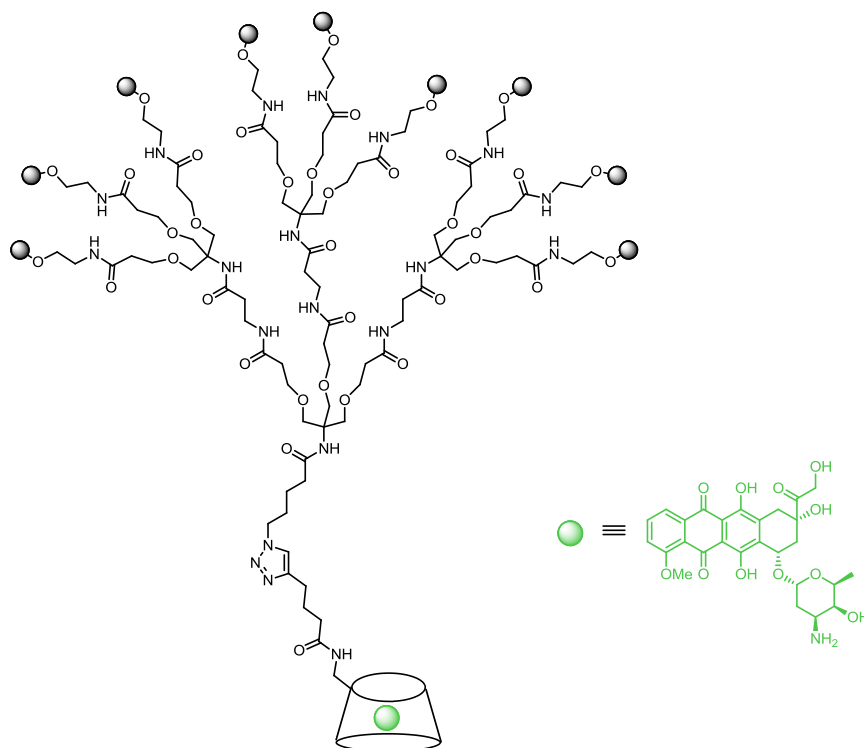


Figure 11. Schematic representation of the glycodendrimers loaded with doxorubicin. CD glycodendrimer consisting of CD (cylinder), the engaged doxorubicin (green ball), and terminal D-Gal residues (grey ball). Figure modified from (221).

2.2.3.7 Stimulation studies of PECs

Mouse peritoneal exudate cells (PECs) were elicited by i.p. injection of 1 mL 4% thioglycolate solution into 8–12-week-old female C57BL/6 mice. After 5 days, mice were sacrificed and PECs were isolated by lavage of the peritoneum with 10 mL ice-cold PBS. Upon erythrocyte lysis by addition of ammonium chloride, PECs were suspended in complete IMDM medium. Fibers functionalized with mannose, galactose (specific control), or aminoethanol (unspecific control) with similar dimensions (mat size, mat density, fiber diameter) (Figure 12) were placed in the wells of a 96-well plate. Fibers were manually attached to the bottom of the wells of the cell culture plates used. Fibers were not prewet, but no air bubbles could be seen when checking through a light microscope. Subsequently, 2×10^5 freshly prepared PECs were seeded in each well and were allowed to adhere to the fiber meshes for 2 h. The attachment was checked by microscope at regular intervals. Nonadherent

cells were removed by replacing the medium with prewarmed cell culture medium. Cells were then stimulated by adding the TLR4 agonist LPS at a final concentration of 10 ng/mL. Cells were cultivated overnight at 37°C and 5% CO₂, the culture supernatant was removed from the cells, and cytokine concentrations were analyzed by ELISA.

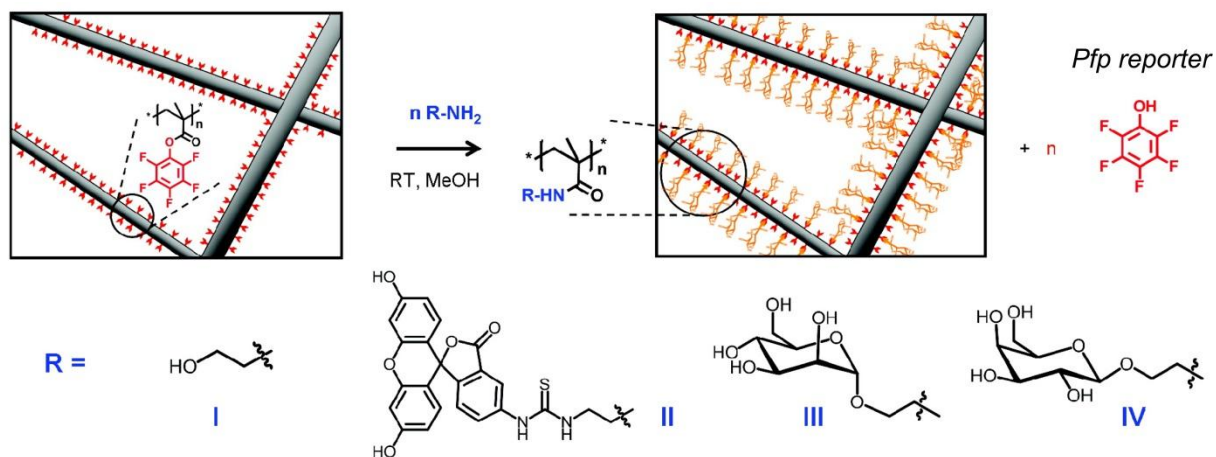


Figure 12. Fiber meshes for multivalent carbohydrate presentation. Functionalization of poly(pentafluorophenyl methacrylate) and poly(ϵ - caprolactone) (PCL/PPfpMA) blend fiber meshes with 2-aminoethanol (I), aminofluorescein (II), 2-aminoethyl- α -D-mannopyranoside (III), or β -D-galactopyranoside (IV). Figure obtained from (222).

Indirect sandwich ELISA was performed for the quantification of TNF- α . Antibody pairs and cytokine standards were from PeproTech and the protocol was performed according to the manufacturer's instructions. After incubation with the detection antibody, plates were washed three times and incubated with Avidin-HRP at RT for 30 minutes. ELISA development was performed by using the ABTS substrate. Absorbance was measured with an ELISA plate reader at 405 nm (reference wavelength 650 nm).

2.2.3.8 Stable transfection into CHO cells

CHO cells were stably transfected with plasmid DNA using the LipofectamineTM reagent according to the manufacturer's protocol for transfection in a 6-well plate format. 1×10^6 CHO cells in 500 μ l complete antibiotics-free RPMI medium were plated on each well. 2.5 μ g of plasmid DNA was added followed by the addition of 10 μ l of LipofectamineTM. The cells were incubated for 24 hours before adding 250 μ g/ml zeocin. After a few days, the medium of the surviving cells was replenished with complete RPMI medium with 250 μ g/ml zeocin.

To check the protein expression of transfected DNA into cells, intracellular staining was done following the procedure as outlined in the BD Cytofix/CytopermTM

Fixation/Permeabilization Kit. Briefly, cells were incubated with 100 μ l Fixation/Permeabilization buffer at 4°C for 20 minutes. The cells were then washed two times with 1x PermWash buffer (10x PermWash provided in the kit; buffer was diluted down to 1x by addition of water). The cells were incubated with 50 μ l of polyclonal goat anti-human IgG Fc-PE, diluted 1:20 in PermWash at 4°C for 20 minutes, followed by washing 2 times with 1x PermWash buffer. The cells were resuspended in FACS staining buffer and subsequent measurement was done by flow cytometry using FACSCanto™ II flow cytometer.

2.2.3.9 Fusion protein production in bioreactors

CHO cell lines expressing CLR-Fc proteins were cultivated in CELLline CL 350 bioreactors according to the manufacturer's procedure. The bioreactor was equilibrated by adding 10 ml of nutrient medium (complete RPMI with 250 μ g/ml zeocin and depleted of bovine IgG) into the inner compartment and letting it stand for 5 minutes. 8×10^6 CHO cells were suspended in 5 ml of nutrient medium and placed in the inner compartment. 80 ml of complete RPMI medium with 250 μ g/ml zeocin was added into the outer compartment. Cell harvests were done every week for 8 weeks. During each harvest, the nutrient medium was collected while some cells were placed back into the inner compartment with fresh nutrient medium. Cells were monitored for growth and production by removing a small sample of cells and testing for protein expression by flow cytometry.

2.2.3.10 Isolation of spleen cell subsets

Spleens were removed from sacrificed mice and, using a fine needle, spleen cells were flushed with complete RPMI. The cells were passed through 40- μ m cell strainers to filter out cell aggregates and centrifuged at $300 \times g$ for 5 minutes. The cell pellets were resuspended in erythrocyte lysis buffer and incubated at RT for 3-5 minutes. Cells were washed with complete RPMI and resuspended in MACS buffer. Spleen cells from C67BL/6 mice were incubated with anti-CD16/32 to block cell surface Fc γ RII/RIII receptors. CD11c⁺ DCs were obtained from C57BL/6 mice spleen and T cells from OT-II transgenic mice by magnetic-activated cell sorting (MACS) using CD11c microbeads and Pan T Cell Isolation Kit II, respectively. Cells which bound to the magnetic microbeads were loaded onto a column placed in a magnetic field and unbound cells were washed away with MACS buffer. CD11c⁺ cells were eluted by taking of the column from the magnetic field and flushing with MACS buffer. The procedure was repeated using the eluted CD11c⁺ cells and applying on a 2nd column to increase the purity. To isolate T cells, non-target cells were magnetically labeled

and T cells were allowed to flow through. Isolated cell subsets were then centrifuged and resuspended in complete IMDM.

2.2.3.11 *In vitro* stimulation by OVA-carbohydrate conjugates

MACS purified CD11c⁺ cells were seeded on a 96-well round bottom culture plate at a concentration of 2×10^4 cells/well in complete IMDM. 30 minutes later, cells were pulsed with OVA and OVA conjugates at a final concentration of 30 µg/ml. After one hour, MACS purified T cells were added. Activation of CD11c⁺ cells and T cells were then analyzed by flow cytometry after 48 and 72 hours. To measure the cytokines in the supernatant, ELISA was performed.

2.2.4 *In vivo* studies

2.2.4.1 Ethics statement

Animal experiments were performed in strict accordance with the German regulations of the Society for Laboratory Animal Science (GV-SOLAS) and the European Health Law of the Federation of Laboratory Animal Science Associations (FELASA). The protocol were approved by the Landesamt für Gesundheit und Soziales (LAGeSo) Berlin. All efforts were made to minimize suffering.

2.2.4.2 Adoptive transfer

Splenic cells were obtained from 10-week old female OT-II transgenic mice and the erythrocytes were lysed in lysis buffer. The cells were washed twice with PBS to remove any serum and resuspended in PBS at twice the desired final concentration of 1×10^7 cells/ml. A solution of 10 µM Cell Proliferation Dye eFluor[®] 670 in the same volume as the cells was prepared. While vortexing the cells, the dye was then mixed 1:1 with the 2x cell suspension to obtain a final concentration of 5 µM. The mixture was incubated at 37°C in the dark for 10 minutes. The labeling was stopped by adding 4-5 volumes of cold complete RPMI medium and incubated on ice for 5 minutes. The cells were washed three times with complete medium and resuspended in PBS at 1.5×10^7 labeled cells in 100 µl.

1.5×10^7 labeled cells were injected i.v. into female wild-type C57BL/6 mice, 10 to 12 weeks old. To verify if the transfer of cells was successful, heparinized tail blood was obtained from the recipient mice 2 hours after the i.v. injection. Labeling was checked using flow cytometry.

2.2.4.3 Immunization

24 hours after the adoptive transfer of labeled OT-II transgenic spleen cells into wild-type C57BL/6 mice, pre-immunization sera were obtained from the recipient mice. These mice were then immunized by i.p. injection with PBS, 22 µg OVA, OVA-Alum (22 µg OVA; 1:1 mixture of OVA and Alum), 22 µg OVA-Lewis X, 22 µg OVA-1,3-lactosamine, or 22 µg OVA-Gb5. Days 7 and 13 post-immunization sera were also obtained.

2.2.4.4 Stabilate preparation

Fresh stabilates were prepared by infection of the MRA-311 PbA stabilate through Balb/c mice. On day 12 post-infection, mice were sacrificed and the pooled heparinized blood was collected. Stabilates containing 1×10^7 PbA-infected erythrocytes in stabilate buffer were frozen in liquid N₂ until further use.

2.2.4.5 PbA infection of mice

Female DCIR^{-/-}, SIGNR3^{-/-}, or C57BL/6 wild-type mice, 6-8 weeks old, were infected by i.p. injection of 1×10^6 PbA-infected erythrocytes as described previously (223). Parasitemia was determined by examining Wright-stained tail blood smears on glass slides, and results were expressed as the percentage of infected red blood cells. Mice were monitored daily for early signs of CM. C57BL/6 mice infected with blood stages of PbA are known to develop neurological symptoms such as ataxia, convulsions, and coma. Accordingly, in our study about 80% of PbA-infected wild-type mice exhibited signs of CM between day 8 and day 10 p.i. Mice were immediately euthanized in case of clinical symptoms of CM such as ataxia to avoid unnecessary suffering.

2.2.4.6 Brain histology

On day 7 post-infection, infected mice were sacrificed and the brains were removed. Sections were fixed in neutrally buffered 4 % formaldehyde, in Davidson's fixative solution for at least 24 hours, or were placed in tissue freezing medium. Tissues were routinely embedded in paraffin and tissue sections of 2 µm size were cut. These sections were subsequently stained with haematoxylin and eosin (H&E) according to standard protocols.

CD3 and CD31 immunostaining on paraffin or Davidson's sections was performed using the ABC method as previously described (224). Primary antibodies were diluted in Tris-buffered saline (TBS, 50 mM, pH 7.6). Polyclonal rabbit anti-human CD3, diluted 1:1500 in PBS, and polyclonal rat anti-mouse CD31, diluted 1:100, required a microwave/citric acid-

pretreatment. Both primary antibodies were incubated at 4°C overnight after a blocking step with 50% goat serum in TBS at RT for 30 minutes. The secondary antibodies, goat anti-rat, goat anti-rabbit and goat anti-mouse were used at a dilution of 1:200 in TBS and incubated at RT for 1 hour. Diaminobenzidine tetrahydrochloride was used as chromogen and slides were counterstained with haematoxylin. For negative controls, sections were incubated without a primary antibody or with an irrelevant rabbit anti-murine calcium-activated chloride channel (CLCA) antiserum. CD3 staining was scored as 1, 2, and 3 indicating very few, single positive lymphocytes, few, scattered, positive lymphocytes, and frequent, single and small accumulations of lymphocytes, respectively. Scoring for CD31 was 0 and 1 corresponding to the absence and presence of endothelial cells, respectively. Presence of intravascular leukocytes, endothelial activation and vessel wall hyalinization was evaluated in sagittal H&E-stained sections of the cerebrum and cerebellum. Presence of intravascular leukocytes was evaluated positive (score 1) if the majority of intracerebral and -cerebellar vessels contained more than one nucleated cell or were otherwise scored as 0. CD3 staining was used to increase the sensitivity of intravascular and perivascular lymphocyte detection. Sections were evaluated as positive (1) if the majority of vessels contained one or more CD3-positive cells or otherwise scored as 0.

2.2.4.7 Determination of spleen and brain cell populations

On day 7 post-infection, infected mice were sacrificed and spleens were removed. Red blood cells were lysed by addition of lysis buffer. Staining was performed by using anti-mouse CD4-FITC, anti-mouse CD8-APC-H7, anti-mouse CD62L-PE, and anti-mouse CD69-PerCP-Cy5.5. Cells were analyzed flow cytometry.

For analysis of cell populations in brain, brains were homogenized and erythrocyte lysis was done by addition of ammonium chloride. Staining was done by using anti-mouse CD45-PerCP-Cy5.5, anti-CD8-APC-H7, and anti-CD62L-PE. Cells were analyzed by flow cytometry as described. Initial gating was performed on CD45⁺ cells, and subsequently the number of CD45⁺CD8⁺CD62L^{low} cells was quantified.

2.2.4.8 Binding studies with pRBCs

For DCIR/pRBCs interaction studies, heparinized blood was taken from a highly parasitemic C57BL/6 mouse and RBCs were fluorescently labeled with Cell Proliferation Dye eFluor 670 according to manufacturer's instructions. 1 µl of Protein A-coated fluorescent

particles was incubated with 5 μg of mDCIR-hIgG1Fc at RT for 1 hour, followed by incubation with 1×10^5 fluorescently labeled RBCs at 4°C for 1 hour. Binding of fluorescently labeled pRBCs to the DCIR-Ig-Protein A particle was measured by flow cytometry.

2.2.5 Statistical analysis

Statistical analyses were performed using GraphPad Prism (GraphPad Software, Inc., La Jolla, CA, USA). Unpaired Student's *t* test was used for analyzing data with nominal values. Unpaired Mann Whitney U test was used for analyzing data with ordinal scaling.

3. Results

3.1 Lectin targeting

Lectin-carbohydrate interactions play a pivotal role in numerous biological systems, thus a deeper understanding of these interactions will provide critical insight into the biological processes involved such as cell communication, proliferation, differentiation, and host-pathogen interactions (225). The weak affinity of lectin-carbohydrate binding serves as a challenge to develop tools and techniques to allow for sophisticated investigation of lectin-carbohydrate complexes. One way to circumvent this weakness is to utilize multivalent presentation of carbohydrates on different carrier systems such as dendrimers (226), micelles (227), quantum dots (81), and cavity-containing templates (228). In this way, the weak interactions can be amplified and significantly enhance the binding effectiveness of the carbohydrate ligands. The potency of multivalent carbohydrate-functionalized systems was elucidated. This was done by first investigating the affinity and kinetics of binding of known lectin-carbohydrate interactions, and then taking it further by looking into the drug delivery as well as immunomodulatory functions of such systems. With this information in hand, the interactions of CLR and their novel carbohydrate ligands could then be examined. For this purpose, the CLR, in the form of fusion proteins, were first produced and then used for ligand identification, followed by binding and immunological evaluation.

3.1.1 Affinity and kinetics of lectin-multivalent carbohydrate system interaction

Multivalent carbohydrate presentation and lectin binding were first examined using ruthenium(II)-cyclodextrin-mannose (RuCdMan) complexes and the mannose-specific plant lectin Concanavalin A (ConA). ConA, present in the legume *Canavalia ensiformis*, is a lectin which binds specifically to terminal mannose and, to a weaker extent, glucose. Given its characteristic binding strength and affinity to mannose, it serves as a convenient tool to explore multivalent carbohydrate interactions. The complexes comprised of a fluorescent ruthenium(II) core surrounded by two, four, or six heptamannosylated cyclodextrin scaffold referred to as RuCdMan14, RuCdMan28, and RuCdMan42, respectively (Figure 9) (220). An RuCd-based scaffold that can accommodate different carbohydrate densities provides the appropriate system to function as the ligand. The template is derived from $[\text{Ru}(\text{bipy})_2]\text{Cl}_2$ to afford a di-adamantyl-(Ru2), tetra-adamantyl-(Ru4), or hexa-adamantyl-(Ru6) ruthenium complex. Around this core, the Cds, each equipped with seven mannose units to form heptamannosylated Cd (CdMan), self-assemble around the template as the adamantane

“hosts” the Cd “guests” around the template. In order to understand the influence of carbohydrate density on lectin binding, multivalent carbohydrate presentation on Cds can be used to investigate carbohydrate-lectin interaction.

To understand the influence of mannose density on lectin binding at the surface of the RuCdMan complexes, the interaction of the complexes with ConA was investigated (229). SPR measurements were performed to obtain a quantitative insight into the role of mannose multivalency in ConA binding. SPR kinetic analyses were based on a 1:1 Langmuir interaction model. This is the simplest model which describes the interaction between the immobilized ligand (ConA) and the analyte (Ru complexes). It predicts that the association and disassociation phases are monoexponential. It has the advantage of allowing slight deviations from the raw data, such as baseline drifts, and even takes into account mass transport limitations. The suggested strategy is to start out with this model and see whether the data fits the curve consistent with this model. If so, then the calculated results obtained can be considered. If the curves are not fitted, then alternative models can be used for more complex interaction patterns (230). Two different concentrations were covalently bound to a polycarboxylated CM5 sensor chip generating low-density (ConA-LD) and high-density (ConA-HD) surfaces. ConA has four mannose binding sites. Immobilizing the lectin at low and high densities was intended to distinguish whether the presence of more mannose-binding sites would stabilize bound complexes, or whether binding site clustering would inhibit this interaction. The SPR analyses of ConA-RuCdMan14 and ConA-RuCdMan28 (Figure 13 and Table 1) indicated that both complexes strongly prefer to bind to ConA-HD over ConA-LD, indicating that high ConA concentration stabilized the binding interaction. This trend correlates well with the prior characterization of ConA binding to mannose (231). Closer examination shows that RuCdMan28 binds to ConA-HD more efficiently than to RuCdMan14 (Figures 13C and D), and also that RuCdMan14 dissociates from ConA much faster than RuCdMan28 (Figures 13A and B). For the ConA-LD complex interactions, K_D for ConA-RuCdMan14 is lower than for ConA-RuCdMan28. The difference in the specific K_D values (Table 1) is most likely attributable to the generally weak binding of low ConA concentration than to the individual binding capacity of RuCdMan14 and RuCdMan28. Interestingly, complex RuCdMan42 did not bind to ConA. The binding curves obtained for the interactions between RuCdMan42 and ConA-HD as well as ConA-LD were comparable to the results obtained using only the buffer HEPES-EP as a negative control. This outcome is not entirely surprising, since similar results have been reported for highly multivalent probes (232). In this case, the addition of two mannose-functionalized cyclodextrin units (the structural difference

between complexes ConA-RuCdMan28 and ConA-RuCdMan42) impeded binding with ConA, despite the greater number of mannose residues available for the interaction.

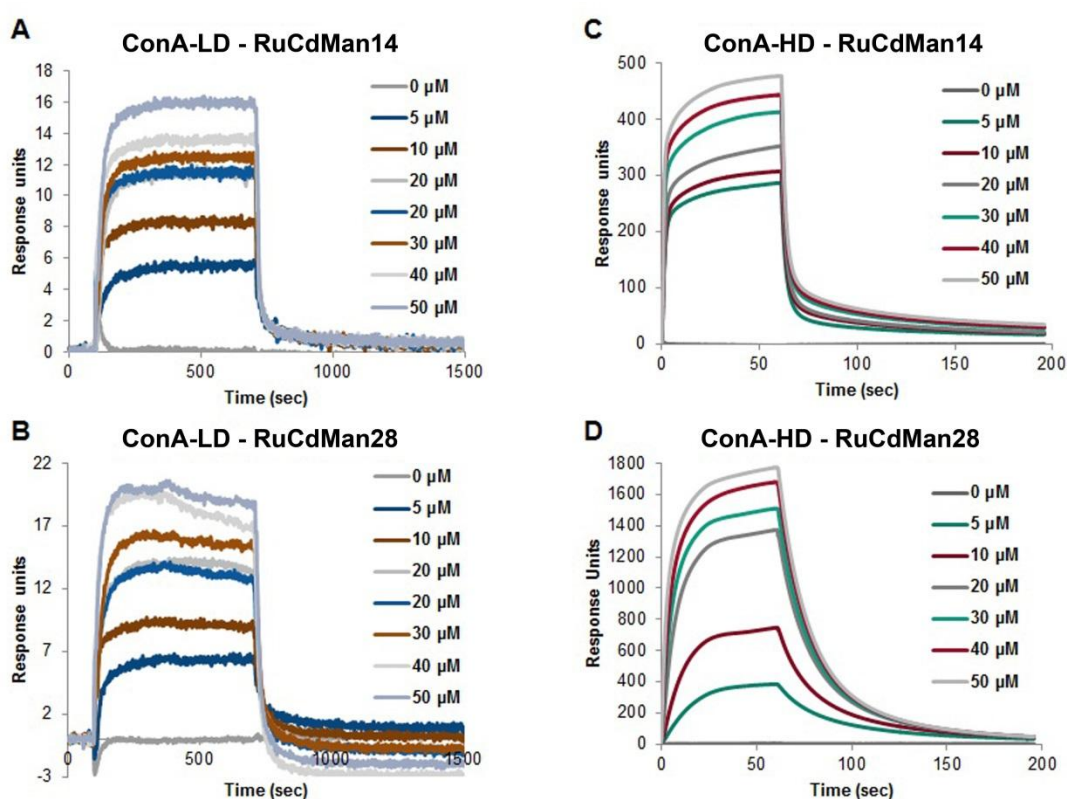


Figure 13. SPR sensorgrams of RuCdMan14 and RuCdMan28 with ConA-LD and ConA-HD. Different concentrations of the Ru complexes were allowed to bind to ConA in low and high densities. Preferential binding was observed in RuCdMan14 to Con A-HD than to Con-LD (**B and C**). A similar tendency was also observed with RuCdMan28 (**C and D**). Furthermore, the binding between RuCdMan28 to Con A-HD was stronger than that of RuCdMan14.

Analyte	K_D (μM)	
	ConA-LD	ConA-HD
RuCdMan14	0.8428	0.2292
RuCdMan28	4.573	0.1380
RuCdMan42	No binding	No binding

Table 1. Equilibrium Dissociation Constants, K_D , of RuCdMan14 and RuCdMan28.

3.1.2 Carbohydrate-functionalized dendrimers and liposomes in *in vitro* cellular uptake and drug delivery

Given the effectiveness of multivalent presentation on carbohydrate ligand binding on ConA, as illustrated in the preceding ConA-RuCdMan interactions, the next step was to probe into the potency of a multivalent system *in vitro* and its utility in drug delivery. The CLR ASGPR was used as a target since it is suitable for liver-specific drug delivery as it is

expressed exclusively by parenchymal hepatocytes (91). ASGPR binds to galactose and GalNAc and the binding strongly depends on the valency of the ligands with a binding hierarchy increasing from monoantennary to tetraantennary ligands (106). Additionally, ASGPR exhibits a 10–50 fold higher affinity to GalNAc compared to galactose residues (107). For targeting ASGPR, cyclodextrins functionalized with galactose dendrimers and liposomes that displayed GalNAc-terminated lipids were used by exploiting multivalent galactose/GalNAc interactions (Figure 10A) (221). Both cyclodextrins and glycoliposomes were equipped with a fluorescent dye, rhodamine B or rhodamine-DHPE, to enable detection of hepatocyte binding and uptake *in vitro*.

The hepatocellular carcinoma cell line HepG2 has been previously employed to investigate ASGPR-mediated uptake of galactosylated polymers and liposomes (233-235). To analyze ASGPR-mediated uptake of cyclodextrin functionalized with glycodendrimers, the hepatocellular carcinoma cell line HepG2 was incubated with three different derivatives of rhodamine B-labeled cyclodextrins: non-functionalized (Cd), mannose-functionalized (Cd-Man) and galactose-functionalized (Cd-Gal). Uptake by HepG2 cells was analyzed by flow cytometry. As expected, the incubation of HepG2 cells with non-functionalized rhodamine B-labeled cyclodextrin did not induce uptake (Figure 14A). Cyclodextrin displaying a mannose dendron was used as a specificity control and indeed, only marginal unspecific uptake of mannose-functionalized cyclodextrin was observed (Figure 14A). In contrast, functionalization of cyclodextrin with galactose dendrons dramatically increased the uptake by HepG2 cells indicating receptor-mediated endocytosis. Liposome-based delivery systems are widely used since liposomes can be loaded with drugs or siRNAs and may be used as efficient carrier systems. Consistently, recent studies have focused on liposomal delivery systems for targeting ASGPR (101, 102). Glycoliposomes were functionalized with rhodamine-DHPE and either GalNAc or GlcNAc (Figure 10B). GlcNAc-functionalized liposomes were used as specificity control. In contrast to the cyclodextrin glycodendrimers where almost no unspecific uptake was observed, background fusion of control liposomes with HepG2 cells was detected to a limited extent (Figure 14B). However, preferential uptake of GalNAc-capped liposomes was observed again indicating specificity of GalNAc-mediated hepatocyte targeting.

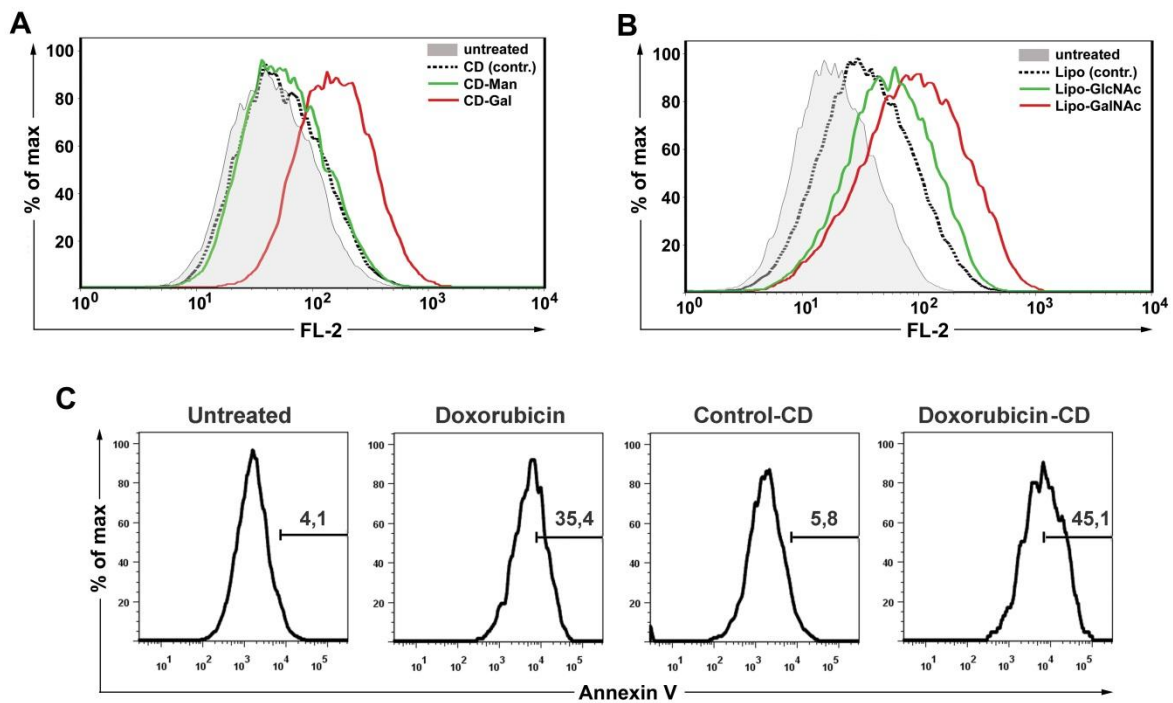


Figure 14. Specific uptake of galactose/GalNAc-functionalized cyclodextrins and liposomes. (A) Targeting of HepG2 cells with cyclodextrin glycodendrimers. HepG2 cells were left untreated (grey area), incubated with 250 nmol rhodamine B-labeled cyclodextrin (dotted line, negative control) or labeled cyclodextrin glycodendrimers containing terminal mannose (green line, specificity control) or galactose residues (red line). Uptake was measured by flow cytometry. Specific uptake of cyclodextrin displaying a galactose dendrimer by HepG2 cells was observed. (B) Targeting of the hepatocellular carcinoma cell line HepG2 with glycoliposomes. HepG2 cells were left untreated (gray area), incubated with rhodamine-DHPE-labeled liposomes (dotted line, negative control) or labeled liposomes containing glycolipids with terminal GlcNAc (green line, specificity control) or GalNAc residues (red line). Uptake was measured by flow cytometry. Preferential uptake of liposomes functionalized with the GalNAc glycolipid was observed. (C) Induction of apoptosis in HepG2 cells treated with doxorubicin-loaded Cd-Gal. Cells were left untreated or were treated with doxorubicin only, Cd-Gal (Control-Cd) or doxorubicin-loaded Cd-Gal (Doxorubicin-CD) for 24 hours. Apoptosis was detected by Annexin-V-APC staining and subsequent measurement by flow cytometry. Bars indicate the frequency of apoptotic cells present in the whole HepG2 cell population. The highest degree of apoptosis was observed in HepG2 cells incubated with Doxorubicin-CD whereas Control-CD induced no apoptosis. Data are representative of three independent experiments.

Cyclodextrin-functionalized systems have been widely explored as molecular vectors for gene (236-238) and drug delivery (239). To evaluate the ability of the aforementioned galactose-functionalized cyclodextrin systems to deliver pharmacologically active species into hepatocytes, Cd-Gal was loaded with doxorubicin (Figure 11), a potent chemotherapy drug used in cancer treatment (240). The potential of this system to induce apoptosis in HepG2 cells was evaluated. Cells were left untreated or were treated with doxorubicin only, Cd-Gal or doxorubicin-loaded Cd-Gal (Figure 14C) for 24 hours. The highest degree of apoptosis was observed in HepG2 cells incubated with doxorubicin-loaded Cd-Gal whereas Cd-Gal alone induced no apoptosis (Figure 4C). This result encourages the use of galactose-functionalized cyclodextrins as a drug delivery system.

3.1.3 Cell stimulation by carbohydrate-functionalized fiber meshes

Mannose-rich glycans of a number of pathogens were reported to be recognized by CLRs such as MR, DC-SIGN, or murine DC-SIGN homologues (216, 241). Specific targeting of HepG2 cells has been achieved by targeting ASGPR using conjugated cyclodextrins and liposomes with carbohydrate ligands galactose and GalNAc. A logical extension of the efficacy of multivalent carbohydrate presentation is its functionality in modulating the immune response by targeting lectins on the cell surface. Fiber meshes consisting of poly(pentafluorophenyl methacrylate) (PPfpMA) and PPfpMA/poly(ϵ -caprolactone) (PCL) blends functionalized with mannose (Figure 12) (222) were utilized to investigate whether LPS-mediated stimulation of APCs, specifically macrophages, could be enhanced. LPS is found in the outer membrane of Gram-negative bacteria and induces cytokine production in antigen-presenting cells through stimulation of the TLR4 signaling pathway (242). To analyze whether macrophage cultivation on the fiber meshes increased cytokine production, freshly prepared mouse peritoneal exudate cells (PECs) consisting mainly of peritoneal macrophages were seeded on the meshes and were stimulated with LPS overnight. Pro-inflammatory cytokines released by APCs upon stimulation such as TNF- α were measured as readout parameters to monitor stimulation of inflammatory pathways. As negative control, aminoethanol-functionalized meshes were included in the study, whereas galactose-functionalized meshes served as specificity control. The meshes alone did not induce the production of TNF- α by macrophages (Figure 14). PEC stimulation in the presence of LPS induced a marked production of TNF- α . However, in the presence of the mannose-functionalized fiber mesh the production of TNF- α was significantly increased. Examining the cytokine profile upon cultivation of cells with carbohydrate-functionalized scaffold provided a means to determine whether multivalent presentation correlates with cell activation. Indeed, the increased levels of TNF- α showed a valency-dependent modulation of PEC functions.

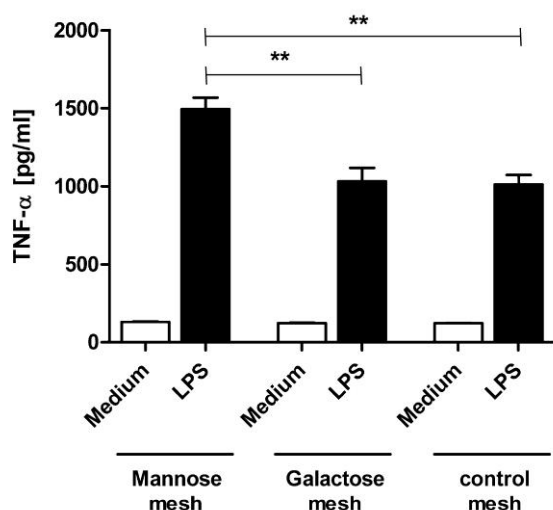


Figure 14. TNF- α production by peritoneal exudate cells (PEC) after stimulation with LPS in combination with the functionalized meshes. PECs were seeded on the meshes and stimulated in the presence (black bars) or absence (white bars) of 10 ng/mL LPS overnight. TNF- α was measured in supernatants of stimulated macrophages. Measurements were performed in triplicates. Data are expressed as mean \pm standard error of mean. Significance was tested with the one-tailed unpaired Student's *t* test (**: $p < 0.01$).

3.1.4 Platform for CLR targeting for immune modulation

Given the state-of-the-art in defining lectin-carbohydrate interactions and the information that can be acquired from them, as illustrated above, I sought to apply the same rationale in order to present a platform that brings together novel CLR ligand identification and their immunological evaluation.

3.1.4.1 Production of CLR fusion proteins

The CLRs DCIR, Clec12b, Dectin 1, M1CL, and M2CL contain a single CRD having a Ca^{2+} binding site and carbohydrate binding ability in their extracellular regions (42). Soluble human IgG Fc fusion proteins have been widely used as a versatile tool for *in vitro* and *in vivo* applications such as immunotherapy, pharmacokinetics, and immunohistochemistry (243). The Fc fragment, which exhibits independent folding, confers stability and functionality on the attached proteins. This stability can enable the expression of proteins in mammalian systems that could be otherwise difficult (244). Aside from the ease in production and purification these fusion proteins provide, they also form dimeric complexes in solution, thus display a higher binding avidity, and are easily detectable due to the Fc fragment. Fusion proteins were generated consisting of the extracellular region of Dectin 1, DCIR, M1CL, M2CL, or Clec12b and the Fc part of human IgG1. The different constructs were expressed in stably transfected CHO cells. The expression of the fusion proteins was verified by flow cytometry after intracellular staining with anti-human IgG-PE (Figure 15).

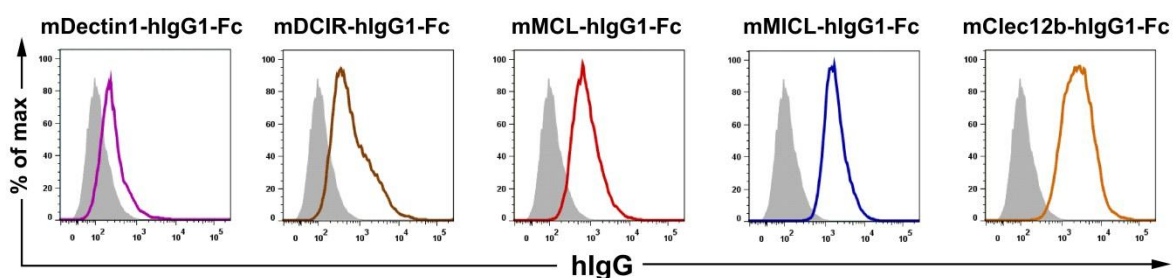


Figure 15. Eukaryotic expression of fusion proteins in CHO cells. In order to confirm the eukaryotic expression of the fusion proteins, intracellular staining was done on stably transfected CHO cells using goat anti-human IgG-PE. Subsequent measurement was done by flow cytometry. Grey area corresponds to untransfected CHO cells which served as negative control.

The fusion proteins were purified from the cell supernatant over a protein G column. Production of the fusion proteins was confirmed by Western Blot using anti-human IgG-HRP (Figure 16). The calculated masses of mDectin1-hlgG1-Fc, mDCIR-hlgG1-Fc, mMCL-

hIgG1-Fc, mMICL-hIgG1-Fc, and mClec12b-hIgG1-Fc were 39 kDa, 42 kDa, 38 kDa, 49 kDa, and 42 kDa, respectively.

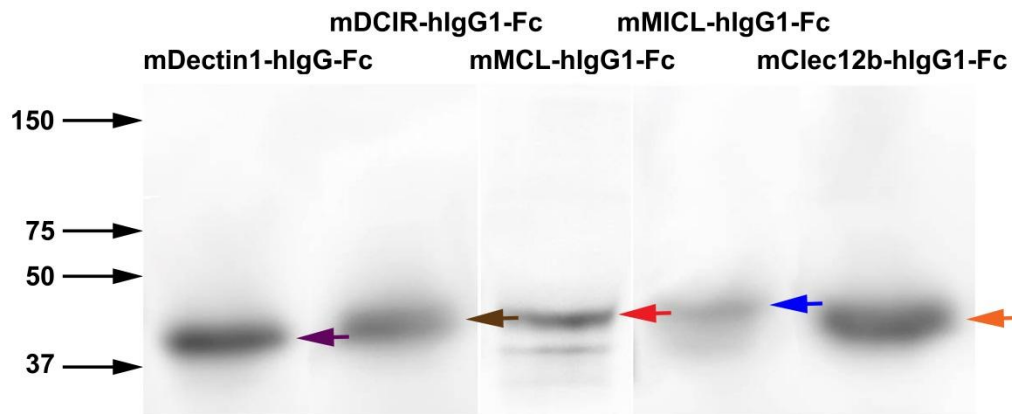


Figure 16. Production and purification of fusion proteins. Supernatants of stably transfected CHO cells were purified and Western Blot analysis was performed to check the success of the production. The arrows correspond to the calculated masses of each fusion protein. The calculated masses of mDCIR-hIgG1-Fc, mClec12b-hIgG1-Fc, mDectin1-hIgG1-Fc, mMICL-hIgG1-Fc, and mMCL-hIgG1-Fc are 39 kDa, 42 kDa, 38 kDa, 49 kDa, and 42 kDa, respectively.

Dectin 1 recognizes β -1,3-glucans derived from zymosan as well as intact yeast particles (245). In order to check the functionality of the mDectin1-hIgG1-Fc fusion protein as well as to verify that the method to produce the fusion proteins did indeed generate functional proteins with correct folding of the extracellular region, ELISA was performed using intact zymosan to capture Dectin 1. Using hIgG1-Fc as a control, mDectin1-hIgG1-Fc showed binding to zymosan (Figure 17). No additional functionality studies for the other CLR-hIg1-Fc fusion proteins were performed since their ligands are unknown.

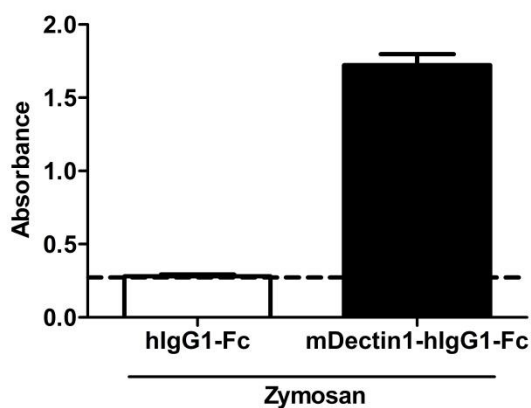


Figure 17. Verification of functionality of Dectin 1. ELISA was performed to verify the functionality of mDectin1-hIgG1-Fc. The wells were coated with zymosan and incubated with hIgG1-Fc, mDectin1-hIgG1-Fc, or buffer. mDectin1-hIgG1-Fc showed a markedly high absorbance indicative of binding to zymosan. Dashed lines represent the absorbance after incubation with buffer only.

3.1.4.2 Glycan microarray reveals novel ligands of CLRs

Screening for carbohydrate ligands for mDectin1-hIgG1-Fc, mDCIR-hIgG1-Fc, mMCL-hIgG1-Fc, mMICL-hIgG1-Fc, mClec12b-hIgG1-Fc, and mMGL1-hIgG1-Fc (fusion protein obtained from Magdalena Eriksson) was performed using a glycan array analysis consisting of 52 monosaccharides, disaccharides, sialylated oligosaccharides, sulfated saccharides, heparins (208, 209), blood group antigens (211), high mannose structures (213), lipoarabinomannan (214, 215), phosphatidylmyo-inositol mannosides (PIMs) (216), and tumor antigens (217, 218) (SI1.2). The glycans were immobilized through their amino- and thiol-functional groups on epoxy slides in triplicates, incubated with the fusion proteins, followed by addition of anti-hIgG-Alex Fluor 488. The binding read-out, in mean fluorescent intensity (MFI), was measured by a fluorescent scanner. A summary of the MFI of the glycan screening of the fusion proteins is shown in Figures 18 and 19. Figure 18 indicates the binding of the fusion proteins based on the terminal carbohydrates, while Figure 19 indicates binding to the general structure of each glycan. Each glycan is assigned a microarray identification (ID) number. All CLRs bound to the heparin structures; since heparins are highly charged, the binding can be accredited towards a charge-charge interaction. There were no ligand hits for Dectin 1, DCIR, and MCL among the glycans in this array. Nevertheless, MICL, Clec12b, and MGL1 did indeed show binding to some of the glycans. MICL showed binding affinity towards terminal galactose (21), glucose (41), GlcNAc (42), and more interestingly to PIM structures, PIM₂ (46) and PIM₃ (47) (Table 2). Clec12b exhibited binding to terminal GlcNAc (42), GalNAc (20) and to terminal galactose (18, 21, 32, 40, and 50 or Gb5). For its binding to terminal mannose, it showed that it recognized both α 1-3 (27) and β 1-6 (35, 45, and 46) linkages (Table 3). On the other hand, it showed affinity towards terminal galactose with β 1-4 (17 and 32) and β 1-3 (18, 21, 40, and Gb5) linkages. MGL1 bound to terminal GalNAc (20), and to a remarkable extent, to terminal galactose (17, 18, 19, 21, 22, 23, 40, and Gb5) (Table 4). It bound to different terminal galactose linkages: β 1-2 (22), β 1-4 (17 and 19), and β 1-3 (18, 21, 23, 40, and Gb5), essentially demonstrating no specific affinity towards a particular linkage. Of importance to note, binding of MGL1 to carbohydrates with terminal galactose is markedly stronger than that of Clec12b that it is prudent to acknowledge this difference.

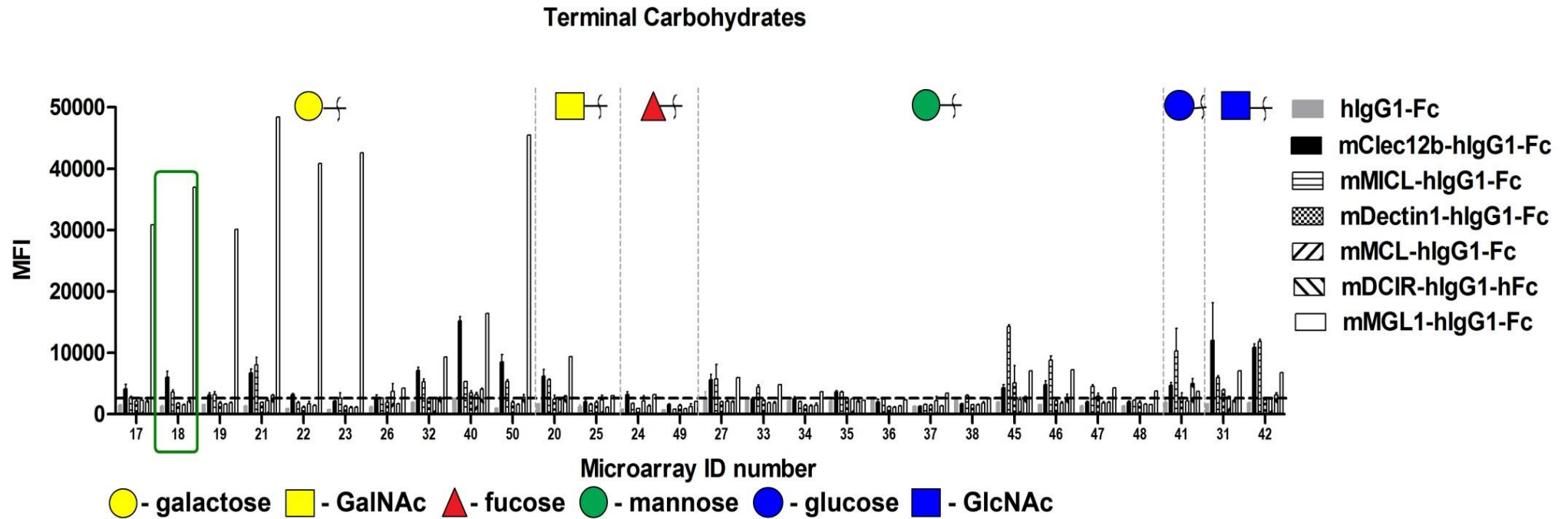


Figure 18. mMGL1-hlgG1-Fc and mClec12b-hlgG1-Fc showed strong and weak binding, respectively, to 1,3-lactosamine (boxed in green). Analysis of carbohydrate ligands of mDectin1-hlgG1-Fc, mDCIR-hlgG1-Fc, mMCL-hlgG1-Fc, mMICL-hlgG1-Fc, mClec12b-hlgG1-Fc, and mMGL1-hlgG1-Fc on a 52-sugar microarray based on the terminal carbohydrates. The amino- and thiol-functionalized carbohydrates were printed in triplicates on epoxy-coated glass slides. The fusion proteins were incubated on the slide. Detection was done by incubation with anti-hlgG-Alex Fluor 488. Results are shown as MFI \pm SEM.

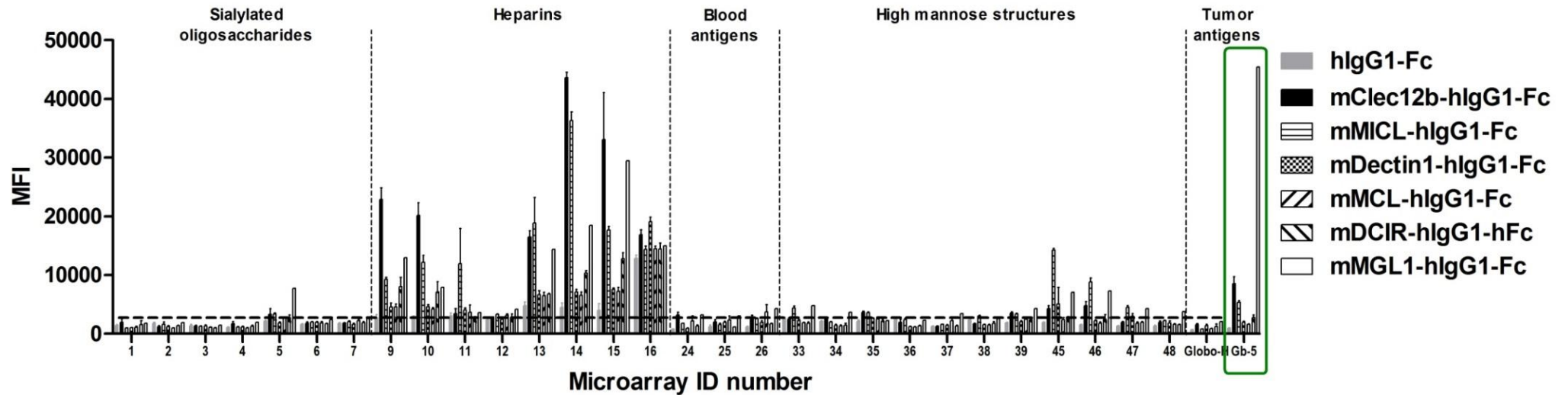


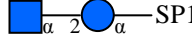
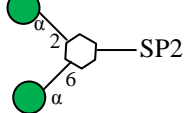
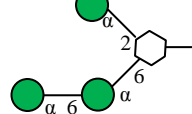


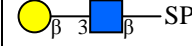

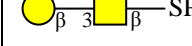
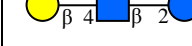
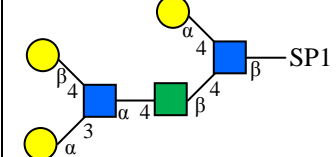
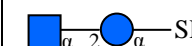
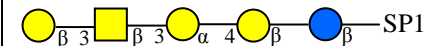
Figure 19. mMGL1-hIgG1-Fc and mClec12b-hIgG1-Fc showed strong and weak binding, respectively, to glycan 50 (Gb5) (boxed in green). Analysis of carbohydrate ligands of mDectin1-hIgG1-Fc, mDCIR-hIgG1-Fc, mMCL-hIgG1-Fc, mMICL-hIgG1-Fc, mClec12b-hIgG1-Fc, and mMGL1-hIgG1-Fc on a 52-sugar microarray based on the general structure of the glycans. The amino- and thiol-functionalized carbohydrates were printed in triplicates on epoxy-coated glass slides. The fusion proteins were incubated on the slide. Detection was done by incubation with anti-hIgG-Alex Fluor 488. Results are shown as MFI \pm SEM.

Table 2. Carbohydrates with relatively high binding affinity to MICL.

ID Number	Structure	MFI \pm SEM
21	 Gal(β 1-3)GalNAc β 1-O(CH ₂) ₅ SH	8072 \pm 1202
41	 Glc(β 1-4)Glc β 1-O(CH ₂) ₅ SH	10298 \pm 3727
42	 GlcNAc(α 1-2)Glc α 1-O(CH ₂) ₅ SH	11911 \pm 331
46	 Man(α 1-2)[Man(α 1-6)] <i>myo</i> -Ins1-OPO ₃ H(CH ₂) ₆ SH (PIM ₂)	8796 \pm 732
47	 Man(α 1-6)Man(α 1-6)[Man(α 1-2)] <i>myo</i> -Ins1-OPO ₃ H(CH ₂) ₆ SH (PIM ₃)	4507 \pm 308

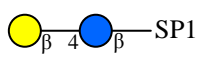
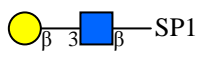
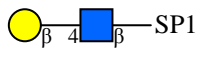
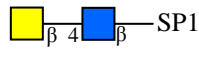
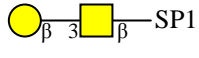
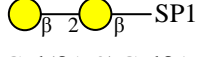
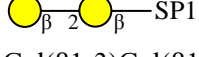
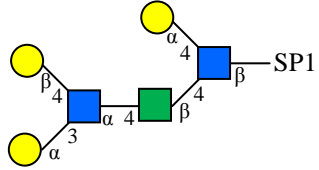
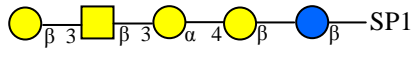
Spacers: SP1: -O(CH₂)₅SH; SP2: -OPO₃H(CH₂)₆SH

Table 3. Carbohydrates with relatively high binding affinity to Clec12b.

ID Number	Structure	MFI \pm SEM
18	 Gal(β 1-3)GlcNAc β 1-O(CH ₂) ₅ SH (1,3-lactosamine)	6003 \pm 1038
20	 GalNAc(β 1-4)GlcNAc β 1-O(CH ₂) ₅ SH	6205 \pm 1104
21	 Gal(β 1-3)GalNAc β 1-O(CH ₂) ₅ SH	6723 \pm 619
32	 Gal(β 1-4)GlcNAc(β 1-2)Glc α 1-O(CH ₂) ₅ SH	7101 \pm 552
40	 Gal(α 1-3)[Gal(β 1-4)]GlcNAc(α 1-4)ManNAc(β 1-4)[Gal(α 1-4)]GlcNAc β 1-O(CH ₂) ₅ SH	15219 \pm 710
42	 GlcNAc(α 1-2)Glc α 1-O(CH ₂) ₅ SH	10887 \pm 579
50	 Gal(β 1-3)GalNAc(β 1-3)Gal(α 1-4)Gal(β 1-4)Glc β 1-O(CH ₂) ₅ SH (Gb5)	8523 \pm 1220

Spacer: SP1: -O(CH₂)₅SH

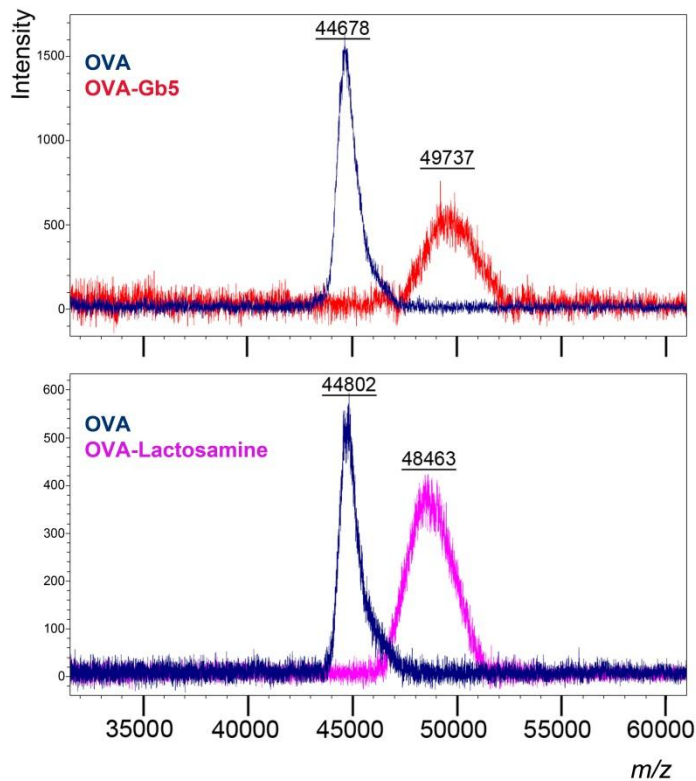
Table 4. Carbohydrates with relatively high binding affinity to MGL1.

ID Number	Structure	MFI \pm SEM
17	 Gal(β 1-4)Glc β 1-O(CH ₂) ₅ SH	30912 \pm 3335
18	 Gal(β 1-3)GlcNAc β 1-O(CH ₂) ₅ SH (1,3-lactosamine)	37028 \pm 2589
19	 Gal(β 1-4)GlcNAc β 1-O(CH ₂) ₅ SH	30165 \pm 1779
20	 GalNAc(β 1-4)GlcNAc β 1-O(CH ₂) ₅ SH	9397 \pm 1008
21	 Gal(β 1-3)GalNAc β 1-O(CH ₂) ₅ SH	48430 \pm 1731
22	 Gal(β 1-2)Gal β 1-O(CH ₂) ₅ SH	40842 \pm 3037
23	 Gal(β 1-3)Gal(β 1-4)Glc β 1-O(CH ₂) ₅ SH	42618 \pm 2332
40	 Gal(α 1-3)[Gal(β 1-4)]GlcNAc(α 1-4)ManNAc(β 1-4)[Gal(α 1-4)]GlcNAc β 1-O(CH ₂) ₅ SH	16453 \pm 3645
50	 Gal(β 1-3)GalNAc(β 1-3)Gal(α 1-4)Gal(β 1-4)Glc β 1-O(CH ₂) ₅ SH (Gb5)	45459 \pm 8770

Spacer: SP1: -O(CH₂)₅SH

3.1.4.3 Carbohydrate modification of OVA enhanced T_H1 cytokine production *in vitro*

The screening for novel CLR ligands was a collaborative approach performed jointly with Magdalena Eriksson. The results for the *in vitro* and *in vivo* analyses are also described in (246). It has been shown that DCs pulsed with the native glycosylated form of the OVA antigen containing mannose moieties targeted antigen to the MR to induce cross-presentation (247). I sought to examine OVA modified by the newly identified ligands of MGL1 and Clec12b, 1,3-lactosamine or Gb5, the rationale being that the engagement of sugar modified OVA with CLRs on DCs will enhance antigen uptake and activation of DCs, thereby influencing MHC-II presentation and CD4⁺ T cell proliferation. OVA was conjugated with



either 1,3-lactosamine or Gb5 using the DSAP linker and the conjugation, as verified by MALDI (Figure 20), revealed that 4.6-4.8 sugars were attached to OVA.

Figure 20. MALDI analysis of OVA (blue) conjugated with Gb-5 (red, upper panel) and 1,3-lactosamine (pink, bottom panel) revealed that an average of 4.6-4.8 sugars per OVA molecule were conjugated.

Co-culture of CD11c⁺ DCs of wild-type C57BL/6 mice with T cells from OT-II transgenic mice was done followed by incubation with OVA, OVA-Gb5, or OVA-1,3-lactosamine (hereinafter referred to as OVA-lactosamine). T cells from transgenic OT-II mice have a T cell receptor specific for the OVA₃₂₃₋₃₃₉ peptide presented by MHC-II molecule I-A^b, as this is expressed specifically by APCs from C57BL/6 mice. By pulsing wild-type CD11c⁺ DCs cells with whole OVA protein, it is endocytosed and degraded intracellularly. The generated OVA-sugar conjugate is loaded and presented by the MHC-II molecule I-A^b to the TCR thus being recognized by OT-II T cells. By using transgenic OT-II T cells, the T cell response can be analyzed whereas T cells from wild-type mice would exhibit no measurable cytokine production. Interestingly, both OVA-lactosamine and OVA-Gb5 targeted to DCs significantly enhanced the production of IL-2 by OT-II T cells, and in the case of Gb5, to a much higher extent (Figure 21A). Additionally, OVA-lactosamine and OVA-Gb5 also showed a tendency to boost IFN- γ production (Figure 21B). IL-4 was also measured but the results were below detection level.

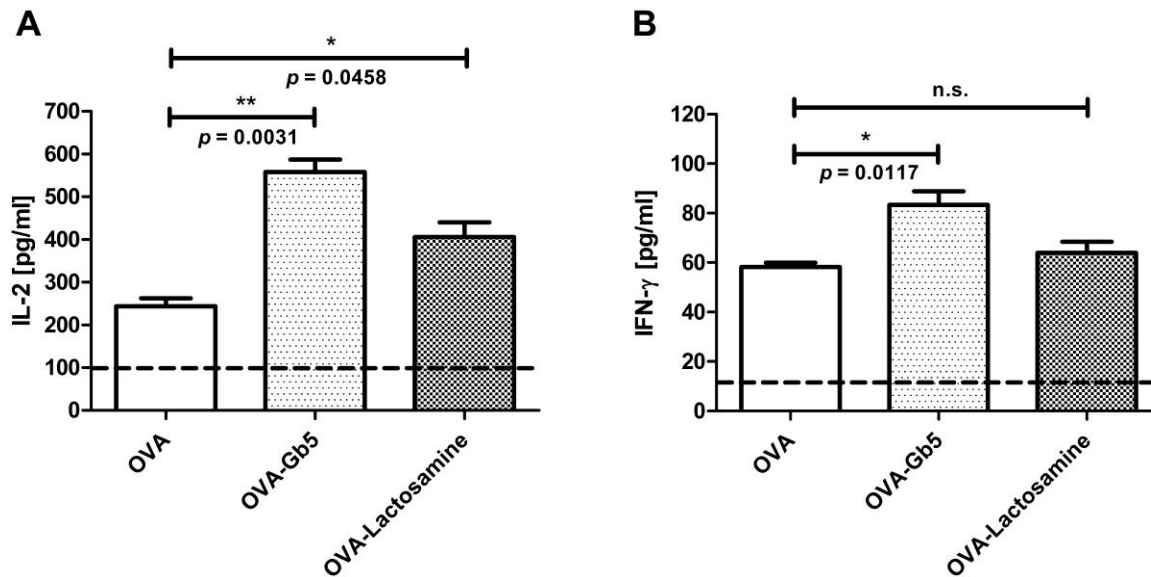


Figure 21. Enhanced T_H1 cytokine production in *in vitro* stimulation with OVA conjugates. CD11c⁺ DCs from C57BL/6 were co-cultured with T cells from OT-II transgenic mice, followed by stimulation with OVA, OVA-Gb-5, or OVA-lactosamine. **(A)** Quantification of cytokines showed a significant increase in IL-2 in both OVA-Gb5 and OVA-lactosamine stimulated cultures. **(B)** IFN- γ production showed a tendency for higher levels in OVA-Gb5 or OVA-lactosamine stimulated cultures compared to OVA alone. Dashed lines represent cytokine levels of unstimulated mouse spleens from C57BL/6 mice which did not undergo adoptive transfer. Data are expressed as mean \pm SEM for each group. Statistical analysis was performed using Student's *t* test (*, $p \leq 0.05$; **, $p \leq 0.001$; *ns* = not significant).

3.1.4.4 CLR targeting *in vivo* using OVA conjugates dampens humoral response

To corroborate the *in vitro* findings, *in vivo* targeting of DCs by MGL1 and Clec12b was performed. Splenic cells were taken from OT-II transgenic mice, labeled with the cell proliferation dye eFluor 670, and adoptively transferred into groups of C57BL/6 mice. Twenty-four hours later, the latter were prime-immunized with PBS, OVA, OVA-Gb5, and OVA-lactosamine. After 21 days, the mice underwent a boost immunization with the same formulations as in the prime immunization. On day 30 post-prime immunization, mice were sacrificed. The serum of each mouse was analyzed for anti-OVA antibody titers by ELISA (Figure 22A). Plates were coated with OVA, followed by incubation with the serum samples, then the detection using AP-labeled anti-mIgG+IgM. The antibody titers taken from mice immunized with OVA-Gb5 and OVA-lactosamine were lower than the mice immunized with OVA only (Figure 22A). To further analyze the IgG subclass the antibodies belong to, the sera were tested to differentiate whether they were IgG₁ or IgG₂ using a similar ELISA procedure as aforementioned only using either AP-labeled anti-mIgG₁ or anti-mIgG₂. For all three groups, OVA, OVA-Gb5, and OVA-lactosamine, the antibodies were classified as mainly IgG₁ (Figure 22B). To analyze cytokine production, the spleen cells were restimulated with OVA₃₂₃₋₃₃₉ peptide and the cytokine levels were quantified by ELISpot. The same tendency in

IL-2 (Figure 23A) and IFN- γ (Figure 23B) production was observed as in the *in vitro* assays, i.e. the levels were higher in mice immunized with OVA-Gb5 and OVA-lactosamine than with OVA though values did not reach statistical significance. Thus, OVA conjugated with either Gb5 or 1,3-lactosamine might indeed lead to a T_H1 response while modulating T_H2 response.

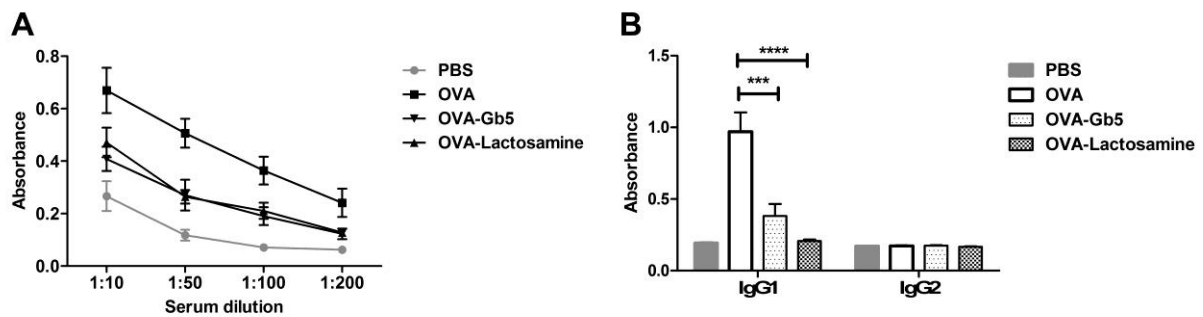


Figure 22. Antibody production is decreased upon immunization with OVA-sugar conjugates. C57BL/6 mice received 1.5×10^7 splenic cells isolated from OT-II transgenic mice. 24 hours after, mice were prime immunized with PBS ($n=3$), 22 μ g OVA ($n=4$), 22 μ g OVA-Gb5 ($n=5$), and 22 μ g OVA-lactosamine ($n=4$). On day 21 post-prime immunization, the mice were given a boost with the same concentrations and formulations of OVA and the OVA conjugates. On day 30, serum samples were analyzed for antibody production by ELISA. (A) Plates were coated with OVA, followed by the incubation of serum samples in different dilutions, thereafter anti-hIgG-AP was added. Mice immunized with OVA-Gb5 or OVA-lactosamine showed less antibody production compared to OVA alone. (B) To identify the subclass of the antibodies produced, the same procedure was performed as in A, but the readout was done using either anti-hIgG₁-AP or anti-IgG₂-AP. The results show that the antibodies produced by mice immunized with either OVA-Gb5 or OVA-lactosamine mainly belong to the IgG₁ subclass. Data are expressed as mean \pm SEM for each group. Statistical analysis was performed using Student's *t* test (****, $p \leq 0.0001$; ***, $p \leq 0.0001$).

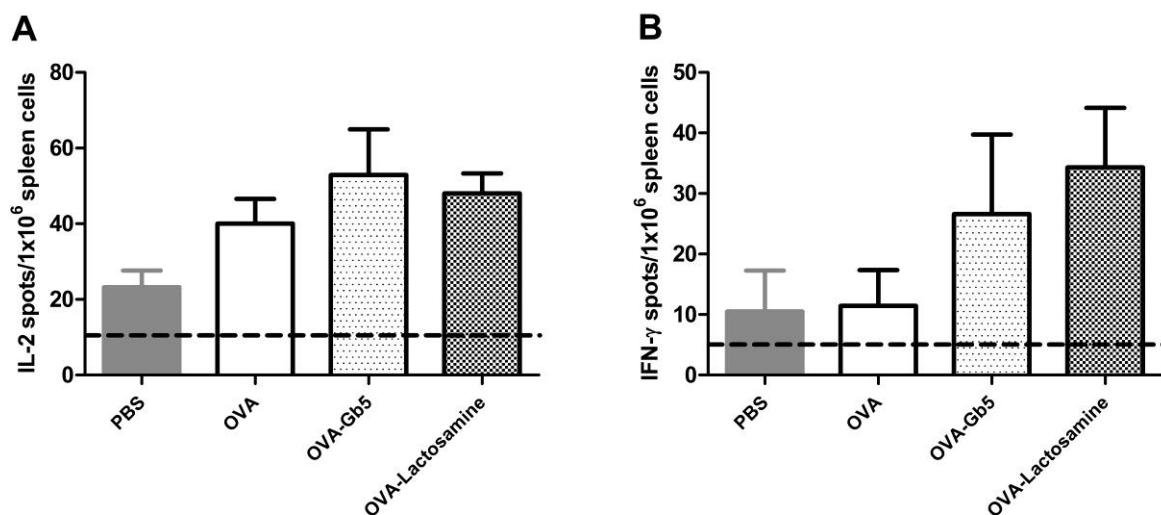


Figure 23. Increasing tendency for IL-2 and IFN- γ production is observed upon immunization with OVA-sugar conjugates. C57BL/6 mice received 1.5×10^7 splenic cells isolated from OT-II transgenic mice. 24 hours after, mice were prime immunized with PBS ($n=3$), OVA ($n=4$), OVA-Gb5 ($n=5$), and OVA-lactosamine ($n=4$). On day 21 post-prime immunization, the mice were given a boost with the same formulations of OVA and the OVA conjugates. On day 30, spleen cells were restimulated with OVA₃₂₃₋₃₃₉ peptide. (A) IL-2 and (B) IFN- γ levels are higher among mice immunized with either OVA-Gb5 or OVA-lactosamine than with OVA alone. Dashed lines represent spot numbers of stimulated mouse spleen cells from C57BL/6 mice which did not undergo adoptive transfer. Data are expressed as mean \pm SEM for each group. Statistical analysis was performed using Student's *t* test. No statistical significance was obtained for any of the groups.

3.2 Role of CLRs in cerebral malaria

The following chapters describe the procedure conducted to determine the role of the CLRs DCIR and SIGNR3 in murine cerebral malaria. Mice deficient in DCIR or SIGNR3 were used for the experiments. Some experiments included all three groups namely DCIR^{-/-} mice, SIGNR3^{-/-} mice, and wild-type mice. For others, only the DCIR^{-/-} or the SIGNR3^{-/-} mice were used as well as the corresponding wild-type mice.

3.2.1 Role of DCIR in cerebral malaria

3.2.1.1 Genotyping of DCIR^{-/-} mice by PCR

The generation of DCIR^{-/-} mice (031932-UCD, DCIR KO/Mmcd) is described in detail on the homepage of the Consortium for Functional Glycomics. For genotyping, PCR, as outlined by CFG, was performed using genomic DNA taken from tail biopsies of C57BL/6 wild-type (DCIR^{+/+}), heterozygous (DCIR^{+/-}), and DCIR-deficient (DCIR^{-/-}) mice. The wild-type band has a size of 748 bp, while the DCIR knockout band is 457 bp (Figure 24).

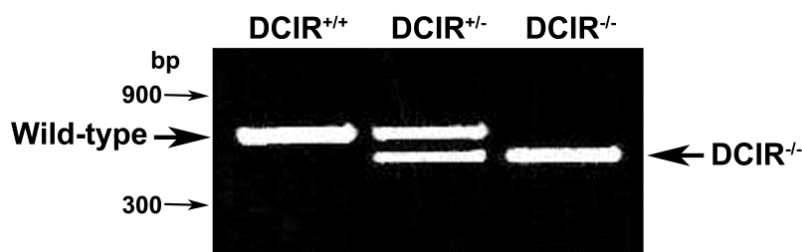


Figure 24. Genotyping of DCIR^{-/-} mice by PCR. Genotyping of DCIR^{-/-} mice was performed by PCR and the genomic DNA acquired from the tail biopsies of DCIR^{+/+}, DCIR^{+/-}, and DCIR^{-/-}. The DCIR^{+/+} band has a size of 748 bp, while the DCIR^{-/-} band is 457 bp.

3.2.1.2 Reduced CM incidence in DCIR^{-/-} mice

The murine C-type lectin receptor DCIR is predominantly expressed by antigen-presenting cells including DCs (44). To elucidate the impact of DCIR deficiency on CM incidence, DCIR^{-/-} mice and the respective wild-type control mice were infected i.p. with PbA and parasitemia and clinical symptoms were monitored daily. The PbA infection model of C57BL/6 mice is currently the model of choice to analyze malaria-associated pathology, namely CM, with survival rates between 0-40% (165, 166). While CM induction occurred in 80% of infected wild-type mice, less than 15% of infected DCIR^{-/-} mice developed neurological symptoms, thus were highly protected from CM (Figure 25A). However, no

difference was observed in the parasitemia levels between DCIR^{-/-} and wild-type mice (Figure 25B) suggesting that DCIR deficiency did not impact parasite replication directly.

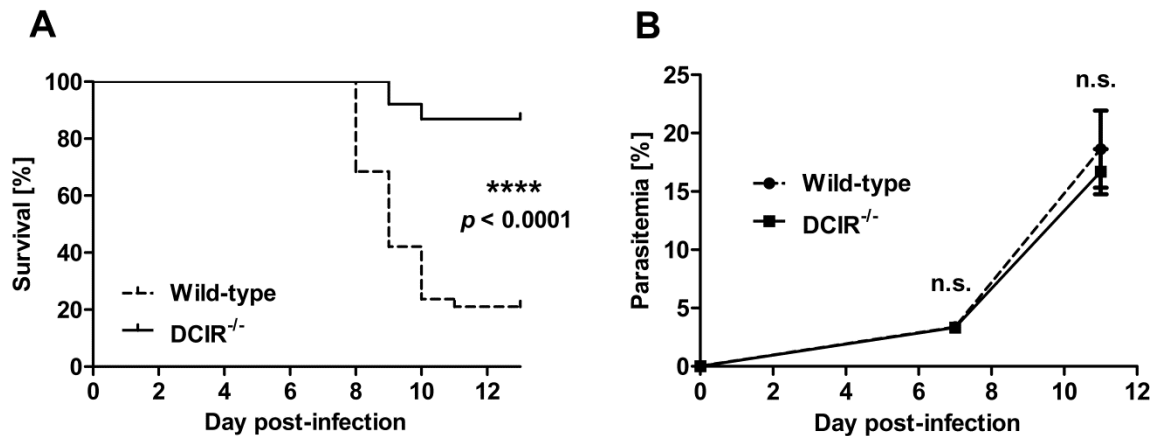


Figure 25. PbA-infected DCIR^{-/-} mice are significantly protected from CM induction. DCIR^{-/-} mice ($n=38$) and the respective C57BL/6 control mice ($n=38$) were infected i.p. with 1×10^6 PbA-infected RBCs. (A) Mice were monitored daily for early signs of CM and were euthanized in case of clinical symptoms such as ataxia, convulsions, or coma. Survival was determined using log rank test (****, $p \leq 0.0001$). The survival curves represent a summary of 5 independent experiments with 5 to 10 mice each. (B) Parasitemia was determined on days 7 and 11 p.i. On day 11 p.i., the number of PbA-infected wild-type mice used for determination of parasitemia was significantly lower ($n=8$) because ~80% of mice had developed CM by that time point. Data are expressed as mean \pm SEM for each group. Statistical analysis was performed using Student's t test (ns = not significant).

3.2.1.3 Reduced T cell sequestration in brain of DCIR^{-/-} mice

Numerous studies have demonstrated that leukocytes in the brain, particularly CD8⁺ T cells, are important for CM induction in the murine PbA infection model. To determine whether the absence of DCIR influenced the sequestration of CD8⁺ T cells into the brain, CD45⁺ leukocytes in the brain were stained and the number of activated CD45⁺CD8⁺ T cells (which were CD62L^{low}) was analyzed by flow cytometry (Figure 26A). Indeed, upon PbA infection the number of CD45⁺ cells in the brain of DCIR^{-/-} mice was significantly reduced compared to infected wild-type mice (Figure 26B). This was mainly due to a reduced sequestration of activated CD8⁺ T cells into the brain of DCIR^{-/-} mice (Figure 26C). This finding demonstrates that the reduced incidence of CM among DCIR^{-/-} mice is accompanied by a decreased migration of activated CD8⁺ T cells into the brain compared to wild-type mice.

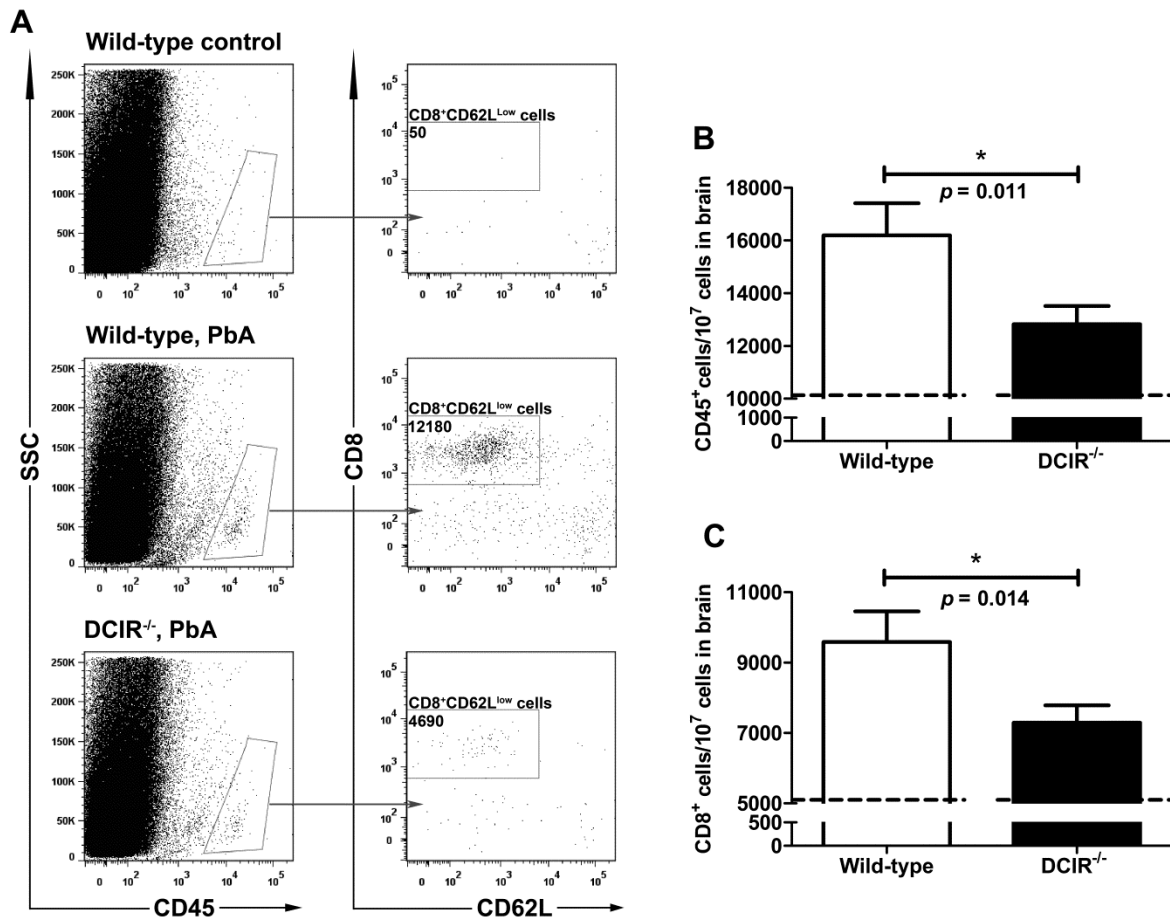


Figure 26. Decreased sequestration of CD8⁺ T cells in the brain of DCIR^{-/-} mice upon PbA-infection. C57BL/6 mice ($n=18$) and DCIR^{-/-} mice ($n=18$) were infected i.p. with 1×10^6 PbA-infected RBCs. On day 7 p.i., brains were homogenized and cells were stained with anti-CD45-PerCP-Cy5.5, anti-CD8-APC-H7, and anti-CD62L-PE and analyzed by flow cytometry. Cells were gated on CD45⁺ cells in the brain. **(A)** Representative dot plots are shown for uninfected wild-type mice (top panel), PbA-infected wild-type mice (middle panel), and infected DCIR^{-/-} mice (bottom panel). **(B)** Bar diagrams showing the frequency of CD45⁺ cells and **(C)** CD45⁺CD8⁺CD62L^{low} T cells per 1×10^7 cells in the brain of PbA-infected wild-type and DCIR^{-/-} mice. Dashed lines represent cell numbers in brain of uninfected DCIR^{-/-} and wild-type mice. A summary of 3 independent experiments is shown with 6 to 8 mice each. Data are expressed as mean \pm SEM for each group. Statistical analysis was performed using unpaired Student's *t* test (*, $p < 0.05$). The results indicate a significantly reduced sequestration of CD45⁺ leukocytes and CD8⁺CD62L^{low} T cells in the brain of PbA-infected DCIR^{-/-} mice.

To corroborate these findings, the expression of the endothelium marker CD31 and the number of CD3⁺ T cells in the brain were determined by immunohistochemistry on brain sections of PbA-infected wild-type and DCIR^{-/-} mice (Figure 27). As CD31 is an integral marker for endothelial cells, no difference in CD31 expression by wild-type, PbA-infected wild-type, and infected DCIR^{-/-} mice was observed (Figure 27A upper panel). On the contrary, CD3 staining showed a significantly higher number of intravascular and extravascular lymphocytes in PbA-infected wild-type mice than in DCIR^{-/-} mice (Figures 27A middle panel and B). The release of cytolytic molecules granzyme B and perforin, expressed by the CD8⁺ T cells sequestered in the brain, promote CM (177). Hence, the production of the apoptosis-inducing serine protease granzyme B was measured in PbA-infected wild-type and DCIR^{-/-}

mice. The presence of granzyme B is significantly higher in infected wild-type than in DCIR^{-/-} mice (Figures 27A bottom panel and C).

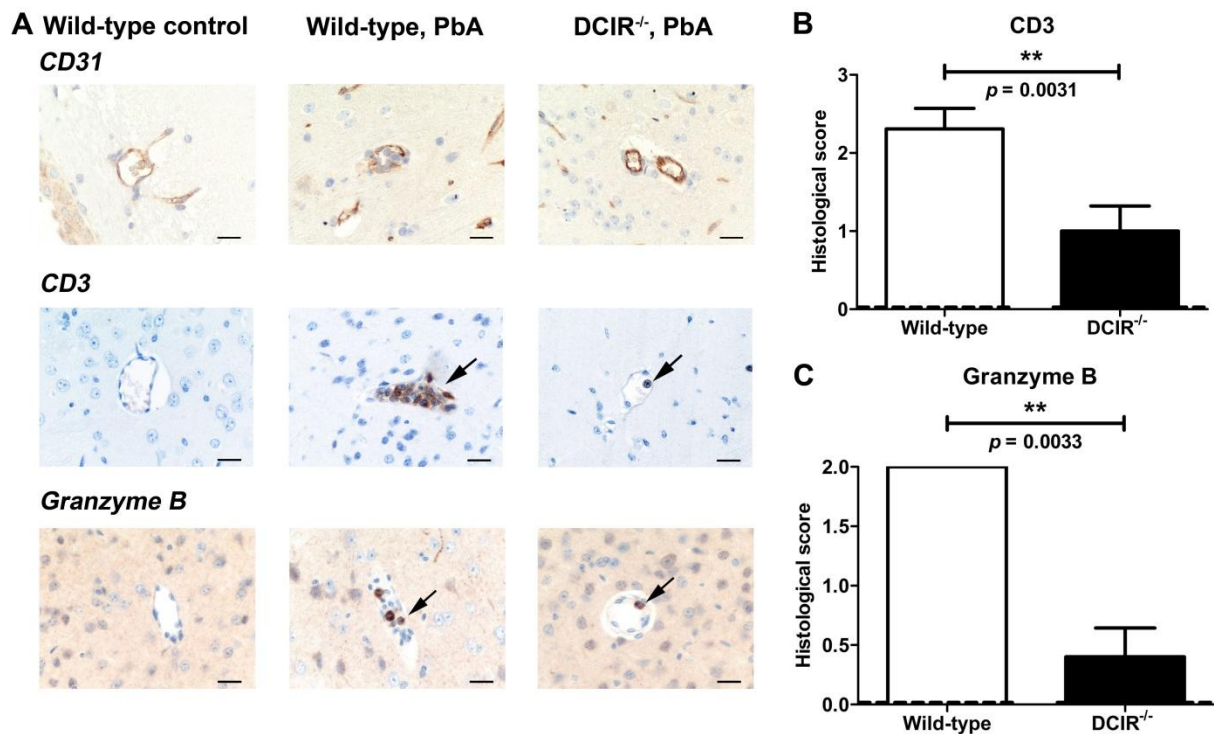


Figure 27. Decreased number of sequestered T cells in the brain of PbA-infected DCIR^{-/-} mice. Brain sections from PbA-infected C57BL/6 and DCIR^{-/-} mice were taken on day 7 p.i. These sections were then stained for CD31, CD3, and granzyme B. (A) Representative figures of uninfected wild-type, PbA-infected wild-type and infected DCIR^{-/-} are shown for CD31 expression (top panel), CD3⁺ T cell sequestration (middle panel), and granzyme B expression (bottom panel). All mice resulted positive for the presence of endothelial cells as confirmed by CD31 staining (top panel). In the case of CD3 staining, a significantly higher number of intravascular and extravascular lymphocytes was observed among PbA-infected wild-type mice (black arrow) compared to DCIR^{-/-} mice, which only exhibited rare CD3-positive cells in few cerebral and cerebellar vessels. Bar scale = 40 μ m. (B) Analysis was performed using a scoring system to determine the degree of lymphocyte presence. A summary of 3 independent experiments is shown with 6 to 8 mice each. (C) Analysis was performed using a scoring system to determine the degree of granzyme B-expressing cell presence. All data are presented as mean \pm SEM for each group. Dashed lines represent scores of uninfected DCIR^{-/-} and wild-type mice. Statistical significance was determined by unpaired Mann Whitney U test (**, $p < 0.01$).

To further analyze the effect of DCIR deficiency on brain pathology, histological examination of brain sections was performed using a clinical scoring system as described in Materials and Methods. Brain sections were analyzed for the presence of vessel wall hyalinization, endothelial activation, and intravascular leukocytes (Figure 28A). A significantly increased eosinophilic thickening of intracerebral vessel walls, a distinct feature characterizing vessel wall hyalinization, was observed in PbA-infected wild-type mice compared to DCIR^{-/-} mice (Figures 28A top panel and B). Consistently, there was also an enlargement of endothelial nuclei indicating endothelial activation that was predominantly observed in PbA-infected wild-type mice but only to a significantly lower level in DCIR^{-/-}

mice (Figures 28A middle panel and C). Additionally, the abundance of leukocytes in vessels observed was also higher among PbA-infected wild-type mice compared to DCIR^{-/-} mice though differences did not reach statistical significance (Figures 18A bottom panel and D). These findings demonstrate that brain inflammation is indeed ameliorated in PbA-infected DCIR^{-/-} mice.

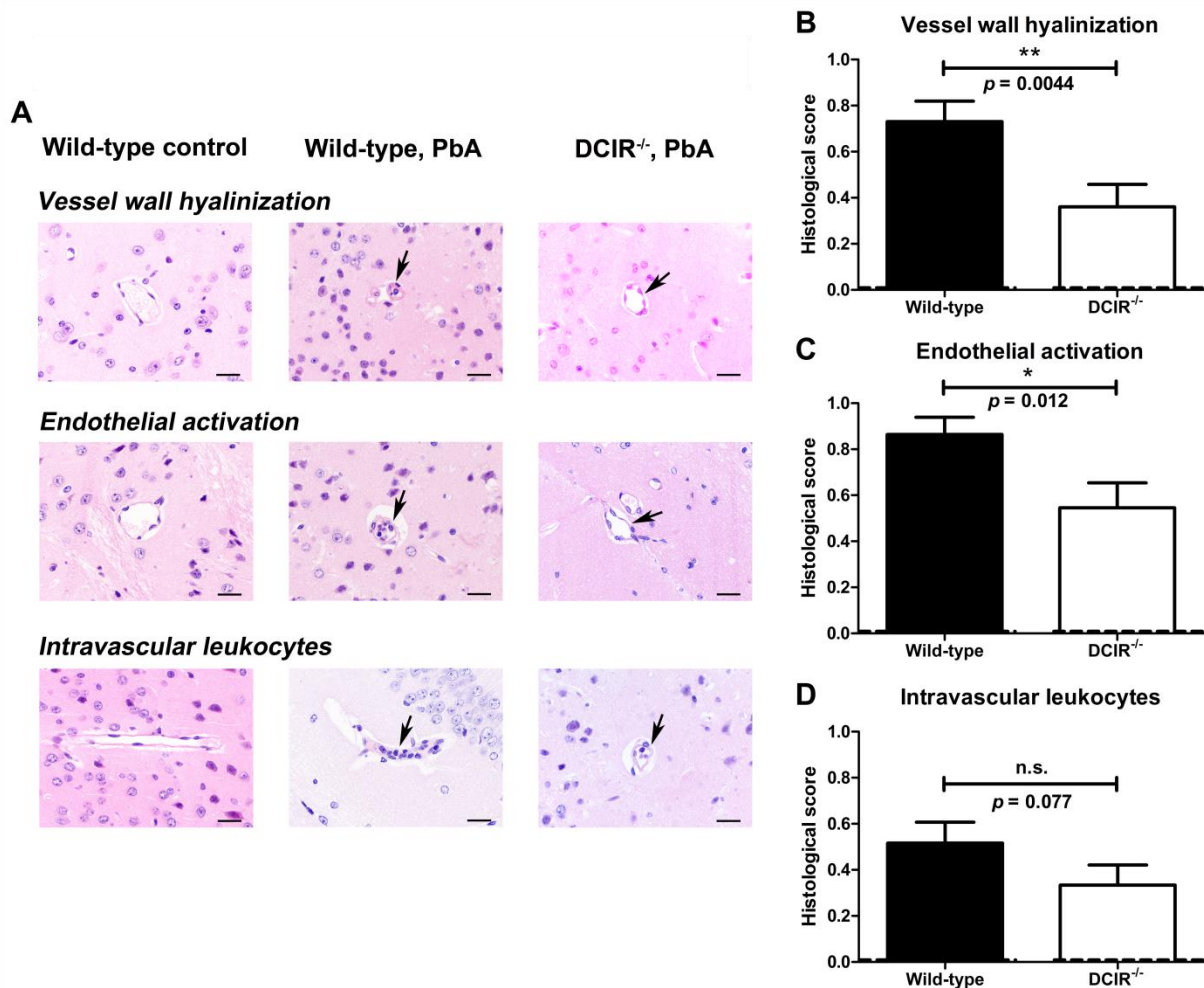


Figure 28. Reduced inflammation in the brain of PbA-infected DCIR^{-/-} mice. Brain sections from PbA-infected C57BL/6 and DCIR^{-/-} mice were taken on day 7 p.i. Brain histology of uninfected and infected mice was assessed. (A) Representative figures of uninfected wild-type mice as well as PbA-infected wild-type and DCIR^{-/-} mice are shown to depict the histological differences among the groups. Infected wild-type mice exhibited vessel wall hyalinization characterized by eosinophilic thickening of intracerebral vessel walls (black arrow), which was significantly reduced in infected DCIR^{-/-} mice (top panel). Enlargement of endothelial nuclei (black arrow), indicative of endothelial activation, was observed in most PbA-infected wild-type mice but only few infected DCIR^{-/-} mice (middle panel). The presence of intravascular leukocytes was observed (black arrow), with higher tendency, in PbA-infected wild-type mice than DCIR^{-/-} mice (lower panel). Bar scale = 40 μ m. Histological analysis was performed using a scoring system to determine the degree of vessel wall hyalinization (B), endothelial activation (C), and the presence of intravascular leukocytes (D). A summary of 6 independent experiments is shown with 4 to 8 mice each. Data are presented as mean \pm SEM for each group. Dashed lines represent scores of uninfected DCIR^{-/-} and wild-type mice (0 for all parameters analyzed). Statistical significance was determined by unpaired Mann Whitney U test (*, $p < 0.05$; **, $p < 0.01$, *ns* = not significant).

3.2.1.4 Reduced TNF- α levels in serum of DCIR^{-/-} mice

ECM is associated with high levels of pro-inflammatory cytokines with TNF- α and IFN- γ playing a crucial role in CM induction (181, 182). Thus, I examined whether the levels of IL-1 β , IL-12p70, IL-12p40, TNF- α , IL-10, and IFN- γ in sera of PbA-infected WT and DCIR^{-/-} mice differed. Indeed, the level of the pro-inflammatory cytokine TNF- α in serum was significantly lower in PbA-infected DCIR^{-/-} mice than in wild-type mice (Figure 29A). Interestingly, no significant differences in the levels of IFN- γ , IL-10, and IL-12p40 were observed (Figures 29B and C). The levels of IL-1 β , IL-12p70, IL-6 and IL-4 were at or below detection level for both groups. Increased levels of TNF- α are an important indicator of the pathogenesis of CM (181). Thus, DCIR deficiency exclusively impacted TNF- α release which might explain the reduced CM incidence in DCIR^{-/-} mice.

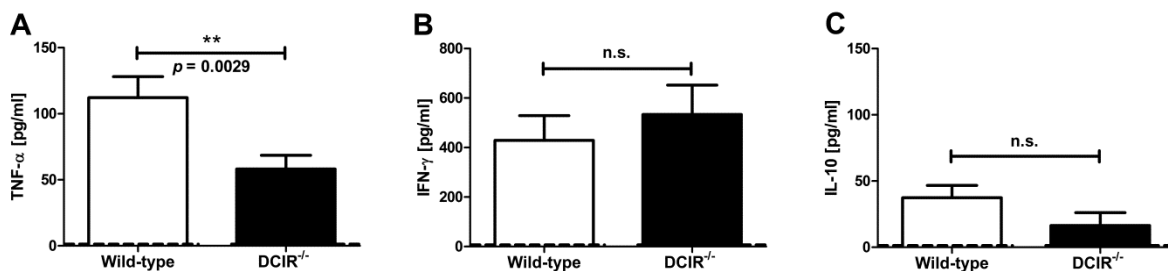


Figure 29. Decreased TNF- α levels in sera of PbA-infected DCIR^{-/-} mice. Sera from PbA-infected wild-type and DCIR^{-/-} mice were taken on day 7 p.i. Levels of the cytokines TNF- α (A), IFN- γ (B), and IL-10 (C) were evaluated using cytometric bead array. Production of TNF- α was markedly reduced in PbA-infected DCIR^{-/-} mice compared to wild-type mice. Data are expressed as mean \pm SEM for each group. The summary of 6 independent experiments is shown with 5-6 mice each. The dashed lines represent cytokine levels in sera of uninfected wild-type and DCIR^{-/-} mice. Statistical analysis was performed using unpaired Student's *t* test (**, $p < 0.01$).

3.2.5 Modulated T cell activation in spleen of DCIR^{-/-} mice

The activation of CD4⁺ and CD8⁺ T cells in spleen is important for these leukocyte populations to migrate to the brain and to contribute to CM induction (176, 248). Thus, I determined the frequency of activated CD4⁺ and CD8⁺ T cells in the spleen during PbA infection (Figure 30). While whole splenic composition was unaltered in uninfected as well as PbA-infected wild-type and DCIR^{-/-} mice (Figure 30A), the frequency of activated CD4⁺ and CD8⁺ T cells in spleen expressing the early activation marker CD69 was significantly lower in PbA-infected DCIR^{-/-} mice compared to infected wild-type mice (Figure 30B and C). This finding indicates that DCIR deficiency affects T cell priming in spleen which finally impacts T cell sequestration in the brain.

DCIR is an attachment factor for HIV-1 (132) but no other ligands have been identified yet. In the 52-glycan microarray analysis as described in the previous chapter, there

was no binding to mDCIR-hIgG-Fc observed. A supplemental glycan microarray was prepared consisting of synthetic glycosylphosphatidylinositol (GPI) glycolipids (249) which are found on the cell surface of *P. falciparum* during the merozoite stage. GPI has demonstrated potency in activating the host immune response and in inducing pro-inflammatory cytokines (250, 251). There was no binding detected between mDCIR-hIgG-Fc and the GPI structures (data not shown). Binding of DCIR fusion protein to pRBCs was also not observed (data not shown). These findings suggest that DCIR does not bind to parasitic glycans directly but might rather interact with DAMPs released during the course of malaria or that DCIR influences the activation state of DCs directly.

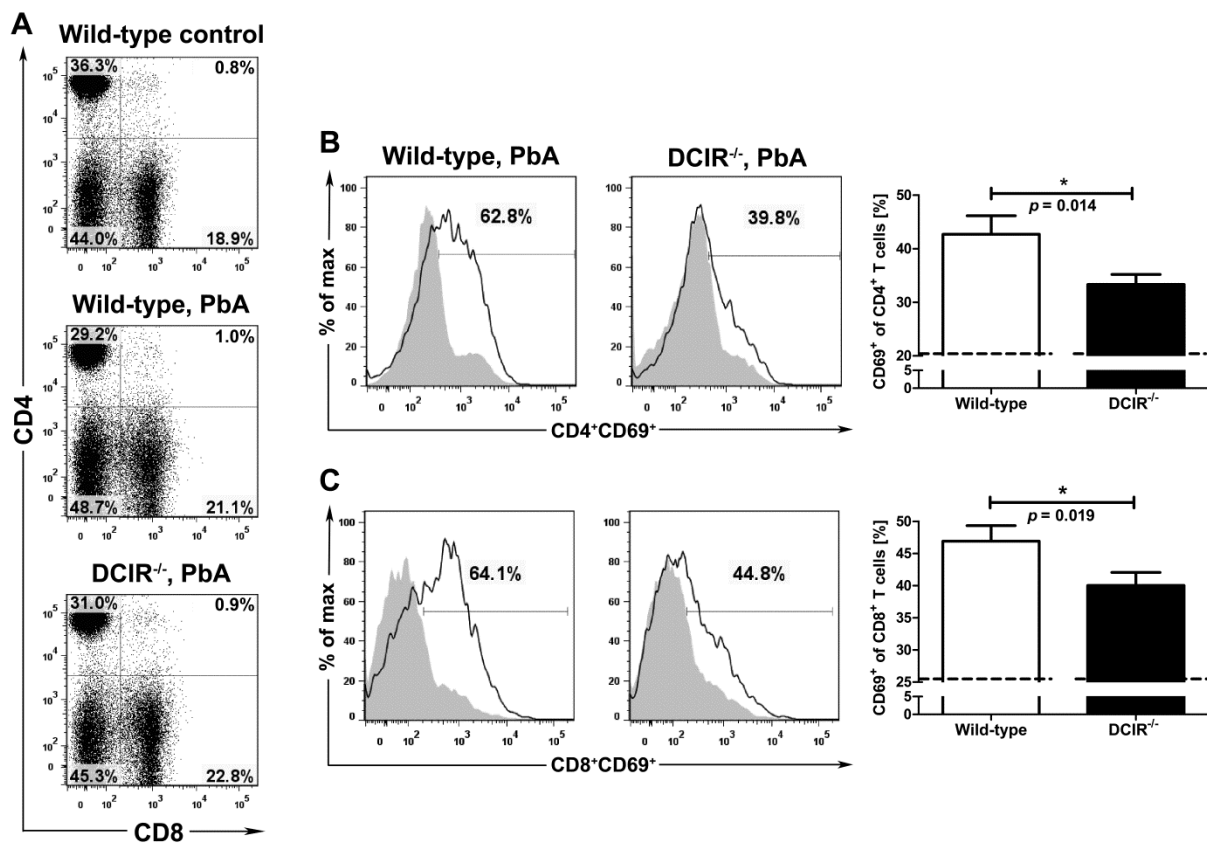


Figure 30. Reduced T cell activation in spleen of PbA-infected DCIR^{-/-} mice. C57BL/6 mice ($n=5$) and DCIR^{-/-} mice ($n=5$) were infected i.p. with 1×10^6 PbA-infected RBCs. On day 7 p.i., spleen cells were isolated, stained with anti-CD4-FITC, anti-CD8-APC-H7, and anti-CD69-PerCP-Cy5.5, and analyzed by flow cytometry. Cells were gated on lymphocytes. (A) Representative dot plots are shown for uninfected wild-type mice (top panel), PbA-infected wild-type mice (middle panel), and infected DCIR^{-/-} mice (bottom panel). (B) Cells were gated on CD4⁺ T cells. The frequency of CD4⁺ T cells expressing the early activation marker CD69 is shown. PbA-infected DCIR^{-/-} mice exhibited a lower frequency of activated CD4⁺ T cells in spleen than infected wild-type mice. (C) Cells were gated on CD8⁺ T cells. The frequency of CD8⁺ T cells expressing CD69 is shown. The frequency of activated CD8⁺ T cells was also lower in PbA-infected DCIR^{-/-} mice than infected wild-type mice. Dashed lines represent frequencies of activated CD4⁺ and CD8⁺ T cells in spleen of uninfected wild-type and DCIR^{-/-} mice. Data are expressed as mean \pm SEM for each group. Statistical analysis was performed using unpaired Student's *t* test (*, $p < 0.05$).

3.2.2 Role of *SIGNR3*^{-/-} in cerebral malaria

3.2.2.1 Genotyping of *SIGNR3*^{-/-} mice by PCR

In order to verify the genotype of the *SIGNR3*^{-/-} mice (031934-UCD, *SIGNR3* KO/Mmcd), PCR was performed as outlined in detail on the homepage of the Consortium for Functional Glycomics. Genomic DNA was obtained from tail biopsies of C57BL/6 wild-type (*SIGNR3*^{+/+}), heterozygous (*SIGNR3*^{+/-}), and *SIGNR3* knockout (*SIGNR3*^{-/-}) mice. The wild-type band has a size of 129 bp, while the *SIGNR3* knockout band is 243 bp (Figure 31).

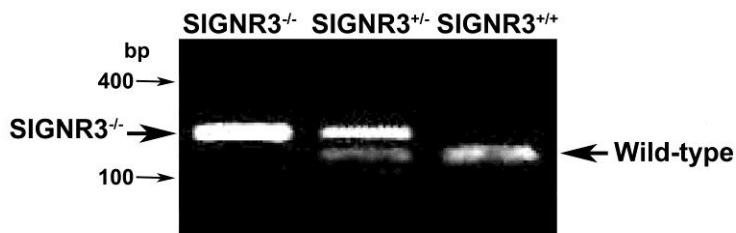


Figure 31. Genotyping of *SIGNR3*^{-/-} mice by PCR. To verify the genotype of *SIGNR3*^{-/-} mice, PCR was performed by with the genomic DNA taken from the tail biopsies of *DCIR*^{+/+}, *DCIR*^{+/-}, and *DCIR*^{-/-}. The *SIGNR3*^{+/+} band has a size of 129 bp, while the *SIGNR3*^{-/-} band is 243 bp.

3.2.2.2 Reduced CM incidence in *SIGNR3*^{-/-} mice

To shed light on the effect of *SIGNR3* deficiency on CM incidence, *SIGNR3*^{-/-} mice and the respective wild-type control mice were infected i.p. with PbA and parasitemia and clinical symptoms were monitored daily.

While CM induction resulted in more than 80% mortality of infected wild-type mice, only 40% of infected *SIGNR3*^{-/-} mice developed neurological symptoms, hence, were highly protected from CM (Figure 32A). No difference was observed in the parasitemia levels between *SIGNR3*^{-/-} and wild-type mice (Figure 32B) suggesting that *SIGNR3* deficiency did not affect parasite replication directly.

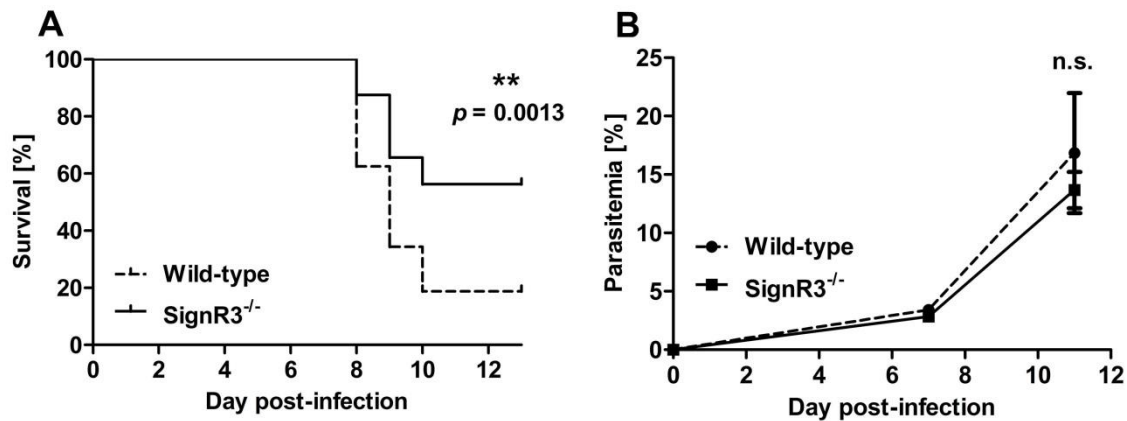


Figure 32. PbA-infected *SIGNR3*^{-/-} mice are significantly protected from CM induction. *SIGNR3*^{-/-} mice ($n=22$) and the respective C57BL/6 control mice ($n=22$) were infected i.p. with 1×10^6 PbA-infected RBCs. Mice were monitored daily for early signs of CM and were euthanized in case of clinical symptoms such as ataxia, convulsions, or coma. Survival was determined using log rank test (**, $p \leq 0.01$). The survival curves represent a summary of 4 independent experiments with 5 to 10 mice each. Parasitemia was determined on days 7 and 11 p.i. On day 11 p.i., the number of PbA-infected wild-type mice used for determination of parasitemia was significantly lower ($n=6$) because ~80% of mice had developed CM by that time point. Data are expressed as mean \pm SEM for each group. Statistical analysis was performed using Student's *t* test (*n.s.*=not significant).

3.2.2.3 Similar T cell sequestration in brain of *SIGNR3*^{-/-} and wild-type mice

The presence of CD8⁺ T cells in the brain is a firm indication of CM induction in the murine PbA infection model. To determine whether the absence of *SIGNR3* influenced the sequestration of CD8⁺ T cells into the brain, CD45⁺ leukocytes in the brain were stained and the number of activated CD45⁺CD8⁺CD62L^{low} T cells was analyzed by flow cytometry (Figure 33A). Upon PbA infection, the number of CD45⁺ cells in the brain of *SIGNR3*^{-/-} showed no significant difference to the CD45⁺ cell profile observed in infected wild-type mice (Figure 33B). This is even validated by the insignificant difference in the presence of activated CD8⁺ T cells also found in the brain (Figure 33C). There was also no difference in the number of CD45⁺CD8⁺CD62L^{low} T cells between the two groups demonstrating that *SIGNR* deficiency had no influence in the sequestration of activated CD8⁺ T cells into the brain.

3.2.2.4 Decreased TNF- α but increased IFN- γ expression

The levels of IL-1 β , IL-12p70, IL-12p40, TNF- α , IL-10, and IFN- γ in sera of PbA-infected wild-type and *SIGNR3*^{-/-} mice were examined. The level of the pro-inflammatory cytokine TNF- α in serum was significantly lower in PbA-infected *SIGNR3*^{-/-} mice than in wild-type mice (Figure 34A). Interestingly, *SIGNR3*^{-/-} exhibited a higher level of IFN- γ compared to the wild-type (Figure 34B). No significant differences in the levels of IL-10, and IL-12p40 were observed (Figure 34C). The levels of IL-1 β , IL-12p70, IL-6 and IL-4 were at or below detection level for both groups. Thus, the contrasting lower levels TNF- α but higher

levels of IFN- γ in SIGNR3^{-/-} could aid in illuminating the higher CM incidence observed in SIGNR3^{-/-} mice.

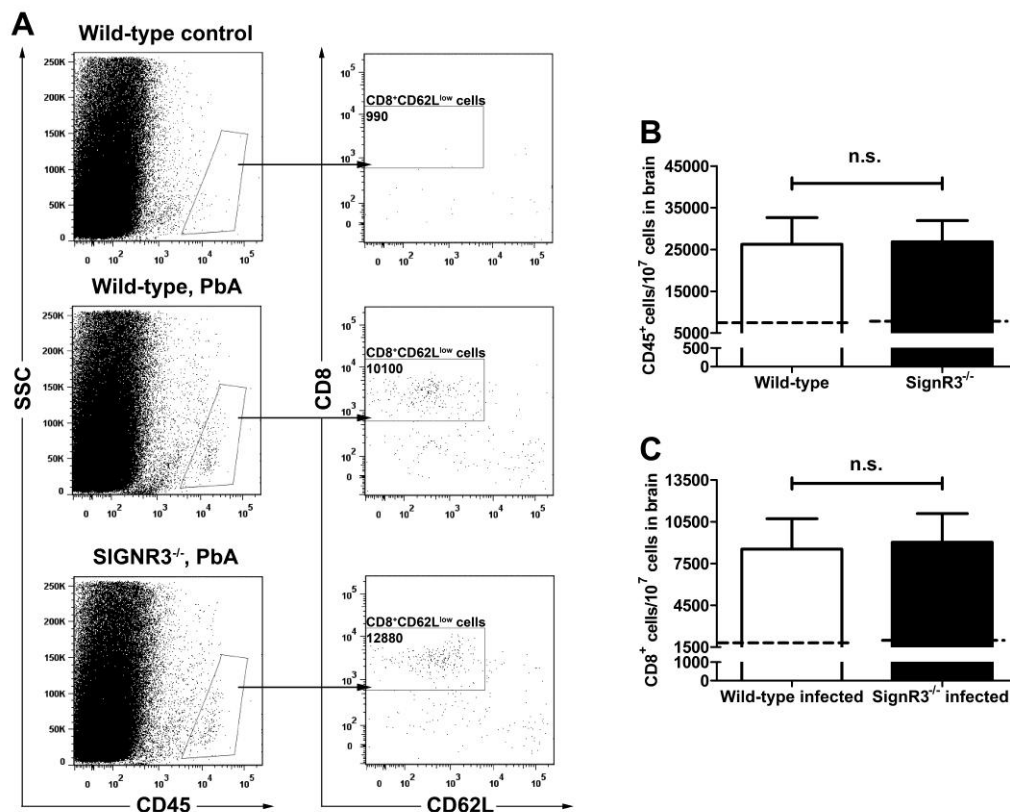


Figure 33. No difference in sequestration of CD8⁺ T cells in the brain of SIGNR3^{-/-} and wild-type mice upon PbA-infection. C57BL/6 mice and SIGNR3^{-/-} mice were infected i.p. with 1×10^6 PbA-infected RBCs. On day 7 p.i., brains were homogenized and cells were stained with anti-CD45-PerCP-Cy5.5, anti-CD8-APC-H7, and anti-CD62L-PE and analyzed by flow cytometry. Cells were gated on CD45⁺ cells in the brain. **(A)** Representative dot plots are shown for uninfected wild-type mice (top panel), PbA-infected wild-type mice (second panel), and infected SIGNR3^{-/-} mice (bottom panel). **(B)** Bar diagrams showing the frequency of CD45⁺ cells for infected SIGNR3^{-/-} mice; and **(C)** CD45⁺CD8⁺CD62L^{low} T cells per 1×10^7 cells in the brain of PbA-infected SIGNR3^{-/-} mice. Dashed lines represent cell numbers in brain of the involved uninfected SIGNR3^{-/-} and wild-type mice. A summary of 4 independent experiments is shown with 2 to 3 mice each (SIGNR3^{-/-} mice $n=12$; wild-type mice $n=12$). Data are expressed as mean \pm SEM for each group. Statistical analysis was performed using unpaired Student's *t* test (*n.s.*=not significant). The results indicate no significant difference in the the sequestration of CD45⁺ leukocytes and CD8⁺CD62L^{low} T cells in the brain of PbA-infected SIGNR3^{-/-} mice compared to PbA-infected wild-type mice.

3.2.2.5 Modulated spleen cell activation in SIGNR3^{-/-} mice

The frequency of activated CD4⁺ and CD8⁺ T cells in the spleen during PbA infection was determined (Figure 35). While whole splenic composition was unaltered in uninfected as well as PbA-infected wild-type and SIGNR3^{-/-} mice (Figure 35A), the frequency of activated CD4⁺ and CD8⁺ T cells in spleen expressing the early activation marker CD69 was significantly lower in PbA-infected SIGNR3^{-/-} mice compared to infected wild-type mice (Figure 35B and C). This finding indicates that SIGNR3 deficiency affects T cell priming in spleen which may finally impact T cell sequestration in the brain.

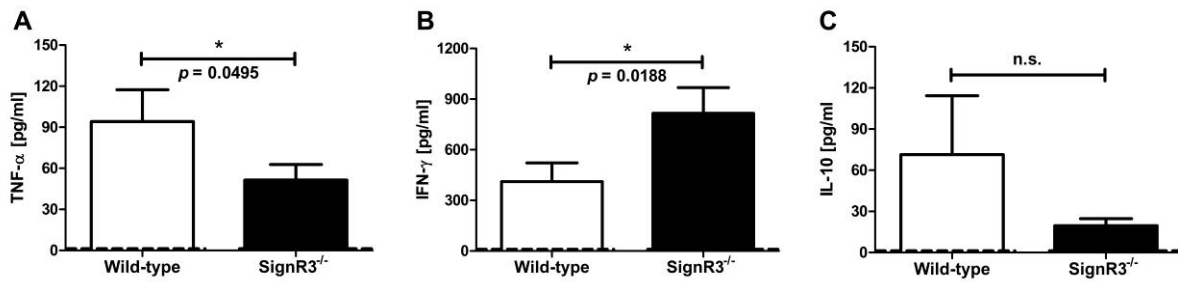


Figure 34. Decreased TNF- α but increased IFN- γ levels in sera of PbA-infected SIGNR3^{-/-} mice. Sera from PbA-infected wild-type and SIGNR3^{-/-} mice were taken on day 7 p.i. Levels of the cytokines TNF- α (A), IFN- γ (B), and IL-10 (C) were evaluated using cytometric bead array. Production of TNF- α was markedly reduced in PbA-infected SIGNR3^{-/-} mice compared to wild-type mice. In contrast, significantly higher levels of IFN- γ were observed in infected SIGNR3^{-/-} mice. Data are expressed as mean \pm SEM for each group. A summary of 4 independent experiments is shown with 4 to 6 mice each. The dashed lines represent cytokine levels in sera of uninfected wild-type and SIGNR3^{-/-} mice. Statistical analysis was performed using unpaired Student's *t* test (*, $p < 0.05$).

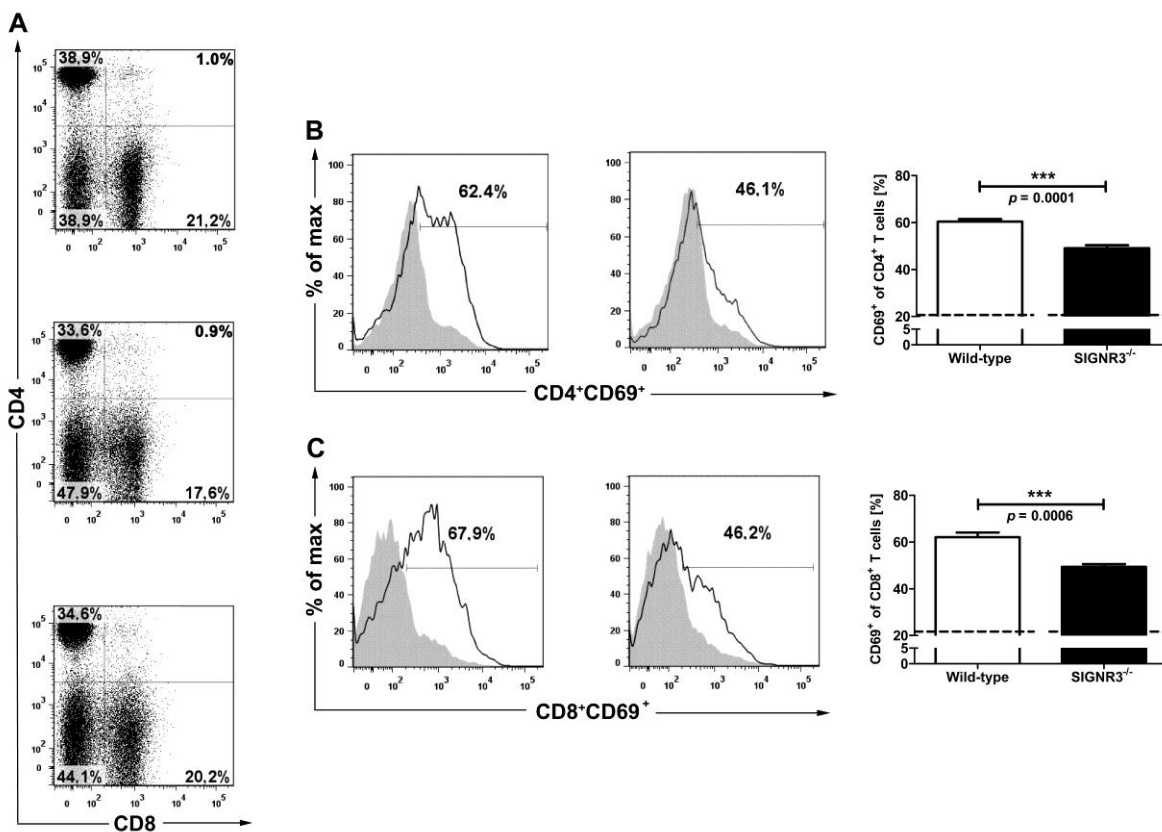


Figure 35. Reduced T cell activation in spleen of PbA-infected SIGNR3^{-/-} mice. C57BL/6 mice ($n=5$) and SIGNR3^{-/-} mice ($n=5$) were infected i.p. with 1×10^6 PbA-infected RBCs. On day 7 p.i., spleen cells were isolated, stained with anti-CD4-FITC, anti-CD8-APC-H7, and anti-CD69-PerCP-Cy5.5, and analyzed by flow cytometry. Cells were gated on lymphocytes. (A) Representative dot plots are shown for uninfected wild-type mice (top panel), PbA-infected wild-type mice (middle panel), and infected SIGNR3^{-/-} mice (bottom panel). (B) Cells were gated on CD4⁺ T cells. Representative frequency of CD4⁺ T cells expressing the early activation marker CD69 is shown. The frequencies of CD4⁺ T cells expressing the early activation marker CD69 is shown in PbA-infected SIGNR3^{-/-} mice. Both PbA-infected SIGNR3^{-/-} mice exhibited lower frequencies of activated CD4⁺ T cells in spleen than infected wild-type mice. (C) Cells were gated on CD8⁺ T cells. The frequencies of CD8⁺ T cells expressing CD69 is shown. The frequencies of activated CD8⁺ T cells were also lower in PbA-infected SIGNR3^{-/-} mice than in infected wild-type mice. Dashed lines represent frequencies of activated CD4⁺ and CD8⁺ T cells in spleen of uninfected wild-type and SIGNR3^{-/-} mice. Data are expressed as mean \pm SEM for each group. Statistical analysis was performed using unpaired Student's *t* test (***, $p < 0.001$).

The studies regarding the role of CLR_s in malaria infection indicate that CLR_s influence the pathogenesis of CM. DCIR deficiency demonstrated a crucial function in CM development. This is essentially characterized by prompting protection against CM induction. SIGNR3 revealed an impact in the genesis of CM, nevertheless, the mechanism of its role needs to be further investigated.

4. Discussion

4.1 Lectin targeting

In this thesis, the role of CLRs in cell-specific targeting and immune modulation was investigated by using different strategies: first, by identifying the ligands of CLRs and subsequently substantiating the potential adjuvanticity of CLR targeting; and second, by employing an animal model to determine the function of CLRs in infection in a murine malaria model.

The potential of CLR carbohydrate ligands as adjuvants is a promising venture. CLR targeting not only facilitates increased uptake of antigen by APCs, it also facilitates the recruitment and activation of DCs by stimulating CLRs, thereby enabling priming B and T cell responses (1). Indeed, PRR-based vaccine adjuvants approved for use in human vaccines have already been established albeit these are still limited. These adjuvants include the alum-TLR4 agonist MPL combination Adjuvant System [AS]04 (GlaxoSmithKline Biologicals), oil-in-water emulsions MF59 and AS03, and reconstituted influenza virosomes (252). To study the capability of CLR carbohydrate ligands to act as adjuvants, the general and inherent problem of weak affinity in lectin-carbohydrate ligand binding was first addressed and already known lectin-ligand interactions in evaluating biological functions were employed as proof-of-concepts. With these studies in hand, I sought to develop a platform that could bring about a rational strategy principally involving CLR-ligand interactions, an approach that combines glycan analysis with *in vivo* studies.

4.1.1 Multivalency enhances carbohydrate-lectin interaction

Lectin-carbohydrate interactions are generally weak, hence, in order to resolve this, multivalency in carbohydrate presentation on a scaffold was applied to generate insight into the binding profiles from both the lectin's and the ligand's roles. The multivalent Ru(II) complexes, with their sophisticated design, displayed different numbers of mannose residues on the surfaces with unique spatial orientation and the binding interactions between the carbohydrate epitopes and the lectin ConA was investigated by SPR. The mannose-carrying Ru(II) complexes were recognized by Con A; this was proven by the increase in RUs upon introducing the RuCdMan14 and RuCdMan28 complexes onto the ConA-immobilized surface. SPR experiments clearly demonstrated that the presence of more mannose residues as in the case of RuCdMan28 yielded a more efficient binding to ConA, and the affinity to ConA is higher than obtained for RuCdMan14. Additionally, the immobilization level of ConA affected the interaction; high density ConA exhibited stronger binding as compared to the low

density ConA. More importantly, results showed that the ConA binding to mannose on the ruthenium complexes is profoundly affected by the number of mannose residues displayed on their surface. By increasing the number of mannose on the surface, the binding performance was improved. RU values for RuCdMan14 were much lower and weaker binding was observed. Interestingly, the most potent multivalent template was not the compound with the highest functionalization of mannose residues. No binding was detected between RuCdMan42 and ConA-LD nor ConA-HD. This is presumably due to the steric hindrance afforded by the two additional CdMan encapsulating the ruthenium complex. This outcome is not entirely surprising, since similar results have been reported for highly multivalent probes (232, 253). The finding demonstrates that multivalent presentation of lectin ligand has a heightened effect on the binding to the lectin, however, it also shows that it is possible that strong binding can be achieved not necessarily with the maximum presentation of carbohydrates on a given carrier system. The effect of avidity is constructive only until a certain level. One explanation for this is that the inherent bulkiness of RuCdMan42 may impede the formation of stable interactions between mannose and ConA. Additionally, the spatial arrangement may need to be optimized further in order to improve potency. To further improve binding affinity, not a higher functionalization, but a careful study on the spatial arrangement of the ligands that would be deemed highly appropriate to provide the appropriate spacing of ligands for lectin binding. This study has allowed us to identify the effect of multivalency on lectin binding and that higher numbers of carbohydrate presentation do enhance the binding strength of carbohydrate-lectin interaction; there is an apparent upper limit to that number, beyond which binding efficiency declines.

4.1.2 Multivalent carbohydrate presentation affords cell-specific targeting

The data presented in this thesis show the effective targeting of the CLR ASGPR on HepG2 cells using cyclodextrins and liposomes. This is due to the recognition of ASGPR of its ligands, galactose or GalNAc, which are multivalently presented on these two systems. *In vitro* studies demonstrated that higher HepG2 uptake was observed in both galactose-functionalized cyclodextrins and GalNAc-functionalized liposomes. Conversely, cyclodextrins or liposome alone had no effect on the uptake by HepG2 cells. Although the cyclodextrin and the liposome controls helped to establish the general effectiveness of the galactose or GalNAc functionalities, the use of specificity controls was performed to rule out the possibility of unspecific binding. The uptake experiments were conducted with specificity controls, mannose-functionalized cyclodextrin for the cyclodextrin system and GlcNAc-

functionalized liposomes for the liposome system. Flow cytometry analysis revealed that there was no HepG2 uptake of mannose-functionalized cyclodextrin (uptake was the same degree as the cyclodextrin control) and a distinctly less uptake of GlcNAc-functionalized liposomes, confirming that the presence of galactose or GalNAc accounts for the specificity of uptake by HepG2 cells. To complement studies establishing the usefulness of carbohydrate-based targeting, the galactose-functionalized cyclodextrin system was loaded with doxorubicin, a potent chemotherapy drug used in cancer treatment, to induce apoptosis in HepG2 cells. The degree of apoptosis was substantially higher in HepG2 cells incubated with doxorubicin-loaded galactose-functionalized cyclodextrin than with doxorubicin alone. As expected, the degree of apoptosis in HepG2 cells treated with only galactose-functionalized cyclodextrin was at the same level as that of cells left untreated. Taken together, galactose- or GalNAc-based delivery systems for targeting ASGPR expressed by hepatocytes enable for multivalent receptor interactions. Furthermore, the galactose-functionalized cyclodextrin-based system is a molecular carrier for doxorubicin inducing a high degree of apoptosis in hepatocytes *in vitro*.

Several studies have examined targeting focusing on receptor-mediated endocytosis by ASGPR for gene and drug delivery (81, 233, 254). Multivalent delivery systems based on galactose/GalNAc-macromolecule conjugates have yielded HepG2-specific targeting more potent than monovalent agents. The results obtained in this thesis are in line with previous studies and show that valency-dependent uptake can be increased significantly.

4.1.3 CLR targeting modulates immune response

Carbohydrate structures on pathogens participate in the induction of host immune response that can be exploited for vaccination (79, 92). One important mechanism by which the immune system senses bacteria, viruses, fungi, or parasites is the recognition of microorganism-specific oligosaccharide motifs by innate immune receptors. A common receptor-ligand complex is formed between the TLR4–MD2–CD14 complex and bacterial lipopolysaccharides (LPS) (242). Host recognition of pathogenic microorganisms induces an immune response by producing antibacterial substances and recruitment of phagocytic cells such as neutrophils or macrophages. Sugars such as mannose-containing oligosaccharides contribute to this process by interacting with macrophages via MR, which mediates endocytosis and cytokine production (255). These are important compounds for signaling cascades to trigger the immune reaction.

Another strategy for targeting CLR employed in this thesis was using a multivalent mannose-functionalized fiber mesh with the carbohydrate residues interacting with MR on macrophages. This system was aimed to shed light into the influence of MR targeting by multivalent presentation of mannose on LPS-mediated stimulation of macrophages. The results indicate that stimulation with the plate-bound mannose-functionalized fibers in the presence of LPS had a synergistic effect in that TNF- α production by macrophages was increased. The sugar-functionalized fibers afforded a functional surface that is accessible. The aminoethanol- and galactose-functionalized fiber meshes show a significantly lower (~30%) activation under comparable conditions, which proved that the increase in TNF- α production upon mannose fiber stimulation is indeed specific. It is also consistent with previous publications where murine macrophages were efficiently targeted by mannosylated proteins such as mannosylated bovine serum albumin (256-258). For DC-SIGN, mannose-dependent enhancement of TLR-4 induced cytokine production has been proven (241). In sum, the increased effect of LPS/mannose meshes on macrophage cytokine production in this study is most likely due to the engagement of mannose-binding lectins such as MR or DC-SIGN homologues.

4.1.4 Platform for surveying CLR ligand adjuvanticity

The studies discussed thus far have illustrated the potency of multivalent carbohydrate presentation in targeting lectins and its application in enhancing immune responses. This schematic progression was then applied to elucidate the role of CLR targeting with novel ligands. Before any interaction studies can be performed, the carbohydrate ligands first need to be identified. For this purpose, the CLR fusion proteins, consisting of the extracellular region of the CLR and the human IgG1-Fc, were produced. These proteins form dimeric complexes in solution, thus displaying a higher binding avidity, and are easily detectable due to the Fc fragment. mDectin1-hIgG1-Fc, containing the extracellular region of the CLR Dectin 1, recognized zymosan, a known ligand of Dectin 1, which confirmed the functionality of the fusion proteins.

The creation of a library of fusion proteins allows for a high throughput screening of novel carbohydrate ligands by glycan microarray analysis, but its utility is not only limited to glycan arrays. It is a versatile tool that can be used in a diverse array of strategies and assays. Fc fusion proteins can be used for lectin arrays wherein the proteins are attached to the solid surface via interactions between the Fc part and the surface-bound protein G/A (259, 260). This method enables investigations on carbohydrate-protein and protein-protein interactions,

and on interactions with microbial particles. Moreover, Fc fusion proteins can be multivalently presented on scaffolds such as protein G/A microbeads and subsequent interaction studies can be performed with macromolecule conjugates and even cells (261). Strategies which necessitate immobilization such as ELISA or SPR can also make use of the Fc fusion proteins (262, 263). The fusion proteins mDectin1-hIgG1-Fc, mDCIR-hIgG1-Fc, mMCL-hIgG1-Fc, mMICL-hIgG1-Fc, mClec12b-hIgG1-Fc, and mMGL1-hIgG1-Fc, mClec12b-hIgG1-Fc and mMGL1-hIgG1-Fc were screened directly on a carbohydrate microarray to determine any binding partners. There were no interactions observed among Dectin 1, DCIR, and MCL and the respective carbohydrates. MICL showed binding affinity towards terminal mannose structures, particularly PIM₂ and PIM₃. This is an interesting result since MICL does not contain the EPN motif, which pertains to mannose recognition (264). MGL1 exhibited recognition to 1,3-lactosamine and to Gb5. Similar binding activity was observed on Clec12b albeit to a weaker extent than that of MGL1. It is important to note that both CLRs exhibited broader specificity, recognizing galactose-terminal glycans. This is not actually surprising in the case of MGL1 since its CRD contains the galactose-binding motif QPD and its binding to galactose-containing Lewis X and Lewis Y glycans is known (70). The tumor antigen Gb5 (stage-specific embryonic antigen-3; SSEA-3) is highly expressed in the fertilized egg and at the 8-cell embryo stage in mice, and in embryonic stem cells and embryonal carcinoma cells in humans (265). It is involved in the metastatic spread of testicular, lung, and breast tumors as well as teratocarcinoma (266). Since Gb5 plays a mechanistic role in cancer pathogenesis, binding of MGL1 and Clec12b to Gb5 holds a promising venture into the role of CLRs in cancer.

Targeting of CLRs on DCs using their carbohydrate ligands has been explored by employing multivalent carbohydrate presentation to promote efficient delivery of cargo to intracellular compartments responsible for antigen processing and presentation. Nanoparticles such as liposomes and micelles have been used as antigen delivery systems and the CLR MR has been extensively investigated (97). The engagement of MR on DCs with mannose-functionalized polyanhydride nanoparticles facilitates the cell surface expression of MHC-II and co-stimulatory molecules (267). Higher efficiency of endocytosis was exhibited by MR-mediated uptake of mannose-functionalized nanoparticles by DCs (97, 268). Aside from using nanoparticles as carbohydrate-functionalized delivery systems, the model antigen ovalbumin (OVA) has been employed for multivalent ligand presentation with the primary goal of targeting CLRs to induce immune responses. OVA conjugated with Lewis^b structures, fucose-containing ligands of DC-SIGN, enhanced CD4⁺ and CD8⁺ T cell responses by targeting bone

marrow DCs and splenic DCs (269). Modification of OVA with GalNAc, ligand of MGL2, and targeting to DCs also augmented T cell responses (76).

Having identified novel ligands for MGL1 and Clec12b, targeted antigen delivery by modifying OVA was employed with either 1,3-lactosamine or Gb5. To overcome the disadvantage of weak carbohydrate-lectin interactions, multivalent presentation of the sugars on OVA was carried out and verified by MALDI. In both *in vitro* and *in vivo* studies, OVA-Gb5 and OVA-lactosamine showed a tendency in higher IL-2 production than with OVA alone, even slightly higher in the case of OVA-Gb5. The levels of IFN- γ also showed a tendency to be higher in OVA-Gb5 and OVA-lactosamine than in OVA. The same tendency in IL-2 and IFN- γ production was observed *in vivo*, i.e. the levels were higher in mice immunized with OVA-Gb5 and OVA-lactosamine than with OVA alone, was observed *in vivo*. This might indicate that engagement of OVA-Gb5 or OVA-lactosamine influence CD4⁺ T cell differentiation into IL-2 and IFN- γ -producing T_H1 cells. Furthermore, antibody titers showed a decrease in IgG, specifically IgG₁, production among OVA-Gb5- and OVA-lactosamine-immunized mice than those immunized with OVA alone. This suggests that the T_H2 humoral response is dampened consistent with the increased T_H1.

Taken together, the strategy---from ligand identification to *in vivo* studies---presents a platform in the pursuit for adjuvant candidates. Protein, peptide and DNA antigens alone are generally insufficient in inducing immunogenicity to initiate DC-mediated adaptive immune responses giving pertinence to the approach that the antigens are delivered to DCs with an adjuvant (270). Adjuvants stimulate the innate immune system by activating APCs, which subsequently enables the development of a long-lasting and antigen-specific immune response. Thus, the long-term effectiveness of antigen vaccines significantly relies on effective adjuvants (271). Aluminum-based adjuvants such as aluminum phosphate and aluminum hydroxide have been used for more than 60 years and are the only ones approved for use in humans by the Food and Drug Administration of the United States to date (272). These adjuvants boost the efficacy of the vaccine by indirectly activating APCs in various ways, which include the formation of an antigen depot and the accumulation of antigen to increase uptake by APCs (273). Though these adjuvants have been proven to be safe in humans, they do not strongly induce antibody production and weakly initiate cell-mediated immunity. On the other hand, there are other potential adjuvants that have been shown to activate APCs more directly, e.g. LPS and CpG DNA which are binding moieties for TLRs. Though they induce upregulation of MHC-I and MHC-II molecules and secretion of inflammatory cytokines such as IL-6 and TNF- α , they are toxic. Derivatives of these

adjuvants are being explored with the aim of developing reduced toxic effects (274). Still, the broader aim is to develop adjuvants which are strongly immunogenic as well as non-toxic.

CLR targeting can serve as an effective approach to activate DCs which could then influence skewing of immune responses. Antigens modified by CLR ligands afford an adaptable and robust platform which can facilitate antigen presentation and cytokine secretion, and perhaps even co-stimulatory molecules, leading to the initiation of a protective adaptive immune response. By engaging CLR-mediated DC activation, this thesis provides a basis to develop an immunization protocol that effectively induces immune response by CLR-mediated DC activation. The approach outlined in this study presents a rationale design of CLR ligands as feasible adjuvants.

4.2 CLRs in cerebral malaria

As another approach in examining the role of CLRs, the murine *P. berghei* ANKA infection model was employed to determine whether DCIR has a functional role in the control and/or genesis of CM. Pathogenic diseases can be tempered by homeostasis, however, in severe cases as in cerebral malaria, this can be subjugated leading to fatal consequences (180). DCs play a crucial role in the initiation of an overwhelming immune response against malaria. DCs need to detect danger signals through PRRs in order to direct trafficking towards the appropriate response. To date, numerous studies focus on the role of TLRs in immunity to malaria and in the pathogenesis of severe/cerebral malaria whereas studies on the relevance of CLRs are lacking. TLRs are involved in the recognition of parasitic pathogen-associated molecular patterns (PAMPs) such as TLR2/4 in binding to *P. falciparum* glycosylphosphatidylinositol (GPI) (275, 276) or TLR9 in the interaction with hemozoin/*P. falciparum* DNA (277, 278). In a study employing *P. chabaudi* infection, priming of TLR responses corresponds to the increased expression of TLR mRNA, and TLR9-deficient mice were protected against LPS-induced lethality during acute infection (279). The TLR/MyD88 pathway was shown to be crucial for CM development (280) and targeting of nucleic acid-sensing TLRs protected mice from clinical signs of CM (281). In other studies, only a limited role for TLRs in the genesis of CM was found (195, 197). A recent study indicated that the impact of TLR signaling on pathology might depend on the genetic background of the mice (282). Moreover, TLRs 2/4/9 were found to be dispensable in the induction of cerebral malaria and also parasite control (197). It is mainly MyD88, in its role as core adaptor protein in IL-18 signaling, which is pivotal in blood stage parasite control and induction of pro-inflammatory cytokines (196). In addition to TLR signaling, the STING,

TBK1 and IRF3-IRF7 signaling pathways are important for malaria-associated pathology (283). These signaling molecules were shown to be involved in sensing of AT-rich *P. falciparum* DNA and mice lacking IRF3, IRF7, the kinase TBK1 or the type I IFN receptor were resistant to CM (283). In contrast, CM genesis is independent of the Nod pathway. Though cytokine levels such as IL-1 β or IFN- γ were decreased in Nod1/Nod2^{-/-} mice during PbA infection, there was no difference in survival or parasitemia compared to wild-type mice (284).

The extracellular part of DCIR is homologous to other members of the CLR superfamily and contains a CRD (42). Human DCIR functions as an attachment receptor for HIV-1 and promotes virus uptake into cells (132), however, these results were obtained by DCIR transfection experiments and were not based on direct interaction studies with purified ligands. No ligand for DCIR has yet been identified and the glycan microarrays, one of which consisted of GPI structures, conducted in this study yielded no positive ligand for DCIR. DCIR binding to glycoprotein or protein ligands might be more likely albeit this finding does not formally exclude an interaction with carbohydrate ligands. Binding to protein ligands was shown for other CLRs such as Clec9a, which binds to the F-actin component of the cellular cytoskeleton (285, 286). Binding studies between mDCIR-hIgG1-Fc and pRBCs was performed; however there was no specific interaction observed. Moreover, parasitemia levels in blood were comparable between PbA-infected DCIR^{-/-} and control mice. These findings suggest that DCIR might not bind to parasitic PAMPs directly but rather indicate that DCIR acts as a recognition receptor for self-antigens released by the rupture of pRBCs during malaria progression and/or DC activation. Indeed, CLRs such as Mincle or Clec9a sense DAMPs such as necrotic cells highlighting the dual role of CLRs in the recognition of pathogens, non-self, and self-antigens (42). Accordingly, the nature of the DCIR ligand still remains to be identified.

This thesis demonstrates that DCIR deficiency impacted T cell activation in the spleen and modulated TNF- α production. Previous studies have shown the importance of PRRs expressed by APCs for cell activation and T cell priming. Since DCs become refractory to TLR-mediated IL-12 and TNF- α production during the course of the disease, TLRs are deemed essential players in DC activation and cross-priming during malaria infection (287). Moreover, cross-priming of CD8⁺ T cells by activated DCs is hindered during PbA infection (187). In *P. yoelii* infection, TLR9 and MyD88 were shown to play crucial roles in the regulation of cytokine production, T_H1/T_H2 development, and in the development of cellular

and humoral responses (194). Thus far, the role of CLRs in these processes is not fully elucidated.

Regarding the role of PRRs in immunity to malaria, most studies focus on the contribution of TLRs to immune pathology. Since CLRs are another major family of PRRs in DCs, it is reasonable to suggest a possible pivotal role of CLRs in malaria pathology and indeed the influence of CLRs in the pathogenesis of CM has just started to be elucidated. The adaptor protein CARD9 mediates a number of CLR signaling, hence, the susceptibility of *CARD9*^{-/-} mice to PbA infection has been investigated (200). An up-regulated *CARD9* expression was observed in the brains of PbA-infected wild-type mice, however, PbA-infected *CARD9*^{-/-} mice succumbed to neurological signs and blood-brain barrier disruption similar to wild-type mice (200). This study indicates that CM develops independently of the *CARD9* signaling pathway. DCIR signaling does not engage the adaptor protein *CARD9*, but instead is mediated through ITIM (44). Surprisingly, in spite of the presence of an intracellular ITIM, DCIR deficiency did not exacerbate immune pathology, but led to a reduced incidence of CM, accompanied by a decreased T cell sequestration into the brain, and modulated T cell activation in spleen. Previous studies on antibody-mediated DCIR targeting resulted in efficient T helper cell priming and T cell proliferation (48) which might help explain the latter. Moreover, targeting of human DCIR also induced efficient CD8⁺ T cell cross-priming (47). These studies are in agreement with the findings shown here that the frequencies of activated CD4⁺ and CD8⁺ T cells in spleen expressing CD69 were reduced in PbA-infected DCIR^{-/-} mice compared to wild-type mice. The differential T cell priming in spleen might be a key factor responsible for the decreased susceptibility of the DCIR^{-/-} mice to CM. In this respect, our results are consistent with a recent study analyzing the role of the CD11c^{high}CD8⁺ DC subset in CM immunopathology. Selective depletion of the Clec9a⁺ DC subset caused reduced activation of splenic CD4⁺ and CD8⁺ T cells that was accompanied by a reduced CD8⁺ T cell sequestration in brain and ameliorated brain inflammation (149). The evidence for an essential role of a single CLR in this process is provided in this thesis.

In this thesis, the reduced T cell priming in spleen was complemented by lower levels of TNF- α in serum of PbA-infected DCIR^{-/-} mice. The causal relationship between TNF- α levels and malaria pathology has been established from studies on the association of higher TNF- α levels in sera of patients suffering from CM as well as studies demonstrating the critical role of TNF- α in PbA infection of mice (181). More recently, a number of other TNF and TNFR superfamily members were shown to be involved in malaria pathology (199). Interestingly, there were no significant changes in IFN- γ levels detected during PbA infection

in DCIR^{-/-} mice indicating that DCIR deficiency exclusively influenced the level of the pro-inflammatory cytokine TNF- α .

Taken together, this study establishes a crucial role for DCIR in CM development during PbA infection of mice (Figure 36). To the best of my knowledge, this is the first report showing the importance of a specific DC-expressed CLR in malaria-associated pathology. The only CLR that was reported to be associated with placental malaria is the complement protein mannan-binding lectin (MBL) (288). Evidence that DCIR affects T cell priming in spleen, contributes to TNF- α production, impacts CD8⁺ T cell sequestration in the brain and triggers the pathogenesis of CM is provided here. Thus, interference with DCIR signaling might be a means to modulate APC function during the course of malaria.

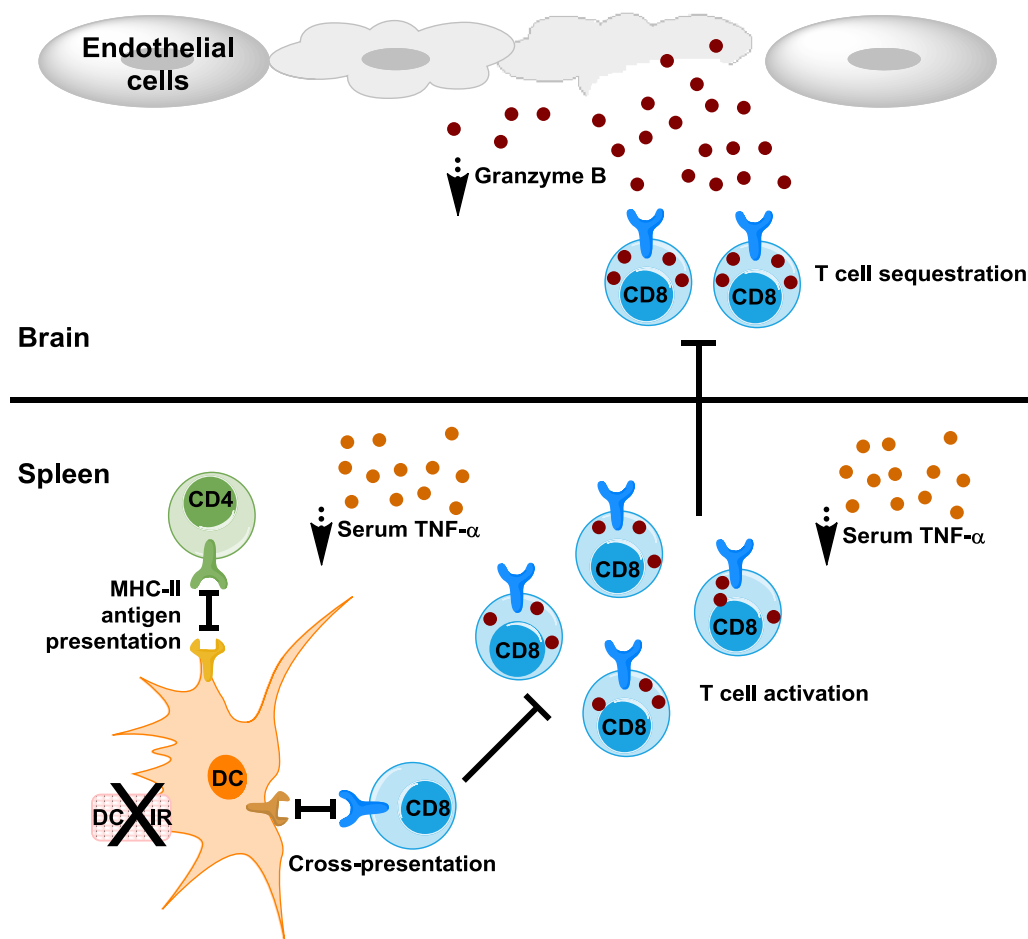


Figure 36. A schematic representation of the influence of DCIR deficiency in the development of ECM. Upon PbA infection of DCIR^{-/-} mice, there was modulated activation of CD4⁺ and CD8⁺ T cells. Systemic TNF- α production is also modulated, which reduces the permeability of the brain endothelium impeding T cell sequestration into the brain. Activated CD4⁺ T cells also migrate into the brain which produce IFN- γ and activate endothelial cells. Activated CD8⁺ T cells proliferate and sequester into the brain. They secrete the cytolytic molecule perforin to lyse the antigen-presenting endothelial cells and the apoptosis-inducing protease granzyme B. Destruction of the brain endothelium leads to breakdown of the blood brain barrier. There are decreased levels of activated T cells in DCIR^{-/-} mice, particularly CD8⁺ T cells, which might explain that there are less sequestered T cells in the brain resulting in the reduced release of granzyme B as well as histological features of inflammation.

On the other hand, the effect of SIGNR3 on the induction of CM cannot be compellingly established. SIGNR3 deficiency did not influence the parasitemia levels, but led to a significantly higher survival rate (60%) compared to wild-type mice. Furthermore, PbA-infected SIGNR3^{-/-} and wild-type mice exhibited similar numbers of sequestered CD45⁺CD8⁺CD62L^{low} T cells in the brain. Interestingly, TNF- α levels were significantly reduced, whereas IFN- γ levels were increased in PbA-infected SIGNR3^{-/-} compared to wild-type mice. These contrasting outcomes suggest that an alternative mechanism leading to the release of these cytokines may be involved and be even more important than SIGNR3-mediated gene expression. Additionally, activation of CD8⁺ and CD4⁺ T cells in the spleen was remarkably lower in SIGNR3^{-/-} than in wild-type mice. The results on the role of SIGNR3 on cerebral malaria suggest that SIGNR3 plays a role, however, its mechanism needs to be further investigated. This may be, in part, due to the different signaling cascade following SIGNR3 activation. SIGNR3 as well as its human homologue, DC-SIGN, has an intracellular hemITAM. DC-SIGN is exploited by pathogens such as HIV-1 and *M. tuberculosis* to escape immunosurveillance and to promote its survival by hiding within DCs (40, 136). A similar mechanism could play a role in PbA infection. Moreover, SIGNR3 binds to high-mannose and, notably, the *P. falciparum* GPI is a mannosylated structure. Binding of SIGNR3 to GPI has not been determined, but if confirmed, this can help illustrate a CLR/GPI-mediated protection or susceptibility in CM. It is also imperative to characterize the sequestered CD8⁺ T cells in the brain in terms of the expression of inflammation markers such as TNF- α , IFN- γ , and IL-10. Nevertheless, this is still currently investigated and possible approaches to address the issues mentioned above are being developed.

4.3 Conclusion

The two strategies, the adjuvant platform approach and the animal model studies, though would initially seem as distinct and separate can in fact be brought together to be complementary. The detection of PAMPs or DAMPs by CLRs activates signaling pathways to mount an effective antimicrobial response targeting the invading pathogen. Understanding how the innate immune system senses individual pathogens and the crosstalk among CLRs is critical for understanding the complexities in regulating the innate immune system. Targeting CLRs within the context of malaria to modulate immune responses can be feasible by utilizing the adjuvanticity of CLR carbohydrate ligands. Furthermore, knowledge of these processes, particularly the immunological outcomes of CLR signaling, will provide new insights facilitating the design of novel vaccine adjuvants that target CLRs and appropriately guide

protective immunity. A better understanding of how individual cell signaling pathways such as Syk-dependent signaling influence regulation of the adaptive immune system, thereby underlying immunity to infection, will be important. This will enable the generation of more effective and safe vaccine adjuvants that not only target CLRs but also manipulate downstream signaling pathways to influence the immune response.

Supplemental Information

SI.1 Fusion protein sequences

SI.2 Genotyping protocols from the Consortium for Functional Glycomics

SI.3 List of microarray carbohydrates

SI.1 Fusion protein sequences

SI.1.1 mDectin1-hIgG1-Fc sequence

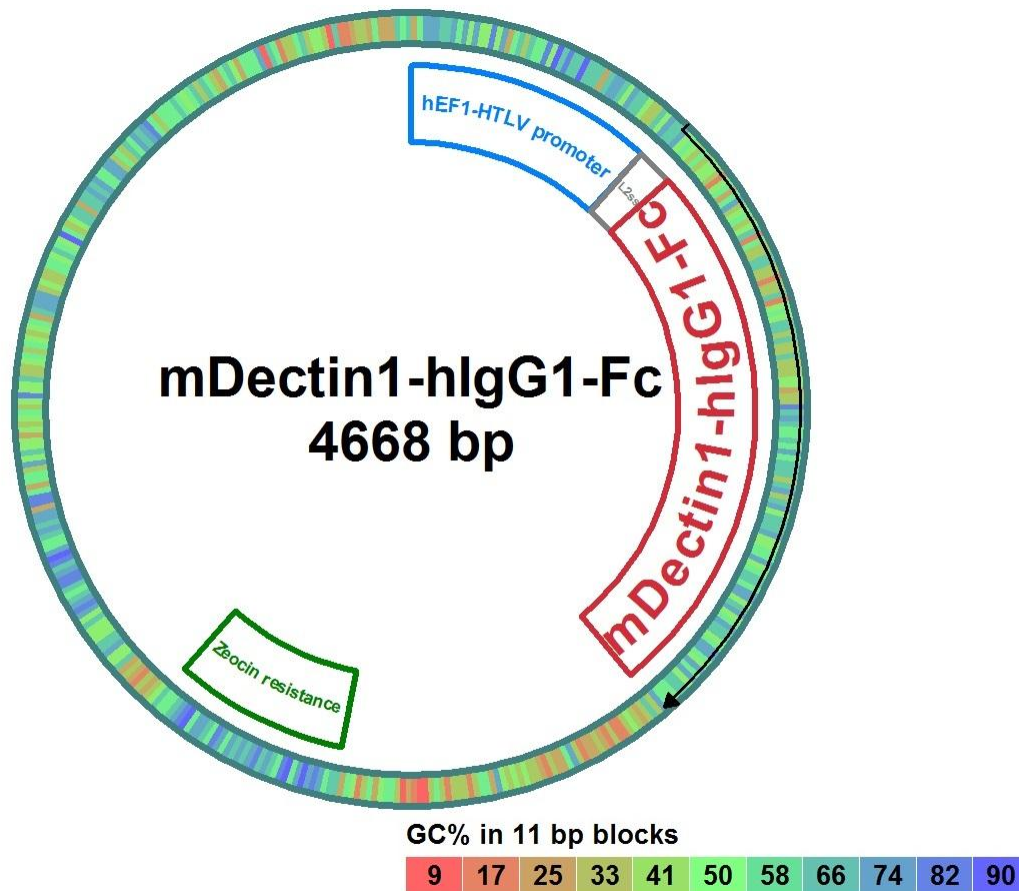
hEF1-HTLV promoter

IL2 ss

mDectin1-hIgG1-Fc

Zeocin resistance

Black arrow (→) represents an open reading frame (ORF).



```

1 GGATCTGCGA TCGCTCCGGT GCCCGTCAGT GGGCAGAGCG CACATCGCCC
51 ACAGTCCCCG AGAAGTTGGG GGGAGGGGTC GGCAATTGAA CGGGTGCCTA
101 GAGAAGGTGG CGCGGGGTAA ACTGGGAAAG TGATGTCGTG TACTGGCTCC
151 GCCTTTTTTC CGAGGGTGGG GGAGAACCGT ATATAAGTGC AGTAGTCGCC
201 GTGAACGTTT TTTTTCGCAA CGGGTTTGCC GCCAGAACAC AGCTGAAGCT
251 TCGAGGGGCT CGCATCTCTC CTTACGCGC CCGCCGCCCT ACCTGAGGCC
301 GCCATCCACG CCGGTTGAGT CGCGTTCTGC CGCCTCCCGC CTGTGGTGCC
351 TCCTGAACTG CGTCCGCCGT CTAGGTAAGT TTAAAGCTCA GGTCGAGACC
401 GGGCCTTTGT CCGGCGCTCC CTTGGAGCCT ACCTAGACTC AGCCGGCTCT
451 CCACGCTTTG CCTGACCCTG CTTGCTCAAC TCTACGTCTT TGTTTCGTTT
501 TCTGTTCTGC GCCGTTACAG ATCCAAGCTG TGACCGGCGC CTACCTGAGA
551 TCACCGGCGA AGGAGGGCCA CCATGTACAG GATGCAACTC CTGTCTTGCA
601 TTGCACTAAG TCTTGCACCT GTCACGAATT CTTCAGGGAG AAATCCAGAG
651 GAGAAAGACA ACTTCCTATC AAGAAATAAA GAGAACCACA AGCCACAGA
701 ATCATCTTTA GATGAGAAGG TGGCTCCCTC CAAGGCATCC CAAACTACAG

```

751 GAGGTTTTTC TCAGCCTTGC CTTCTAATT GGATCATGCA TGGGAAGAGC
801 TGTTACCTAT TTAGCTTCTC AGGAAATTCC TGGTATGGAA GTAAGAGACA
851 CTGCTCCCAG CTAGGTGCTC ATCTACTGAA GATAGACAAC TCAAAGAAT
901 TTGAGTTCAT TGAAAGCCAA ACATCGTCTC ACCGTATTAA TGCATTTTGG
951 ATAGGCCTTT CCCGCAATCA GAGTGAAGGG CCATGGTTCT GGGAGGATGG
1001 ATCAGCATT CTTCCCAACT CGTTTCAAGT CAGAAATACA GCTCCCAGG
1051 AAAGCTTACT GCACAATTGT GTATGGATT ATGGATCAGA GGTCTACAAC
1101 CAAATCTGCA ATACTTCTTC AAGATCTGAC AAAACTCACA CATGCCACC
1151 GTGCCCAGCA CCTGAACTCC TGGGGGGACC GTCAGTCTTC CTCTTCCCCC
1201 CAAAACCCAA GGACACCCTC ATGATCTCCC GGACCCTGA GGTACATGC
1251 GTGGTGGTGG ACGTGAGCCA CGAAGACCTT GAGGTCAAGT TCAACTGGTA
1301 CGTGGACGGC GTGGAGGTGC ATAATGCCAA GACAAAGCCG CGGGAGGAGC
1351 AGTACAACAG CACGTACCGT GTGGTCAGCG TCCTCACCGT CCTGCACCAG
1401 GACTGGCTGA ATGGCAAGGA GTACAAGTGC AAGGTCTCCA ACAAGCCCT
1451 CCCAGCCCC ATCGAGAAAA CCATCTCCA AGCCAAAGGG CAGCCCCGAG
1501 AACCACAGGT GTACACCCTG CCCCATCCC GGGAGGAGAT GACCAAGAAC
1551 CAGGTCAGCC TGACCTGCCT GGTCAAAGGC TTCTATCCA GCGACATCGC
1601 CGTGGAGTGG GAGAGCAATG GGCAGCCGGA GAACAACACTAC AAGACCACGC
1651 CTCCCGTGCT GGACTCCGAC GGCTCCTTCT TCCTCTACAG CAAGCTCACC
1701 GTGGACAAGA GCAGGTGGCA GCAGGGGAAC GTCTTCTCAT GCTCCGTGAT
1751 GCACGAGGCT CTGCACAACC ACTACACGCA GAAGAGCCTC TCCCTGTCTC
1801 CGGGTAAATG AGTGCTAGCT GGCCAGACAT GATAAGATAC ATTGATGAGT
1851 TTGGACAAAC CACAAC TAGA ATGCAGTGAA AAAAATGCTT TATTTGTGAA
1901 ATTTGTGATG CTATTGCTTT ATTTGTAACC ATTATAAGCT GCAATAACA
1951 AGTTAACAAC AACAAATGCA TTCATTTTAT GTTTCAGGTT CAGGGGGAGG
2001 TGTGGGAGGT TTTTAAAGC AAGTAAAACC TCTACAAATG TGGTATGGAA
2051 TTAATTCTAA AATACAGCAT AGCAAACTT TAACCTCCA ATCAAGCCTC
2101 TACTTGAATC CTTTTCTGAG GGATGAATAA GGCATAGGCA TCAGGGGCTG
2151 TTGCCAATGT GCATTAGCTG TTTGCAGCCT CACCTTCTTT CATGGAGTTT
2201 AAGATATAGT GTATTTTCCC AAGGTTTGAA CTAGCTCTTC ATTTCTTTAT
2251 GTTTTAAATG CACTGACCTC CCACATTCCC TTTT TAGTAA AATATTCAGA
2301 AATAATTTAA ATACATCATT GCAATGAAAA TAAATGTTTT TTATTAGGCA
2351 GAATCCAGAT GCTCAAGGCC CTTCATAATA TCCCCAGTT TAGTAGTTGG
2401 ACTTAGGGAA CAAAGGAACC TTTAATAGAA ATTGGACAGC AAGAAAGCGA
2451 GCTTCTAGCT TATCCTCAGT CCTGCTCCTC TGCCACAAG TGCACGCAGT
2501 TGCCGGCCGG GTCGCGCAGG GCGAACTCCC GCCCCACGG CTGCTCGCCG
2551 ATCTCGGTCA TGGCCGGCCC GGAGGCGTCC CGGAAGTTCG TGGACACGAC
2601 CTCCGACCAC TCGGCGTACA GCTCGTCCAG GCCGCGCACC CACACCAGG
2651 CCAGGGTGTG GTCCGGCACC ACCTGGTCTT GGACCGCGCT GATGAACAGG
2701 GTCACGTCGT CCCGGACCAC ACCGGCGAAG TCGTCTCCA CGAAGTCCCG
2751 GGAGAACCCG AGCCGGTCCG TCCAGAACTC GACCGCTCCG GCGACGTCGC
2801 GCGCGGTGAG CACCGGAACG GCACTGGTCA ACTTGGCCAT GATGGCTCCT
2851 CCTGTCAGGA GAGGAAAGAG AAGAAGGTTA GTACAATTGC TATAGTGAGT
2901 TGTATTATAC TATGCAGATA TACTATGCCA ATGATTAATT GTCAAAC TAG
2951 GGCTGCAGGG TTCATAGTGC CACTTTTCTT GCACTGCCCC ATCTCCTGCC
3001 CACCCTTCC CAGGCATAGA CAGTCAGTGA CTTACCAAAC TCACAGGAGG
3051 GAGAAGGCAG AAGCTTGAGA CAGACCCGCG GGACCGCCA ACTGCGAGGG
3101 GACGTGGCTA GGGCGGCTTC TTTTATGGTG CGCCGGCCCT CGGAGGCAGG
3151 GCGCTCGGGG AGGCCTAGCG GCCAATCTGC GGTGGCAGGA GGCGGGGCCG
3201 AAGGCCGTGC CTGACCAATC CGGAGCACAT AGGAGTCTCA GCCCCCCGCC
3251 CCAAAGCAAG GGAAGTCAC GCGCCTGTAG CGCCAGCGTG TTGTGAAATG
3301 GGGGCTTGGG GGGGTGGGG CCCTGACTAG TCAAACAAA CTCCCATTGA

3351 CGTCAATGGG GTGGAGACTT GGAAATCCCC GTGAGTCAAA CCGCTATCCA
3401 CGCCCATTTGA TGTACTGCCA AAACCGCATC ATCATGGTAA TAGCGATGAC
3451 TAATACGTAG ATGTACTGCC AAGTAGGAAA GTCCCATAAG GTCATGTACT
3501 GGGCATAATG CCAGGCGGGC CATTTACCGT CATTGACGTC AATAGGGGGC
3551 GTACTTGGCA TATGATACAC TTGATGTACT GCCAAGTGGG CAGTTTACCG
3601 TAAATACTCC ACCCATTTGAC GTCAATGGAA AGTCCCTATT GGC GTTACTA
3651 TGGGAACATA CGTCATTATT GACGTCAATG GCGGGGGTTC GTTGGGCGGT
3701 CAGCCAGGCG GGCCATTTAC CGTAAGTTAT GTAACGCCTG CAGGTTAATT
3751 AAGAACATGT GAGCAAAAGG CCAGCAAAAG GCCAGGAACC GTAAAAAGGC
3801 CGCGTTGCTG GCGTTTTTCC ATAGGCTCCG CCCCCCTGAC GAGCATCACA
3851 AAAATCGACG CTCAAGTCAG AGGTGGCGAA ACCCGACAGG ACTATAAAGA
3901 TACCAGGCGT TTCCCCCTGG AAGCTCCCTC GTGCGCTCTC CTGTTCCGAC
3951 CCTGCCGCTT ACCGGATACC TGTCCGCCTT TCTCCCTTCG GGAAGCGTGG
4001 CGCTTTCTCA TAGCTCACGC TGTAGGTATC TCAGTTCGGT GTAGGTCGTT
4051 CGTCCAAGC TGGGCTGTGT GCACGAACCC CCCGTTCAGC CCGACCGCTG
4101 CGCCTTATCC GGTAACTATC GTCTTGAGTC CAACCCGGTA AGACACGACT
4151 TATCGCCACT GGCAGCAGCC ACTGGTAACA GGATTAGCAG AGCGAGGTAT
4201 GTAGGCGGTG CTACAGAGTT CTTGAAGTGG TGGCCTAACT ACGGCTACAC
4251 TAGAAGAACA GTATTTGGTA TCTGCGCTCT GCTGAAGCCA GTTACCTTCG
4301 GAAAAAGAGT TGGTAGCTCT TGATCCGGCA AACAAACCAC CGCTGGTAGC
4351 GGTGGTTTTT TTGTTTGCAA GCAGCAGATT ACGCGCAGAA AAAAAGGATC
4401 TCAAGAAGAT CCTTTGATCT TTTCTACGGG GTCTGACGCT CAGTGGAACG
4451 AAAACTCACG TTAAGGGATT TTGGTCATGG CTAGTTAATT AACATTTAAA
4501 TCAGCGGCCG CAATAAAATA TCTTTATTTT CATTACATCT GTGTGTTGGT
4551 TTTTTGTGTG AATCGTAACT AACATACGCT CTCCATCAAA ACAAACGAA
4601 ACAAACAAA CTAGCAAAAT AGGCTGTCCC CAGTGCAAGT GCAGGTGCCA
4651 GAACATTTCT CTATCGAA

SI.1.2 mMICL-hIgG1-Fc sequence

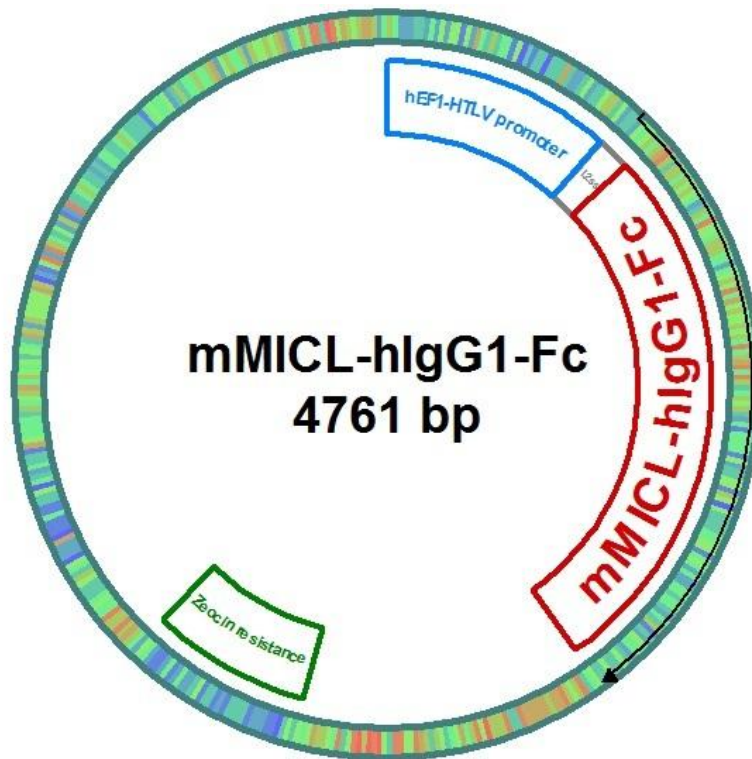
hEF1-HTLV promoter

IL2 ss

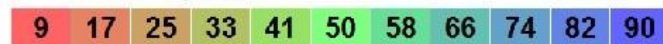
mMICL-hIgG1-Fc

Zeocin resistance

Black arrow (→) represents an open reading frame (ORF).



GC% in 11 bp blocks



```

1  GGATCTGCGA  TCGCTCCGGT  GCCCGTCAGT  GGGCAGAGCG  CACATCGCCC
51  ACAGTCCCGG  AGAAGTTGGG  GGGAGGGGTC  GGCAATTGAA  CGGGTGCCTA
101 GAGAAGGTGG  CGCGGGGTAA  ACTGGGAAAG  TGATGTCGTG  TACTGGCTCC
151 GCCTTTTTC  CGAGGGTGGG  GGAGAACCGT  ATATAAGTGC  AGTAGTCGCC
201 GTGAACGTT  TTTTTCGCAA  CGGGTTTGCC  GCCAGAACAC  AGCTGAAGCT
251 TCGAGGGGCT  CGCATCTCTC  CTTACGCGC  CCGCCGCCCT  ACCTGAGGCC
301 GCCATCCACG  CCGGTTGAGT  CGCGTTCTGC  CGCCTCCCGC  CTGTGGTGCC
351 TCCTGAACTG  CGTCCGCCGT  CTAGGTAAGT  TTAAAGCTCA  GGTCGAGACC
401 GGGCCTTTGT  CCGGCGCTCC  CTTGGAGCCT  ACCTAGACTC  AGCCGGCTCT
451 CCACGCTTTG  CCTGACCCTG  CTTGCTCAAC  TCTACGTCTT  TGTTTCGTTT
501 TCTGTTCTGC  GCCGTTACAG  ATCCAAGCTG  TGACCGGCGC  CTACCTGAGA
551 TCACCGGCGA  AGGAGGGCCA  CCATGTACAG  GATGCAACTC  CTGTCTTGCA
601 TTGCACTAAG  TCTTGCACCT  GTCACGAAT  CTTTGGCAAC  AGAAATGATA
651 AAATCGAATC  AATTGCAAAG  GGCCAAGGAA  GAACTTCAGG  AAAATGTTTC
701 CCTACAGCTG  AAGCACAATC  TCAACAGCTC  CAAGAAAATC  AAGAACCTTT
751 CTGCCATGCT  GCAAAGCACA  GCCACCCAGC  TGTGCCGAGA  GCTGTATAGC
801 AAAGAACCAG  AGCACAAATG  TAAACCATGT  CCAAAGGGTT  CAGAAATGGTA
851 CAAGGACAGC  TGTTATTCTC  AACTCAATCA  GTATGGAACA  TGGCAAGAGA

```

901 GTGTCATGGC CTGCTCTGCT CGGAATGCCA GCCTCCTGAA GGTTAAGAAC
951 AAGGATGTGC TGGAAATTTAT AAAGTACAAG AAGCTACGCT ATTTTTGGCT
1001 TGCATTGTTG CCCAGAAAAG ATCGCACACA ATATCCACTA AGTGAGAAGA
1051 TGTTCCCTCTC TGAAGAGTCT GAAAGAAGCA CAGATGACAT AGATAAGAAG
1101 TACTGCGGAT ATATAGACAG GGTC AATGTT TATTATACAT ACTGCACTGA
1151 TGAGAACAAT ATCATATGTG AAGAGACAGC CAGCAAGGTG CAGTTGGAAA
1201 GTGTGTTGAA TGGCAGATCT GACAAAACCTC ACACATGCCC ACCGTGCCCA
1251 GCACCTGAAC TCCTGGGGGG ACCGTCAAGTTC TTCCTCTTCC CCCCAAACC
1301 CAAGGACACC CTCATGATCT CCCGGACCCC TGAGGTCACA TGCGTGTTGG
1351 TGGACGTGAG CCACGAAGAC CCTGAGGTCA AGTTCAACTG GTACGTGGAC
1401 GCGTGAGG TGCATAATGC CAAGACAAAG CCGCGGGAGG AGCAGTACAA
1451 CAGCACGTAC CGTGTGGTCA GCGTCCTCAC CGTCCTGCAC CAGGACTGGC
1501 TGAATGGCAA GGAGTACAAG TGCAAGGTCT CCAACAAAGC CCTCCCAGCC
1551 CCCATCGAGA AAACCATCTC CAAAGCCAAA GGGCAGCCCC GAGAACCACA
1601 GGTGTACACC CTGCCCCCAT CCCGGGAGGA GATGACCAAG AACCAGGTCA
1651 GCCTGACCTG CCTGGTCAA GGCTTCTATC CCAGCGACAT CGCCGTGGAG
1701 TGGGAGAGCA ATGGGCAGCC GGAGAACAAC TACAAGACCA CGCCTCCCGT
1751 GCTGGACTCC GACGGCTCCT TCTTCTCTA CAGCAAGCTC ACCGTGGACA
1801 AGAGCAGGTG GCAGCAGGGG AACGTCTTCT CATGCTCCGT GATGCACGAG
1851 GCTCTGCACA ACCACTACAC GCAGAAGAGC CTCTCCCTGT CTCCGGGTAA
1901 ATGAGTGCTA GCTGGCCAGA CATGATAAGA TACATTGATG AGTTTGGACA
1951 AACCACAAC AGAATGCAGT GAAAAAATG CTTTATTTGT GAAATTTGTG
2001 ATGCTATTGC TTTATTTGTA ACCATTATAA GCTGCAATAA ACAAGTTAAC
2051 AACACAATT GCATTCATTT TATGTTTCAG GTTCAGGGGG AGGTGTGGGA
2101 GGTTTTTTAA AGCAAGTAAA ACCTCTACAA ATGTGGTATG GAATTAATTC
2151 TAAAATACAG CATAGCAAAA CTTTAACCTC CAAATCAAGC CTCTACTTGA
2201 ATCCTTTTCT GAGGGATGAA TAAGGCATAG GCATCAGGGG CTGTTGCCAA
2251 TGTGCATTAG CTGTTTGCAG CCTCACCTTC TTTCATGGAG TTTAAGATAT
2301 AGTGTATTTT CCCAAGGTTT GAACTAGCTC TTCATTTCTT TATGTTTTAA
2351 ATGCACTGAC CTCCCACATT CCCTTTTTAG TAAAATATTC AGAAATAATT
2401 TAAATACATC ATTGCAATGA AAATAAATGT TTTTTATTAG GCAGAATCCA
2451 GATGCTCAAG GCCCTTCATA ATATCCCCCA GTTTAGTAGT TGGACTTAGG
2501 GAACAAAGGA ACCTTTAATA GAAATTGGAC AGCAAGAAAG CGAGCTTCTA
2551 GCTTATCCTC AGTCCTGCTC CTCTGCCACA AAGTGCACGC AGTTGCCGGC
2601 CGGGTCGCGC AGGGCGAACT CCCGCCCCA CGGCTGCTCG CCGATCTCGG
2651 TCATGGCCGG CCCGGAGGCG TCCCGGAAGT TCGTGGACAC GACCTCCGAC
2701 CACTCGGCGT ACAGCTCGTC CAGGCCGCGC ACCCACACC AGGCCAGGGT
2751 GTTGTCCGGC ACCACCTGGT CCTGGACCGC GCTGATGAAC AGGGTCACGT
2801 CGTCCCAGAC CACACCGGCG AAGTCGTCTT CCACGAAGTC CCGGGAGAAC
2851 CCGAGCCGGT CCGTCCAGAA CTCGACCGCT CCGGCGACGT CGCGCGGGT
2901 GAGCACCGBA ACGGCACTGG TCAACTTGGC CATGATGGCT CCTCCTGTCA
2951 GGAGAGGAAA GAGAAGAAGG TTAGTACAAT TGCTATAGTG AGTTGTATTA
3001 TACTATGCAG ATATACTATG CCAATGATTA ATTGTCAAAC TAGGGCTGCA
3051 GGGTTCATAG TGCCACTTTT CCTGCACTGC CCCATCTCCT GCCCACCCTT
3101 TCCCAGGCAT AGACAGTCAG TGACTTACCA AACTCACAGG AGGGAGAAGG
3151 CAGAAGCTTG AGACAGACCC GCGGGACCGC CGAACTGCGA GGGGACGTGG
3201 CTAGGGCGGC TTCTTTTATG GTGCGCCGGC CCTCGGAGGC AGGGCGCTCG
3251 GGGAGGCCTA GCGGCCAATC TGCGGTGGCA GGAGGCGGGG CCGAAGGCCG
3301 TGCCTGACCA ATCCGGAGCA CATAGGAGTC TCAGCCCCC GCCCAAAGC
3351 AAGGGGAAGT CACGCGCCTG TAGCGCCAGC GTGTTGTGAA ATGGGGGCTT
3401 GGGGGGGTTG GGGCCCTGAC TAGTCAAAC AACTCCCAT TGACGTCAAT
3451 GGGGTGGAGA CTTGGAAATC CCCGTGAGTC AAACCGCTAT CCACGCCCAT

3501 TGATGTACTG CAAAACCGC ATCATCATGG TAATAGCGAT GACTAATACG
3551 TAGATGTACT GCCAAGTAGG AAAGTCCCAT AAGGTCATGT ACTGGGCATA
3601 ATGCCAGGCG GGCCATTTAC CGTCATTGAC GTCAATAGGG GGCGTACTTG
3651 GCATATGATA CACTTGATGT ACTGCCAAGT GGCAGTTTA CCGTAAATAC
3701 TCCACCCATT GACGTCAATG GAAAGTCCCT ATTGGCGTTA CTATGGGAAC
3751 ATACGTCATT ATTGACGTCA ATGGGCGGGG GTCGTTGGGC GGTCAGCCAG
3801 GCGGGCCATT TACCGTAAGT TATGTAACGC CTGCAGGTTA ATTAAGAACA
3851 TGTGAGCAAA AGGCCAGCAA AAGGCCAGGA ACCGTAAAAA GGCCGCGTTG
3901 CTGGCGTTTT TCCATAGGCT CCGCCCCCT GACGAGCATC AAAAAATCG
3951 ACGCTCAAGT CAGAGGTGGC GAAACCCGAC AGGACTATAA AGATACCAGG
4001 CGTTTCCCCC TGGAAGCTCC CTCGTGCGCT CTCCTGTTCC GACCCTGCCG
4051 CTTACCGGAT ACCTGTCCGC CTTTCTCCCT TCGGGAAGCG TGGCGCTTTC
4101 TCATAGCTCA CGCTGTAGGT ATCTCAGTTC GGTGTAGGTC GTTCGCTCCA
4151 AGCTGGGCTG TGTGCACGAA CCCCCGTTT AGCCCGACCG CTGCGCCTTA
4201 TCCGGTAACT ATCGTCTTGA GTCCAACCCG GTAAGACACG ACTTATCGCC
4251 ACTGGCAGCA GCCACTGGTA ACAGGATTAG CAGAGCGAGG TATGTAGGCG
4301 GTGCTACAGA GTTCTTGAAG TGGTGGCCTA ACTACGGCTA CACTAGAAGA
4351 ACAGTATTTG GTATCTGCGC TCTGCTGAAG CCAGTTACCT TCGAAAAAAG
4401 AGTTGGTAGC TCTTGATCCG GCAAACAAAC CACCGCTGGT AGCGGTGGTT
4451 TTTTTGTTTG CAAGCAGCAG ATTACGCGCA GAAAAAAGG ATCTCAAGAA
4501 GATCCTTTGA TCTTTTCTAC GGGGTCTGAC GCTCAGTGGA ACGAAAATC
4551 ACGTTAAGGG ATTTTGGTCA TGGCTAGTTA ATTAACATTT AAATCAGCGG
4601 CCGCAATAAA ATATCTTTAT TTTCATTACA TCTGTGTGTT GTTTTTTTGT
4651 GTGAATCGTA ACTAACATAC GCTCTCCATC AAAACAAAAC GAAACAAAAC
4701 AAAC TAGCAA AATAGGCTGT CCCCAGTGCA AGTGCAGGTG CCAGAACATT
4751 TCTCTATCGA A

SI.1.3 mDCIR-hIgG1-Fc sequence

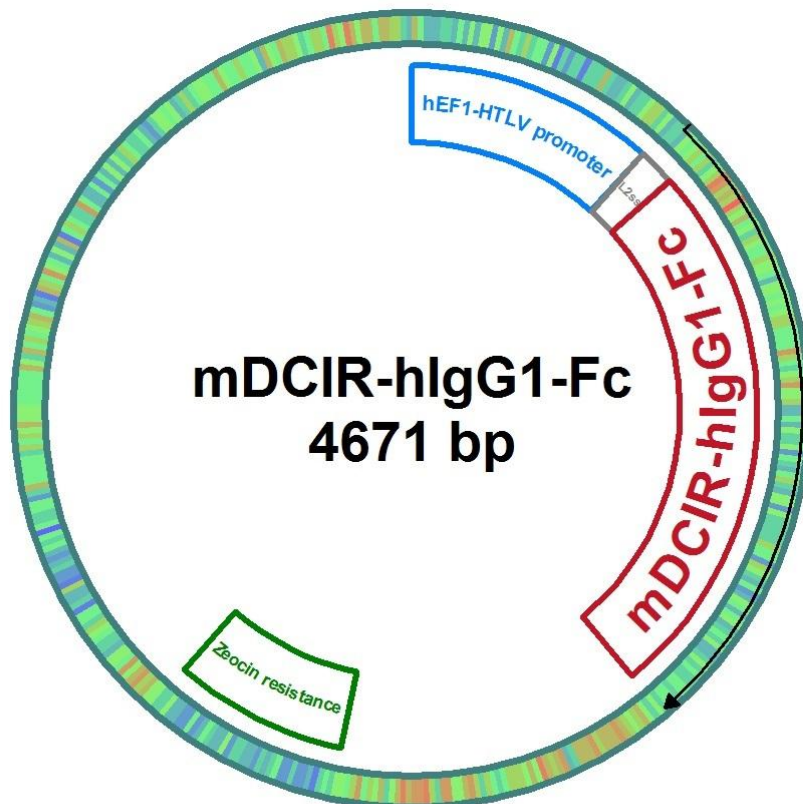
hEF1-HTLV promoter

IL2 ss

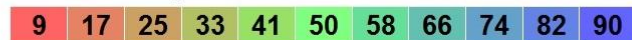
mDCIR-hIgG1-Fc

Zeocin resistance

Black arrow (→) represents an open reading frame (ORF).



GC% in 11 bp blocks



```

1  GGATCTGCGA  TCGCTCCGGT  GCCCGTCAGT  GGGCAGAGCG  CACATCGCCC
51  ACAGTCCCCG  AGAAGTTGGG  GGGAGGGGTC  GGCAATTGAA  CGGGTGCCTA
101 GAGAAGGTGG  CGCGGGGTAA  ACTGGGAAAG  TGATGTCGTG  TACTGGCTCC
151 GCCTTTTTTC  CGAGGGTGGG  GGAGAACCGT  ATATAAGTGC  AGTAGTCGCC
201 GTGAACGTTT  TTTTTCGCAA  CGGGTTTGCC  GCCAGAACAC  AGCTGAAGCT
251 TCGAGGGGCT  CGCATCTCTC  CTTACGCGC  CCGCCGCCCT  ACCTGAGGCC
301 GCCATCCACG  CCGGTTGAGT  CGCGTTCGTC  CGCCTCCCGC  CTGTGGTGCC
351 TCCTGAACTG  CGTCCGCCGT  CTAGGTAAGT  TTAAAGCTCA  GGTCGAGACC
401 GGGCCTTTGT  CCGGCGCTCC  CTTGGAGCCT  ACCTAGACTC  AGCCGGCTCT
451 CCACGCTTTG  CCTGACCCTG  CTTGCTCAAC  TCTACGTCTT  TGTTTCGTTT
501 TCTGTTCTGC  GCCGTTACAG  ATCCAAGCTG  TGACCGGCGC  CTACCTGAGA
551 TCACCGGCGA  AGGAGGGCCA  CCATGTACAG  GATGCAACTC  CTGTCTTGCA
601 TTGCACTAAG  TCTTGCACCT  GTCACGAATT  CGTACTTCTT  CCTGCTGCTG
651 GCAATCACAT  TCTTAGTTGC  TTTTATCATT  TATTTTCAA  AGTACTCTCA
701 ACTTCTTGAA  GAAAAAAAAG  CTGCAAAAA  TATAATGCAC  AATGAATTGA
751 ACTGCACAAA  AAGTGTTTCA  CCCATGGAAG  ACAAAGTCTG  GAGCTGTTGC
801 CCAAAGGATT  GGAGGCTATT  TGGTTCAC  TGCTACTTGG  TTCCACAGT
851 TTCTTCATCA  GCATCTTGGA  ACAAGAGTGA  GGAGAACTGC  TCCCGCATGG

```

901 GTGCTCATCT AGTGGTGATC CAAAGCCAGG AAGAGCAGGA TTTCATCACT
951 GGGATCTTGG ACACTCATGC TGCTTATTTT ATAGGGTGT GGGATACAGG
1001 CCATCGGCAA TGGCAATGGG TTGATCAGAC ACCATATGAA GAAAGTATCA
1051 CATTCTGGCA CAATGGTGAG CCCAGCAGTG GCAATGAAAA ATGTGCTACA
1101 ATAATTTACC GTTGGGAAGAC TGGAAGATCT GACAAAAC TC ACACATGCCC
1151 ACCGTGCCCA GCACCTGAAC TCCTGGGGGG ACCGT CAGTC TTCCTCTTCC
1201 CCCAAAACC CAAGGACACC CTCATGATCT CCCGGACCCC TGAGGTCACA
1251 TGCCTGGTGG TGGACGTGAG CCACGAAGAC CCTGAGGTCA AGTTCAACTG
1301 GTACGTGGAC GGCCTGGAGG TGCATAATGC CAAGACAAAG CCGCGGGAGG
1351 AGCAGTACAA CAGCACGTAC CGTGTGGTCA GCGTCCTCAC CGTCCTGCAC
1401 CAGGACTGGC TGAATGGCAA GGAGTACAAG TGCAAGGTCT CCAACAAAGC
1451 CCTCCCAGCC CCCATCGAGA AAACCATCTC CAAAGCCAAA GGGCAGCCCC
1501 GAGAACCACA GGTGTACACC CTGCCCCAT CCCGGGAGGA GATGACCAAG
1551 AACCAGGTCA GCCTGACCTG CCTGGTCAA GGCTTCTATC CCAGCGACAT
1601 CGCCGTGGAG TGGGAGAGCA ATGGGCAGCC GGAGAACAAC TACAAGACCA
1651 CGCCTCCCGT GCTGGACTCC GACGGCTCCT TCTTCCTCTA CAGCAAGCTC
1701 ACCGTGGACA AGAGCAGGTG GCAGCAGGGG AACGTCTTCT CATGCTCCGT
1751 GATGCACGAG GCTCTGCACA ACCACTACAC GCAGAAGAGC CTCTCCCTGT
1801 CTCCGGGTAA ATGAGTGCTA GCTGGCCAGA CATGATAAGA TACATTGATG
1851 AGTTTGGACA AACCACAAC AGAATGCAGT GAAAAAATG CTTTATTTGT
1901 GAAATTTGTG ATGCTATTGC TTTATTTGTA ACCATTATAA GCTGCAATAA
1951 ACAAGTTAAC AACAACAATT GCATTCATTT TATGTTTCAG GTTCAGGGGG
2001 AGGTGTGGGA GTTTTTTTAA AGCAAGTAAA ACCTCTACAA ATGTGGTATG
2051 GAATTAATTC TAAAATACAG CATAGCAAAA CTTTAACCTC CAAATCAAGC
2101 CTCTACTTGA ATCCTTTTCT GAGGGATGAA TAAGGCATAG GCATCAGGGG
2151 CTGTTGCCAA TGTGCATTAG CTGTTTGCAG CCTCACCTTC TTTCATGGAG
2201 TTTAAGATAT AGTGTATTTT CCCAAGGTTT GAACTAGCTC TTCATTTCTT
2251 TATGTTTTAA ATGCACTGAC CTCCCACATT CCCTTTTTAG TAAAATATTC
2301 AGAAATAATT TAAATACATC ATTGCAATGA AAATAAATGT TTTTTATTAG
2351 GCAGAATCCA GATGCTCAAG GCCCTTCATA ATATCCCCCA GTTTAGTAGT
2401 TGGACTTAGG GAACAAAGGA ACCTTTAATA GAAATTGGAC AGCAAGAAAG
2451 CGAGCTTCTA GCTTATCCTC AGTCCTGCTC CTCTGCCACA AAGTGCACGC
2501 AGTTGCCGGC CGGGTCGCGC AGGGCGAACT CCCGCCCCA CGGCTGCTCG
2551 CCGATCTCGG TCATGGCCGG CCCGGAGGCG TCCCGGAAGT TCGTGGACAC
2601 GACCTCCGAC CACTCGGCGT ACAGCTCGTC CAGGCCGCGC ACCCACACCC
2651 AGGCCAGGGT GTTGTCCGGC ACCACCTGGT CCTGGACCGC GCTGATGAAC
2701 AGGGTCACGT CGTCCCGGAC CACACCGGCG AAGTCGTCTT CCACGAAGTC
2751 CCGGGAGAAC CCGAGCCGGT CGGTCCAGAA CTCGACCGCT CCGGCGACGT
2801 CGCGCGCGGT GAGCACC GGA ACGGCACTGG TCAACTTGGC CATGATGGCT
2851 CCTCCTGTCA GGAGAGGAAA GAGAAGAAGG TTAGTACAAT TGCTATAGTG
2901 AGTTGTATTA TACTATGCAG ATATACTATG CCAATGATTA ATTGTCAAAC
2951 TAGGGCTGCA GGGTTCATAG TGCCACTTTT CCTGCACTGC CCCATCTCCT
3001 GCCACCCCTT TCCCAGGCAT AGACAGTCAG TGA CTTACCA AACTCACAGG
3051 AGGGAGAAGG CAGAAGCTTG AGACAGACCC GCGGGACCGC CGAACTGCGA
3101 GGGGACGTGG CTAGGGCGGC TTCTTTTATG GTGCGCCGGC C TCGGAGGC
3151 AGGGCGCTCG GGGAGCCTA GCGGCCAATC TGCGGTGGCA GGAGGCGGGG
3201 CCGAAGGCCG TGCTGACCA ATCCGGAGCA CATAGGAGTC TCAGCCCCC
3251 GCCCAAAGC AAGGGGAAGT CACGCGCCTG TAGCGCCAGC GTGTTGTGAA
3301 ATGGGGGCTT GGGGGGGTTG GGGCCCTGAC TAGTCAAAC AA ACTCCCAT
3351 TGACGTCAAT GGGGTGGAGA CTTGGAAATC CCCGTGAGTC AAACCGCTAT
3401 CCACGCCCAT TGATGTACTG CCAAACCGC ATCATCATGG TAATAGCGAT
3451 GACTAATACG TAGATGTACT GCCAAGTAGG AAAGTCCCAT AAGGTCATGT

3501 ACTGGGCATA ATGCCAGGCG GGCCATTTAC CGTCATTGAC GTCAATAGGG
3551 GGCGTACTTG GCATATGATA CACTTGATGT ACTGCCAAGT GGGCAGTTTA
3601 CCGTAAATAC TCCACCCATT GACGTCAATG GAAAGTCCCT ATTGGCGTTA
3651 CTATGGGAAC ATACGTCATT ATTGACGTCA ATGGGCGGGG GTCGTTGGGC
3701 GGTGAGCCAG GCGGGCCATT TACCGTAAGT TATGTAACGC CTGCAGGTTA
3751 ATTAAGAACA TGTGAGCAA AGGCCAGCAA AAGGCCAGGA ACCGTAAAAA
3801 GGCCGCGTTG CTGGCGTTTT TCCATAGGCT CCGCCCCCT GACGAGCATC
3851 ACAAAAATCG ACGCTCAAGT CAGAGGTGGC GAAACCCGAC AGGACTATAA
3901 AGATACCAGG CGTTTCCCCC TGGAAGCTCC CTCGTGCGCT CTCCTGTTCC
3951 GACCCTGCCG CTTACCGGAT ACCTGTCCGC CTTTCTCCCT TCGGGAAGCG
4001 TGGCGCTTTC TCATAGCTCA CGCTGTAGGT ATCTCAGTTC GGTGTAGGTC
4051 GTTCGCTCCA AGCTGGGCTG TGTGCACGAA CCCCCGTTT AGCCCGACCG
4101 CTGCGCCTTA TCCGGTAACT ATCGTCTTGA GTCCAACCCG GTAAGACACG
4151 ACTTATCGCC ACTGGCAGCA GCCACTGGTA ACAGGATTAG CAGAGCGAGG
4201 TATGTAGGCG GTGCTACAGA GTTCTTGAAG TGGTGGCCTA ACTACGGCTA
4251 CACTAGAAGA ACAGTATTTG GTATCTGCGC TCTGCTGAAG CCAGTTACCT
4301 TCGGAAAAAG AGTTGGTAGC TCTTGATCCG GCAAACAAAC CACCGCTGGT
4351 AGCGGTGGTT TTTTTGTTTG CAAGCAGCAG ATTACGCGCA GAAAAAAGG
4401 ATCTCAAGAA GATCCTTTGA TCTTTTCTAC GGGGTCTGAC GCTCAGTGGA
4451 ACGAAAATC ACGTTAAGGG ATTTTGGTCA TGGCTAGTTA ATTAACATTT
4501 AAATCAGCGG CCGCAATAAA ATATCTTTAT TTCATTACA TCTGTGTGTT
4551 GGTTTTTTGT GTGAATCGTA ACTAACATAC GCTCTCCATC AAAACAAAAC
4601 GAAACAAAAC AAAC TAGCAA AATAGGCTGT CCCAGTGCA AGTGCAGGTG
4651 CCAGAACATT TCTCTATCGA A

SI.1.4 mMCL-hIgG1-Fc sequence

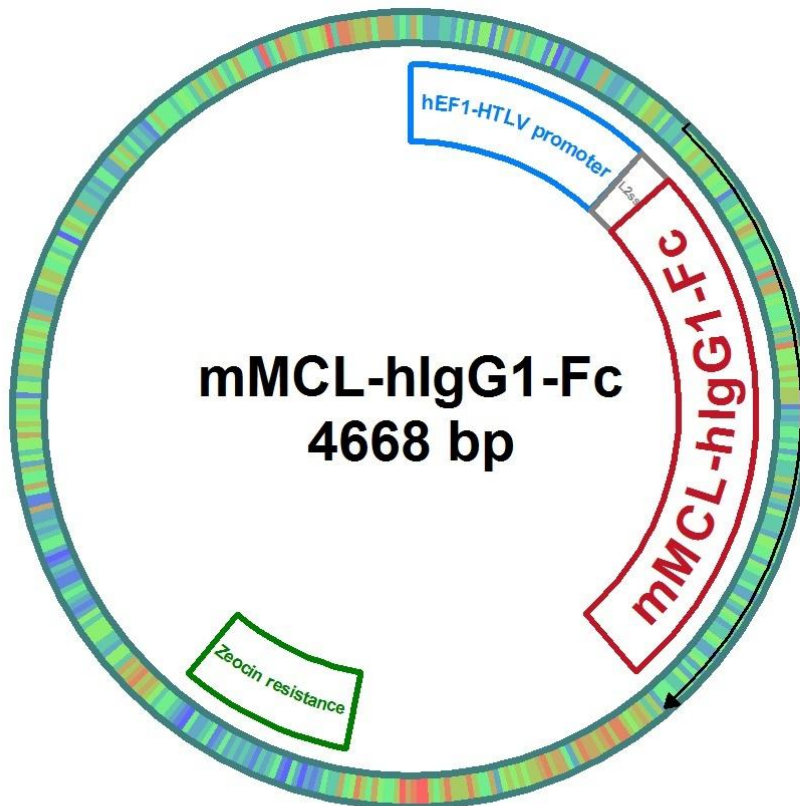
hEF1-HTLV promoter

IL2 ss

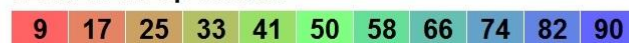
mMCL-hIgG1-Fc

Zeocin resistance

Black arrow (→) represents an open reading frame (ORF).



GC% in 11 bp blocks



```

1  GGATCTGCGA  TCGCTCCGGT  GCCCGTCAGT  GGGCAGAGCG  CACATCGCCC
51  ACAGTCCCCG  AGAAGTTGGG  GGGAGGGGTC  GGCAATTGAA  CGGGTGCCTA
101 GAGAAGGTGG  CGCGGGGTAA  ACTGGGAAAG  TGATGTCGTG  TACTGGCTCC
151 GCCTTTTTTC  CGAGGGTGGG  GGAGAACCGT  ATATAAGTGC  AGTAGTCGCC
201 GTGAACGTTT  TTTTTCGCAA  CGGGTTTGCC  GCCAGAACAC  AGCTGAAGCT
251 TCGAGGGGCT  CGCATCTCTC  CTTACGCGC  CCGCCGCCCT  ACCTGAGGCC
301 GCCATCCACG  CCGGTTGAGT  CGCGTTCTGC  CGCCTCCCGC  CTGTGGTGCC
351 TCCTGAACTG  CGTCCGCCGT  CTAGGTAAGT  TTAAAGCTCA  GGTCGAGACC
401 GGGCCTTTGT  CCGGCGCTCC  CTTGGAGCCT  ACCTAGACTC  AGCCGGCTCT
451 CCACGCTTTG  CCTGACCCTG  CTTGCTCAAC  TCTACGTCTT  TGTTTCGTTT
501 TCTGTTCTGC  GCCGTTACAG  ATCCAAGCTG  TGACCGGCGC  CTACCTGAGA
551 TCACCGGCGA  AGGAGGGCCA  CCATGTACAG  GATGCAACTC  CTGTCTTGCA
601 TTGCACTAAG  TCTTGCACCT  GTCACCCATG  GTCATTACTT  TTTACGCTGG
651 ACGAGAGGAA  GTGTGGTGAA  ACTGTCAGAC  TACCACACGA  GAGTAACGTG
701 CATCCGAGAG  GGGCCACAGC  CTGGAGCTAC  AGGAGGTACT  TGGACCTGCT
751 GTCCTGTTAG  CTGGAGAGCC  TTCCAGTCTA  ACTGTTACTT  TCCTCTTAAT
801 GACAACCAGA  CCTGGCATGA  GAGCGAGAGG  AACTGCTCAG  GGATGAGCAG

```

851 TCATCTGGTG ACCATCAACA CCGAAGCAGA ACAGAATTTT GTGACCCAGC
901 TTTTGGATAA ACGGTTTTCT TATTTCTGG GACTTGCTGA TGAGAATGTG
951 GAAGGCCAAT GGCAGTGGGT GGACAAGACG CCATTTAACC CACACACGGT
1001 ATTCTGGGAA AAGGGGGAAT CCAATGACTT TATGGAAGAA GACTGTGTTG
1051 TCCTTGTTCA TGTCCATGAA AAATGGGTCT GGAATGACTT TCCTTGTCAC
1101 TTTGAGGTGA GAAGGATTTG TAGATCTGAC AAAACTCACA CATGCCACC
1151 GTGCCCAGCA CCTGAACTCC TGGGGGGACC GTCAGTCTTC CTCTTCCCC
1201 CAAAACCCAA GGACACCCTC ATGATCTCCC GGACCCTGA GGTCACATGC
1251 GTGGTGGTGG ACGTGAGCCA CGAAGACCTT GAGGTCAAGT TCAACTGGTA
1301 CGTGGACGGC GTGGAGGTGC ATAATGCCAA GACAAAGCCG CGGGAGGAGC
1351 AGTACAACAG CACGTACCGT GTGGTCAGCG TCCTCACCGT CCTGCACCAG
1401 GACTGGCTGA ATGGCAAGGA GTACAAGTGC AAGGTCTCCA ACAAAGCCCT
1451 CCCAGCCCC ATCGAGAAAA CCATCTCAA AGCCAAAGGG CAGCCCCGAG
1501 AACCACAGGT GTACACCCTG CCCCATCCC GGGAGGAGAT GACCAAGAAC
1551 CAGGTCAGCC TGACCTGCCT GGTCAAAGGC TTCATCCCA GCGACATCGC
1601 CGTGGAGTGG GAGAGCAATG GGCAGCCGGA GAACAACACTAC AAGACCACGC
1651 CTCCCGTGCT GGACTCCGAC GGCTCCTTCT TCCTCTACAG CAAGCTCACC
1701 GTGGACAAGA GCAGGTGGCA GCAGGGGAAC GTCTTCTCAT GCTCCGTGAT
1751 GCACGAGGCT CTGCACAACC ACTACACGCA GAAGAGCCTC TCCCTGTCTC
1801 CGGGTAAATG AGTGCTAGCT GGCCAGACAT GATAAGATAC ATTGATGAGT
1851 TTGGACAAAC CACAAC TAGA ATGCAGTGAA AAAAATGCTT TATTTGTGAA
1901 ATTTGTGATG CTATTGCTTT ATTTGTAACC ATTATAAGCT GCAATAAACA
1951 AGTTAACAAC AACAATTGCA TTCATTTTAT GTTTCAGGTT CAGGGGGAGG
2001 TGTGGGAGGT TTTTTAAAGC AAGTAAAACC TCTACAAATG TGGTATGGAA
2051 TTAATTCTAA AATACAGCAT AGCAAACTT TAACCTCAA ATCAAGCCTC
2101 TACTTGAATC CTTTTCTGAG GGATGAATAA GGCATAGGCA TCAGGGGCTG
2151 TTGCCAATGT GCATTAGCTG TTTGCAGCCT CACCTTCTTT CATGGAGTTT
2201 AAGATATAGT GTATTTTCCC AAGGTTTGAA CTAGCTCTTC ATTTCTTTAT
2251 GTTTTAAATG CACTGACCTC CCACATTCCC TTTT TAGTAA AATATTCAGA
2301 AATAATTTAA ATACATCATT GCAATGAAAA TAAATGTTTT TTATTAGGCA
2351 GAATCCAGAT GCTCAAGGCC CTTCATAATA TCCCCAGTT TAGTAGTTGG
2401 ACTTAGGGAA CAAAGGAACC TTTAATAGAA ATTGGACAGC AAGAAAGCGA
2451 GCTTCTAGCT TATCCTCAGT CCTGCTCCTC TGCCACAAAG TGCACGCAGT
2501 TGCCGGCCGG GTCGCGCAGG GCGAACTCCC GCCCCACGG CTGCTCGCCG
2551 ATCTCGGTCA TGGCCGGCCC GGAGGCGTCC CGGAAGTTCG TGGACACGAC
2601 CTCCGACCAC TCGGCGTACA GCTCGTCCAG GCCGCGCACC CACACCAGG
2651 CCAGGGTGTG GTCCGGCACC ACCTGGTCTT GGACCGCGCT GATGAACAGG
2701 GTCACGTCGT CCCGGACCAC ACCGGCGAAG TCGTCTCCA CGAAGTCCCG
2751 GGAGAACCCG AGCCGGTCGG TCCAGAACTC GACCGCTCCG GCGACGTCCG
2801 GCGCGGTGAG CACCGGAACG GCACTGGTCA ACTTGGCCAT GATGGCTCCT
2851 CCTGTCAGGA GAGGAAAGAG AAGAAGGTTA GTACAATTGC TATAGTGAGT
2901 TGTATTATAC TATGCAGATA TACTATGCCA ATGATTAATT GTCAAAC TAG
2951 GGCTGCAGGG TTCATAGTGC CACTTTTCTT GCACTGCCCC ATCTCCTGCC
3001 CACCCTTTC CAGGCATAGA CAGTCAGTGA CTTACCAAAC TCACAGGAGG
3051 GAGAAGGCAG AAGCTTGAGA CAGACCCGCG GGACCGCCGA ACTGCGAGGG
3101 GACGTGGCTA GGGCGGCTTC TTTTATGGTG CGCCGGCCCT CGGAGGCAGG
3151 GCGCTCGGGG AGGCCTAGCG GCCAATCTGC GGTGGCAGGA GGCGGGGCCG
3201 AAGGCCGTGC CTGACCAATC CGGAGCACAT AGGAGTCTCA GCCCCCCGCC
3251 CCAAAGCAAG GGGAAGTCAC GCGCCTGTAG CGCCAGCGTG TTGTGAAATG
3301 GGGGCTTGGG GGGGTTGGGG CCCTGACTAG TCAAACAAA CTCCCATTGA
3351 CGTCAATGGG GTGGAGACTT GGAAATCCCC GTGAGTCAA CCGCTATCCA
3401 CGCCCATGTA TGTACTGCCA AAACCGCATC ATCATGGTAA TAGCGATGAC

3451 TAATACGTAG ATGTACTGCC AAGTAGGAAA GTCCCATAAG GTCATGTACT
3501 GGGCATAATG CCAGGCGGGC CATTTACCGT CATTGACGTC AATAGGGGGC
3551 GTA CTTGGCA TATGATACAC TTGATGTACT GCCAAGTGGG CAGTTTACCG
3601 TAAATACTCC ACCCATTGAC GTCAATGGAA AGTCCCTATT GCGGTTACTA
3651 TGGGAACATA CGTCATTATT GACGTCAATG GCGGGGGGTC GTTGGGCGGT
3701 CAGCCAGGCG GGCCATTTAC CGTAAGTTAT GTAACGCCTG CAGGTTAATT
3751 AAGAACATGT GAGCAAAAGG CCAGCAAAAG GCCAGGAACC GTAAAAAGGC
3801 CGCGTTGCTG GCGTTTTTCC ATAGGCTCCG CCCCCCTGAC GAGCATCACA
3851 AAAATCGACG CTCAAGTCAG AGGTGGCGAA ACCCGACAGG ACTATAAAGA
3901 TACCAGGCGT TTCCCCCTGG AAGCTCCCTC GTGCGCTCTC CTGTTCCGAC
3951 CCTGCCGCTT ACCGGATACC TGTCCGCCTT TCTCCCTTCG GGAAGCGTGG
4001 CGCTTTCTCA TAGCTCACGC TG TAGGTATC TCAGTTCGGT GTAGGTCGTT
4051 CGCTCCAAGC TGGGCTGTGT GCACGAACCC CCCGTT CAGC CCGACCGCTG
4101 CGCCTTATCC GGTA ACTATC GTCTTGAGTC CAACCCGGTA AGACACGACT
4151 TATCGCCACT GGCAGCAGCC ACTGGTAACA GGATTAGCAG AGCGAGGTAT
4201 GTAGGCGGTG CTACAGAGTT CTTGAAGTGG TGGCCTAACT ACGGCTACAC
4251 TAGAAGAACA GTATTTGGTA TCTGCGCTCT GCTGAAGCCA GTTACCTTCG
4301 GAAAAAGAGT TGGTAGCTCT TGATCCGGCA AACAAACCAC CGCTGGTAGC
4351 GGTGGTTTTT TTGTTTGCAA GCAGCAGATT ACGCGCAGAA AAAAAGGATC
4401 TCAAGAAGAT CCTTTGATCT TTTCTACGGG GTCTGACGCT CAGTGGAACG
4451 AAAACTCACG TTAAGGGATT TTGGTCATGG CTAGTTAATT AACATTTAAA
4501 TCAGCGGCCG CAATAAAATA TCTTTATTTT CATTACATCT GTGTGTTGGT
4551 TTTTTGTGTG AATCGTAACT AACATACGCT CTCCATCAAA ACAAACGAA
4601 ACAAACAAA CTAGCAAAT AGGCTGTCCC CAGTGCAAGT GCAGGTGCCA
4651 GAACATTTCT CTATCGAA

SI.1.5 mClec12b-hIgG1-Fc sequence

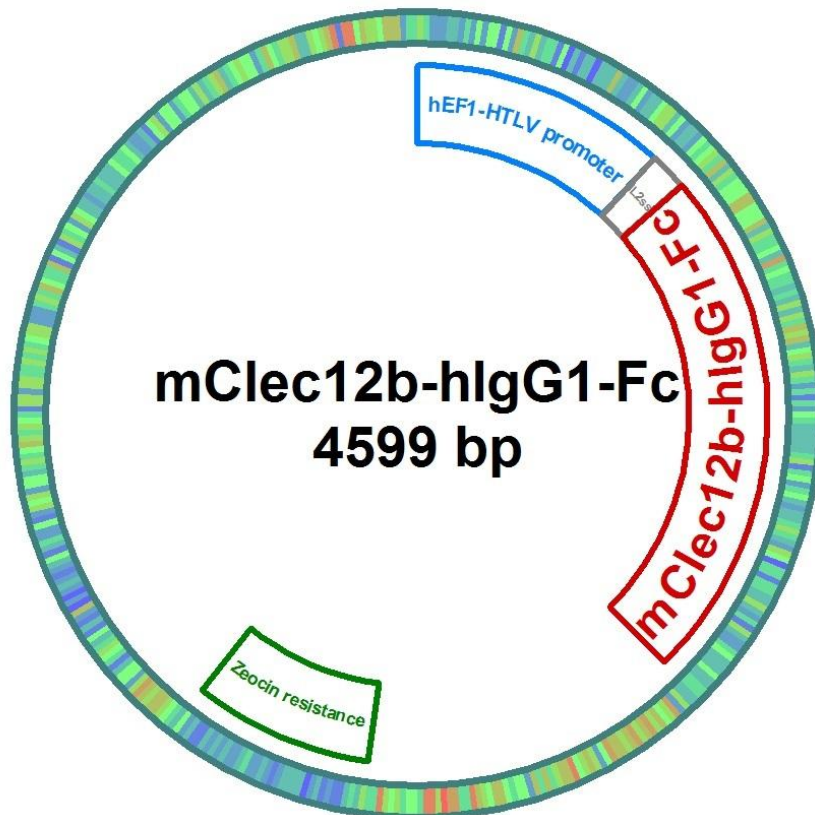
hEF1-HTLV promoter

IL2 ss

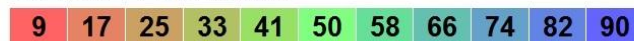
mClec12b-hIgG1-Fc

Zeocin resistance

Black arrow (→) represents an open reading frame (ORF).



GC% in 11 bp blocks



```

1  GGATCTGCGA  TCGCTCCGGT  GCCCGTCAGT  GGCAGAGCG  CACATCGCCC
51  ACAGTCCCCG  AGAAGTTGGG  GGGAGGGGTC  GGCAATTGAA  CGGGTGCCTA
101 GAGAAGGTGG  CGCGGGGTAA  ACTGGGAAAG  TGATGTCGTG  TACTGGCTCC
151 GCCTTTTTTC  CGAGGGTGGG  GGAGAACCGT  ATATAAGTGC  AGTAGTCGCC
201 GTGAACG TTC  TTTTTCGCAA  CGGGTTTGCC  GCCAGAACAC  AGCTGAAGCT
251 TCGAGGGGCT  CGCATCTCTC  CTTACGCGC  CCGCCGCCCT  ACCTGAGGCC
301 GCCATCCACG  CCGGTTGAGT  CGCGTTCTGC  CGCCTCCCGC  CTGTGGTGCC
351 TCCTGAACTG  CGTCCGCCGT  CTAGGTAAGT  TTAAAGCTCA  GGTCGAGACC
401 GGGCCTTTGT  CCGGCGCTCC  CTTGGAGCCT  ACCTAGACTC  AGCCGGCTCT
451 CCACGCTTTG  CCTGACCCTG  CTTGCTCAAC  TCTACGTC TT  TGTTTCGTTT
501 TCTGTTCTGC  GCCGTTACAG  ATCCAAGCTG  TGACCGGCGC  CTACCTGAGA
551 TCACCGGCGA  AGGAGGGCCA  CCATGTACAG  GATGCAACTC  CTGTCTTGCA
601 TTGACTAAG  TCTTGCAC TT  GTCACGAAT T  CGATATCGGC  CATGGCTTCT
651 GACCATAAAT  GCAACCCTTG  TCCCAAGACA  TGGCAATGGT  ATGAAACAG
701 TTGCTACTAT  TTCTCAATCA  ATGAAGAGAA  ATCCTGGAGT  GATAGCAGAA
751 AGGACTGTAT  AGACAAGAAT  GCCACTCTGG  TGAAGATTGA  CAGCACCGAA
801 GAAAGGGATC  TCCTTCAGTC  ACAGCTGTCC  CTCACATTTT  CTTTCTTTTG

```

851 GCTGGGATTG TCCTGGA ACT CATCTGGCAG AACTGGCTG TGGGAGGATG
901 GTTCATTCCC CCCTCCAACC CTGCTTAGTG ACAAGGAGCT TGCGAGTTTC
951 AATGGATCCA GAGAGTGTGC TTATTTTGAA AGAGGGAATA TTTACACTTC
1001 TCGCTGTCGT GCTGAAATCC CTTGGATTTG TGAGAAGAGA GCCTCCCTGG
1051 TGAGATCTGA CAAAACCTCAC ACATGCCAC CGTGCCACGC ACCTGAACTC
1101 CTGGGGGGAC CGTCAGTCTT CCTCTTCCCC CCAAACCCA AGGACACCCT
1151 CATGATCTCC CGGACCCCTG AGGTCACATG CGTGGTGGTG GACGTGAGCC
1201 ACGAAGACCC TGAGGTCAAG TTCAACTGGT ACGTGGACGG CGTGGAGGTG
1251 CATAATGCCA AGACAAAGCC GCGGGAGGAG CAGTACAACA GCACGTACCG
1301 TGTGGTCAGC GTCCTCACCG TCCTGCACCA GGA CTGGCTG AATGGCAAGG
1351 AGTACAAGTG CAAGGTCTCC AACAAAGCCC TCCAGCCCC CATCGAGAAA
1401 ACCATCTCCA AAGCCAAAGG GCAGCCCCGA GAACCACAGG TGTACACCCT
1451 GCCCCATCC CGGGAGGAGA TGACCAAGAA CCAGGTCAGC CTGACCTGCC
1501 TGGTCAAAGG CTTCTATCCC AGCGACATCG CCGTGGAGTG GGAGAGCAAT
1551 GGGCAGCCGG AGAACA ACTA CAAGACCAG CCTCCCGTGC TGGACTCCGA
1601 CGGCTCCTTC TTCCTCTACA GCAAGCTCAC CGTGGACAAG AGCAGGTGGC
1651 AGCAGGGGAA CGTCTTCTCA TGCTCCGTGA TGCACGAGGC TCTGCACAAC
1701 CACTACACGC AGAAGAGCCT CTCCC TGCT CCGGGTAAAT GAGTGCTAGC
1751 TGCCAGACA TGATAAGATA CATTGATGAG TTTGGACAAA CCACA ACTAG
1801 AATGCAGTGA AAAAAATGCT TTATTTGTGA AATTTGTGAT GCTATTGCTT
1851 TATTTGTAAC CATTATAAGC TGCAATAAAC AAGTTAACAA CAACAATTGC
1901 ATTCATTTTA TGTTTCAGGT TCAGGGGGAG GTGTGGGAGG TTTTTTAAAG
1951 CAAGTAAAAC CTCTACAAAT GTGGTATGGA ATTAATTCTA AAATACAGCA
2001 TAGCAAACT TTAACCTCCA AATCAAGCCT CTA CTTGAAT CTTTTTCTGA
2051 GGGATGAATA AGGCATAGGC ATCAGGGGCT GTTGCCAATG TGCATTAGCT
2101 GTTTGCAGCC TCACCTTCTT TCATGGAGTT TAAGATATAG TGTATTTTCC
2151 CAAGGTTTGA ACTAGCTCTT CATTTCCTTA TGT TTTAAAT GCACTGACCT
2201 CCCACATTCC CTTTTTAGTA AAATATTCAG AAATAATTTA AATACATCAT
2251 TGCAATGAAA ATAAATGTTT TTTATTAGGC AGAATCCAGA TGCTCAAGGC
2301 CCTTCATAAT ATCCCCAGT TTAGTAGTTG GACTTAGGGA ACAAAGGAAC
2351 CTTTAATAGA AATTGGACAG CAAGAAAGCG AGCTTCTAGC TTATCCTCAG
2401 TCC TGCTCCT CTGCCACAAA GTGCACGCAG TTGCCGGCCG GGTCCGCGCAG
2451 GGC GAACTCC CGCCCCACG GCTGCTCGCC GATCTCGGTC ATGGCCGGCC
2501 CGGAGGCGTC CCGGAAGTTC GTGGACACGA CCTCCGACCA CTCGGCGTAC
2551 AGCTCGTCCA GGCCGCGCAC CCACACCAG GCCAGGGTGT TGTCCGGCAC
2601 CACCTGGTCC TGGACCGCGC TGATGAACAG GGT CACGTCG TCCCGGACCA
2651 CACCGGCGAA GTCGTCCTCC ACGAAGTCCC GGGAGAACCC GAGCCGGTCCG
2701 GTCCAGAACT CGACCGCTCC GCGGACGTCG CCGCGGCTGA GCACCGGAAC
2751 GGC ACTGGTC AACTTGGCCA TGATGGCTCC TCCTGTCAGG AGAGGAAAGA
2801 GAAGAAGGTT AGTACAATTG CTATAGTGAG TTGTATTATA CTATGCAGAT
2851 A TACTATGCC AATGATTAAT TG TCAA ACTA GGGCTGCAGG GTTCATAGTG
2901 CCACTTTTCC TGCACTGCCC CATCTCCTGC CCACCCTTTC CCAGGCATAG
2951 ACAGTCAGTG ACTTACCAA CTCACAGGAG GGAGAAGGCA GAAGCTTGAG
3001 ACAGACCCGC GGGACCGCCG AACTGCGAGG GGACGTGGCT AGGGCGGCTT
3051 CTTTTATGGT GCGCCGGCCC TCGGAGGCAG GGCCTCGGG GAGGCTTAGC
3101 GGCCAATCTG CGGTGGCAGG AGGCGGGGCC GAAGGCCGTG CCTGACCAAT
3151 CCGGAGCACA TAGGAGTCTC AGCCCCCGC CCCAAAGCAA GGGGAAGTCA
3201 CGCGCCTGTA GCGCCAGCGT GTTGTGAAAT GGGGGCTTGG GGGGGTTGGG
3251 GCCCTGACTA GTCAAAACAA ACTCCCAT TG ACGTCAATGG GGTGGAGACT
3301 TGAAATCCC CGTGAGTCAA ACCGCTATCC ACGCCCAT TG ATGTACTGCC
3351 AAAACCGCAT CATCATGGTA ATAGCGATGA CTAATACGTA GATGTACTGC
3401 CAAGTAGGAA AGTCCCATAA GGT CATGTAC TGGGCATAAT GCCAGGCGGG

3451 CCATTTACCG TCATTGACGT CAATAGGGGG CGTACTTGGC ATATGATACA
3501 CTTGATGTAC TGCCAAGTGG GCAGTTTACC GTAAATACTC CACCCATTGA
3551 CGTCAATGGA AAGTCCCTAT TGGCGTTACT ATGGGAACAT ACGTCATTAT
3601 TGACGTCAAT GGGCGGGGGT CGTTGGGCGG TCAGCCAGGC GGGCCATTTA
3651 CCGTAAGTTA TGTAACGCCT GCAGGTTAAT TAAGAACATG TGAGCAAAAG
3701 GCCAGCAAAA GGCCAGGAAC CGTAAAAAGG CCGCGTTGCT GGC GTTTTTTC
3751 CATAGGCTCC GCCCCCTGA CGAGCATCAC AAAAATCGAC GCTCAAGTCA
3801 GAGGTGGCGA AACCCGACAG GACTATAAAG ATACCAGGCG TTTCCCCCTG
3851 GAAGCTCCCT CGTGCGCTCT CCTGTTCCGA CCCTGCCGCT TACCGGATAC
3901 CTGTCCGCCT TTCTCCCTTC GGG AAGCGTG GCGCTTTCTC ATAGCTCACG
3951 CTGTAGGTAT CTCAGTTCGG TGTAGGTCGT TCGCTCCAAG CTGGGCTGTG
4001 TGCACGAACC CCCC GTTCAG CCCGACCGCT GCGCCTTATC CGGTA ACTAT
4051 CGTCTTGAGT CCAACCCGGT AAGACACGAC TTATCGCCAC TGGCAGCAGC
4101 CACTGGTAAC AGGATTAGCA GAGCGAGGTA TGTAGGCGGT GCTACAGAGT
4151 TCTTGAAGTG GTGGCCTAAC TACGGCTACA CTAGAAGAAC AGTATTTGGT
4201 ATCTGCGCTC TGCTGAAGCC AGTTACCTTC GGAAAAAGAG TTGGTAGCTC
4251 TTGATCCGGC AAACAAACCA CCGCTGGTAG CCGTGGTTTT TTTGTTTGCA
4301 AGCAGCAGAT TACGCGCAGA AAAAAAGGAT CTCAAGAAGA TCCTTTGATC
4351 TTTTCTACGG GGTCTGACGC TCAGTGGAAC GAAA ACTCAC GTTAAGGGAT
4401 TTTGGTCATG GCTAGTTAAT TAACATTTAA ATCAGCGGCC GCAATAAAAT
4451 ATCTTTATTT TCATTACATC TGTGTGTTGG TTTTTTGTGT GAATCGTAAC
4501 TAACATACGC TCTCCATCAA AACAAAACGA AACAAAACAA ACTAGCAAAA
4551 TAGGCTGTCC CCAGTGCAAG TGCAGGTGCC AGAACATTTT TCTATCGAA

SI.2.1 Genotyping protocol for DCIR^{-/-} mice from the homepage of the Consortium for Functional Glycomics

DR		12	samples	Condition		
10X EX buff	2.5	30		Temp (°C)	Time (Min:Sec)	
dNTP (2.5mM)	2	24		95	5:00	
Ex Taq HS	0.125	1.5		94	0:30	
Primer WT DR 177 (20uM)	0.5	6		58	0:30	
Primer comm DR 483 (20uM)	0.25	3		72	1:00	
Primer null DR 484 (20uM)	0.25	3		72	5:00	
H2O	17.7	212.4		4	∞	
	23.325	Take 23/sample				
DNA Template	2			Exp. Size (BPs)	WT	748
∑ Total in rxn mix	25				Null	457
Primer WT DR 177 (20uM)	GCC&CATGCTC&GCCTTC&G					
Primer comm DR 483 (20uM)	CACTGTGGG&CGTTACTGTC					
Primer null DR 484 (20uM)	GG&CCATTTTCTTCTGCCT&GA					
Vector NTI files available upon request. Send to ar						

SI.2.2 Genotyping protocol for DCIR^{-/-} mice from the homepage of the Consortium for Functional Glycomics

SD.SignR3		18	Condition			
			samples			
10X EX buff	2.5	45	Temp (°C)		Time (Min:Sec)	
dNTP (2.5mM)	2	36	95	5:00		
Ex Taq	0.15	2.7	94	0:30		
common SD.378 (20uM)	0.5	9	58	0:30		
imer null SD.375 (20uM)	0.25	4.5	72	0:30		
imer WT SD.200 (20uM)	0.25	4.5	72	5:00		
H2O	17.6	316.8	4	∞		
	23.25	Take 23/sample				
DNA Template	2		Exp. Siz (BPs)		WT	129
V Total in rxn mix	25				Null	243
common SD.378 (20uM)	TCCCCCTTCTGCCCTTTTGG					
imer null SD.375 (20uM)	CCAATTCCCAGCTTCCACGG					
imer WT SD.200 (20uM)	GTTTGGGGGAAATCCAGCTG					
Vector NTI files available upon request. Send to annacrie@scripps.edu						

SI.3 List of microarray carbohydrates

ID number	Structure
1	Neu5Ac(α 1-3)Gal(β 1-3)GlcNAc(β 1-3)Gal(β 1-4)Glc β 1-O(CH ₂) ₆ NH ₂
2	Neu5Ac(α 1-3)Gal(β 1-4)GlcNAc(β 1-3)Gal(β 1-4)Glc β 1-O(CH ₂) ₆ NH ₂
3	Neu5Ac(α 1-6)Gal(β 1-3)GlcNAc(β 1-3)Gal(β 1-4)Glc β 1-O(CH ₂) ₆ NH ₂
4	Neu5Ac(α 1-6)Gal(β 1-4)GlcNAc(β 1-3)Gal(β 1-4)Glc β 1-O(CH ₂) ₆ NH ₂
5	Neu5Ac(α 1-3)Gal(β 1-4)GlcNAc6S β 1-O(CH ₂) ₆ NH ₂
6	Neu5Ac(α 1-3)Gal(β 1-4)Glc β 1-O(CH ₂) ₆ NH ₂
7	Neu5Ac(α 1-6)Gal(β 1-4)Glc β 1-O(CH ₂) ₆ NH ₂
8	Gal(β 1-4)Glc β 1-O(CH ₂) ₆ NH ₂
9	GlcNS(6S)(α 1-4)IdoA(2S)(α 1-4)GlcNS(6S)(α 1-4)IdoA(2S)(α 1-4)GlcNS(6S)(α 1-4)IdoA(2S) α 1-O(CH ₂) ₅ SO ₂ (CH ₂) ₂ NH ₂
10	GlcNAc(6S)(α 1-4)IdoA(2S)(α 1-4)GlcNAc(6S)(α 1-4)IdoA(2S)(α 1-4)GlcNAc(6S)(α 1-4)IdoA(2S) α 1-O(CH ₂) ₅ NH ₂
11	GlcNS(α 1-4)IdoA(α 1-4)GlcNS(α 1-4)IdoA(α 1-4)GlcNS(α 1-4)IdoA α 1-O(CH ₂) ₅ NH ₂
12	GlcNAc(α 1-4)IdoA(α 1-4)GlcNAc(α 1-4)IdoA(α 1-4)GlcNAc(α 1-4)IdoA α 1-O(CH ₂) ₅ NH ₂
13	IdoA(2S)(α 1-4)GlcNS(α 1-4)IdoA(2S)(α 1-4)GlcNS(α 1-4)IdoA(2S)(α 1-4)GlcNS α 1-O(CH ₂) ₅ NH ₂
14	IdoA(2S)(α 1-4)GlcNAc(α 1-4)IdoA(2S)(α 1-4)GlcNAc(α 1-4)IdoA(2S)(α 1-4)GlcNAc α 1-O(CH ₂) ₅ NH ₂
15	IdoA(2S)(4S) α 1-O(CH ₂) ₅ SO ₂ (CH ₂) ₂ NH ₂
16	Natural heparin (5 kDa)
17	Gal(β 1-4)Glc β 1-O(CH ₂) ₅ SH
18	Gal(β 1-3)GlcNAc β 1-O(CH ₂) ₅ SH
19	Gal(β 1-4)GlcNAc β 1-O(CH ₂) ₅ SH
20	GalNAc(β 1-4)GlcNAc β 1-O(CH ₂) ₅ SH
21	Gal(β 1-3)GalNAc β 1-O(CH ₂) ₅ SH
22	Gal(β 1-2)Gal β 1-O(CH ₂) ₅ SH
23	Gal(β 1-3)Gal(β 1-4)Glc β 1-O(CH ₂) ₅ SH
24	Fuc(α 1-2)Gal(β 1-4)GlcNAc β 1-O(CH ₂) ₅ SH
25	GalNAc(α 1-3)Fuc(α 1-2)Gal(β 1-4)GlcNAc β 1-O(CH ₂) ₅ SH
26	Gal(α 1-3)Fuc(α 1-2)Gal(β 1-4)GlcNAc β 1-O(CH ₂) ₅ SH
27	Man(α 1-3)Fuc(α 1-2)Gal(β 1-4)GlcNAc β 1-O(CH ₂) ₅ SH
28	Gal(3S) β 1-O(CH ₂) ₅ NHC(NH)(CH ₂) ₃ SH
29	Gal(6S) β 1-O(CH ₂) ₅ NHC(NH)(CH ₂) ₃ SH
30	Gal α 1-(OCH ₂ CH ₂) ₃ SH
31	GlcNAc β 1-O(CH ₂) ₅ SH
32	Gal(β 1-4)GlcNAc(β 1-2)Glc α 1-O(CH ₂) ₅ SH
33	Man(α 1-2)Man α 1-O(CH ₂) ₅ SH
34	Man(α 1-2)Man(α 1-6)[Man(α 1-2)Man(α 1-3)]Man(α 1-6)[Man(α 1-2)Man(α 1-2)Man(α 1-3)]Man α 1-(OCH ₂ CH ₂) ₃ SH
35	Man(α 1-6)Man(α 1-6)[Man(α 1-2)]Man(α 1-6)Man(α 1-6)Man α 1-O(CH ₂) ₆ SH
36	Man(α 1-2)Man(α 1-2)Man α 1-O(CH ₂) ₆ SH
37	Man(α 1-6)Man(α 1-6)[Man(α 1-2)]Man(α 1-6)Man(α 1-6)Man α 1-O(CH ₂) ₆ SH
38	Man(α 1-2)Man(α 1-6)Man(α 1-6)Man α 1-O(CH ₂) ₆ SH
39	Ara(α 1-6)Ara(α 1-3)[Ara(α 1-6)]Ara(α 1-6)Ara(α 1-6)Ara(α 1-2)[Man(α 1-

40	6)]Man(α 1-6)[Man(α 1-2)] Man(α 1-6) Man(α 1-6) Man α 1-O(CH ₂) ₆ SH Gal(α 1-3)[Gal(β 1-4)]GlcNAc(α 1-4)ManNAc(β 1-4)[Gal(α 1- 4)]GlcNAc β 1-O(CH ₂) ₅ SH
41	Glc(β 1-4)Glc β 1-O(CH ₂) ₅ SH
42	GlcNAc(α 1-2)Glc α 1-O(CH ₂) ₅ SH
43	Fuc α 1-O(CH ₂) ₅ SH
44	<i>myo</i> -Ins1-OPO ₃ H(CH ₂) ₆ SH (Phosphatidylmyo-inositol; PI)
45	Man(α 1-2) <i>myo</i> -Ins1-OPO ₃ H(CH ₂) ₆ SH (Phosphatidylmyo-inositol mannoside; PIM ₁)
46	Man(α 1-2)[Man(α 1-6)] <i>myo</i> -Ins1-OPO ₃ H(CH ₂) ₆ SH (PIM ₂)
47	Man(α 1-6)Man(α 1-6)[Man(α 1-2)] <i>myo</i> -Ins1-OPO ₃ H(CH ₂) ₆ SH (PIM ₃)
48	Man(α 1-6)Man(α 1-6)Man(α 1-6)[Man(α 1-2)] <i>myo</i> -Ins1- OPO ₃ H(CH ₂) ₆ SH (PIM ₄)
49	Fuc(α 1-2)Gal(β 1-3)GalNAc(β 1-3)Gal(α 1-4)Gal(β 1-4)Glc β 1- O(CH ₂) ₅ SH (Globo-H)
50	Gal(β 1-3)GalNAc(β 1-3)Gal(α 1-4)Gal(β 1-4)Glc β 1-O(CH ₂) ₅ SH (Gb5 or SSEA-3)
51	Glc β 1-O(CH ₂) ₂ NH ₂
52	Gal β 1-O(CH ₂) ₂ NH ₂

Summary

C-type lectin receptors (CLRs) represent a family of pattern recognition receptors (PRRs) that recognize carbohydrate structures on pathogens and self-antigens often in a Ca^{2+} -dependent manner. By virtue of their expression on dendritic cells (DCs), they can be exploited for the induction of antigen-specific immunity or tolerance. A platform was established to screen for novel CLR carbohydrate ligands and to use these ligands for CLR targeting. 1,3-lactosamine and the tumor antigen Gb5 were identified as novel ligands for MGL1 and Clec12b by glycan microarray screening of synthetic carbohydrates. The sugars were coupled to a model antigen, ovalbumin (OVA), and each conjugate was evaluated for its ability to skew the immune response. Both *in vitro* and *in vivo* assays demonstrated that carbohydrate modification of OVA leads to $\text{T}_{\text{H}1}$ response while dampening humoral response. These data established a promising strategy to determine the adjuvant capacity of CLR carbohydrate ligands, which not only is cell-specific but also stimulates immune responses.

Furthermore, the role of CLRs in the genesis of experimental cerebral malaria (ECM) was investigated. Cerebral malaria (CM) is the most severe complication of malaria. The murine *Plasmodium berghei* ANKA (PbA) infection model has helped identify crucial players in the pathogenesis of CM. Here it is shown that the CLR dendritic cell immunoreceptor (DCIR) is critical for the development of CM. While PbA infection led to 80% CM in wild-type C57BL/6 mice, DCIR-deficient mice were highly protected with only 15% CM development. In accordance with the reduced CM incidence in DCIR^{-/-} mice, CD8⁺ T cell sequestration was markedly reduced in brains of PbA-infected DCIR^{-/-} mice that was accompanied by reduced brain inflammation. Reduced T cell sequestration in the brain was caused by decreased TNF- α levels in sera as well as a modulated activation of CD4⁺ and CD8⁺ T cells in spleen of PbA-infected DCIR^{-/-} mice. This study indicates that DCIR is critically involved in CM induction, thus highlighting the importance of this CLR in innate immunity during malaria infection.

Zusammenfassung

Unter C-Typ Lektin-Rezeptoren (CLRs) versteht man eine Familie von Mustererkennungsrezeptoren welche - oftmals calciumabhängig - Strukturen auf Pathogenen und Selbstantigenen erkennen. Aufgrund ihrer Expression auf dendritischen Zellen können sie sowohl für die Induktion einer antigenspezifischen Immunität, als auch für die Ausbildung von immunologischer Toleranz eingesetzt werden. Es wurde eine Plattform entwickelt um neue CLR-Kohlenhydratliganden zu identifizieren und für das Targeting von CLRs zu verwenden. 1,3-Laktosamin und das Tumorantigen Gb5 wurden als neue Liganden für MGL1 und Clec12b anhand eines Screenings synthetischer Kohlenhydrate mittels Glykan-Array identifiziert. Diese Strukturen wurden mit dem Modellantigen Ovalbumin (OVA) konjugiert, wobei jedes Konjugat hinsichtlich seiner Eignung zur Modellierung der Immunantwort getestet wurde. Sowohl *in vitro*- als auch *in vivo*-Studien zeigten, dass die Kohlenhydratmodifikation von OVA eine T_H1 -Antwort auslöst und die humorale Antwort inhibiert. Diese Daten eröffnen eine vielversprechende neue Strategie zur Evaluation von CLR-Kohlenhydratliganden als Adjuvantien, welche nicht nur zellspezifisch wirken, sondern ebenfalls die Immunantwort stimulieren.

Des Weiteren wurde die Rolle von CLRs in der Entwicklung der experimentellen zerebralen Malaria (ECM) untersucht. Zerebrale Malaria (CM) stellt die schwerwiegendste Komplikation der Malaria dar. Das murine *Plasmodium berghei* ANKA (PbA)-Infektionsmodell hat maßgeblich zur Identifizierung an der Pathogenese beteiligter Zelltypen und Proteine beigetragen. Im Rahmen der vorliegenden Arbeit konnte gezeigt werden, dass der C-Typ Lektin-Rezeptor „dendritic cell immunoreceptor“ (DCIR) kritisch an der Entwicklung der CM beteiligt ist. Während eine Infektion mit PbA zu 80% CM in Wildtyp-C57BL/6-Mäusen führte, waren DCIR-defiziente Mäuse mit nur 15% CM hochgradig geschützt. Analog zur reduzierten CM-Inzidenz in DCIR^{-/-}-Mäusen lag eine auffallend inhibierte Sequestration von CD8⁺ T-Zellen bei gleichzeitig verminderter Inflammation im Gehirn PbA-infizierter Mäuse vor. Die verminderte Sequestration von CD8⁺ T-Zellen wurde sowohl durch eine geringere Konzentration von TNF- α im Serum, als auch eine modulierte Aktivierung von CD4⁺ und CD8⁺ T-Zellen in der Milz PbA-infizierter DCIR^{-/-}-Mäuse hervorgerufen. Diese Untersuchungen zeigen, dass DCIR kritisch an der Entstehung der CM beteiligt ist und heben somit die Bedeutung dieses C-Typ Lektin-Rezeptors für die innate Immunantwort während der Malariainfektion hervor.

List of Publications

- Raghavendra Kikkeri*, Gonçalo J.L. Bernardes*, **Maha Maglinao**, Paola Laurino, Mayeul Collot, Bernd Lepenies, Peter H. Seeberger (2010). “Design, synthesis and biological evaluation of carbohydrate-functionalized cyclodextrins and liposomes for hepatocyte-specific targeting.” *Org Biomol Chem*; 8(21): 4987-96. DOI: 10.1039/c0ob00372g. **Chosen as HOT article and top ten most accessed article in Org Biomol Chem (10/2010).**

- Rafael Gentsch, Falko Pippig, Katja Nilles, Kersin T. Wiss, Patrick Theato, Raghavendra Kikkeri, **Maha Maglinao**, Bernd Lepenies, Peter H. Seeberger, and Hans G. Börner (2010). “Modular approach toward bioactive fiber meshes carrying oligosaccharides.” *Macromolecules*; 43(21): 9239-9247. DOI: 10.1021/ma101607a.

- Dan Gruenstein, **Maha Maglinao**, Raghavendra Kikkeri, Mayeul Collot, Konstantin Barylyuk, Bernd Lepenies, Faustin Kamena, Renato Zenobi, and Peter H. Seeberger (2011). “Hexameric supramolecular scaffold orients carbohydrates to sense bacteria.” *J Am Chem Soc*; 133(35): 13957-13966. DOI: 10.1021/ja2036767.

- **Maha Maglinao**, Robert Klopffleisch, Peter H. Seeberger, and Bernd Lepenies (2013). “The C-type Lectin Receptor DCIR Is Crucial for the Development of Experimental Cerebral Malaria.” *J. Immunol*; 191(5): 2551-2559. DOI:10.4049/jimmunol.1203451.

- **Maha Maglinao***, Magdalena Eriksson*, Mark K. Schlegel, Peter H. Seeberger, and Bernd Lepenies. “A Novel Platform to Screen for Immune Modulatory Properties of C-type Lectin Receptor-Binding Carbohydrates.” *In preparation*.

- Magdalena Eriksson*, **Maha Maglinao***, Sonia Serna, Mark K. Schlegel, Peter H. Seeberger, Niels-Christian Reichardt, and Bernd Lepenies. “Biological evaluation of multivalent Lewis X - MGL1 interactions.” *In preparation*.

*Authors contributed equally to this work.

References

1. Banchereau, J. and R.M. Steinman, Dendritic cells and the control of immunity. *Nature*, 1998. **392**(6673): p. 245-52.
2. Medzhitov, R. and C. Janeway, Jr., Innate immunity. *N Engl J Med*, 2000. **343**(5): p. 338-44.
3. Steinman, R.M., D. Hawiger, and M.C. Nussenzweig, Tolerogenic dendritic cells. *Ann Rev Immunol*, 2003. **21**: p. 685-711.
4. Matzinger, P., The danger model: a renewed sense of self. *Science*, 2002. **296**(5566): p. 301-5.
5. Figdor, C.G., Y. van Kooyk, and G.J. Adema, C-type lectin receptors on dendritic cells and Langerhans cells. *Nat Rev Immunol*, 2002. **2**(2): p. 77-84.
6. Kawai, T. and S. Akira, The role of pattern-recognition receptors in innate immunity: update on Toll-like receptors. *Nat Immunol*, 2010. **11**(5): p. 373-384.
7. Akira, S. and K. Takeda, Toll-like receptor signalling. *Nat Rev Immunol*, 2004. **4**(7): p. 499-511.
8. Chen, G., M.H. Shaw, Y.G. Kim, and G. Nunez, NOD-like receptors: role in innate immunity and inflammatory disease. *Annu Rev Pathol*, 2009. **4**: p. 365-98.
9. Loo, Y.M. and M. Gale, Jr., Immune signaling by RIG-I-like receptors. *Immunity*, 2011. **34**(5): p. 680-92.
10. Medzhitov, R. and C.A. Janeway, Jr., Innate immune recognition and control of adaptive immune responses. *Semin Immunol*, 1998. **10**(5): p. 351-3.
11. Chen, X. and P. Jensen, The role of B lymphocytes as antigen-presenting cells. *Arch Immunol Ther Exp*, 2008. **56**(2): p. 77-83.
12. Guermonprez, P., J. Valladeau, L. Zitvogel, C. Thery, and S. Amigorena, Antigen presentation and T cell stimulation by dendritic cells. *Annu Rev Immunol*, 2002. **20**: p. 621-67.
13. Steinman, R.M. and J. Banchereau, Taking dendritic cells into medicine. *Nature*, 2007. **449**(7161): p. 419-426.
14. Joffre, O.P., E. Segura, A. Savina, and S. Amigorena, Cross-presentation by dendritic cells. *Nat Rev Immunol*, 2012. **12**(8): p. 557-569.
15. Banchereau, J., F. Briere, C. Caux, J. Davoust, S. Lebecque, Y.-J. Liu, B. Pulendran, and K. Palucka, Immunobiology of Dendritic Cells. *Ann Rev Immunol*, 2000. **18**(1): p. 767-811.
16. Drickamer, K., C-type lectin-like domains. *Curr Opin Struct Biol*, 1999. **9**(5): p. 585-90.
17. Geijtenbeek, T.B. and S.I. Gringhuis, Signalling through C-type lectin receptors: shaping immune responses. *Nat Rev Immunol*, 2009. **9**(7): p. 465-79.
18. Lowell, C.A., Src-family and Syk Kinases in Activating and Inhibitory Pathways in Innate Immune Cells: Signaling Cross Talk. *Cold Spring Harbor Perspect Biol*, 2011. **3**(3).
19. Billadeau, D.D. and P.J. Leibson, ITAMs versus ITIMs: striking a balance during cell regulation. *J Clin Invest*, 2002. **109**(2): p. 161-168.
20. Graham, L.M. and G.D. Brown, The Dectin-2 family of C-type lectins in immunity and homeostasis. *Cytokine*, 2009. **48**(1-2): p. 148-155.
21. Zelensky, A.N. and J.E. Gready, The C-type lectin-like domain superfamily. *FEBS J*, 2005. **272**(24): p. 6179-6217.
22. Huysamen, C. and G.D. Brown, The fungal pattern recognition receptor, Dectin-1, and the associated cluster of C-type lectin-like receptors. *FEMS Microbiol Lett*, 2009. **290**(2): p. 121-8.

23. Taylor, P.R., G.D. Brown, D.M. Reid, J.A. Willment, L. Martinez-Pomares, S. Gordon, and S.Y.C. Wong, The β -Glucan Receptor, Dectin-1, Is Predominantly Expressed on the Surface of Cells of the Monocyte/Macrophage and Neutrophil Lineages. *J Immunol*, 2002. **169**(7): p. 3876-3882.
24. Martin, B., K. Hirota, D.J. Cua, B. Stockinger, and M. Veldhoen, Interleukin-17-Producing $\gamma\delta$ T Cells Selectively Expand in Response to Pathogen Products and Environmental Signals. *Immunity*, 2009. **31**(2): p. 321-330.
25. Willment, J.A., S. Gordon, and G.D. Brown, Characterization of the Human β -Glucan Receptor and Its Alternatively Spliced Isoforms. *J Biol Chem*, 2001. **276**(47): p. 43818-43823.
26. Willment, J.A., A.S.J. Marshall, D.M. Reid, D.L. Williams, S.Y.C. Wong, S. Gordon, and G.D. Brown, The human β -glucan receptor is widely expressed and functionally equivalent to murine Dectin-1 on primary cells. *Eur J Immunol*, 2005. **35**(5): p. 1539-1547.
27. Olynych, T.J., D.L. Jakeman, and J.S. Marshall, Fungal zymosan induces leukotriene production by human mast cells through a dectin-1-dependent mechanism. *J Allergy Clin Immunol*, 2006. **118**(4): p. 837-843.
28. Kerrigan, A.M. and G.D. Brown, Syk-coupled C-type lectin receptors that mediate cellular activation via single tyrosine based activation motifs. *Immunol Rev*, 2010. **234**(1): p. 335-352.
29. Palma, A.S., T. Feizi, Y.B. Zhang, M.S. Stoll, A.M. Lawson, E. Diaz-Rodriguez, M.A. Campanero-Rhodes, J. Costa, S. Gordon, G.D. Brown, and W.G. Chai, Ligands for the beta-glucan receptor, Dectin-1, assigned using "designer" microarrays of oligosaccharide probes (neoglycolipids) generated from glucan polysaccharides. *J Biol Chem*, 2006. **281**(9): p. 5771-5779.
30. Brown, G.D., Dectin-1: a signalling non-TLR pattern-recognition receptor. *Nat Rev Immunol*, 2006. **6**(1): p. 33-43.
31. Tsoni, S.V. and G.D. Brown, β -Glucans and Dectin-1. *Ann N Y Acad Sci*, 2008. **1143**(1): p. 45-60.
32. Gringhuis, S.I., B.A. Wevers, T.M. Kaptein, T.M. van Capel, B. Theelen, and T. Boekhout, Selective C-Rel activation via Malt1 controls anti-fungal T(H)-17 immunity by dectin-1 and dectin-2. *PLoS Pathog*, 2011. **1143**(1).
33. Gringhuis, S.I., J. den Dunnen, M. Litjens, M. van der Vlist, B. Wevers, S.C.M. Bruijns, and T.B.H. Geijtenbeek, Dectin-1 directs T helper cell differentiation by controlling noncanonical NF- κ B activation through Raf-1 and Syk. *Nat Immuno*, 2009. **10**(2): p. 203-213.
34. Gross, O., H. Poeck, M. Bscheider, C. Dostert, N. Hanneschläger, S. Endres, G. Hartmann, A. Tardivel, E. Schweighoffer, V. Tybulewicz, A. Mocsai, J. Tschopp, and J. Ruland, Syk kinase signalling couples to the Nlrp3 inflammasome for anti-fungal host defence. *Nature*, 2009. **459**(7245): p. 433-436.
35. Vautier, S., D.M. MacCallum, and G.D. Brown, C-type lectin receptors and cytokines in fungal immunity. *Cytokine*, 2012. **58**(1): p. 89-99.
36. Cheng, S.C., F.L. van de Veerdonk, M. Lenardon, M. Stoffels, T. Plantinga, S. Smeekens, L. Rizzetto, L. Mukaremera, K. Preechasth, D. Cavalieri, T.D. Kanneganti, J.W.M. van der Meer, B.J. Kullberg, L.A.B. Joosten, N.A.R. Gow, and M.G. Netea, The dectin-1/inflammasome pathway is responsible for the induction of protective T-helper 17 responses that discriminate between yeasts and hyphae of *Candida albicans*. *J Leukocyte Biol*, 2011. **90**(2): p. 357-366.
37. Goodridge, H.S., R.M. Simmons, and D.M. Underhill, Dectin-1 stimulation by *Candida albicans* yeast or zymosan triggers NFAT activation in macrophages and dendritic cells. *J Immunol*, 2007. **178**(5): p. 3107-3115.

38. Powlesland, A.S., E.M. Ward, S.K. Sadhu, Y. Guo, M.E. Taylor, and K. Drickamer, Widely divergent biochemical properties of the complete set of mouse DC-SIGN-related proteins. *J Biol Chem*, 2006. **281**(29): p. 20440-9.
39. Geijtenbeek, T.B.H., R. Torensma, S.J. van Vliet, G.C.F. van Duijnhoven, G.J. Adema, Y. van Kooyk, and C.G. Figdor, Identification of DC-SIGN, a Novel Dendritic Cell-Specific ICAM-3 Receptor that Supports Primary Immune Responses. *Cell*, 2000. **100**(5): p. 575-585.
40. Geijtenbeek, T.B.H., D.S. Kwon, R. Torensma, S.J. van Vliet, G.C.F. van Duijnhoven, J. Middel, I.L.M.H.A. Cornelissen, H.S.L.M. Nottet, V.N. KewalRamani, D.R. Littman, C.G. Figdor, and Y. van Kooyk, DC-SIGN, a Dendritic Cell-Specific HIV-1-Binding Protein that Enhances trans-Infection of T Cells. *Cell*, 2000. **100**(5): p. 587-597.
41. Nagaoka, K., K. Takahara, K. Minamino, T. Takeda, Y. Yoshida, and K. Inaba, Expression of C-type lectin, SIGNR3, on subsets of dendritic cells, macrophages, and monocytes. *J Leukocyte Biol*, 2010. **88**(5): p. 913-924.
42. Sancho, D. and C. Reis e Sousa, Signaling by myeloid C-type lectin receptors in immunity and homeostasis. *Annu Rev Immunol*, 2012. **30**: p. 491-529.
43. Bates, E.E.M., N. Fournier, E. Garcia, J. Valladeau, I. Durand, J.-J. Pin, S.M. Zurawski, S. Patel, J.S. Abrams, S. Lebecque, P. Garrone, and S. Saeland, APCs Express DCIR, a Novel C-Type Lectin Surface Receptor Containing an Immunoreceptor Tyrosine-Based Inhibitory Motif. *J Immunol*, 1999. **163**(4): p. 1973-1983.
44. Kanazawa, N., T. Okazaki, H. Nishimura, K. Tashiro, K. Inaba, and Y. Miyachi, DCIR acts as an inhibitory receptor depending on its immunoreceptor tyrosine-based inhibitory motif. *J Invest Dermatol*, 2002. **118**(2): p. 261-6.
45. Richard, M., P. Veilleux, M. Rouleau, R. Paquin, and A.D. Beaulieu, The expression pattern of the ITIM-bearing lectin CLECSF6 in neutrophils suggests a key role in the control of inflammation. *J Leukocyte Biol*, 2002. **71**(5): p. 871-880.
46. Fujikado, N., S. Saijo, T. Yonezawa, K. Shimamori, A. Ishii, S. Sugai, H. Kotaki, K. Sudo, M. Nose, and Y. Iwakura, Dcir deficiency causes development of autoimmune diseases in mice due to excess expansion of dendritic cells. *Nat Med*, 2008. **14**(2): p. 176-80.
47. Klechevsky, E., A.-L. Flamar, Y. Cao, J.-P. Blanck, M. Liu, A. O'Bar, O. Agouna-Deciat, P. Klucar, L. Thompson-Snipes, S. Zurawski, Y. Reiter, A.K. Palucka, G. Zurawski, and J. Banchereau, Cross-priming CD8+ T cells by targeting antigens to human dendritic cells through DCIR. *Blood*, 2010. **116**(10): p. 1685-1697.
48. Dudziak, D., A.O. Kamphorst, G.F. Heidkamp, V.R. Buchholz, C. Trumpfheller, S. Yamazaki, C. Cheong, K. Liu, H.-W. Lee, C.G. Park, R.M. Steinman, and M.C. Nussenzweig, Differential Antigen Processing by Dendritic Cell Subsets in Vivo. *Science*, 2007. **315**(5808): p. 107-111.
49. Richard, M., N. Thibault, P. Veilleux, G. Gareau-Pagé, and A.D. Beaulieu, Granulocyte macrophage-colony stimulating factor reduces the affinity of SHP-2 for the ITIM of CLECSF6 in neutrophils: A new mechanism of action for SHP-2. *Mol Immunol*, 2006. **43**(10): p. 1716-1721.
50. Marshall, A.S.J., J.A. Willment, H.-H. Lin, D.L. Williams, S. Gordon, and G.D. Brown, Identification and Characterization of a Novel Human Myeloid Inhibitory C-type Lectin-like Receptor (MICAL) That Is Predominantly Expressed on Granulocytes and Monocytes. *J Biol Chem*, 2004. **279**(15): p. 14792-14802.
51. Han, Y., M. Zhang, N. Li, T. Chen, Y. Zhang, T. Wan, and X. Cao, KLRL1, a novel killer cell lectinlike receptor, inhibits natural killer cell cytotoxicity. *Blood*, 2004. **104**(9): p. 2858-2866.

52. Bakker, A.B.H., S. van den Oudenrijn, A.Q. Bakker, N. Feller, M. van Meijer, J.A. Bia, M.A.C. Jongeneelen, T.J. Visser, N. Bijl, C.A.W. Geuijen, W.E. Marissen, K. Radosevic, M. Throsby, G.J. Schuurhuis, G.J. Ossenkoppele, J. de Kruif, J. Goudsmit, and A.M. Kruisbeek, C-Type Lectin-Like Molecule-1: A Novel Myeloid Cell Surface Marker Associated with Acute Myeloid Leukemia. *Cancer Res*, 2004. **64**(22): p. 8443-8450.
53. Lahoud, M.H., A.I. Proietto, F. Ahmet, S. Kitsoulis, L. Eidsmo, L. Wu, P. Sathe, S. Pietersz, H.-W. Chang, I.D. Walker, E. Maraskovsky, H. Braley, A.M. Lew, M.D. Wright, W.R. Heath, K. Shortman, and I. Caminschi, The C-Type Lectin Clec12A Present on Mouse and Human Dendritic Cells Can Serve as a Target for Antigen Delivery and Enhancement of Antibody Responses. *J Immunol*, 2009. **182**(12): p. 7587-7594.
54. Pyż, E., C. Huysamen, A.S.J. Marshall, S. Gordon, P.R. Taylor, and G.D. Brown, Characterisation of murine MICL (CLEC12A) and evidence for an endogenous ligand. *Eur J Immunol*, 2008. **38**(4): p. 1157-1163.
55. Sattler, S., H. Ghadially, and E. Hofer, Evolution of the C-type lectin-like receptor genes of the DECTIN-1 cluster in the NK gene complex. *ScientificWorldJournal*, 2012. **2012**: p. 931386.
56. Hoffmann, S.C., C. Schellack, S. Textor, S. Konold, D. Schmitz, A. Cerwenka, S. Pflanz, and C. Watzl, Identification of CLEC12B, an inhibitory receptor on myeloid cells. *J Biol Chem*, 2007. **282**(31): p. 22370-5.
57. Higashi, N., K. Fujioka, K. Denda-Nagai, S. Hashimoto, S. Nagai, T. Sato, Y. Fujita, A. Morikawa, M. Tsuiji, M. Miyata-Takeuchi, Y. Sano, N. Suzuki, K. Yamamoto, K. Matsushima, and T. Irimura, The macrophage C-type lectin specific for galactose/N-acetylgalactosamine is an endocytic receptor expressed on monocyte-derived immature dendritic cells. *J Biol Chem*, 2002. **277**(23): p. 20686-93.
58. van Vliet, S.J., S.I. Gringhuis, T.B.H. Geijtenbeek, and Y. van Kooyk, Regulation of effector T cells by antigen-presenting cells via interaction of the C-type lectin MGL with CD45. *Nat Immunol*, 2006. **7**(11): p. 1200-1208.
59. van Vliet, S.J., E. van Liempt, E. Saeland, C.A. Aarnoudse, B. Appelmek, T. Irimura, T.B. Geijtenbeek, O. Blixt, R. Alvarez, I. van Die, and Y. van Kooyk, Carbohydrate profiling reveals a distinctive role for the C-type lectin MGL in the recognition of helminth parasites and tumor antigens by dendritic cells. *Int Immunol*, 2005. **17**(5): p. 661-9.
60. van Liempt, E., S.J. van Vliet, A. Engering, J.J. Garcia Vallejo, C.M. Bank, M. Sanchez-Hernandez, Y. van Kooyk, and I. van Die, Schistosoma mansoni soluble egg antigens are internalized by human dendritic cells through multiple C-type lectins and suppress TLR-induced dendritic cell activation. *Mol Immunol*, 2007. **44**(10): p. 2605-15.
61. Takada, A., K. Fujioka, M. Tsuiji, A. Morikawa, N. Higashi, H. Ebihara, D. Kobasa, H. Feldmann, T. Irimura, and Y. Kawaoka, Human Macrophage C-Type Lectin Specific for Galactose and N-Acetylgalactosamine Promotes Filovirus Entry. *J Virol*, 2004. **78**(6): p. 2943-2947.
62. Van Sorge, N.M., N.M.C. Bleumink, S.J. Van Vliet, E. Saeland, W.L. Van Der Pol, Y. Van Kooyk, and J.P.M. Van Putten, N-glycosylated proteins and distinct lipooligosaccharide glycoforms of Campylobacter jejuni target the human C-type lectin receptor MGL. *Cell Microbiol*, 2009. **11**(12): p. 1768-1781.
63. van Vliet, S.J., L. Steeghs, S.C.M. Bruijns, M.M. Vaezirad, C. Snijders Blok, J.A. Arenas Busto, M. Deken, J.P.M. van Putten, and Y. van Kooyk, Variation of *Neisseria gonorrhoeae* Lipooligosaccharide Directs Dendritic Cell-Induced T Helper Responses. *PLoS Pathog*, 2009. **5**(10): p. e1000625.

64. van Vliet, S.J., E. Saeland, and Y. van Kooyk, Sweet preferences of MGL: carbohydrate specificity and function. *Trends Immunol*, 2008. **29**(2): p. 83-90.
65. Saeland, E., S. Vliet, M. Bäckström, V.M. Berg, T.H. Geijtenbeek, G. Meijer, and Y. Kooyk, The C-type lectin MGL expressed by dendritic cells detects glycan changes on MUC1 in colon carcinoma. *Cancer Immunol Immunother*, 2007. **56**(8): p. 1225-1236.
66. Napoletano, C., A. Rughetti, M.P. Agervig Tarp, J. Coleman, E.P. Bennett, G. Picco, P. Sale, K. Denda-Nagai, T. Irimura, U. Mandel, H. Clausen, L. Frati, J. Taylor-Papadimitriou, J. Burchell, and M. Nuti, Tumor-Associated Tn-MUC1 Glycoform Is Internalized through the Macrophage Galactose-Type C-Type Lectin and Delivered to the HLA Class I and II Compartments in Dendritic Cells. *Cancer Res*, 2007. **67**(17): p. 8358-8367.
67. Sato, M., K. Kawakami, T. Osawa, and S. Toyoshima, Molecular cloning and expression of cDNA encoding a galactose/N-acetylgalactosamine-specific lectin on mouse tumoricidal macrophages. *J Biochem*, 1992. **111**(3): p. 331-6.
68. Tsuiji, M., M. Fujimori, Y. Ohashi, N. Higashi, T.M. Onami, S.M. Hedrick, and T. Irimura, Molecular cloning and characterization of a novel mouse macrophage C-type lectin, mMGL2, which has a distinct carbohydrate specificity from mMGL1. *J Biol Chem*, 2002. **277**(32): p. 28892-901.
69. van Vliet, S.J., E. van Liempt, T.B. Geijtenbeek, and Y. van Kooyk, Differential regulation of C-type lectin expression on tolerogenic dendritic cell subsets. *Immunobiology*, 2006. **211**(6-8): p. 577-85.
70. Singh, S.K., I. Streng-Ouwehand, M. Litjens, D.R. Weelij, J.J. Garcia-Vallejo, S.J. van Vliet, E. Saeland, and Y. van Kooyk, Characterization of murine MGL1 and MGL2 C-type lectins: distinct glycan specificities and tumor binding properties. *Mol Immunol*, 2009. **46**(6): p. 1240-9.
71. Saba, K., K. Denda-Nagai, and T. Irimura, A C-type lectin MGL1/CD301a plays an anti-inflammatory role in murine experimental colitis. *Am J Pathol*, 2009. **174**(1): p. 144-52.
72. Ichii, S., Y. Imai, and T. Irimura, Tumor site-selective localization of an adoptively transferred T cell line expressing a macrophage lectin. *J Leukocyte Biol*, 1997. **62**(6): p. 761-70.
73. Ichii, S., Y. Imai, and T. Irimura, Initial steps in lymph node metastasis formation in an experimental system: possible involvement of recognition by macrophage C-type lectins. *Cancer Immunol Immunother*, 2000. **49**(1): p. 1-9.
74. Mizuochi, S., Y. Akimoto, Y. Imai, H. Hirano, and T. Irimura, Immunohistochemical study on a macrophage calcium-type lectin in mouse embryos: transient expression in chondroblasts during endochondral ossification. *Glycoconj J*, 1998. **15**(4): p. 397-404.
75. Yuita, H., M. Tsuiji, Y. Tajika, Y. Matsumoto, K. Hirano, N. Suzuki, and T. Irimura, Retardation of removal of radiation-induced apoptotic cells in developing neural tubes in macrophage galactose-type C-type lectin-1-deficient mouse embryos. *Glycobiology*, 2005. **15**(12): p. 1368-75.
76. Singh, S.K., I. Streng-Ouwehand, M. Litjens, H. Kalay, E. Saeland, and Y. van Kooyk, Tumour-associated glycan modifications of antigen enhance MGL2 dependent uptake and MHC class I restricted CD8 T cell responses. *Int J Cancer*, 2011. **128**(6): p. 1371-83.
77. Graham, L.M., V. Gupta, G. Schafer, D.M. Reid, M. Kimberg, K.M. Dennehy, W.G. Hornsell, R. Guler, M.A. Campanero-Rhodes, A.S. Palma, T. Feizi, S.K. Kim, P. Sobieszczuk, J.A. Willment, and G.D. Brown, The C-type lectin receptor CLECSF8 (CLEC4D) is expressed by myeloid cells and triggers cellular activation through Syk kinase. *J Biol Chem*, 2012. **287**(31): p. 25964-74.

78. Sharon, N., Lectins: Carbohydrate-specific reagents and biological recognition molecules. *J Biol Chem*, 2006.
79. Lepenies, B., J.A. Yin, and P.H. Seeberger, Applications of synthetic carbohydrates to chemical biology. *Curr Opin Chem Biol*, 2010. **14**(3): p. 404-411.
80. Kikkeri, R., D. Grunstein, and P.H. Seeberger, Lectin biosensing using digital analysis of Ru(II)-glycodendrimers. *J Am Chem Soc*, 2010. **132**(30): p. 10230-2.
81. Kikkeri, R., B. Lepenies, A. Adibekian, P. Laurino, and P.H. Seeberger, In Vitro Imaging and in Vivo Liver Targeting with Carbohydrate Capped Quantum Dots. *J Am Chem Soc*, 2009. **131**(6): p. 2110-2112.
82. Kikkeri, R., I. Garcia-Rubio, and P.H. Seeberger, Ru(II)-carbohydrate dendrimers as photoinduced electron transfer lectin biosensors. *Chem Comm*, 2009(2): p. 235-7.
83. Gutierrez Gallego, R., S.R. Haseley, V.F. van Miegem, J.F. Vliegthart, and J.P. Kamerling, Identification of carbohydrates binding to lectins by using surface plasmon resonance in combination with HPLC profiling. *Glycobiology*, 2004. **14**(5): p. 373-86.
84. Leriche, V., P. Sibille, and B. Carpentier, Use of an enzyme-linked lectinsorbent assay to monitor the shift in polysaccharide composition in bacterial biofilms. *Appl Environ Microbiol*, 2000. **66**(5): p. 1851-6.
85. Lotan, R., E. Skutelsky, D. Danon, and N. Sharon, The purification, composition, and specificity of the anti-T lectin from peanut (*Arachis hypogaea*). *J Biol Chem*, 1975. **250**(21): p. 8518-23.
86. Dam, T.K. and C.F. Brewer, Thermodynamic studies of lectin-carbohydrate interactions by isothermal titration calorimetry. *Chem Rev*, 2002. **102**(2): p. 387-429.
87. Stallforth, P., B. Lepenies, A. Adibekian, and P.H. Seeberger, Carbohydrates: A Frontier in Medicinal Chemistry. *J Med Chem*, 2009. **52**(18): p. 5561-5577.
88. Bernardes, G.J.L., B. Castagner, and P.H. Seeberger, Combined Approaches to the Synthesis and Study of Glycoproteins. *Chem Biol*, 2009. **4**(9): p. 703-713.
89. Zhang, H., Y. Ma, and X.L. Sun, Recent developments in carbohydrate-decorated targeted drug/gene delivery. *Med Res Rev*, 2010. **30**(2): p. 270-89.
90. Davis, B.G. and M.A. Robinson, Drug delivery systems based on sugar-macromolecule conjugates. *Curr Opin Drug Discov Devel*, 2002. **5**(2): p. 279-88.
91. Wu, J., M.H. Nantz, and M.A. Zern, Targeting hepatocytes for drug and gene delivery: emerging novel approaches and applications. *Front Biosci*, 2002. **7**: p. d717-25.
92. Lepenies, B. and P.H. Seeberger, The promise of glycomics, glycan arrays and carbohydrate-based vaccines. *Immunopharm Immunot*, 2010. **32**(2): p. 196-207.
93. Kurmyshkina, O., E. Rapoport, E. Moiseeva, E. Korchagina, T. Ovchinnikova, G. Pazynina, I. Belyanchikov, and N. Bovin, Glycoprobes as a tool for the study of lectins expressed on tumor cells. *Acta Histochem*, 2010. **112**(2): p. 118-126.
94. Brewer, C.F., Thermodynamic binding studies of galectin-1, -3 and -7. *Glycoconj J*, 2004. **19**(7-9): p. 459-465.
95. Jubeli, E., L. Moine, J. Vergnaud-Gauduchon, and G. Barratt, E-selectin as a target for drug delivery and molecular imaging. *J Controlled Release*, 2012. **158**(2): p. 194-206.
96. Kiessling, L.L., J.E. Gestwicki, and L.E. Strong, Synthetic Multivalent Ligands as Probes of Signal Transduction. *Angew Chem Int Ed*, 2006. **45**(15): p. 2348-2368.
97. Irache, J., H. Salman, C. Gamazo, and S. Espuelas, Mannose-targeted systems for the delivery of therapeutics. *Expert Opin Drug Delivery*, 2008. **5**(6): p. 703-724.
98. Platt, V.M. and F.C. Szoka, Anticancer therapeutics: targeting macromolecules and nanocarriers to hyaluronan or CD44, a hyaluronan receptor. *Mol Pharm*, 2008. **5**(4): p. 474-486.
99. Lunney, J. and G. Ashwell, Hepatic Receptor of Avian Origin Capable of Binding Specifically Modified Glycoproteins. *PNAS*, 1976. **73**(2): p. 341-343.

100. Yik, J.H.N., A. Saxena, and P.H. Weigel, The minor subunit splice variants, H2b and H2c, of the human asialoglycoprotein receptor are present with the major subunit H1 in different hetero-oligomeric receptor complexes. *J Biol Chem*, 2002. **277**(25): p. 23076-23083.
101. Sun, X., L. Hai, Y. Wu, H.-Y. Hu, and Z.-R. Zhang, Targeted gene delivery to hepatoma cells using galactosylated liposome-polycation-DNA complexes (LPD). *J Drug Targeting*, 2005. **13**(2): p. 121-128.
102. Shigeta, K., S. Kawakami, Y. Higuchi, T. Okuda, H. Yagi, F. Yamashita, and M. Hashida, Novel histidine-conjugated galactosylated cationic liposomes for efficient hepatocyte-selective gene transfer in human hepatoma HepG2 cells. *J Controlled Release*, 2007. **118**(2): p. 262-270.
103. Letrou-Bonneval, E., R. Chevre, O. Lambert, P. Costet, C. Andre, C. Tellier, and B. Pitard, Galactosylated multimodular lipoplexes for specific gene transfer into primary hepatocytes. *J Gene Med*, 2008. **10**(11): p. 1198-1209.
104. Wang, X., P. Mani, D.P. Sarkar, N. Roy-Chowdhury, and J. Roy-Chowdhury, Ex vivo gene transfer into hepatocytes. *Methods Mol Biol*, 2009. **481**: p. 117-40.
105. Morille, M., C. Passirani, E. Letrou-Bonneval, J.P. Benoit, and B. Pitard, Galactosylated DNA lipid nanocapsules for efficient hepatocyte targeting. *Int J Pharm*, 2009. **379**(2): p. 293-300.
106. Lee, R.T. and Y.C. Lee, Affinity enhancement by multivalent lectin-carbohydrate interaction. *Glycoconj J*, 2000. **17**(7-9): p. 543-51.
107. Lee, R.T. and Y.C. Lee, Facile Synthesis of a High-Affinity Ligand for Mammalian Hepatic Lectin Containing Three Terminal N-Acetylgalactosamine Residues. *Bioconjugate Chem*, 1997. **8**(5): p. 762-765.
108. Diebold, S.S., C. Plank, M. Cotten, E. Wagner, and M. Zenke, Mannose receptor-mediated gene delivery into antigen presenting dendritic cells. *Somat Cell Mol Genet*, 2002. **27**(1-6): p. 65-74.
109. Tacke, P.J., R. Torensma, and C.G. Figdor, Targeting antigens to dendritic cells in vivo. *Immunobiology*, 2006. **211**(6-8): p. 599-608.
110. Delneste, Y., G. Magistrelli, J.-F. Gauchat, J.-F. Haeuw, J.-P. Aubry, K. Nakamura, N. Kawakami-Honda, L. Goetsch, T. Sawamura, J.-Y. Bonnefoy, and P. Jeannin, Involvement of LOX-1 in Dendritic Cell-Mediated Antigen Cross-Presentation. *Immunity*, 2002. **17**(3): p. 353-362.
111. Unger, W.W.J. and Y. van Kooyk, 'Dressed for success' C-type lectin receptors for the delivery of glyco-vaccines to dendritic cells. *Curr Opin Immunol*, 2011. **23**(1): p. 131-137.
112. Gurer, C., T. Strowig, F. Brilot, M. Pack, C. Trumfheller, F. Arrey, C.G. Park, R.M. Steinman, and C. Münz, Targeting the nuclear antigen 1 of Epstein-Barr virus to the human endocytic receptor DEC-205 stimulates protective T-cell responses. *Blood*, 2008. **112**(4): p. 1231-1239.
113. Birkholz, K., M. Schwenkert, C. Kellner, S. Gross, G. Fey, B. Schuler-Thurner, G. Schuler, N. Schaft, and J. Dörrie, Targeting of DEC-205 on human dendritic cells results in efficient MHC class II-restricted antigen presentation. *Blood*, 2010. **116**(13): p. 2277-2285.
114. Bonifaz, L.C., D.P. Bonnyay, A. Charalambous, D.I. Darguste, S. Fujii, H. Soares, M.K. Brimnes, B. Moltedo, T.M. Moran, and R.M. Steinman, In vivo targeting of antigens to maturing dendritic cells via the DEC-205 receptor improves T cell vaccination. *J Exp Med*, 2004. **199**(6): p. 815-24.
115. McKenzie, E.J., P.R. Taylor, R.J. Stillion, A.D. Lucas, J. Harris, S. Gordon, and L. Martinez-Pomares, Mannose receptor expression and function define a new population of murine dendritic cells. *J Immunol*, 2007. **178**(8): p. 4975-83.

116. Lahoud, M.H., F. Ahmet, S. Kitsoulis, S.S. Wan, D. Vremec, C.N. Lee, B. Phipson, W. Shi, G.K. Smyth, A.M. Lew, Y. Kato, S.N. Mueller, G.M. Davey, W.R. Heath, K. Shortman, and I. Caminschi, Targeting antigen to mouse dendritic cells via Clec9A induces potent CD4 T cell responses biased toward a follicular helper phenotype. *J Immunol*, 2011. **187**(2): p. 842-50.
117. Sancho, D., D. Mourão-Sá, O.P. Joffre, O. Schulz, N.C. Rogers, D.J. Pennington, J.R. Carlyle, and C.R. Sousa, Tumor therapy in mice via antigen targeting to a novel, DC-restricted C-type lectin. *J Clin Invest*, 2008. **118**(6): p. 2098-2110.
118. Caminschi, I., A.I. Proietto, F. Ahmet, S. Kitsoulis, J.S. Teh, J.C.Y. Lo, A. Rizzitelli, L. Wu, D. Vremec, S.L.H. Van Dommelen, I.K. Campbell, E. Maraskovsky, H. Braley, G.M. Davey, P. Mottram, N. Van De Velde, K. Jensen, A.M. Lew, M.D. Wright, W.R. Heath, K. Shortman, and M.H. Lahoud, The dendritic cell subtype-restricted C-type lectin Clec9A is a target for vaccine enhancement. *Blood*, 2008. **112**(8): p. 3264-3273.
119. Meyer-Wentrup, F., D. Benitez-Ribas, P.J. Tacken, C.J. Punt, C.G. Figdor, I.J. de Vries, and G.J. Adema, Targeting DCIR on human plasmacytoid dendritic cells results in antigen presentation and inhibits IFN-alpha production. *Blood*, 2008. **111**(8): p. 4245-53.
120. Nchinda, G., J. Kuroiwa, M. Oks, C. Trumpfheller, G.P. Chae, Y. Huang, D. Hannaman, S.J. Schlesinger, O. Mizenina, M.C. Nussenzweig, K. Überla, and R.M. Steinman, The efficacy of DNA vaccination is enhanced in mice by targeting the encoded protein to dendritic cells. *J Clin Invest*, 2008. **118**(4): p. 1427-1436.
121. Maynard, J. and G. Georgiou, ANTIBODY ENGINEERING. *Ann Rev Biomed Eng*, 2000. **2**(1): p. 339-376.
122. Winter, G. and W.J. Harris, Humanized antibodies. *Immunol Today*, 1993. **14**(6): p. 243-6.
123. Tacken, P.J., I.J.M. de Vries, K. Gijzen, B. Joosten, D. Wu, R.P. Rother, S.J. Faas, C.J.A. Punt, R. Torensma, G.J. Adema, and C.G. Figdor, Effective induction of naive and recall T-cell responses by targeting antigen to human dendritic cells via a humanized anti-DC-SIGN antibody. *Blood*, 2005. **106**(4): p. 1278-1285.
124. Mukhopadhyaya, A., T. Hanafusa, I. Jarchum, Y.G. Chen, Y. Iwai, D.V. Serreze, R.M. Steinman, K.V. Tarbell, and T.P. DiLorenzo, Selective delivery of β cell antigen to dendritic cells in vivo leads to deletion and tolerance of autoreactive CD8+ T cells in NOD mice. *PNAS*, 2008. **105**(17): p. 6374-6379.
125. Yamazaki, S., D. Dudziak, G.F. Heidkamp, C. Fiorese, A.J. Bonito, K. Inaba, M.C. Nussenzweig, and R.M. Steinman, CD80+CD205+ splenic dendritic cells are specialized to induce Foxp3+ regulatory T cells. *J Immunol*, 2008. **181**(10): p. 6923-6933.
126. Kovacsovics-Bankowski, M. and K.L. Rock, A phagosome-to-cytosol pathway for exogenous antigens presented on MHC class I molecules. *Science*, 1995. **267**(5195): p. 243-246.
127. Sallusto, F., M. Cella, C. Danieli, and A. Lanzavecchia, Dendritic cells use macropinocytosis and the mannose receptor to concentrate macromolecules in the major histocompatibility complex class II compartment: Downregulation by cytokines and bacterial products. *J Exp Med*, 1995. **182**(2): p. 389-400.
128. Thiele, L., H.P. Merkle, and E. Walter, Phagocytosis and phagosomal fate of surface-modified microparticles in dendritic cells and macrophages. *Pharm Res*, 2003. **20**(2): p. 221-228.
129. Joshi, M.D., W.J. Unger, G. Storm, Y. van Kooyk, and E. Mastrobattista, Targeting tumor antigens to dendritic cells using particulate carriers. *J Controlled Release*, 2012. **161**(1): p. 25-37.

130. van den Berg, L.M., S.I. Gringhuis, and T.B. Geijtenbeek, An evolutionary perspective on C-type lectins in infection and immunity. *Ann N Y Acad Sci*, 2012. **1253**: p. 149-58.
131. Long, K.M., A.C. Whitmore, M.T. Ferris, G.D. Sempowski, C. McGee, B. Trollinger, B. Gunn, and M. Heise, Dendritic cell immune receptor (DCIR) regulates Chikungunya virus pathogenesis in mice. *J Virol*, 2013.
132. Lambert, A.A., C. Gilbert, M. Richard, A.D. Beaulieu, and M.J. Tremblay, The C-type lectin surface receptor DCIR acts as a new attachment factor for HIV-1 in dendritic cells and contributes to trans- and cis-infection pathways. *Blood*, 2008. **112**(4): p. 1299-1307.
133. Hodges, A., K. Sharrocks, M. Edelmann, D. Baban, A. Moris, O. Schwartz, H. Drakesmith, K. Davies, B. Kessler, A. McMichael, and A. Simmons, Activation of the lectin DC-SIGN induces an immature dendritic cell phenotype triggering Rho-GTPase activity required for HIV-1 replication. *Nat Immunol*, 2007. **8**(6): p. 569-77.
134. Gringhuis, S.I., J. den Dunnen, M. Litjens, B. van het Hof, Y. van Kooyk, and Teunis B.H. Geijtenbeek, C-Type Lectin DC-SIGN Modulates Toll-like Receptor Signaling via Raf-1 Kinase-Dependent Acetylation of Transcription Factor NF- κ B. *Immunity*, 2007. **26**(5): p. 605-616.
135. Kang, P.B., A.K. Azad, J.B. Torrelles, T.M. Kaufman, A. Beharka, E. Tibesar, L.E. DesJardin, and L.S. Schlesinger, The human macrophage mannose receptor directs Mycobacterium tuberculosis lipoarabinomannan-mediated phagosome biogenesis. *J Exp Med*, 2005. **202**(7): p. 987-999.
136. van Kooyk, Y. and T.B. Geijtenbeek, DC-SIGN: escape mechanism for pathogens. *Nat Rev Immunol*, 2003. **3**(9): p. 697-709.
137. Tanne, A., B. Ma, F. Boudou, L. Tailleux, H. Botella, E. Badell, F. Levillain, M.E. Taylor, K. Drickamer, J. Nigou, K.M. Dobos, G. Puzo, D. Vestweber, M.K. Wild, M. Marcinko, P. Sobieszczuk, L. Stewart, D. Lebus, B. Gicquel, and O. Neyrolles, A murine DC-SIGN homologue contributes to early host defense against Mycobacterium tuberculosis. *J Exp Med*, 2009. **206**(10): p. 2205-20.
138. Marakalala, M.J., R. Guler, L. Matika, G. Murray, M. Jacobs, F. Brombacher, A.G. Rothfuchs, A. Sher, and G.D. Brown, The Syk/CARD9-coupled receptor Dectin-1 is not required for host resistance to Mycobacterium tuberculosis in mice. *Microbes Infect*, 2011. **13**(2): p. 198-201.
139. Ishikawa, E., T. Ishikawa, Y.S. Morita, K. Toyonaga, H. Yamada, O. Takeuchi, T. Kinoshita, S. Akira, Y. Yoshikai, and S. Yamasaki, Direct recognition of the mycobacterial glycolipid, trehalose dimycolate, by C-type lectin Mincle. *J Exp Med*, 2009. **206**(13): p. 2879-2888.
140. Schoenen, H., B. Bodendorfer, K. Hitchens, S. Manzanero, K. Werninghaus, F. Nimmerjahn, E.M. Agger, S. Stenger, P. Andersen, J. Ruland, G.D. Brown, C. Wells, and R. Lang, Cutting Edge: Mincle Is Essential for Recognition and Adjuvanticity of the Mycobacterial Cord Factor and its Synthetic Analog Trehalose-Dibehenate. *J Immunol*, 2010. **184**(6): p. 2756-2760.
141. Bergman, M., G. Del Prete, Y. van Kooyk, and B. Appelmelk, Helicobacter pylori phase variation, immune modulation and gastric autoimmunity. *Nat Rev Microbiol*, 2006. **4**(2): p. 151-9.
142. Gross, O., A. Gewies, K. Finger, M. Schafer, T. Sparwasser, C. Peschel, I. Forster, and J. Ruland, Card9 controls a non-TLR signalling pathway for innate anti-fungal immunity. *Nature*, 2006. **442**(7103): p. 651-6.
143. Iliiev, I.D., V.A. Funari, K.D. Taylor, Q. Nguyen, C.N. Reyes, S.P. Strom, J. Brown, C.A. Becker, P.R. Fleshner, M. Dubinsky, J.I. Rotter, H.L. Wang, D.P. McGovern, G.D. Brown, and D.M. Underhill, Interactions between commensal fungi and the C-type lectin receptor Dectin-1 influence colitis. *Science*, 2012. **336**(6086): p. 1314-7.

144. Vazquez-Mendoza, A., J.C. Carrero, and M. Rodriguez-Sosa, Parasitic infections: a role for C-type lectins receptors. *Biomed Res Int*, 2013. **2013**: p. 456352.
145. Hespanhol, R.C., M.D.N.C. Soeiro, M.B. Meuser, M.D.N.S.L. Meirelles, and S. Côrte-Real, The expression of mannose receptors in skin fibroblast and their involvement in *Leishmania (L.) amazonensis* invasion. *J Histochem Cytochem*, 2005. **53**(1): p. 35-44.
146. Chakraborty, P., D. Ghosh, and M.K. Basu, Modulation of macrophage mannose receptor affects the uptake of virulent and avirulent *Leishmania donovani* promastigotes. *J Parasitol*, 2001. **87**(5): p. 1023-1027.
147. Raes, G., L. Brys, B.K. Dahal, J. Brandt, J. Grooten, F. Brombacher, G. Vanham, W. Noël, P. Bogaert, T. Boonefaes, A. Kindt, R. Van Den Bergh, P.J.M. Leenen, P. De Baetselier, and G.H. Ghassebeh, Macrophage galactose-type C-type lectins as novel markers for alternatively activated macrophages elicited by parasitic infections and allergic airway inflammation. *J Leukocyte Biol*, 2005. **77**(3): p. 321-327.
148. Garrido, V.V., L.R. Dulgerian, C.C. Stempin, and F.M. Cerban, The increase in mannose receptor recycling favors arginase induction and *Trypanosoma cruzi* survival in macrophages. *Int J Biol Sci*, 2011. **7**(9): p. 1257-72.
149. Piva, L., P. Tetlak, C. Claser, K. Karjalainen, L. Renia, and C. Ruedl, Cutting edge: Clec9A⁺ dendritic cells mediate the development of experimental cerebral malaria. *J Immunol*, 2012. **189**(3): p. 1128-32.
150. Paveley, R.A., S.A. Aynsley, J.D. Turner, C.D. Bourke, S.J. Jenkins, P.C. Cook, L. Martinez-Pomares, and A.P. Mountford, The Mannose Receptor (CD206) is an important pattern recognition receptor (PRR) in the detection of the infective stage of the helminth *Schistosoma mansoni* and modulates IFN γ production. *Int J Parasitol*, 2011. **41**(13-14): p. 1335-45.
151. WHO, World Malaria Report 2011, 2011.
152. Sturm, A., R. Amino, C. van de Sand, T. Regen, S. Retzlaff, A. Rennenberg, A. Krueger, J.-M. Pollok, R. Menard, and V.T. Heussler, Manipulation of Host Hepatocytes by the Malaria Parasite for Delivery into Liver Sinusoids. *Science*, 2006. **313**(5791): p. 1287-1290.
153. Miller, L.H., D.I. Baruch, K. Marsh, and O.K. Doumbo, The pathogenic basis of malaria. *Nature*, 2002. **415**(6872): p. 673-679.
154. Amino, R., R. Ménard, and F. Frischknecht, In vivo imaging of malaria parasites — recent advances and future directions. *Curr Opin Microbiol*, 2005. **8**(4): p. 407-414.
155. Severe falciparum malaria. World Health Organization, Communicable Diseases Cluster. *Trans R Soc Trop Med Hyg*, 2000. **94 Suppl 1**: p. S1-90.
156. Svenson, J.E., J.D. MacLean, T.W. Gyorkos, and J. Keystone, Imported malaria. Clinical presentation and examination of symptomatic travelers. *Arch Intern Med*, 1995. **155**(8): p. 861-8.
157. Trampuz, A., M. Jereb, I. Muzlovic, and R.M. Prabhu, Clinical review: Severe malaria. *Crit Care*, 2003. **7**(4): p. 315-23.
158. Dondorp, A.M., C.I. Fanello, I.C.E. Hendriksen, E. Gomes, A. Seni, K.D. Chhaganlal, K. Bojang, R. Olaosebikan, N. Anunobi, K. Maitland, E. Kivaya, T. Agbenyega, S.B. Nguah, J. Evans, S. Gesase, C. Kahabuka, G. Mtove, B. Nadjm, J. Deen, J. Mwanga-Amumpaire, M. Nansumba, C. Karema, N. Umulisa, A. Uwimana, O.A. Mokuolu, O.T. Adedoyin, W.B.R. Johnson, A.K. Tshefu, M.A. Onyamboko, T. Sakulthaew, W.P. Ngum, K. Silamut, K. Stepniewska, C.J. Woodrow, D. Bethell, B. Wills, M. Oneko, T.E. Peto, L. von Seidlein, N.P.J. Day, and N.J. White, Artesunate versus quinine in the treatment of severe falciparum malaria in African children (AQUAMAT): an open-label, randomised trial. *Lancet*. **376**(9753): p. 1647-1657.
159. Artesunate versus quinine for treatment of severe falciparum malaria: a randomised trial. *Lancet*. **366**(9487): p. 717-725.

160. Clark, I.A., M.M. Awburn, R.O. Whitten, C.G. Harper, N.G. Liomba, M.E. Molyneux, and T.E. Taylor, Tissue distribution of migration inhibitory factor and inducible nitric oxide synthase in falciparum malaria and sepsis in African children. *Malar J*, 2003. **2**: p. 6.
161. Taylor, T.E., W.J. Fu, R.A. Carr, R.O. Whitten, J.S. Mueller, N.G. Fosiko, S. Lewallen, N.G. Liomba, and M.E. Molyneux, Differentiating the pathologies of cerebral malaria by postmortem parasite counts. *Nat Med*, 2004. **10**(2): p. 143-5.
162. Idro, R., N.E. Jenkins, and C.R. Newton, Pathogenesis, clinical features, and neurological outcome of cerebral malaria. *Lancet Neurol*, 2005. **4**(12): p. 827-40.
163. Wykes, M.N. and M.F. Good, What really happens to dendritic cells during malaria? *Nat Rev Microbiol*, 2008. **6**(11): p. 864-70.
164. Wykes, M.N. and M.F. Good, What have we learnt from mouse models for the study of malaria? *Eur J Immunol*, 2009. **39**(8): p. 2004-2007.
165. Craig, A.G., G.E. Grau, C. Janse, J.W. Kazura, D. Milner, J.W. Barnwell, G. Turner, J. Langhorne, and M. on behalf of the participants of the Hinxtion Retreat meeting on "Animal Models for Research on Severe, The Role of Animal Models for Research on Severe Malaria. *PLoS Pathog*, 2012. **8**(2): p. e1002401.
166. Engwerda, C., E. Belnoue, A.C. Grüner, and L. Rénia, Experimental Models of Cerebral Malaria, in *Immunology and Immunopathogenesis of Malaria*, J. Langhorne, Editor 2005, Springer Berlin Heidelberg. p. 103-143.
167. Brian de Souza, J. and E.M. Riley, Cerebral malaria: the contribution of studies in animal models to our understanding of immunopathogenesis. *Microbes Infect*, 2002. **4**(3): p. 291-300.
168. Taylor-Robinson, A.W., Validity of Modelling Cerebral Malaria in Mice: Argument and Counter Argument. *J Neuroparasitol*, 2010. **1**: p. 5.
169. Penet, M.F., A. Viola, S. Confort-Gouny, Y. Le Fur, G. Duhamel, F. Kober, D. Ibarrola, M. Izquierdo, N. Coltel, B. Gharib, G.E. Grau, and P.J. Cozzone, Imaging experimental cerebral malaria in vivo: significant role of ischemic brain edema. *J Neurosci*, 2005. **25**(32): p. 7352-8.
170. Lackner, P., R. Beer, R. Helbok, G. Broessner, K. Engelhardt, C. Brenneis, E. Schmutzhard, and K. Pfaller, Scanning electron microscopy of the neuropathology of murine cerebral malaria. *Malar J*, 2006. **5**: p. 116.
171. Hearn, J., N. Rayment, D.N. Landon, D.R. Katz, and J.B. de Souza, Immunopathology of cerebral malaria: morphological evidence of parasite sequestration in murine brain microvasculature. *Infect Immun*, 2000. **68**(9): p. 5364-76.
172. Desruisseaux, M.S., M. Gulinello, D.N. Smith, S.C. Lee, M. Tsuji, L.M. Weiss, D.C. Spray, and H.B. Tanowitz, Cognitive dysfunction in mice infected with Plasmodium berghei strain ANKA. *J Infect Dis*, 2008. **197**(11): p. 1621-7.
173. Grau, G.E., T.E. Taylor, M.E. Molyneux, J.J. Wirima, P. Vassalli, M. Hommel, and P.-H. Lambert, Tumor Necrosis Factor and Disease Severity in Children with Falciparum Malaria. *N Engl J Med*, 1989. **320**(24): p. 1586-1591.
174. Pais, T.F. and S. Chatterjee, Brain macrophage activation in murine cerebral malaria precedes accumulation of leukocytes and CD8+ T cell proliferation. *J Neuroimmunol*, 2005. **163**(1-2): p. 73-83.
175. de Souza, J.B., J.C. Hafalla, E.M. Riley, and K.N. Couper, Cerebral malaria: why experimental murine models are required to understand the pathogenesis of disease. *Parasitology*, 2010. **137**(5): p. 755-72.
176. Belnoue, E., M. Kayibanda, A.M. Vigario, J.C. Deschemin, N. van Rooijen, M. Viguier, G. Snounou, and L. Renia, On the pathogenic role of brain-sequestered alphabeta CD8+ T cells in experimental cerebral malaria. *J Immunol*, 2002. **169**(11): p. 6369-75.

177. Haque, A., S.E. Best, K. Unosson, F.H. Amante, F. de Labastida, N.M. Anstey, G. Karupiah, M.J. Smyth, W.R. Heath, and C.R. Engwerda, Granzyme B Expression by CD8⁺ T Cells Is Required for the Development of Experimental Cerebral Malaria. *J Immunol*, 2011. **186**(11): p. 6148-6156.
178. Claser, C., B. Malleret, S.Y. Gun, A.Y.W. Wong, Z.W. Chang, P. Teo, P.C.E. See, S.W. Howland, F. Ginhoux, and L. Rénia, CD8⁺ T Cells and IFN- γ Mediate the Time-Dependent Accumulation of Infected Red Blood Cells in Deep Organs during Experimental Cerebral Malaria. *PLoS ONE*, 2011. **6**(4): p. e18720.
179. Grau, G.E., G. Bieler, P. Pointaire, S. De Kossodo, F. Tacchini-Cotier, P. Vassalli, P.F. Piguet, and P.H. Lambert, Significance of cytokine production and adhesion molecules in malarial immunopathology. *Immunol Lett*, 1990. **25**(1-3): p. 189-194.
180. Schofield, L. and G.E. Grau, Immunological processes in malaria pathogenesis. *Nat Rev Immunol*, 2005. **5**(9): p. 722-35.
181. Grau, G.E., L.F. Fajardo, P.F. Piguet, B. Allet, P.H. Lambert, and P. Vassalli, Tumor necrosis factor (cachectin) as an essential mediator in murine cerebral malaria. *Science*, 1987. **237**(4819): p. 1210-2.
182. Grau, G.E., H. Heremans, P.F. Piguet, P. Pointaire, P.H. Lambert, A. Billiau, and P. Vassalli, Monoclonal antibody against interferon gamma can prevent experimental cerebral malaria and its associated overproduction of tumor necrosis factor. *PNAS*, 1989. **86**(14): p. 5572-4.
183. Villegas-Mendez, A., R. Greig, T.N. Shaw, J.B. de Souza, E. Gwyer Findlay, J.S. Stumhofer, J.C. Hafalla, D.G. Blount, C.A. Hunter, E.M. Riley, and K.N. Couper, IFN-gamma-producing CD4⁺ T cells promote experimental cerebral malaria by modulating CD8⁺ T cell accumulation within the brain. *J Immunol*, 2012. **189**(2): p. 968-79.
184. Freitas do Rosário, A.P., T. Lamb, P. Spence, R. Stephens, A. Lang, A. Roers, W. Muller, A. O'Garra, and J. Langhorne, IL-27 Promotes IL-10 Production by Effector Th1 CD4⁺ T Cells: A Critical Mechanism for Protection from Severe Immunopathology during Malaria Infection. *J Immunol*, 2012. **188**(3): p. 1178-1190.
185. Medzhitov, R., Recognition of microorganisms and activation of the immune response. *Nature*, 2007. **449**(7164): p. 819-826.
186. Urban, B.C., D.J. Ferguson, A. Pain, N. Willcox, M. Plebanski, J.M. Austyn, and D.J. Roberts, Plasmodium falciparum-infected erythrocytes modulate the maturation of dendritic cells. *Nature*, 1999. **400**(6739): p. 73-7.
187. Wilson, N.S., G.M. Behrens, R.J. Lundie, C.M. Smith, J. Waithman, L. Young, S.P. Forehan, A. Mount, R.J. Steptoe, K.D. Shortman, T.F. de Koning-Ward, G.T. Belz, F.R. Carbone, B.S. Crabb, W.R. Heath, and J.A. Villadangos, Systemic activation of dendritic cells by Toll-like receptor ligands or malaria infection impairs cross-presentation and antiviral immunity. *Nat Immunol*, 2006. **7**(2): p. 165-72.
188. Ing, R., M. Segura, N. Thawani, M. Tam, and M.M. Stevenson, Interaction of Mouse Dendritic Cells and Malaria-Infected Erythrocytes: Uptake, Maturation, and Antigen Presentation. *J Immunol*, 2006. **176**(1): p. 441-450.
189. Perry, J.A., A. Rush, R.J. Wilson, C.S. Olver, and A.C. Avery, Dendritic Cells from Malaria-Infected Mice Are Fully Functional APC. *J Immunol*, 2004. **172**(1): p. 475-482.
190. Sponaas, A.-M., E.T. Cadman, C. Voisine, V. Harrison, A. Boonstra, A. O'Garra, and J. Langhorne, Malaria infection changes the ability of splenic dendritic cell populations to stimulate antigen-specific T cells. *J Exp Med*, 2006. **203**(6): p. 1427-1433.
191. Lundie, R.J., T.F. de Koning-Ward, G.M. Davey, C.Q. Nie, D.S. Hansen, L.S. Lau, J.D. Mintern, G.T. Belz, L. Schofield, F.R. Carbone, J.A. Villadangos, B.S. Crabb, and

- W.R. Heath, Blood-stage Plasmodium infection induces CD8⁺ T lymphocytes to parasite-expressed antigens, largely regulated by CD8 α ⁺ dendritic cells. *PNAS*, 2008. **105**(38): p. 14509-14514.
192. Stevenson, M.M., R. Ing, F. Berretta, and J. Miu, Regulating the adaptive immune response to blood-stage malaria: role of dendritic cells and CD4(+)Foxp3(+) regulatory T cells. *Int J Biol Sci*, 2011. **7**(9): p. 1311-22.
193. Coban, C., S. Uematsu, N. Arisue, S. Sato, M. Yamamoto, T. Kawai, O. Takeuchi, H. Hisaeda, T. Horii, and S. Akira, Pathological role of Toll-like receptor signaling in cerebral malaria. *Int Immunol*, 2007. **19**(1): p. 67-79.
194. Gowda, N.M., X. Wu, and D.C. Gowda, TLR9 and MyD88 Are Crucial for the Development of Protective Immunity to Malaria. *J Immunol*, 2012. **188**(10): p. 5073-5085.
195. Togbe, D., L. Schofield, G.E. Grau, B. Schnyder, V. Boissay, S. Charron, S. Rose, B. Beutler, V.F. Quesniaux, and B. Ryffel, Murine cerebral malaria development is independent of toll-like receptor signaling. *Am J Pathol*, 2007. **170**(5): p. 1640-8.
196. Cramer, J.P., B. Lepenies, F. Kamena, C. Holscher, M.A. Freudenberg, G.D. Burchard, H. Wagner, C.J. Kirschning, X. Liu, P.H. Seeberger, and T. Jacobs, MyD88/IL-18-dependent pathways rather than TLRs control early parasitaemia in non-lethal Plasmodium yoelii infection. *Microbes Infect*, 2008. **10**(12-13): p. 1259-65.
197. Lepenies, B., J.P. Cramer, G.D. Burchard, H. Wagner, C.J. Kirschning, and T. Jacobs, Induction of experimental cerebral malaria is independent of TLR2/4/9. *Med Microbiol Immunol*, 2008. **197**(1): p. 39-44.
198. Randall, L.M., F.H. Amante, Y. Zhou, A.C. Stanley, A. Haque, F. Rivera, K. Pfeffer, S. Scheu, G.R. Hill, K. Tamada, and C.R. Engwerda, Cutting Edge: Selective Blockade of LIGHT-Lymphotoxin β Receptor Signaling Protects Mice from Experimental Cerebral Malaria Caused by Plasmodium berghei ANKA. *J Immunol*, 2008. **181**(11): p. 7458-7462.
199. Randall, L.M. and C.R. Engwerda, TNF family members and malaria: Old observations, new insights and future directions. *Exp Parasitol*, 2010. **126**(3): p. 326-331.
200. Hafalla, J.C., J. Burgold, A. Dorhoi, O. Gross, J. Ruland, S.H. Kaufmann, and K. Matuschewski, Experimental cerebral malaria develops independently of caspase recruitment domain-containing protein 9 signaling. *Infect Immun*, 2012. **80**(3): p. 1274-9.
201. Chomczynski, P. and N. Sacchi, Single-step method of RNA isolation by acid guanidinium thiocyanate-phenol-chloroform extraction. *Anal Biochem*, 1987. **162**(1): p. 156-159.
202. Bartlett, J.M. and D. Stirling, A short history of the polymerase chain reaction. *Methods Mol Biol*, 2003. **226**: p. 3-6.
203. Bimboim, H.C. and J. Doly, A rapid alkaline extraction procedure for screening recombinant plasmid DNA. *Nucleic Acids Res*, 1979. **7**(6): p. 1513-1523.
204. Kim, D.W., T. Uetsuki, Y. Kaziro, N. Yamaguchi, and S. Sugano, Use of the human elongation factor 1 α promoter as a versatile and efficient expression system. *Gene*, 1990. **91**(2): p. 217-223.
205. Takebe, Y., M. Seiki, J. Fujisawa, P. Hoy, K. Yokota, K. Arai, M. Yoshida, and N. Arai, SR alpha promoter: an efficient and versatile mammalian cDNA expression system composed of the simian virus 40 early promoter and the R-U5 segment of human T-cell leukemia virus type 1 long terminal repeat. *Mol Cell Biol*, 1988. **8**(1): p. 466-72.

206. Smith, P.K., R.I. Krohn, G.T. Hermanson, A.K. Mallia, F.H. Gartner, M.D. Provenzano, E.K. Fujimoto, N.M. Goeke, B.J. Olson, and D.C. Klenk, Measurement of protein using bicinchoninic acid. *Anal Biochem*, 1985. **150**(1): p. 76-85.
207. Mattson, G., E. Conklin, S. Desai, G. Nielander, M.D. Savage, and S. Morgensen, A practical approach to crosslinking. *Mol Biol Rep*, 1993. **17**(3): p. 167-83.
208. Orgueira, H.A., A. Bartolozzi, P. Schell, R. Litjens, E.R. Palmacci, and P.H. Seeberger, Modular synthesis of heparin oligosaccharides. *Chem-Eur J*, 2003. **9**(1): p. 140-169.
209. Seeberger, P.H., H. Orgueira, and P. Schell, Solid- and solution-phase synthesis of heparin and other glycosaminoglycans, 2005, Massachusetts Institute of Technology.
210. Love, K.R. and P.H. Seeberger, Automated synthesis of the Lewis blood group oligosaccharides. *Abstracts of Papers of ACS*, 2002. **224**(1-2): p. 864-ORGN 864.
211. Love, K.R. and P.H. Seeberger, Solution syntheses of protected type II Lewis blood group oligosaccharides: Study for automated synthesis. *J Org Chem*, 2005. **70**(8): p. 3168-3177.
212. Love, K.R. and P.H. Seeberger, Automated solid-phase synthesis of protected tumor-associated antigen and blood group determinant oligosaccharides. *Angew Chem Int Edit*, 2004. **43**(5): p. 602-605.
213. Ratner, D.M., O.J. Plante, and P.H. Seeberger, Linear synthesis of branched high-mannose oligosaccharides from the HIV-1 viral surface envelope glycoprotein GP1120. *Abstracts of Papers of ACS*, 2002. **224**: p. U273-U273.
214. Hoelemann, A., B.L. Stocker, and P.H. Seeberger, Synthesis of a core arabinomannan oligosaccharide of *Mycobacterium tuberculosis*. *J Org Chem*, 2006. **71**(21): p. 8071-8088.
215. Liu, X., R. Wada, S. Boonyarattanakalin, B. Castagner, and P.H. Seeberger, Automated synthesis of lipomannan backbone alpha(1-6) oligomannoside via glycosyl phosphates: glycosyl tricyclic orthoesters revisited. *Chem Comm*, 2008(30): p. 3510-3512.
216. Boonyarattanakalin, S., X. Liu, M. Michieletti, B. Lepenies, and P.H. Seeberger, Chemical Synthesis of All Phosphatidylinositol Mannoside (PIM) Glycans from *Mycobacterium tuberculosis*. *J Am Chem Soc*, 2008. **130**(49): p. 16791-16799.
217. Bosse, F., L.A. Marcaurelle, and P.H. Seeberger, Linear synthesis of the tumor-associated carbohydrate antigens globo-h, SSEA-3, and Gb3. *J Org Chem*, 2002. **67**(19): p. 6659-6670.
218. Routenberg Love, K. and P.H. Seeberger, Automated solid-phase synthesis of protected tumor-associated antigen and blood group determinant oligosaccharides. *Angew Chem Int Ed*, 2004. **43**(5): p. 602-5.
219. Rich, R.L. and D.G. Myszka, Survey of the year 2007 commercial optical biosensor literature. *J Mol Recognit*, 2008. **21**(6): p. 355-400.
220. Grunstein, D., M. Maglinao, R. Kikkeri, M. Collot, K. Barylyuk, B. Lepenies, F. Kamena, R. Zenobi, and P.H. Seeberger, Hexameric supramolecular scaffold orients carbohydrates to sense bacteria. *J Am Chem Soc*, 2011. **133**(35): p. 13957-66.
221. Bernardes, G.J., R. Kikkeri, M. Maglinao, P. Laurino, M. Collot, S.Y. Hong, B. Lepenies, and P.H. Seeberger, Design, synthesis and biological evaluation of carbohydrate-functionalized cyclodextrins and liposomes for hepatocyte-specific targeting. *Org Biomol Chem*, 2010. **8**(21): p. 4987-96.
222. Gentsch, R., F. Pippig, K. Nilles, P. Theato, R. Kikkeri, M. Maglinao, B. Lepenies, P.H. Seeberger, and H.G. Borner, Modular Approach toward Bioactive Fiber Meshes Carrying Oligosaccharides. *Macromolecules*, 2010. **43**(22): p. 9239-9247.

223. Lepenies, B., K. Pfeffer, M.A. Hurchla, T.L. Murphy, K.M. Murphy, J. Oetzel, B. Fleischer, and T. Jacobs, Ligation of B and T lymphocyte attenuator prevents the genesis of experimental cerebral malaria. *J Immunol*, 2007. **179**(6): p. 4093-100.
224. Klopffleisch, R., P. Klose, A. da Costa, L. Brunnberg, and A.D. Gruber, HEPACAM1 and 2 are differentially regulated in canine mammary adenomas and carcinomas and its lymph node metastases. *BMC Vet Res*, 2010. **6**: p. 15.
225. Drickamer, K. and M.E. Taylor, Biology of Animal Lectins. *Ann Rev Cell Biol*, 1993. **9**(1): p. 237-264.
226. Lepenies, B., J. Yin, and P.H. Seeberger, Applications of synthetic carbohydrates to chemical biology. *Curr Opin Chem Biol*, 2010. **14**(3): p. 404-411.
227. Ryu, J.-H., E. Lee, Y.-b. Lim, and M. Lee, Carbohydrate-Coated Supramolecular Structures: Transformation of Nanofibers into Spherical Micelles Triggered by Guest Encapsulation. *J Am Chem Soc*, 2007. **129**(15): p. 4808-4814.
228. Gómez-García, M., J.M. Benito, D. Rodríguez-Lucena, J.-X. Yu, K. Chmurski, C. Ortiz Mellet, R. Gutiérrez Gallego, A. Maestre, J. Defaye, and J.M. García Fernández, Probing Secondary Carbohydrate-Protein Interactions with Highly Dense Cyclodextrin-Centered Heteroglycoclusters: The Heterocluster Effect. *J Am Chem Soc*, 2005. **127**(22): p. 7970-7971.
229. Hardman, K.D. and C.F. Ainsworth, Structure of concanavalin A at 2.4-Ång resolution. *Biochemistry*, 1972. **11**(26): p. 4910-4919.
230. Hahnefeld, C., S. Drewianka, and F.W. Herberg, Determination of kinetic data using surface plasmon resonance biosensors. *Methods Mol Med*, 2004. **94**: p. 299-320.
231. Munoz, E.M., J. Correa, E. Fernandez-Megia, and R. Riguera, Probing the Relevance of Lectin Clustering for the Reliable Evaluation of Multivalent Carbohydrate Recognition. *J Am Chem Soc*, 2009. **131**(49): p. 17765-17767.
232. Dhayal, M. and D.M. Ratner, XPS and SPR Analysis of Glycoarray Surface Density. *Langmuir*, 2009. **25**(4): p. 2181-2187.
233. Li, Y., G. Huang, J. Diakur, and L.I. Wiebe, Targeted delivery of macromolecular drugs: asialoglycoprotein receptor (ASGPR) expression by selected hepatoma cell lines used in antiviral drug development. *Curr Drug Deliv*, 2008. **5**(4): p. 299-302.
234. Peng, D.J., J. Sun, Y.Z. Wang, J. Tian, Y.H. Zhang, M.H.M. Noteborn, and S. Qu, Inhibition of hepatocarcinoma by systemic delivery of Apoptin gene via the hepatic asialoglycoprotein receptor. *Cancer Gene Ther*, 2006. **14**(1): p. 66-73.
235. Zhang, X.-Q., X.-L. Wang, P.-C. Zhang, Z.-L. Liu, R.-X. Zhuo, H.-Q. Mao, and K.W. Leong, Galactosylated ternary DNA/polyphosphoramidate nanoparticles mediate high gene transfection efficiency in hepatocytes. *J Controlled Release*, 2005. **102**(3): p. 749-763.
236. Díaz-Moscoso, A., L. Le Gourriérec, M. Gómez-García, J.M. Benito, P. Balbuena, F. Ortega-Caballero, N. Guilloteau, C. Di Giorgio, P. Vierling, J. Defaye, C. Ortiz Mellet, and J.M. García Fernández, Polycationic Amphiphilic Cyclodextrins for Gene Delivery: Synthesis and Effect of Structural Modifications on Plasmid DNA Complex Stability, Cytotoxicity, and Gene Expression. *Chem Eur J*, 2009. **15**(46): p. 12871-12888.
237. Mourtzis, N., M. Paravatou, I.M. Mavridis, M.L. Roberts, and K. Yannakopoulou, Synthesis, Characterization, and Remarkable Biological Properties of Cyclodextrins Bearing Guanidinoalkylamino and Aminoalkylamino Groups on Their Primary Side. *Chem Eur J*, 2008. **14**(14): p. 4188-4200.
238. Srinivasachari, S., K.M. Fichter, and T.M. Reineke, Polycationic β -Cyclodextrin "Click Clusters": Monodisperse and Versatile Scaffolds for Nucleic Acid Delivery. *J Am Chem Soc*, 2008. **130**(14): p. 4618-4627.

239. Benito, J.M., M. Gómez-García, C. Ortiz Mellet, I. Baussanne, J. Defaye, and J.M. García Fernández, Optimizing Saccharide-Directed Molecular Delivery to Biological Receptors: Design, Synthesis, and Biological Evaluation of Glycodendrimer–Cyclodextrin Conjugates. *J Am Chem Soc*, 2004. **126**(33): p. 10355-10363.
240. Laginha, K.M., S. Verwoert, G.J.R. Charrois, and T.M. Allen, Determination of Doxorubicin Levels in Whole Tumor and Tumor Nuclei in Murine Breast Cancer Tumors. *Clin Cancer Res*, 2005. **11**(19): p. 6944-6949.
241. Gringhuis, S.I., J. den Dunnen, M. Litjens, M. van der Vlist, and T.B.H. Geijtenbeek, Carbohydrate-specific signaling through the DC-SIGN signalosome tailors immunity to Mycobacterium tuberculosis, HIV-1 and Helicobacter pylori. *Nat Immunol*, 2009. **10**(10): p. 1081-1088.
242. Miller, S.I., R.K. Ernst, and M.W. Bader, LPS, TLR4 and infectious disease diversity. *Nat Rev Micro*, 2005. **3**(1): p. 36-46.
243. Flanagan, M.L., R.S. Arias, P. Hu, L.A. Khawli, and A.L. Epstein, Soluble Fc fusion proteins for biomedical research. *Methods Mol Biol*, 2007. **378**: p. 33-52.
244. Zhang, J., J. Carter, S. Siu, J.W. O'Neill, A.H. Gates, J. Delaney, and C. Mehlin, Fusion partners as a tool for the expression of difficult proteins in mammalian cells. *Curr Pharm Biotechnol*, 2010. **11**(3): p. 241-5.
245. Brown, G.D. and S. Gordon, Immune recognition: A new receptor for [beta]-glucans. *Nature*, 2001. **413**(6851): p. 36-37.
246. Eriksson, M., *C-type Lectin Receptors: from Immunomodulatory Carbohydrate Ligands to a Role in Murine Colitis* (Doctoral Thesis), in Department of Biology, Chemistry, and Pharmacy 2013, Free University Berlin: Berlin.
247. Burgdorf, S., C. Scholz, A. Kautz, R. Tampe, and C. Kurts, Spatial and mechanistic separation of cross-presentation and endogenous antigen presentation. *Nat Immunol*, 2008. **9**(5): p. 558-566.
248. Yañez, D.M., D.D. Manning, A.J. Cooley, W.P. Weidanz, and H.C. van der Heyde, Participation of lymphocyte subpopulations in the pathogenesis of experimental murine cerebral malaria. *J Immunol*, 1996. **157**(4): p. 1620-4.
249. Kamena, F., M. Tamborrini, X. Liu, Y.-U. Kwon, F. Thompson, G. Pluschke, and P.H. Seeberger, Synthetic GPI array to study antitoxic malaria response. *Nat Chem Biol*, 2008. **4**(4): p. 238-240.
250. Schofield, L., S. Novakovic, P. Gerold, R.T. Schwarz, M.J. McConville, and S.D. Tachado, Glycosylphosphatidylinositol toxin of Plasmodium up-regulates intercellular adhesion molecule-1, vascular cell adhesion molecule-1, and E-selectin expression in vascular endothelial cells and increases leukocyte and parasite cytoadherence via tyrosine kinase-dependent signal transduction. *J Immunol*, 1996. **156**(5): p. 1886-1896.
251. Tachado, S.D., P. Gerold, M.J. McConville, T. Baldwin, D. Quilici, R.T. Schwarz, and L. Schofield, Glycosylphosphatidylinositol toxin of Plasmodium induces nitric oxide synthase expression in macrophages and vascular endothelial cells by a protein tyrosine kinase-dependent and protein kinase C-dependent signaling pathway. *J Immunol*, 1996. **156**(5): p. 1897-1907.
252. Didierlaurent, A.M., S. Morel, L. Lockman, S.L. Giannini, M. Bisteau, H. Carlsen, A. Kielland, O. Vosters, N. Vanderheyde, F. Schiavetti, D. Larocque, M. Van Mechelen, and N. Garçon, AS04, an aluminum salt- and TLR4 agonist-based adjuvant system, induces a transient localized innate immune response leading to enhanced adaptive immunity. *J Immunol*, 2009. **183**(10): p. 6186-97.
253. Schlick, K.H. and M.J. Cloninger, Inhibition binding studies of glycodendrimer/lectin interactions using surface plasmon resonance. *Tetrahedron*, 2010. **66**(29): p. 5305-5310.

254. Hashida, M., M. Nishikawa, F. Yamashita, and Y. Takakura, Cell-specific delivery of genes with glycosylated carriers. *Adv Drug Delivery Rev*, 2001. **52**(3): p. 187-96.
255. Taylor, M.E., J.T. Conary, M.R. Lennartz, P.D. Stahl, and K. Drickamer, Primary Structure of the Mannose Receptor Contains Multiple Motifs Resembling Carbohydrate-Recognition Domains. *J Biol Chem*, 1990. **265**(21): p. 12156-12162.
256. Takata, I., K. Chida, M.R. Gordon, Q.N. Myrvik, M.J. Ricardo, Jr., and L.S. Kucera, L-fucose, D-mannose, L-galactose, and their BSA conjugates stimulate macrophage migration. *J Leukocyte Biol*, 1987. **41**(3): p. 248-56.
257. Shimizu, Y., H. Takagi, T. Nakayama, K. Yamakami, T. Tadakuma, N. Yokoyama, and N. Kojima, Intraperitoneal immunization with oligomannose-coated liposome-entrapped soluble leishmanial antigen induces antigen-specific T-helper type immune response in BALB/c mice through uptake by peritoneal macrophages. *Parasite Immunol*, 2007. **29**(5): p. 229-39.
258. Un, K., S. Kawakami, R. Suzuki, K. Maruyama, F. Yamashita, and M. Hashida, Enhanced transfection efficiency into macrophages and dendritic cells by a combination method using mannosylated lipoplexes and bubble liposomes with ultrasound exposure. *Hum Gene Ther*, 2010. **21**(1): p. 65-74.
259. Wright, G.J., Signal initiation in biological systems: the properties and detection of transient extracellular protein interactions. *Mol BioSystems*, 2009. **5**(12): p. 1405-1412.
260. Ramani, S.R., I. Tom, N. Lewin-Koh, B. Wranik, L. DePalatis, J. Zhang, D. Eaton, and L.C. Gonzalez, A secreted protein microarray platform for extracellular protein interaction discovery. *Anal Biochem*, 2012. **420**(2): p. 127-138.
261. Mekhaieel, D.N.A., D.M. Czajkowsky, J.T. Andersen, J. Shi, M. El-Faham, M. Doenhoff, R.S. McIntosh, I. Sandlie, J. He, J. Hu, Z. Shao, and R.J. Pleass, Polymeric human Fc-fusion proteins with modified effector functions. *Sci Rep*, 2011. **1**.
262. Nakanishi, K.S., Takaharu; Kumada, Yoichi; Imamura, Koreyoshi; Imanaka, Hiroyuki, Recent Advances in Controlled Immobilization of Proteins onto the Surface of the Solid Substrate and Its Possible Application to Proteomics *Curr Proteomics*, 2008. **5**(3): p. 15.
263. Schlegel, M.K., J. Hütter, M. Eriksson, B. Lepenies, and P.H. Seeberger, Defined Presentation of Carbohydrates on a Duplex DNA Scaffold. *Chem Bio Chem*, 2011. **12**(18): p. 2791-2800.
264. Weis, W.I., K. Drickamer, and W.A. Hendrickson, Structure of a C-type mannose-binding protein complexed with an oligosaccharide. *Nature*, 1992. **360**(6400): p. 127-134.
265. Muramatsu, T. and H. Muramatsu, Carbohydrate antigens expressed on stem cells and early embryonic cells. *Glycoconj J*, 2004. **21**(1-2): p. 41-5.
266. Heimburg-Molinaro, J., M. Lum, G. Vijay, M. Jain, A. Almogren, and K. Rittenhouse-Olson, Cancer vaccines and carbohydrate epitopes. *Vaccine*, 2011. **29**(48): p. 8802-26.
267. Carrillo-Conde, B., E.-H. Song, A. Chavez-Santoscoy, Y. Phanse, A.E. Ramer-Tait, N.L.B. Pohl, M.J. Wannemuehler, B.H. Bellaire, and B. Narasimhan, Mannose-Functionalized "Pathogen-like" Polyanhydride Nanoparticles Target C-Type Lectin Receptors on Dendritic Cells. *Mol Pharm*, 2011. **8**(5): p. 1877-1886.
268. Espuelas, S., C. Thumann, B. Heurtault, F. Schuber, and B. Frisch, Influence of ligand valency on the targeting of immature human dendritic cells by mannosylated liposomes. *Bioconjugate Chem*, 2008. **19**(12): p. 2385-2393.
269. Singh, S.K., J. Stephani, M. Schaefer, H. Kalay, J.J. García-Vallejo, J. den Haan, E. Saeland, T. Sparwasser, and Y. van Kooyk, Targeting glycan modified OVA to murine DC-SIGN transgenic dendritic cells enhances MHC class I and II presentation. *Mol Immunol*, 2009. **47**(2-3): p. 164-174.

270. Singh, M. and D. O'Hagan, Advances in vaccine adjuvants. *Nat Biotechnol*, 1999. **17**(11): p. 1075-1081.
271. Reddy, S.T., M.A. Swartz, and J.A. Hubbell, Targeting dendritic cells with biomaterials: developing the next generation of vaccines. *Trends Immunol*, 2006. **27**(12): p. 573-579.
272. Gupta, R.K. and G.R. Siber, Adjuvants for human vaccines. Current status, problems and future prospects. *Vaccine*, 1995. **13**(14): p. 1263-1276.
273. Gupta, R.K., Aluminum compounds as vaccine adjuvants. *Adv Drug Delivery Reviews*, 1998. **32**(3): p. 155-172.
274. Hunter, R.L., Overview of vaccine adjuvants: Present and future. *Vaccine*, 2002. **20**(SUPPL. 3): p. S7-S12.
275. Zhu, J., G. Krishnegowda, and D.C. Gowda, Induction of proinflammatory responses in macrophages by the glycosylphosphatidylinositols of *Plasmodium falciparum*: the requirement of extracellular signal-regulated kinase, p38, c-Jun N-terminal kinase and NF-kappaB pathways for the expression of proinflammatory cytokines and nitric oxide. *J Biol Chem*, 2005. **280**(9): p. 8617-27.
276. Krishnegowda, G., A.M. Hajjar, J. Zhu, E.J. Douglass, S. Uematsu, S. Akira, A.S. Woods, and D.C. Gowda, Induction of proinflammatory responses in macrophages by the glycosylphosphatidylinositols of *Plasmodium falciparum*: cell signaling receptors, glycosylphosphatidylinositol (GPI) structural requirement, and regulation of GPI activity. *J Biol Chem*, 2005. **280**(9): p. 8606-16.
277. Coban, C., K.J. Ishii, T. Kawai, H. Hemmi, S. Sato, S. Uematsu, M. Yamamoto, O. Takeuchi, S. Itagaki, N. Kumar, T. Horii, and S. Akira, Toll-like receptor 9 mediates innate immune activation by the malaria pigment hemozoin. *J Exp Med*, 2005. **201**(1): p. 19-25.
278. Parroche, P., F.N. Lauw, N. Goutagny, E. Latz, B.G. Monks, A. Visintin, K.A. Halmen, M. Lamphier, M. Olivier, D.C. Bartholomeu, R.T. Gazzinelli, and D.T. Golenbock, Malaria hemozoin is immunologically inert but radically enhances innate responses by presenting malaria DNA to Toll-like receptor 9. *PNAS*, 2007. **104**(6): p. 1919-24.
279. Franklin, B.S., P. Parroche, M.A. Ataide, F. Lauw, C. Ropert, R.B. de Oliveira, D. Pereira, M.S. Tada, P. Nogueira, L.H. da Silva, H. Bjorkbacka, D.T. Golenbock, and R.T. Gazzinelli, Malaria primes the innate immune response due to interferon-gamma induced enhancement of toll-like receptor expression and function. *PNAS*, 2009. **106**(14): p. 5789-94.
280. Coban, C., K.J. Ishii, T. Horii, and S. Akira, Manipulation of host innate immune responses by the malaria parasite. *Trends Microbiol*, 2007. **15**(6): p. 271-8.
281. Franklin, B.S., S.T. Ishizaka, M. Lamphier, F. Gusovsky, H. Hansen, J. Rose, W. Zheng, M.A. Ataide, R.B. de Oliveira, D.T. Golenbock, and R.T. Gazzinelli, Therapeutic targeting of nucleic acid-sensing Toll-like receptors prevents experimental cerebral malaria. *PNAS*, 2011. **108**(9): p. 3689-94.
282. Griffith, J.W., C. O'Connor, K. Bernard, T. Town, D.R. Goldstein, and R. Bucala, Toll-like receptor modulation of murine cerebral malaria is dependent on the genetic background of the host. *J Infect Dis*, 2007. **196**(10): p. 1553-64.
283. Sharma, S., R.B. DeOliveira, P. Kalantari, P. Parroche, N. Goutagny, Z. Jiang, J. Chan, D.C. Bartholomeu, F. Lauw, J.P. Hall, G.N. Barber, R.T. Gazzinelli, K.A. Fitzgerald, and D.T. Golenbock, Innate immune recognition of an AT-rich stem-loop DNA motif in the *Plasmodium falciparum* genome. *Immunity*, 2011. **35**(2): p. 194-207.

284. Finney, C.A., Z. Lu, L. LeBourhis, D.J. Philpott, and K.C. Kain, Disruption of Nod-like receptors alters inflammatory response to infection but does not confer protection in experimental cerebral malaria. *Am J Trop Med Hyg*, 2009. **80**(5): p. 718-22.
285. Ahrens, S., S. Zelenay, D. Sancho, P. Hanc, S. Kjaer, C. Feest, G. Fletcher, C. Durkin, A. Postigo, M. Skehel, F. Batista, B. Thompson, M. Way, C. Reis e Sousa, and O. Schulz, F-actin is an evolutionarily conserved damage-associated molecular pattern recognized by DNGR-1, a receptor for dead cells. *Immunity*, 2012. **36**(4): p. 635-45.
286. Zhang, J.G., P.E. Czabotar, A.N. Policheni, I. Caminschi, S.S. Wan, S. Kitsoulis, K.M. Tullett, A.Y. Robin, R. Brammananth, M.F. van Delft, J. Lu, L.A. O'Reilly, E.C. Josefsson, B.T. Kile, W.J. Chin, J.D. Mintern, M.A. Olshina, W. Wong, J. Baum, M.D. Wright, D.C. Huang, N. Mohandas, R.L. Coppel, P.M. Colman, N.A. Nicola, K. Shortman, and M.H. Lahoud, The dendritic cell receptor Clec9A binds damaged cells via exposed actin filaments. *Immunity*, 2012. **36**(4): p. 646-57.
287. Perry, J.A., C.S. Olver, R.C. Burnett, and A.C. Avery, Cutting edge: the acquisition of TLR tolerance during malaria infection impacts T cell activation. *J Immunol*, 2005. **174**(10): p. 5921-5.
288. Holmberg, V., P. Onkamo, E. Lahtela, P. Lahermo, G. Bedu-Addo, F.P. Mockenhaupt, and S. Meri, Mutations of complement lectin pathway genes MBL2 and MASP2 associated with placental malaria. *Malar J*, 2012. **11**: p. 61.